2020-01-01

Discovery Of Glycan-Based Biomarkers For Cutaneous Leishmaniasis And Chagas Disease By Reversed Immunoglycomics

Alba Lucia Montoya
University of Texas at El Paso

DISCOVERY OF GLYCAN-BASED BIOMARKERS FOR CUTANEOUS LEISHMANIASIS

AND CHAGAS DISEASE BY REVERSED IMMUNOGLYCOMICS

ALBA LUCIA MONTOYA ARIAS

Doctoral Program in Chemistry

APPROVED:

Katja Michael, Ph.D., Chair

Igor C. Almeida, D.Sc.

Chu Young Kim, Ph.D.

Yaoqiu Zhu, Ph.D.

Stephen L. Crites, Jr., Ph.D.
Dean of the Graduate School

Copyright ©

by

Alba Lucia Montoya Arias

2020

Dedication

To God,

Antonio Montoya & Esperanza Arias,

Family, and closest friends

DISCOVERY OF GLYCAN-BASED BIOMARKERS FOR CUTANEOUS LEISHMANIASIS

AND CHAGAS DISEASE BY REVERSED IMMUNOGLYCOMICS

by

ALBA LUCIA MONTOYA ARIAS, M.Sc.

DISSERTATION

Presented to the Faculty of the Graduate School of

The University of Texas at El Paso

in Partial Fulfillment

of the Requirements

for the Degree of

DOCTOR OF PHILOSOPHY

Department of Chemistry and Biochemistry

THE UNIVERSITY OF TEXAS AT EL PASO

December 2020

Abstract

Protozoa are the causative agents of a number of diseases that affect humans and mammalian animals. Several forms of leishmaniasis are caused by different *Leishmania* species (*Leishmania spp.*), while Chagas disease (CD) is caused by the parasite *Trypanosoma cruzi* (*T. cruzi*). These members of the Trypanosomatidae family have characteristic glycoconjugates broadly distributed on their cell surfaces, which can be useful for diagnosis and follow-up of chemotherapy for the diseases.

Leishmania spp. expresses an "exotic" surface glycocalyx mainly composed of a number of glycosyl-phosphatidylinositol (GPI)-anchored proteins, a complex lipophosphoglycan (LPG) and a family of low-molecular mass glycoinositol-phospholipids (GIPLs), some of them containing terminal α-galactopyranosyl (α-Gal*p*) residues. The complete structure of *Leishmania major* (*L. major*) GIPLs have been solved in the past.[1] It was found that *L. major* express type-2 GIPLs, which are known to be highly immunogenic, most likely due to the presence of unusual α-Gal*p* and β-galactofuranosyl (β-Gal*f*) moieties. However, the exact structures of the immunodominant glycotopes responsible for eliciting IgG antibodies (Abs) in Cutaneous Leishmaniasis (CL) patients have not been determined. The identification of these glycotopes are of great interest as potential biomarkers (BMKs) for the accurate diagnosis of leishmaniasis and possibly CD.

In Chapters 2 and 3, the chemical synthesis of five terminal oligosaccharides of type-2 GIPLs from *L. major* ranging from the disaccharide Gal*f*β1,3Man*p*α to the more complex tetrasaccharide Gal*p*α1,6Gal*p*α1,3Gal*f*β1,3Man*p*α, as well as the tetrasaccharide Gal*f*β1,3Man*p*α1,2-[Gal*f*β1,3Man*p*α] present in the GIPLs of *T. cruzi* will be presented. Some of these glycans were then conjugated to bovine serum albumin (BSA) to produce the corresponding

neoglycoproteins (NGPs) for their use as antigens in chemiluminescent enzyme-linked immunosorbent assay (CL-ELISA) using CL and CD patient sera, and to evaluate them as BMKs for the diagnosis of CL and CD respectively.

In collaboration with Drs. Alvaro Acosta-Serrano (Liverpool School of Tropical Medicine, Dept. of Parasitology) and Igor Almeida (UTEP, Dept. of Biological Sciences) we identified Gal$p$α1,3Gal$f$β and Gal$p$α1,3Gal$f$β1,3Man$p$α as diagnostic BMKs for *L. major* infections, distinguishable from *L. tropica* infections and heterologous diseases, respectively.

T. cruzi has a cell surface heavily coated by glycoproteins such as GPI-anchored mucins (tGPI-MUC), whose *O*-glycans are predominantly branched, and often contain highly immunogenic terminal nonreducing α-Gal$p$ glycotopes that are entirely absent or cryptic in humans. The immunodominant tGPI-MUC α-Gal$p$ glycotope, the trisaccharide Gal$p$α1,3Gal$p$β1,4GlcNAcα (Galα3LN), elicits high levels of protective *T. cruzi*-specific anti-α-Gal Abs in CD patients, in both the acute and chronic phases.[2] Although glycoconjugates are the major parasite glycocalyx antigens, they remain completely unexplored as potential BMKs.

In Chapter 4, we searched for a specific α-Gal-based BMK. There, we will show the synthesis of a NGP, consisting of BSA decorated with multiple copies of the branched trisaccharide Gal$p$α(1,6)[Gal$p$α(1,2)]Gal$p$β and its corresponding CL-ELISA using CD patient sera and Normal Human sera (NHS) of healthy individuals. The biological data obtained in collaboration with Dr. Igor Almeida suggest that Gal$p$α(1,6)[Gal$p$α(1,2)]Gal$p$β-linker-BSA (KM11b) may be an immunodominant partial structure of terminal *T. cruzi* glycans or a mimic thereof, and that NGP is suitable as a diagnostic BMK for CD and for drug efficacy assessment in patients.

Table of Contents

x

xi

Vita 179

List of Tables

List of Figures

List of Schemes

Chapter 1: General Introduction

1.1 GLYCOBIOLOGY

Defined in the widest sense, glycobiology is the study of the structure, biosynthesis, biology, and evolution of carbohydrates that are widely distributed in nature and of the proteins that recognize them. Glycobiology is a science field with high relevance to many areas of basic research, biomedicine, and biotechnology. This field includes the chemistry of carbohydrates, the enzymology of glycan formation and degradation, the recognition of glycans by specific proteins, roles of glycans in complex biological systems, and their analysis or manipulation by different techniques.[3]

1.2 CARBOHYDRATES: GLYCANS AND GLYCOCONJUGATES

In recent years, it has been broadly recognized that oligosaccharides (or glycans) and glycoconjugates (glycoproteins and glycolipids) play important roles in different biological processes, including viral and bacterial infections, cell growth and proliferation, cell-cell communication, immune response as well as lead compounds for drug and vaccine discovery.[4-6] As glycans are involved in all those myriad of biological functions, studies on carbohydrates have drawn unprecedented attention, but still fall behind that on proteins and nucleic acids. A major obstacle is related to the fact that it is difficult to get enough pure and structurally well-defined carbohydrates and glycoconjugates, which often exist in nature at low-concentrations and in micro-heterogeneous forms.[6, 7] As a result, chemical synthesis of oligosaccharides is one of the approaches to solve this problem (**Figure 1**).

Although a lot of progress has been made in the assembly of complex oligosaccharides,[5, 8, 9] their synthesis is still a complicated task by the lack of general methods for the routine preparation. While the retrosynthetic analysis is relatively more obvious for oligosaccharides than

1

other natural products, the chemical synthesis of oligosaccharides has several challenges, including: (*i*) control of stereoselectivity in the glycosidic bond formation; (*ii*) glycosylation of substrates with high-density of functional groups; (*iii*) differentiation of multiple functional groups with orthogonal protection to control the regioselectivity of glycosylation; (*iv*) numerous protections and deprotections, which decrease overall efficiency of synthesis, making oligosaccharide synthesis a tedious and time-consuming process. These emphasized issues, which have to be resolved for at least 10 human-type monosaccharides, explain the absence of one general method for the assembly of glycans.[8, 10]

Nevertheless, due to the high significance of glycans as therapeutically relevant targets and highlighted by the ability to synthesize glycoproteins, carbohydrates chemistry is essential, ongoing and advancing towards new and better synthetic methodologies.
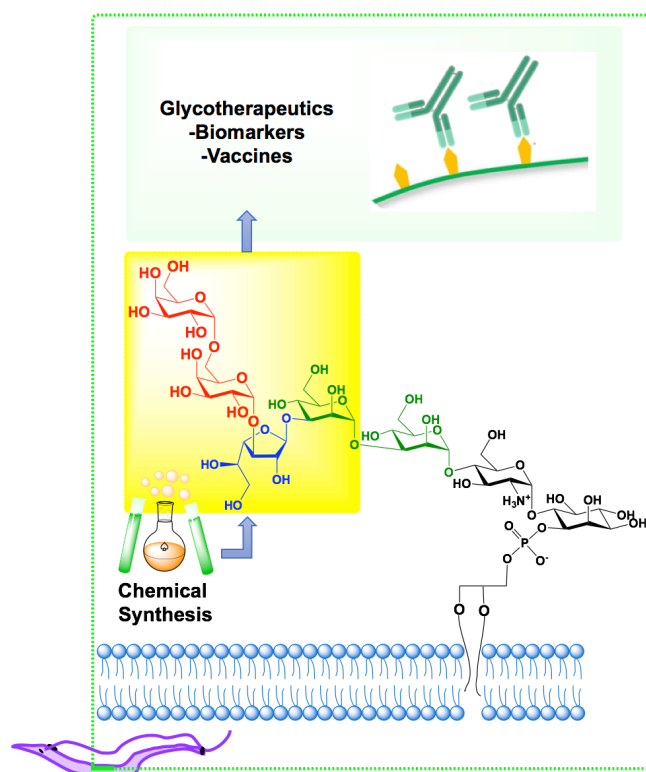
Figure 1. Chemical synthesis and biological evaluation of oligosaccharides present in the cell surface of parasites.

www.manaraa.com

1.3 COMMON MONOSACCHARIDE UNITS OF GLYCOCONJUGATES

While several hundred distinct monosaccharides are known in nature, only a minority of these are commonly found in well-studied glycans.[3] **Table 1** shows the symbol nomenclature for the graphical representation of most common glycans found in *L. major* and *T. cruzi* major surface glycoconjugates, along with their standard abbreviations.

Table 1. Monosaccharide symbol nomenclature for glycans.[11]

Shape	White (Generic)	Blue	Green	Yellow	Purple
Filled Circle	Hexose ◯	Glc 🔵	Man 🟢	Gal 🟡 *f*	
Filled Square	HexNAc □	GlcNAc 🟦		GalNAc 🟨	
Crossed Square	Hexosamine ◻	GlcN ◩			
Filled Diamond	Deoxynonulosanate ◇				Neu5Ac 🔷

1.4 GLYCANS CAN CONSTITUTE A MAJOR PORTION OF THE MASS OF A GLYCOCONJUGATE

In naturally occurring glycoconjugates, the portion of the molecule comprising the glycans can vary greatly in contribution to its overall size. In many cases, the glycans comprise a substantial portion of the mass of the glycoconjugates, as it the case for the mammal-dwelling trypomastigote form of *T. cruzi* in the tGPI-MUC, in which 60% of the glycoprotein is attributed to glycans[12-14] (**Figure 2**). For this reason, the surfaces of all types of cells in nature (which are decorated with diverse kinds of glycoconjugates) are effectively covered with a dense array of sugars, the so-called "glycocalyx". Hence, the density of glycans in the glycocalyx are usually high.[3]

3
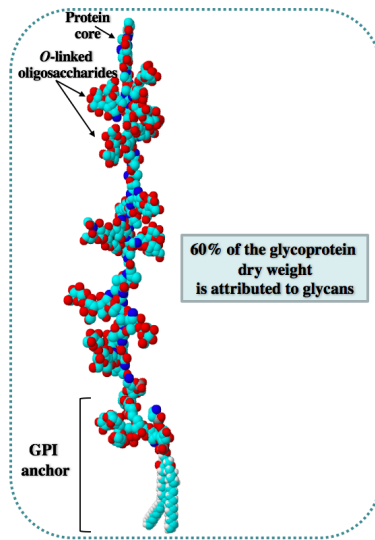
Figure 2. *T. cruzi* trypomastigote (tGPI-MUC) and its calculated percentage of glycans.[15]

1.5 MAJOR CLASSES OF GLYCANS AND GLYCOCONJUGATES

There are two main classes of glycans defined according to the type of covalent attachment to a polypeptide backbone of proteins, usually via *N-* or *O-*linkages. An *N-*glycan, which are the most abundant, (*N-*linked oligossacharide, *N-*[Asn]-linked oligosaccharide) is a sugar chain covalently linked usually through a 2-acetamido-2-deoxy-β-D-glycopyranoside (GlcNAc) to the amide nitrogen of an asparagine (Asn) residue. An *O-*glycan, (*O-*linked oligossacharide, *O-*[Ser/Thr]-linked oligosaccharides) is a sugar chain covalently attached frequently via *N-*acetylgalactosamine (GalNAc) to a hydroxyl group of either serine (Ser) or threonine (Thr) residue, see **Figure 3**.[3]

4
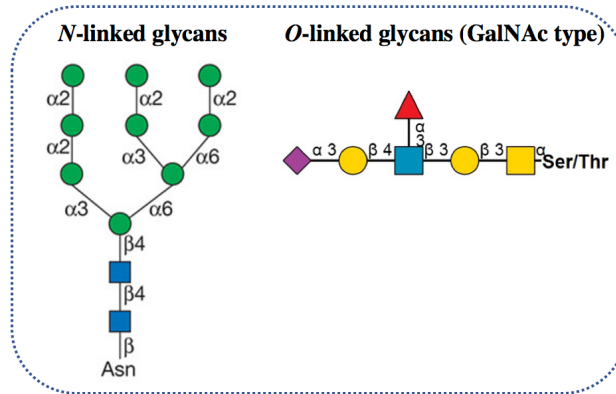
Figure 3. Two main classes of protein glycosylation dominant in mammals.

1.6 GLYCANS CONJUGATED TO CARRIER PROTEINS

The first carrier molecules used for immunogen conjugation were proteins. A foreign protein administered *in vivo* by any one of a number of potential routes nearly assured the elicitation of an immune response. Many proteins can be used as carriers and are chosen based on immunogenicity, solubility, and availability of useful functional groups through which conjugation with the hapten can be achieved.[16] Carrier proteins used to produce the glycoproteins are usually non-toxic, non-reactogenic, homogenous, inexpensive, and stable under standard chemical conditions. They are large and complex and therefore can operate as the initial immunogen, which is an antigen that is capable of inducing an immune response. While, the saccharide is the hapten, which may be bound by Abs, but cannot elicit an immune response. Commonly used carrier proteins are tetanus toxoid (TT; 150 kDa) and diphtheria mutant toxoids (63 kDa) that do not share T-cell epitopes with capsular pathogens, and some commercial functional group-modified proteins, including keyhole limpet hemacyanin (KLH; 350 to 390 kDa), a copper-containing protein found in arthropods and mollusks; (BSA; 67 kDa), a plasma protein in cattle; cationized bovine serum albumin (cBSA), prepared by modifying native BSA with excess ethylenediamine, essentially capping all negatively-charged carboxyl groups with positively-charged primary

amines; and ovalbumin (OVA; 45 kDa), a protein isolated from hen egg whites. These carrier proteins are often modified at their amine-bearing side chains with functional groups such as maleimides, to facilitate easy covalent attachment of molecules.[16]

1.7 IMMUNOGLYCOMICS APPROACH FOR BMKS DEVELOPMENT

Analogous to genomics and proteomics, glycomics represents the systematic methodological elucidation of the "glycome" (the totality of glycan structures) of a given cell type or organism.[3] **Figure 4** illustrates the classic methodology used in immunoglycomics, that generally consists of extracting entire cell types, organs or organisms, then release all the glycan chains from their linkages and, finally identified them by mass spectrometry (left chart); comparison with our explored methodology named reversed immunoglycomics, that is reliable in carbohydrate synthesis based on structural information (right chart).[17, 18]

Immunoglycomics
→
Cultivate the parasites In significant amounts
→
Isolate the glycoconjugates
→
Identification by MS
→
Separate and evaluate

Reversed immunoglycomics
↓
Looking for structural information
↓
Synthesis of partial sugar moiety's that could be immunogenic
↓
Evaluate
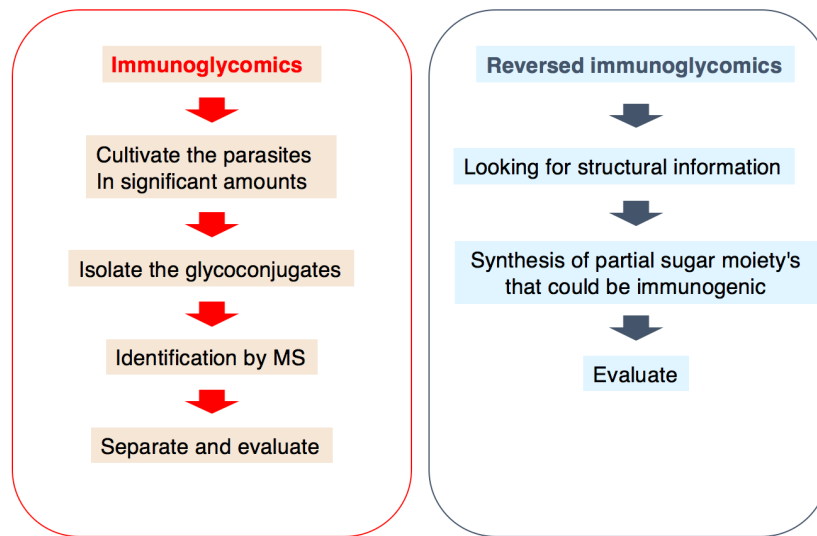
Figure 4. Comparison between immunoglycomics and our reversed immunoglycomics approach.

1.8 CL AND CD GENERALITIES

Protozoa are the most diverse and amongst the most ancient group of organisms in the eukaryotic kingdom. Many of their members are parasitic and some, like those belonging to the family Trypanosomatidae (African trypanosomes, *T. cruzi*, *Leishmania spp.*) and the genera *Plasmodium*, *Eimeria*, *Babesia*, *Theileria*, *Toxoplasma* and *Entamoeba*, are the causative agents of a number of diseases in humans and mammalian animals.[1]

Protozoan parasites of the genus *Leishmania* are members of the family Trypanosomatidae, which infect millions of people worldwide, causing a wide spectrum of diseases collectively termed leishmaniases that vary in their clinical manifestations and symptoms. CL for example, the most common form of the disease is mainly caused by *L. major*, *L. tropica*, and *L. braziliensis*, while *L. donovani* is one of the species that causes life-threatening visceral leishmaniasis[19]. This parasitic disease is endemic in 98 countries and is a public health concern in terms of controlling the transmission reservoirs, for the diagnoses and treatment of the 1 to 2 million patients infected annually. The five major endemic areas are India, Eastern Africa, Brazil, the Mediterranean basin and the Middle East, but the disease is present in all areas favorable to the development of its vector, the sandfly[20]. Leishmaniasis is exclusively transmitted by a blood-sucking of infected female sandflies (Phlebotomus and Lutzomyia), which transmit the parasites into the skin of the host (**Figure 5**). The phenotype of infection depends not only on the parasite species, but also on the immune background of the host, leading to visceral, cutaneous or mucocutaneous leishmaniasis. Even though CL is usually not life-threatening, it causes large disfiguring skin ulcers, often with concomitant secondary infections, mainly by *Staphylococcus aureus[21]*. The skin sores may take months, and in some cases years to heal and often the scarring leads to social stigma. To date, few drugs are available for treatment and all these have significant drawbacks in

terms of cost (liposomal amphotericin B), toxicity (antimonials, miltefosine, and liposomal amphotericin B), teratogenicity (miltefosine) or development of resistance (antimonials, miltefosine, paramomycin)[20]. CL diagnosis usually relies on dermatological examination of the lesion by specialized physicians. Unfortunately, this method fails to detect the disease in a considerable number of patients, because the lesion can closely resemble other skin conditions, such as leprosy or skin cancer. Another way to diagnose the disease is by identifying the parasites using microscopy, but the sensitivity is only ca. 60%. Lastly, PCR is the gold standard of diagnosis, but is often not available or too expensive for clinical laboratories in developing countries and refugee settings. Therefore, an affordable and robust diagnostic tool needs to be developed, allowing for an early and reliable diagnosis, to begin treatment before skin ulcers expand over large areas.
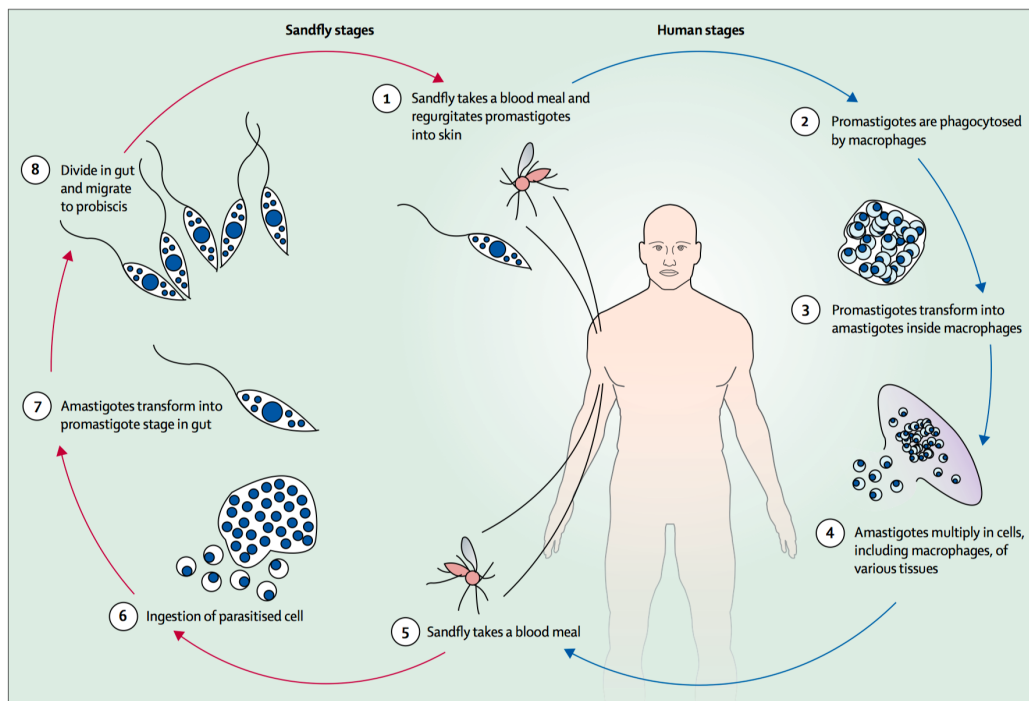
Figure 5. *Leishmania* life cycle. Figure reproduced from reference[22].

CD is a chronic, systemic, parasitic infection caused by the protozoan parasite *T. cruzi*. It is endemic in 21 countries across Latin America, and spreading around the world prevailing in the US, Europe, Australia, New Zealand, and Japan due to the migration of infected individuals into non-endemic regions[23, 24]. Around 6 million people are affected worldwide, and approximately 7000 deaths occur annually, making CD the major cause of death from a parasitic disease in Latin America[25]. *T. cruzi* is transmitted by several routes, including insect-vector transmission (**Figure 6**) and other non-vectorial mechanisms, which include blood transfusion, transplantation, consumption of contaminated foods and fluids, and vertically from mother to infant[26]. CD has effectively an acute and chronic phase (**Figure 7**). As shown, the acute phase lasts up to 2 months, is characterized by elevated parasite load (green) and is usually asymptomatic or unrecognized. *T. cruzi* proliferates actively in the infected individual and invades many host cell types. The host immune system is then activated, resulting in a dramatic reduction in parasite load with subsequent control of the infection. People then enter the so-called chronic phase of the disease, the severity of which (blue) depends on time since infection and host immune status or genetic background. The chronic, symptomatic stage that develops in 10 to 40% of infected patients, often causes cardiomyopathy, megacolon, and megaesophagus, and complications thereof can lead to permanent disability or death. CD can be treated with two old nitro-heterocyclic drugs benznidazole (Abarax/ELEA) and nifurtimox (LAMPIT/Bayer), but they are more effective in the acute phase of the infection. The effectiveness decreases at the chronic phase of the disease[27]. Moreover, the use of these drugs is limited due to their poor bioavailability and side-effects such as allergic dermatitis, pruritus and gastrointestinal manifestations among others[28]. Therefore, early diagnosis is of utmost importance, and there is also a clear need for efficacious and safer drugs and for an effective vaccine, which is not available to date. CD is typically diagnosed by

9

identification of the parasite in the blood using microscopy, or via ELISA using a mixture of purified trypomastigote glycoconjugate and complex epimastigote antigens. However, due to the presence of hundreds or thousands of molecules in the parasite lysate, the assay is not very specific, due to cross-reactivity with heterologous sera (patients with other pathologic conditions or who had been submitted to unrelated immunization procedures)[29]. Another way of diagnosing CD is by direct identification of the parasite's genes via polymerase chain reaction (PCR)[26]. This type of diagnosis is often not available in developing countries, and when the number of circulating parasites is low, the disease may not be detected. A simpler, reliable, affordable, and robust method of diagnosing the disease and for follow up after treatment is needed.
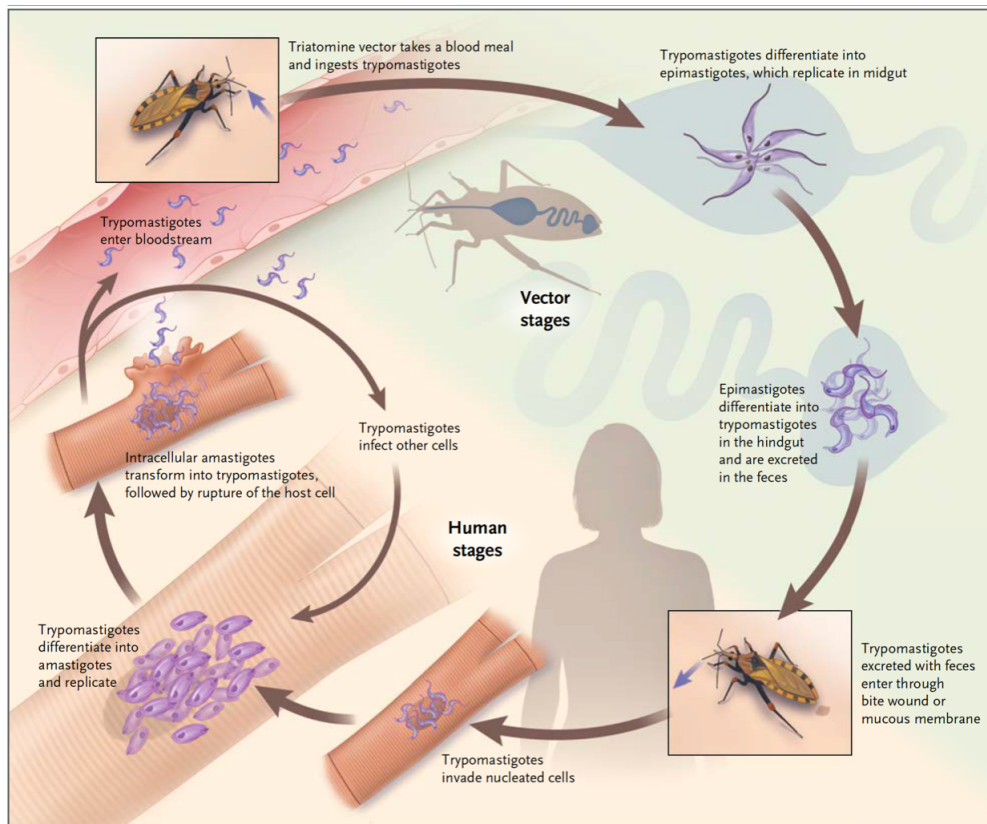
Figure 6. *T. Cruzi* life cycle. Figure reproduced from reference[30].
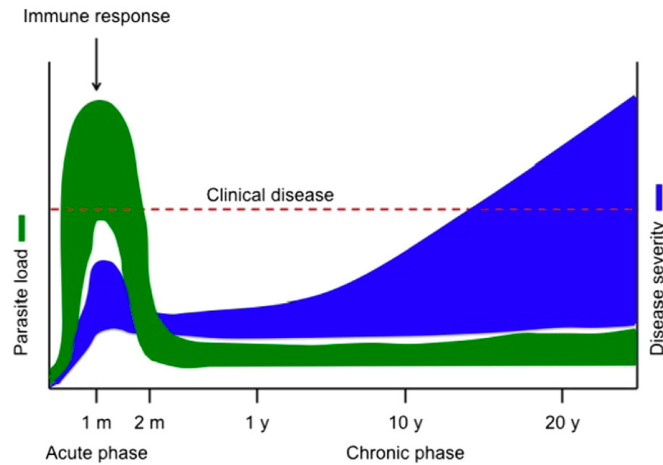
Figure 7. Progression of *T. cruzi* infection over the time; m(months) and y (years)[25].

1.9 THE GLYCOCALYX OF *LEISHMANIA MAJOR* AND *T. CRUZI*

Protozoan parasites, the causative agents of leishmaniasis and CD, exhibit glycoconjugates on the cell surface which frequently play a crucial role in determining parasite survival and infectivity. Many of these molecules are anchored to the plasma membrane via GPI-anchors.

In *Leishmania*, some of these parasitic protozoa, synthesize a number of exotic GPI-related structures, LPGs and GIPLs, which are not covalently linked to protein and which appear to be metabolic end-products[1]. These low-molecular-weight structures are members of the GPI family by virtue of containing the core sequence Man$p$α1,4GlcNα1,6-myo-inositol, but may diverge from the protein anchors beyond this sequence. In several trypanosomatid parasites these glycolipids are the major cellular glycoconjugates[20]. The expression of the LPGs is largely restricted to the promastigote (insect-dwelling) stage where it forms a major component in the densely organized surface glycocalyx. It is present in very low or undetectable levels in the amastigote stage that infects mammalian macrophages. In contrast, the GIPLs are abundant in both major developmental stages of the parasite and are expressed predominantly on the cell surface[1].

11

Most of the GPI and GIPL glycan structures of these parasites are not known, but some of them have been studied and published[1, 31]. For example, it is known that *L. major*, *L. braziliensis* and *L. mexicana* express unusual Gal*p*α1,3Gal*f*β (GIPL-2) and Gal*p*α1,6Gal*p*α1,3Gal*f*β (GIPL-3) moieties attached to the Man*p*α1,3Man*p*α1,4GlcNα trisaccharide, a component that is shared by all GIPLs across all species, see **Figure 8**. They also express LPGs, which contain the same terminal Gal*p*α1,6Gal*p*α1,3Gal*f*β trisaccharide as found in GIPL-3[1]. Furthermore, *L. major* GIPL-1 has a terminal Gal*f*β1,3Man*p*α, which lacks the Gal*p*α moiety.

Most likely, *T. cruzi* contains similar furanoid Gal*f*β residues in its GPIs, like GIPL-1 identified in *L. major*, or possibly elongated with pyranoid Gal*p*α residues, similarly to GIPL-2 and GIPL-3 of *L. major*, *L. braziliensis* and *L. mexicana*. It is believed that in *T. cruzi* several furanoid Gal*f*β residues are directly attached to the GPIs' mannose-rich core saccharide, because treatment with hydrofluoric acid causes the loss of four galactose units [32]. This is indicative of the existence of galactosides in their furanoid form, because it is well known that Gal*f*β glycosides easily hydrolyze under these conditions [33], while the glycosidic linkages of pyranoid galactosides remain stable.

The biological role of Gal*f*β residues (formed in nature by ring contraction of UDP-Gal*p* to UDP-Gal*f*, catalyzed by the enzyme UDP-Gal*p* mutase)[34] is not known. One intriguing hypothesis is that terminal Gal*f*β residues play a central role in the survival of parasites by blocking action of the host's glycosidases against glycoconjugates of the parasites. On the other hand, Gal*f*β may function as a strong immunogen. The absence of Gal*f*β and galactofuranosidases in mammalian host cells makes these molecules potentially useful as specific targets for therapy of parasitic diseases[35].
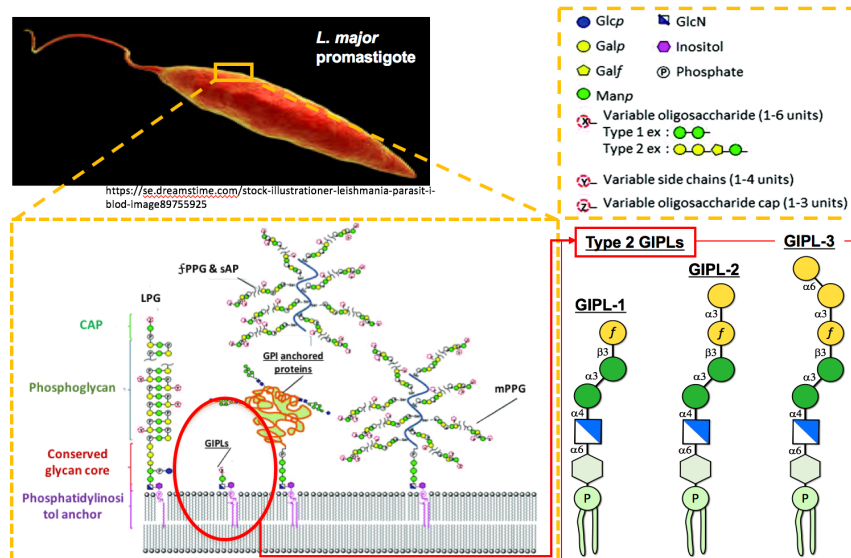
Figure 8. Schematic representation of *Leishmania* surface glycoconjugates: LPG, GIPLs, Glycoproteins (e.g., GP63, sAP), and Proteophosphoglycan (PPG).[20]

The plasma membrane of infective trypomastigote forms of the protozoan parasite *T. cruzi*, is covered by a dense coat of GPI-anchored glycoproteins, including tGPI-MUC, mucin-associated-surface proteins (MASP), and *trans*-sialidases (TS), see **Figure 9** [14, 36-38]. In particular, the highly abundant tGPI-mucins display *O*-glycans containing terminal, nonreducing α-galactosyl (α-Gal) glycotopes, which are absent in human tissues and are therefore highly immunogenic to humans [39-41]. Approximately 10% of these *O*-glycans are comprised of a single immunodominant linear trisaccharide, Galα1,3Galβ1,4GlcNAcα (Galα3LNα), whereas the remaining 90% of the *O*-glycans are branched α-Gal-containing oligosaccharides with as-yet uncharacterized structures [39]. CD patients produce considerable amounts of protective anti-α-Gal antibodies directed to α-Gal glycotopes on tGPI-mucins, in both the acute and chronic phases of the disease [2, 29, 39, 42, 43].

To date, the unique glycostructures of GPIs, which differ from the *O*-glycans of the parasitic cell surface glycoproteins, have never been explored as BMKs. Since the GIPLs and

13

tGPI-MUC of the cell surfaces of the parasites contain sugars that are foreign to humans, they are expected to be highly immunogenic[1, 29, 35, 44], and should therefore be exploitable as BMKs for the diagnosis of leishmaniasis and CD via CL-ELISA[29].
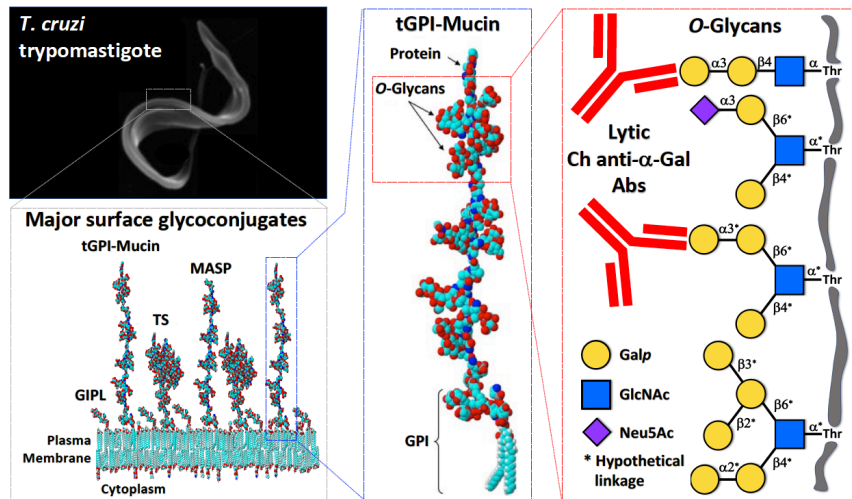
Figure 9. Schematic representation of the *T. cruzi* trypomastigote surface coat. GIPLs and GPI-APs (tGPI-MUC, TS, and MASP). Figure taken from[15]

In this research project, we *hypothesize* that Gal*fα* and/or Gal*pβ* -containing glycans, which are known to exist in the glycolipids of the *L. major* cell surface, cause a strong immune response in CL patients, and that immunodominant glycotopes can be identified and exploited as BMKs for accurate disease diagnosis. We hypothesize further that some of these glycans resemble partial structures of *T. cruzi* glycans, and that these glycans as well as terminal and branched oligosaccharides expressed in tGPI-MUC will have a strong serological response in CD patients, and that these glycans may be used as BMKs for CD.

We believe that using synthetic, well-defined parasitic glycotopes as BMKs may give more reliable data for disease diagnosis and chemotherapy follow-up studies than conventional

14

serology, which uses crude antigenic preparations, which suffers from antibody cross-reactivities[29].

2.0 SPECIFIC AIMS

To address the hypothesis raised above, we propose the following specific aims:

2.1 Specific Aim 1.

▪ To synthesize five α-Gal*p* and β-Gal*f*-containing glycans, which are the terminal saccharides found in type-2 GIPLs of *L. majo*r.

▪ To synthesize two α-Gal*p* and β-Gal*f*-containing oligosaccharides present in the GIPLs and tGPI-MUC of *T. cruzi*

▪ To conjugate the synthetic glycans to BSA using maleimide-thiol chemistry giving NGPs **1-7** needed for CL –ELISA with patient sera.

2.2 Specific Aim 2.

▪ To evaluate whether patients with active CL lesions or CD have IgG Abs that recognize the synthetic glycotopes by CL-ELISA, using a glycoarray consisting of the NGPs **1-7** and various controls. Furthermore, evaluate changes in the Ab levels after chemotherapy for CD.

The CL-ELISA with sera of patients with Old- and new-world CL and CD before and after chemotherapy was conducted in Dr. Almeida's (UTEP) and in Dr. Acosta-Serrano's (Liverpool School of Tropical Medicine) laboratories.

15

Chapter 2: Discovery of Glycan-Based Biomarkers for CL caused by *L. major*

2.1 ABSTRACT

CL is a widespread vector-borne disease caused by protozoan parasites of the genus *Leishmania*. In the Old World, *L. major* and *L. tropica* are the prevailing CL-causing species. Diagnosing CL accurately is challenging because the skin lesions resemble other dermatological conditions, and no specific CL BMK exists. Based on GIPLs, abundant on the *L. major* cell surface, we have developed syntheses for three neoglycoproteins that contain terminal, nonreducing partial glycan structures of these GIPLs, which were probed for their antigenicity by immunoassay using sera from CL patients. This approach identified Gal*p*α1,3Gal*f*β and Gal*p*α1,3Gal*f*β1,3Man*p*α as diagnostic BMKs for *L. major* infections, distinguishable from *L. tropica* infections and heterologous diseases, respectively. These findings are particularly relevant for diagnosing *L. major* infections in areas of large population displacement originating from the Middle East.

2.2 INTRODUCTION

CL is an emerging vector-borne infectious disease, caused by different species of the protozoan parasite *Leishmania*, and is transmitted by infected female sandflies.[45] It is endemic to the Americas, the Mediterranean basin, the Middle East and Central Asia, and it currently affects approximately 12 million people worldwide.[46] CL is usually not life-threatening, but it causes large disfiguring skin ulcers, often associated with secondary infections, that may take months, and in some cases years to heal, and the scarring often leads to social stigma. Furthermore, inadequate treatment of CL may lead to satellite lesions, or nodular lymphangitis.[45] In the absence of a CL protective vaccine, the only feasible way to control the disease is through chemotherapy,

16

most commonly pentavalent antimonials like sodium stibogluconate (also known as SbV). SbV is one of the most affordable drugs for CL,[47] but it is associated with significant side effects, and drug resistance has developed in some regions.[48] Alternative drugs include miltefosine, amphotericin B, liposomal amphotericin B, and pentamidine.[49] However, CL treatment responses vary depending on the infecting parasite species.[50] In Northern Africa and the Middle East, the two predominating CL-causing *Leishmania spp*. are *L. major* and *L. tropica*,[51] each predominating in certain areas. While azole-based drugs (fluconazole, ketoconazole, and itraconazole),[52] and azithromycin,[53] meglumine antimoniate,[54] and miltefosine[54, 55] are effective for CL caused by *L. major*, they are less effective for treating CL caused by *L. tropica*. On the other hand, the imiquimod analog EAPB0503 (1-(3-methoxyphenyl)-*N*-methylimidazo[1,2-a]quinoxalin-4-amine) proved to be efficient against *L. tropica*, but it is inefficient against *L. major*.[56] This underscores the need for species-specific diagnoses.

The current conflict in the Middle East, particularly in Syria, Afghanistan, and Iraq has resulted in a massive displacement of potentially infected individuals. Many refugees moved into regions where different *Leishmania spp*. may be endemic than in the areas of their origin, which complicates the diagnosis by local physicians and can impede treatment. In the last decade, a sharp increase in imported CL cases has been reported in countries of Western Europe due to returning military personnel, labor immigration from endemic zones, and an increased refugee population from the Middle East.[57, 58] In these countries, many physicians have limited experience with CL, hence belated diagnoses and inappropriate treatment have occurred.[58-61]

In the absence of a diagnostic biomarker (BMK), CL is commonly diagnosed by inspection of skin lesions by specialized dermatologists,[21] but unfortunately, the lesions closely resemble other skin conditions, such as skin cancer, sporotrichosis, chromomycosis, lobomycosis, syphilis,

17

and leprosy.[60] Different microscopic and serological methods have been utilized for the identification of *Leishmania* amastigotes, however, with limited sensitivities, and without the ability to differentiate between *Leishmania* species.[45, 62] Polymerase Chain Reaction (PCR) has an extraordinary sensitivity and specificity, [59, 63, 64] but it is an expensive, technologically demanding, and slow assay that is often not available in clinical laboratories in developing countries.[21, 64] There is a pressing need for the development of alternative robust and affordable diagnostic tools for the accurate and fast diagnosis of CL suitable for field hospitals and refugee settings. In addition, the differentiation of different *Leishmania spp.* is a priority, in order to inform best drug treatment regimens.

The glycocalyx of *Leishmania* parasites is predominantly composed of low-molecular mass GIPLs, as well as LPGs and GPI-anchored proteins.[1, 20, 65, 66] *L. major* synthesizes highly abundant Type-2 GIPLs (GIPL-1, GIPL-2, and GIPL-3), which contain unusual α-Gal*p* and β-Gal*f* residues at their non-reducing ends (**Figure 10**).[1] There is considerable evidence that these glycoconjugates are highly immunogenic in mammalian hosts.[1, 67-69] On the other hand, the main GIPLs of *L. tropica* belong to the α-mannose terminating GIPLs iM2, iM3, and iM4.[65] We hypothesized that terminal oligosaccharide partial structures of the GIPLs of *L. major* may be immunodominant glycotopes that are serologically exploitable as diagnostic BMKs specifically for CL caused by *L. major*, and distinguishable from CL caused by *L. tropica*. To address this hypothesis, specific *L. major*-derived glycan partial structures needed to be synthesized and immunologically evaluated.

18
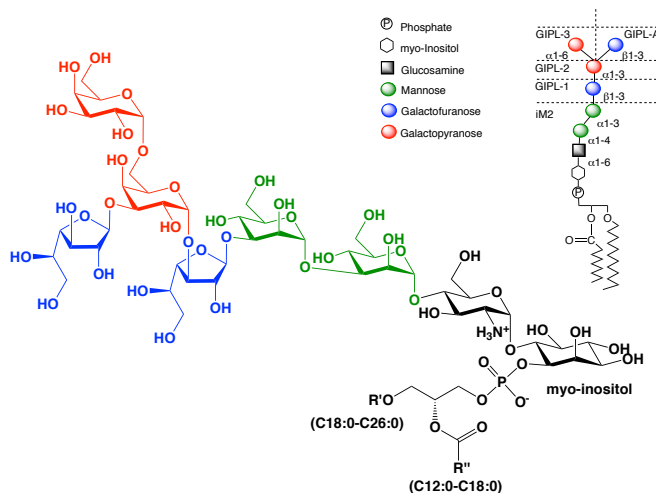
Figure 10. Chemical structure of type-2 GIPLs enriched in galactose in both pyranose and furanose forms described by Ferguson and coworkers.[1]

Here we present reversed immunoglycomics as a combined chemical and serological approach to discover specific glycan BMKs suitable for the diagnosis of *L. major* infection and for the distinction from *L. tropica* infection using synthetic cell surface glycans of the parasite. Instead of isolating glycoconjugates of cultivated parasites and studying their glycoimmunology, we have reversed this classical immunoglycomics approach by probing synthetic partial structures of known cell surface glycans for antibody responses by CL-ELISA. Our previous work showed that the sera of CL patients from Saudi Arabia contain elevated levels of IgG anti-α-Gal Abs,[44] that partially recognize simple α-Gal-containing saccharides, but a specific α-Gal biomarker remained elusive.[70] Therefore, we shifted our focus to α-galactopyranose and β-galactofuranose containing saccharides of the terminal glycan portions of Type-2 GIPLs of *L. major*. The synthesis of a terminal trisaccharide of Type-2 GIPLs and a heptasaccharide present in LPGs of *Leishmania* parasites has been reported.[71] Here we have developed original syntheses for three Type-2 GIPL partial structures with a chemical handle at the reducing end allowing for conjugation. Specifically, mercaptopropyl glycosides of the GIPL-2 derived glycans Gal*p*α1,3Gal*f*β (**G27**) and

19

Galpα1,3Galfβ1,3Manpα (**G30**); as well as the GIPL-3 derived glycan Galpα1,6Galpα1,3Galfβ (**G28**) were synthesized (**Figure 11**). Conjugation of these oligosaccharides to BSA produced NGPs, which, unlike the oligosaccharides by themselves, adhere effectively to microtiter plates. These NGPs served as antigens in CL-ELISA[29, 44] using the sera of CL patients from Saudi Arabia with confirmed *L. major* or *L. tropica* infections.
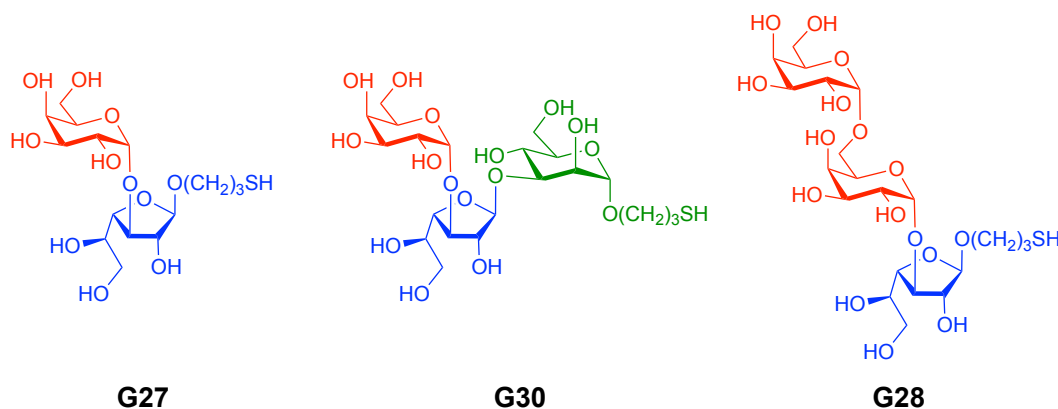
Figure 11. Target mercaptopropyl glycosides of Galpα1,3Galfβ (**G27**), Galpα1,3Galfβ1,3Manα (**G30**), and Galpα1,6Galpα1,3Galfβ (**G28**) derived from GIPL-2 and GIPL-3 of *L. major*.

2.3 RESULTS AND DISCUSSION

2.3.1 Synthesis of NGP27b, NGP28b, and NGP30b

Our synthetic strategy for all three oligosaccharides **G27**, **G28**, and **G30** relied on a) the stereoselective α-galactosylation using Kiso's 4:6-di-*tert*-butylsilylidene-galactosyl trichloroacetimidate donor **3**;[72-74] b) an orthogonal protecting group strategy primarily based on acyl, acetal, and silyl groups, and c) the use of mercaptopropyl glycosides for the conjugation to maleimide-derivatized BSA.[17, 75] The synthesis of GIPL-3 derived trisaccharide **G28** also

included an unprecedented regioselective ring opening of the 4,6-*O*-di-*tert*-butylsilylidene moiety to gain access to a disaccharide acceptor in a single step.

The synthesis of the three target oligosaccharides **G27**, **G28**, and **G30** started with the preparation of the monosaccharide building blocks **1**,[76] **2**,[77-79] and **3**.[72, 80] In order to construct thiopropyl α-D-galactopyranosyl-(1→3)-β-D-galactofuranoside **G27** (**Scheme 1**), Galβ*f* acceptor **1** was glycosylated with Galα*p* donor **3**[72-74] to furnished the fully protected disaccharide **4** in 65% yield. The silylidene and isopropylidene protecting groups were removed using HF·pyridine complex in 88% yield, and aqueous trifluoroacetic acid (TFA) in 77% yield, respectively, to afford **6**. Radical addition of thioacetic acid (AcSH) to the allyl glycoside **6** in dry THF furnished the thioester **7** in 85% yield. Complete deacylation under Zemplén conditions afforded the target disaccharide **G27** quantitatively, which oxidized to disulfide **14**. Upon reduction with TCEP·HCl and conjugation to commercial maleimide-derivatized BSA **15**, **NGP27b** was obtained (**Scheme 2**).

The trisaccharide thiopropyl α-D-galactopyranosyl-(1→3)-β-D-galactofuranosyl-(1→3)-β-D-manopyranoside **G30** was synthesized by two consecutive glycosylations. First, the Galβ*f* acceptor **2**[77-79] was stereoselectively glycosylated with Galα*p* donor **3**[72-74] to produce disaccharide **5** in 67% yield. This donor was used to glycosylate mannosyl acceptor **8**[81] to yield trisaccharide **9** in 47% yield. Afterwards, the silylidene protecting group was removed with HF·pyridine complex, and without purification, both acetal groups were removed by acid catalyzed hydrolysis in 48% yield over two steps. Radical addition of AcSH to the allyl glycoside was achieved in 85% yield. Finally, global removal of all ester groups under Zemplén conditions furnished the desired trisaccharide **G30** quantitatively (**Scheme 1**), which oxidized to disulfide **16**. Upon reduction of **16** and conjugation to maleimide-derivatized BSA **15**, **NGP30b** was obtained (**Scheme 2**).

21

The trisaccharide mercaptopropyl α-D-galactopyranosyl-(1→6)-α-D-galactopyranosyl-(1→3)-β-D-galactofuranoside **G28** was synthesized from disaccharide **4**, which needed to be converted into a suitable acceptor. Instead of a deprotection-reprotection procedure we had the idea to explore a regioselective ring opening of the 4,6-*O*-DTBS group. Based on the known regioselective ring opening of a 3,5-O-DTBS group of a galactofuranoside, this should be accomplishable with tetrabutylammonium fluoride (TBAF).[82] However, the 4,6-O-DTBS group of a galactopyranoside resist reaction via TBAF, even when applied in large access. We found that a novel regioselective ring opening of the 4,6-*O*-DTBS group can be accomplished with HF·pyridine complex at 0°C. Thus, treatment of **4** with 1.2 equiv. HF·pyridine complex exclusively deprotected OH-6 and afforded glycosyl acceptor **11** with a 4-*O*-di-*tert*-butylfluorosilyl ether in 60% yield. One concern was that the bulky silyl group at position 4 could potentially hinder the glycosylation at OH-6, however, to our delight, donor **3**[72-74] was able to glycosylate acceptor **11** to provide the fully protected trisaccharide **12**, with an exclusive α-stereoselectivity in an acceptable yield of 50%. Since acceptor **11** was completely consumed, we looked into the formation of any byproducts and identified the benzoylated disaccharide **20**, which was a minor, but prominent component the product mixture. This finding suggests that acceptor **11** undergoes two competing reactions, i.e., a) the desired glycosylation to produce trisaccharide **12**, and b) a transesterification, presumably via orthoester **19** to give benzoate **20** (**Figure 12**). While orthoesters are known glycosyl donors to yield 1,2-trans glycosides,[83] such a path is not expected to be available for the putative orthoester **19**. Like in Kiso donor **3**[72-74], the presence of the 4,6-DTBS would be expected prevent any nucleophilic attack from the β-side. The silylidene and isopropylidene protecting groups of trisaccharide **12** were removed in 91 and 90% yield, respectively. The thioester derivative was then prepared by radical addition of AcSH in 93% yield.

22

Global deprotection under Zemplén conditions furnished the target mercaptopropyl trisaccharide **G28** quantitatively (**Scheme 1**), which oxidized to disulfide **17**. Reduction and conjugation to maleimide derivatized BSA **15** afforded **NGP28b** (**Scheme 2**).
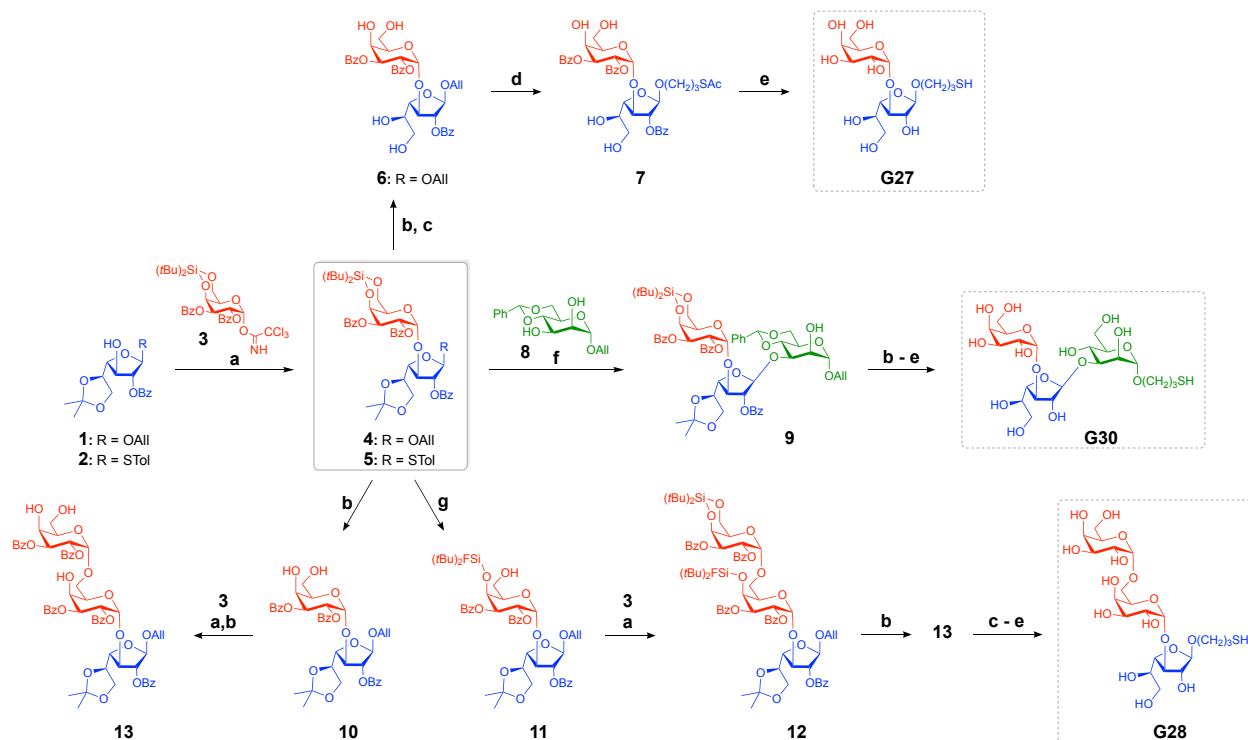
Scheme 1. Synthesis of mercaptopropyl glycosides **G27**, **G28** and **G30**.

a) TMS-OTf, DCM, 0 °C to rt, 1 h, MS 4 Å (50-67%); **b**) HF·pyridine, THF, 0 °C then rt, 1 h (70-91%); **c**) TFA/H$_2$0/DCM 1:1:10, rt, 15 min (70-90%); **d**) AcSH, AIBN, THF, UV light (350 nm), 6-12 h (85-93%); **e**) NaOMe, MeOH, rt, 2 h (quant.); **f**) NIS, AgOTf, DCM, 0 °C to rt, 45 min, MS 4 Å (47%), and **g**) HF·pyridine, THF, 0 °C, 2 h (60%).
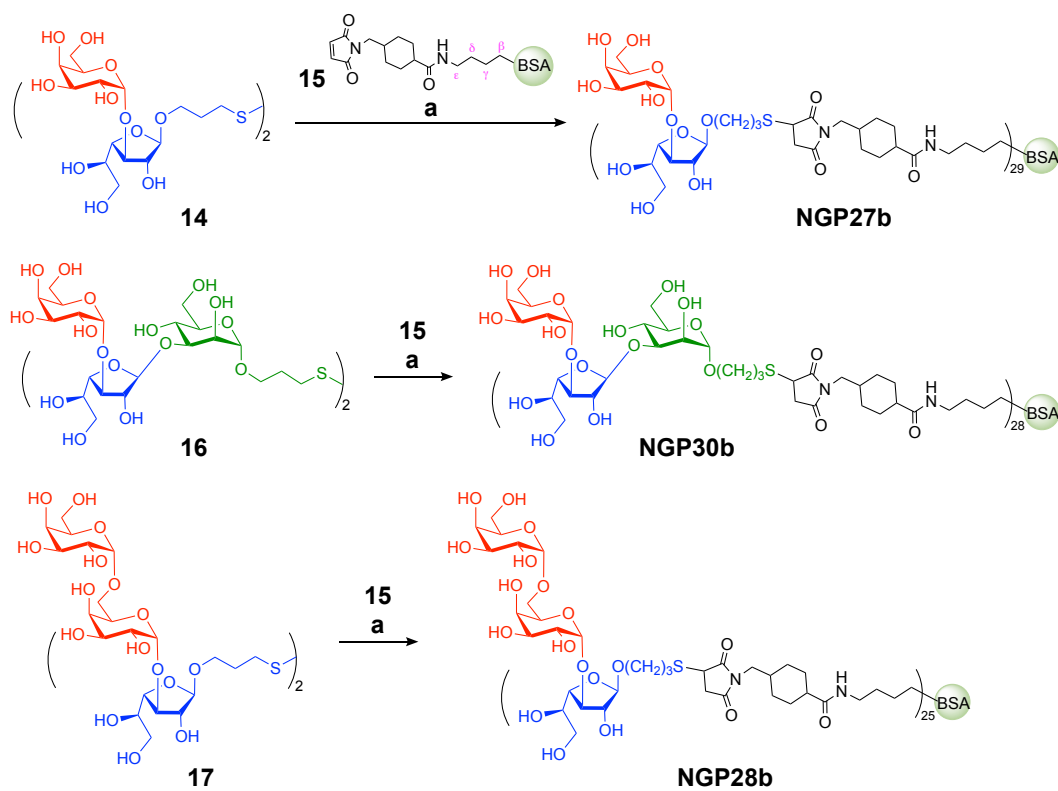
Scheme 2. Conjugation of glycans and maleimide derivatized BSA **15** to produce NGPs.

a) TCEP·HCl, phosphate buffer pH 7.2, rt, 2 h. The average number of glycans per BSA molecule was determined by matrix assisted laser desorption ionization-time of flight (MALDI-TOF) mass spectrometry.
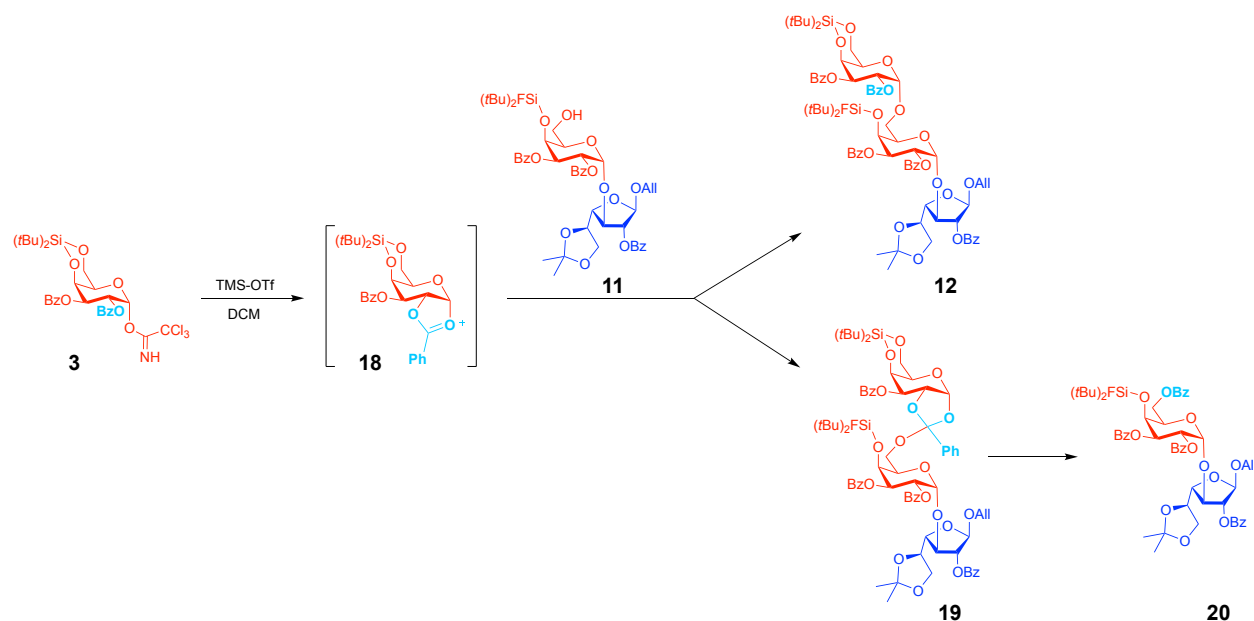
Scheme 3. Proposed mechanism for the obtention of byproduct **20** formed in the synthesis of trisaccharide **12**, likely via putative orthoester **19** (not isolated or observed).

2.3.2 Evaluation of NGP27b, NGP28b, and NGP30b as potential BMKs for Old World CL

With the NGP antigens in hand, IgG antibody responses of CL patient sera with acute *L. major* or *L. tropica* infection, confirmed by PCR, could now be studied by CL-ELISA. The patient sera had been collected from 81 individuals with active *L. major* and 15 individuals with active *L. tropica,* from Saudi Arabia, where *L. major* and *L. tropica* infections are endemic. In addition, pooled sera of 10 healthy individuals, designated NHS, as well as sera from 25 individuals with heterologous diseases from Saudi Arabia were also integrated in the study.

The heterologous sera are from patients who have skin conditions other than cutaneous leishmaniasis. Therefore, these sera represent a real-life, non-CL negative control group, relevant to what a physician may encounter, from which a useful CL biomarker must be able to distinguish. Since all NHS contains anti-α-Gal antibodies directed against α-Gal-containing lipopolysaccharides of Gram-negative enterobacteria, a small amount of cross-reactivity between

25

NHS anti-α-Gal antibodies and the *L. major*-derived glycostructures might be expected, as previously observed with purified *L. major* GIPL-1, -2, and -3.[69] In order to ensure that CL-ELISA responses were not a result of antibody binding to BSA or the crosslinker, 2-MEb, obtained by conjugating 2-mercaptoethanol (2-ME) to maleimide-derivatized BSA **15**, was used as a negative control antigen. In order to identify a suitable protocol for the CL-ELISA, serum pools were prepared and cross-titrated against different concentrations [ng/well] of the three NGPs and 2-MEb. **Figure 12** shows that the *L. major* serum pool exhibited a strong IgG antibody reactivity to NGP27b, NGP28b, and NGP30b, at different dilutions, whereas the *L. tropica* and NHS (healthy) serum pools showed significantly lower antibody reactivity. The cross-titration experiment revealed that a serum dilution of 1:800 and an antigen loading of 25 ng/well exhibited the highest differential antibody reactivity between *L. major*-positive serum pool and serum pools from *L. tropica*-positive or healthy individuals. Under these conditions, the reactivity ratios between *L. major* and healthy serum pools were ~6-, ~9-, and ~56-fold for NGP27b, NGP28b, and NGP30b, respectively. Comparing *L. major* vs. *L. tropica*, the reactivity ratios were ~90-, ~9-, and ~16-fold for NGP27b, NGP28b, and NGP30b, respectively. As expected, the negative control 2-MEb showed no or little reactivity with all pooled sera, indicating that no significant antibody binding occurred to BSA or the crosslinker (**Figure 12**).

Next, NGP27b, NGP28b, and NGP30b were put to a test as potential BMKs for the accurate diagnosis of *L. major* infections, and in particular differentiating these from heterologous diseases, which is a major issue in clinical settings in some endemic and nonendemic regions, where there is a high migration of CL patients from affected areas. Second, we evaluated these NGPs for their utility for distinguishing *L. major* from *L. tropica* infections, which is another challenge in similar clinical settings. To that end, we assessed the three NGPs by CL-ELISA, using conditions

previously established (**Figure 12**). We assayed individual sera from CL patients chronically infected with *L. major* (n = 81) or *L. tropica* (n = 15), or patients with heterologous diseases (n = 24) (**Table 2**). We initially used a CL-ELISA titer cutoff of 1.000, which was determined in each immunoassay microplate by using a pool of negative control sera (healthy individuals from Saudi Arabia, n = 10), in duplicate or triplicate, as described in detail in the experimental section (CL-ELISA). Our data showed that NGP27b diagnosed as positive 77/81 (sensitivity = 95.3 %) of the sera from patients with *L. major* infection, previously confirmed by dermatological examination and laboratory assays (lesion aspirate microscopy and *ITS*1-PCR RFLP) [84] (Cohort description, Experimental Section) (**Figure 13; Table 3**). On the other hand, NGP28b and NGP30b diagnosed as *L. major*-positive 70/81 and 73/81 (sensitivity = 88.0% and 91.0%), respectively. We also evaluated the three NGPs for specificity by comparing sera from *L. major* infections with sera from heterologous diseases or *L. tropica* infections. When we assessed *L. major*-positive sera vs. sera from heterologous diseases, NGP27b, NGP28b and NGP30b exhibited a specificity of 82.8, 80.0, and 80.0%, respectively (**Figure 13; Table 3**). When we compared *L. major*-positive vs. *L. tropica*-positive sera, we found that NGP27b, NGP28b and NGP30b showed a specificity of 93.8, 88.2 and 79.0%, respectively (**Figure 13; Table 4**). No or little reactivity of *L. major*, *L. tropica*, or heterologous sera was observed with the negative control antigen (2-MEb), strongly indicating that the antibody reactivity of all tested sera to the linker or the BSA carrier protein was negligible (**Figure 16**).

To compare the usefulness of the three NGPs for correctly discriminating true-positive from false-positive results, at various threshold (cutoff) values, we plotted receiver operating characteristic (ROC) curves (**Figure 14**). The area under the curve (AUC) values of the ROC curves for NGP27b (0.9421), NGP28b (0.9216), and NGP30b (0.9159), in the comparison of

serum samples from *L. major* infections vs. heterologous diseases, indicated that NGP27b exhibited higher sensitivity and specificity than NGP28b and NGP30b (**Figure 14, top graphs; Table 5**). In the comparison of serum samples from *L. major* vs. *L. tropica* infections, the AUC values for NGP27b (0.9757), NGP28b (0.9280), and NGP30b (0.8951), indicated the same trend (**Figure 14, bottom graphs; Table 6**). Taken together, our data indicated that NGP27b showed a higher sensitivity and specificity than NGP28b and NGP30b, being therefore a more suitable candidate to be pursued as a potential BMK for correctly diagnosing CL infections caused by *L. major* and differentiating those from heterologous diseases and *L. tropica* infections.

Next, to fine-tune the initial cutoff value for each NGP, we performed a two-graph ROC (TG-ROC) analysis by plotting the ROC data (**Figure 14**) for sensitivity (Se) and specificity (Sp) as a function of the cutoff value, as described by Greiner et al.[85] (**Figure 15**). The selection of the cutoff value is always a balance between sensitivity and specificity, and it depends on the context in which the diagnostic BMK is to be applied. Since CL caused by *L. major* or *L. tropica* in endemic countries like Saudi Arabia, where little geographical overlap of the two infections exists, the utility of a new diagnostic BMK test is not a high priority. However, in areas where *L. major* and *L. tropica* infections coexist, for instance in conflict-affected countries (e.g., Afghanistan, Syria, Lebanon) [86] and nonendemic regions (e.g., Europe), with high migration from affected areas, [87] there is an urgent need for new diagnostic BMKs that could accurately diagnose and discriminate CL caused by different *Leishmania* species. In this context, a high specificity is preferred over high sensitivity for any potential new diagnostic BMK for CL.[85] When comparing *L. major* infections vs. heterologous diseases, an adjusted titer cutoff value for NGP27b of 1.140 (instead of 1.000) slightly decreased sensitivity (94.2%), but increased specificity to 85.7% (from 82.8%). When comparing *L. major* infections vs. *L. tropica* infections, we noticed that an adjusted

titer cutoff value for NGP27b of 1.045 afforded a perfect specificity (100%), while maintaining a high sensitivity (95.3%). For NGP28b, in the comparison of *L. major* infections vs. heterologous diseases, an adjusted titer cutoff value of 1.600 gave a lower sensitivity of 83.5% (from 88%), while the specificity considerably improved to 92.3% (from 80%). Nevertheless, when comparing *L. major* vs. *L. tropica* infections, we found that the original NGP28b titer cutoff value of 1.000 could not be significantly improved without drastically affecting the sensitivity. Finally, for NGP30b, when we compared *L. major* infections vs. heterologous diseases, an adjusted titer cutoff value of 1.465 gave a sensitivity of 88% (from 91%), but significantly increased the specificity to 100% (from 80%). When comparing *L. major* vs. *L. tropica* infections with NGP30b, the same adjusted titer cutoff value of 1.465 gave a sensitivity of 88% (from 91%), but significantly increased the specificity to 93.8% (from 79%).

Based on the TG-ROC data with the adjusted titer cutoff values we can propose an algorithm with the two NGPs that exhibited the best outcomes in terms of sensitivity and specificity, i.e., NGP27b and NGP30b, to consecutively screen sera from patients who could be infected with either *L. major* or *L. tropica*, or affected with confounding, non-CL dermatological condition(s). An algorithm to discriminate between these disease states is illustrated in **Figure 17.** First, the serum would be screened by CL-ELISA with NGP27b. A positive result would indicate *L. major* infection or heterologous disease, whereas a negative result would indicate *L. tropica* infection or heterologous disease. A sample with a positive result would undergo a second CL-ELISA with NGP30b to discriminate between *L. major* infection and heterologous disease. Although all three NGPs exhibited similar trends regarding their immunoreactivity with *L. major* sera, on average NGP30b showed titers about twice as high as those of NGP27b and NGP28b.

29

This could be explained by the fact that NGP30b contains a larger portion of the glycotope of type-II GIPL-2, which has been shown to be strongly recognized by sera from *L. major* patients.[68]

Regardless the NGP tested, we observed a small cross-reactivity with sera from *L. tropica* infections and heterologous diseases. A plausible explanation for such a cross-reactivity could be the presence of natural anti-α-Gal antibodies abundantly present in the serum of all individuals, as reported by Galili et al.[88] These antibodies cross-react with the so called Galili epitope (Galα1,3Galβ1,4GlcNAc-R) and other glycans containing terminal nonreducing α-Gal epitopes, in particular melibiose (Galα1,6Glc).[12, 17, 18, 42, 70, 75] In fact, both the Galili trisaccharide and melibiose are regularly used for the purification of natural anti-α-Gal antibodies,[42, 89] which could explain at least in part the cross-reactivity observed here with NGP27b (Galα1,3Gal$f\beta$-BSA) and NGP30b (Galα1,3Gal$f\beta$1,3Manα-BSA), and NGP28b (Galα1,6Galα1,3Gal$f\beta$-BSA), which contain terminal α-Gal residue with the same linkages as observed in the Galili epitope and melibiose.

30
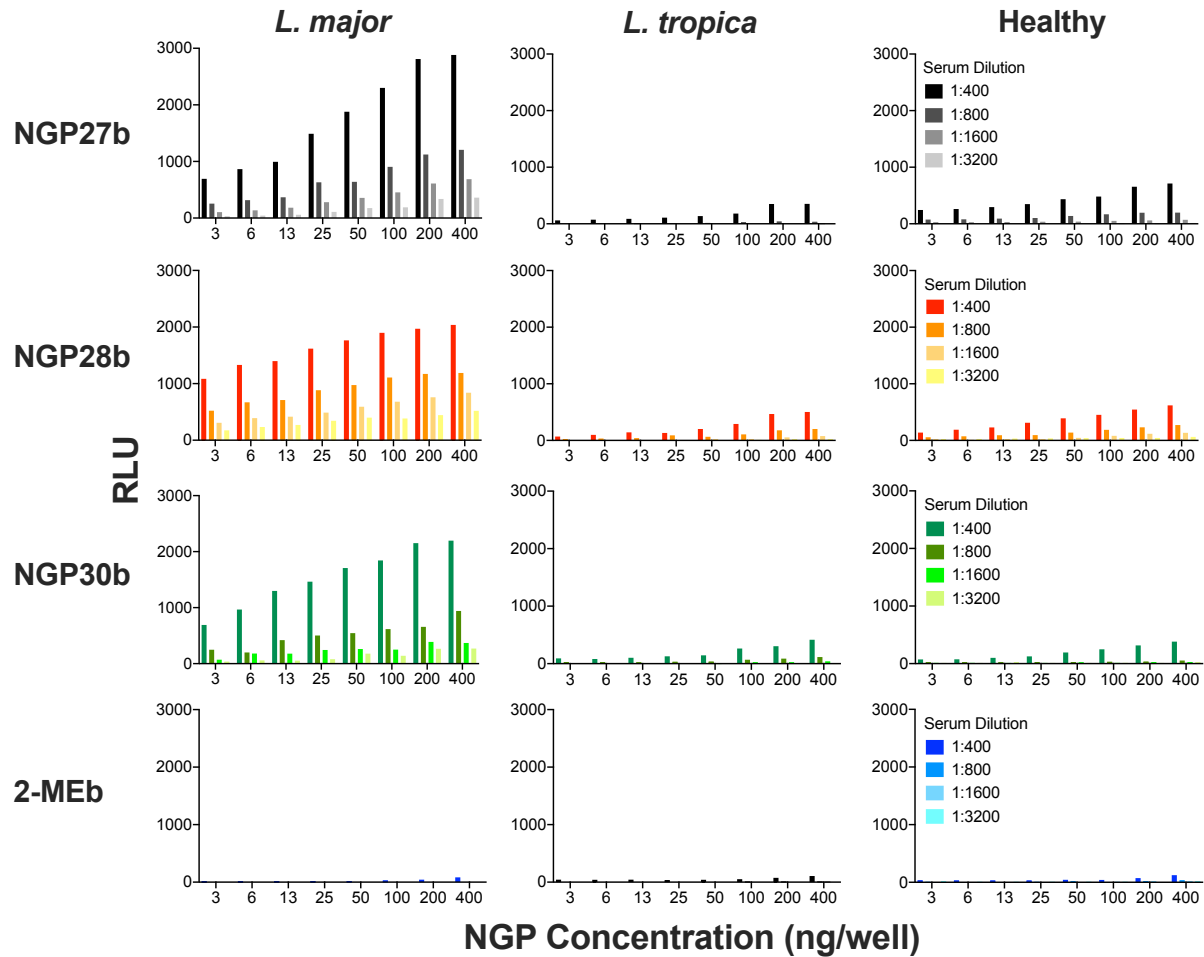
Figure 12. Antigen/serum titrations of **NGP27b**, **NGP28b**, and **NGP30b** as well as **2-ME-BSA** with pools of patient sera with active *L. major*, or *L. tropica* infection, or pooled sera of healthy individuals from **the Kingdom of Saudi Arabia (KSA)**.
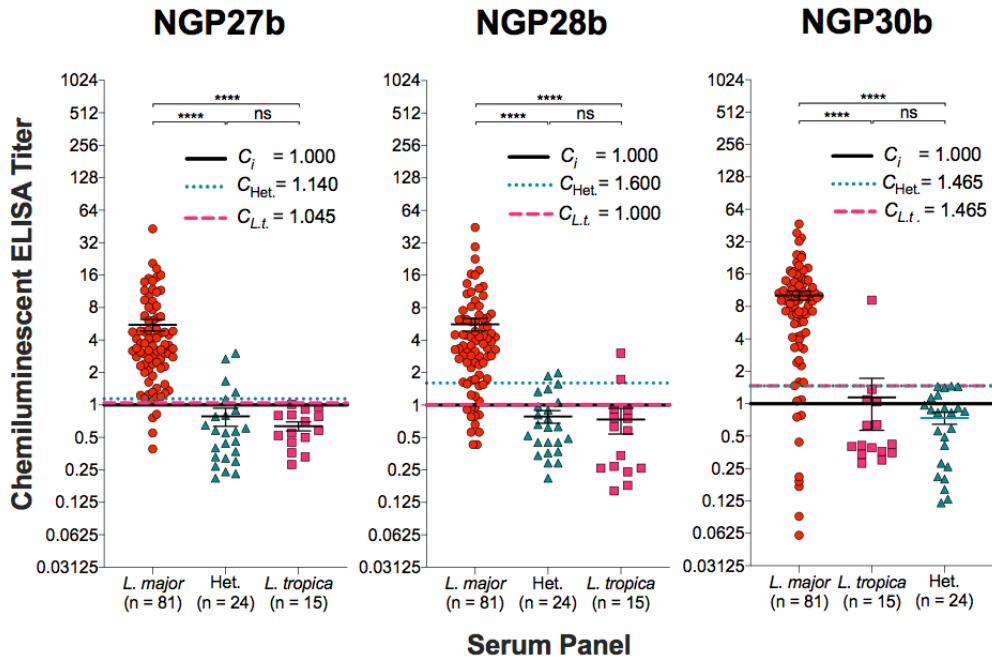
Figure 13. CL-ELISA reactivity of sera from individual patients with active *L. major*, or *L. tropica* infection, or heterologous patients at a sera dilution of 1:800 against **NGP27b**, **NGP28b**, and **NGP30b** (25 ng/well). Relative Luminescence Units (RLU).
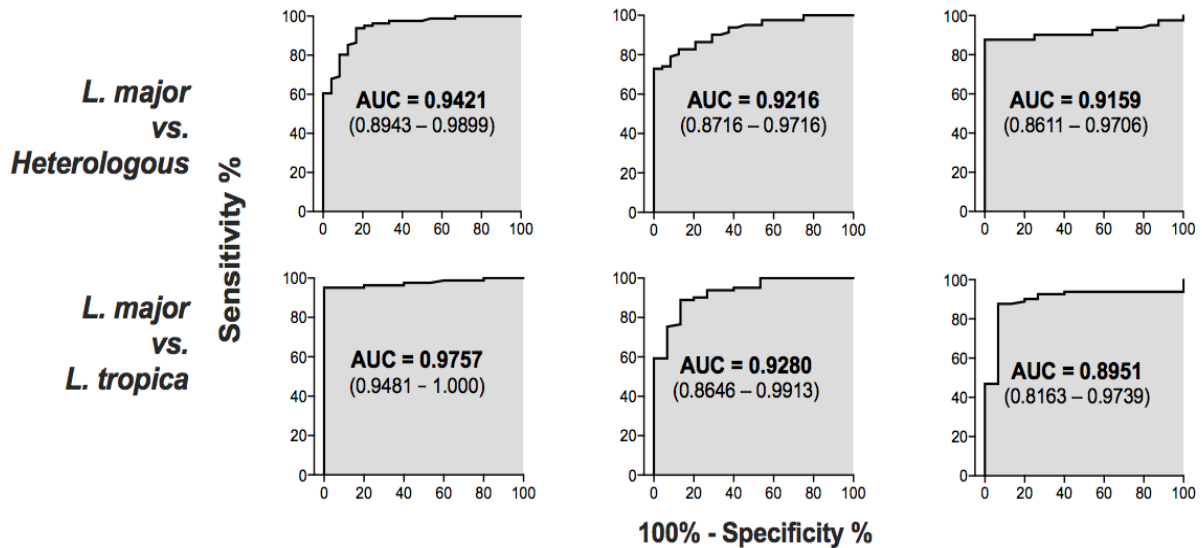
Figure 14. ROC curves.
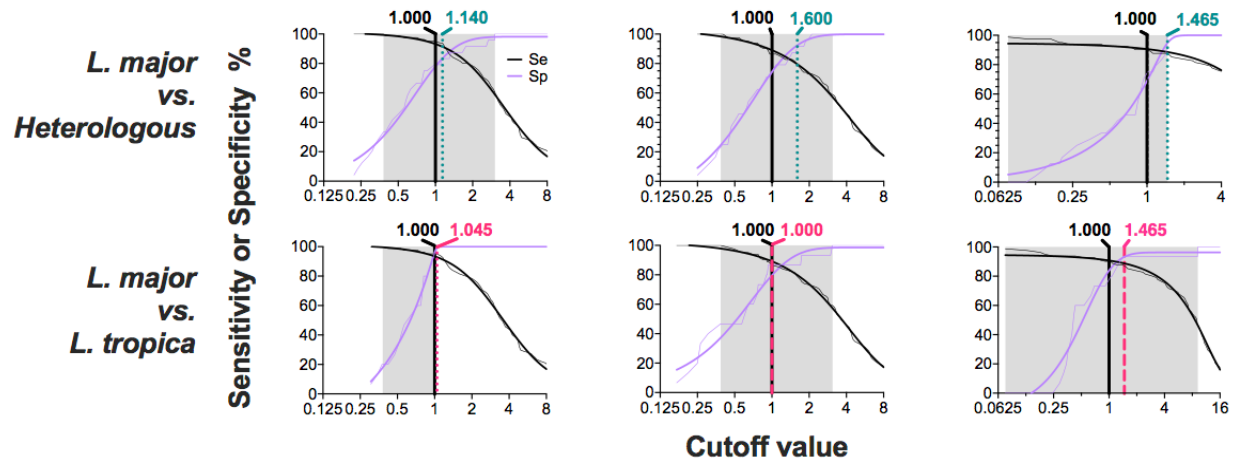
Figure 15. TG-ROC curves.
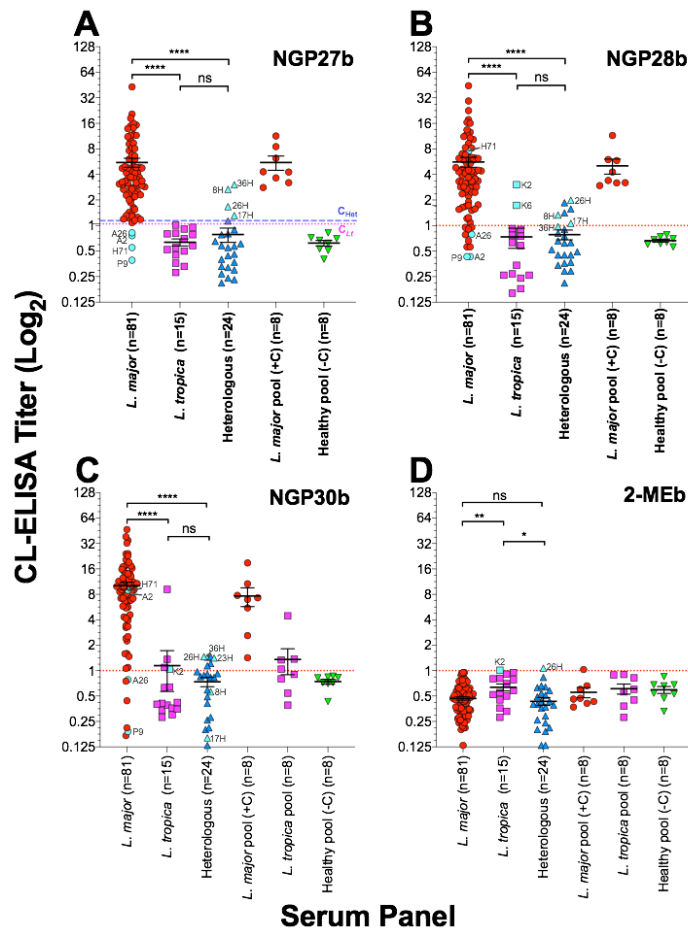
Figure 16. CL-ELISA reactivity of pool sera and sera from individual patients with active *L. major*, or *L. tropica* infection, heterologous, and healthy patients against **NGP27b**, **NGP28b**, and **NGP30b**.

33

Serum

↓

NGP27b

Positive   Negative

↓   ↓

L. major   *L. tropica*
or   or
Het. dis.   Het. dis.

↓

NGP30b

Positive   Negative

↓   ↓

| *L. major* | | Het. dis. |
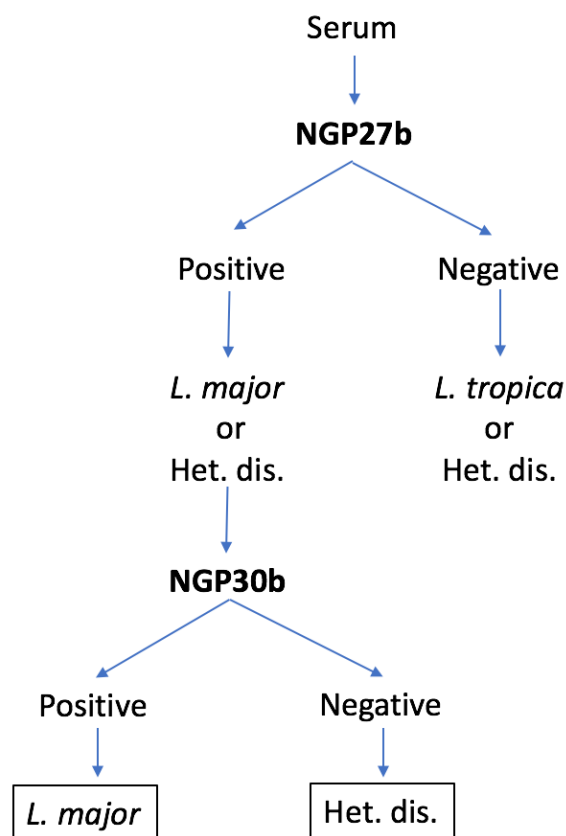
Figure 17. Algorithm to discriminate between *L. major* and *L. tropica* infection, and between *L. major* infection and heterologous diseases using two NGPs.

Table 2. Reactivity of *L. major*, *L. tropica* and heterologous sera with NGP27b, NGP28b, NGP30b, and BME-BSA in CL-ELISA.

Serum	n	NGP27b		NGP28b		NGP30b		2-MEb	
		+	-	+	-	+	-	+	-
L. major	81	77 (95%)	4 (5%)	70 (86%)	11 (14%)	73 (90%)	8 (10%)	0 (0%)	81 (100%)
L. tropica	15	0 (0%)	15 (100%)	2 (13%)	13 (87%)	4 (27%)	11 (73%)	1 (7%)	14 (93%)
Heterologous	24	5 (21%)	19 (79%)	6 (25%)	18 (75%)	6 (25%)	18 (75%)	1 (4%)	23 (96%)

Table 3. Sensitivity, specificity, and predictive values of CL-ELISA using NGP27b, NGP28b, or NGP30b as antigen, and comparing the reactivity of *L. major* vs. heterologous sera.

Parameter	NGP27b	NGP28b	NGP30b
Original values, cutoff	**1.000**	**1.000**	**1.000**
Sensitivity (%)	95.3	88.0	91.0
Specificity (%)	82.8	80.0	80.0
FPR (%)	17.2	20.0	20.0
PPV (%)	94.2	93.1	93.1
NPV (%)	85.7	68.6	75.0
Post-TG-ROC Analysis, cutoff	**1.140**	**1.600**	**1.465**
Sensitivity (%)	94.2	83.5	88.0
Specificity (%)	85.7	92.3	**100.0**
FPR (%)	14.3	7.7	0.0
PPV (%)	95.3	92.0	100.0
NPV (%)	82.8	60.0	75.0

Table 4. Sensitivity, specificity, and predictive values of CL-ELISA using NGP27b, NGP28b, or NGP30b as antigen, and comparing the reactivity of *L. major* vs. *L. tropica* sera.

Parameter	NGP27b	NGP28b	NGP30b
Original values, cutoff	**1.000**	**1.000**	**1.000**
Sensitivity (%)	95.3	88.0	91.0
Specificity (%)	93.8	88.2	79.0

35

FPR (%)	6.2	11.8	21.0
PPV (%)	98.8	97.6	95.3
NPV (%)	79.0	57.7	65.2
Post-TG-ROC Analysis, cutoff	**1.045**	**1.000**	**1.465**
Sensitivity (%)	95.3	88.0	88.0
Specificity (%)	**100.0**	88.2	93.8
FPR (%)	0.0	11.8	6.2
PPV (%)	100.0	96.4	98.8
NPV (%)	75.0	48.4	57.7

Sensitivity: TP/TP + FN

Specificity: TN/TN + FP

FPR (False-Positive Rate): 1 − Specificity = FP/TN + FP

PPV (Positive Predictive Value): TP/TP + FP

NPV (Negative Predictive Value): TN/TN + FN

Table 5. AUC-ROC values of CL-ELISA using NGP27b, NGP28b, or NGP30b as antigen, and comparing the reactivity of *L. major* vs. heterologous sera.

Parameter	NGP27b	NGP28b	NGP30b
Area under ROC curve	**0.9421**	0.9216	0.9159
Std. Error	**0.02439**	0.02551	0.02793
95% confidence interval	**0.8943-0.9899**	0.8716-0.9716	0.8611-0.9706
P value	**<0.0001**	<0.0001	<0.0001
Controls (Heterologous), n	**24**	24	24
Patients (*L. major*), n	**81**	81	81

Table 6. AUC-ROC values of CL-ELISA using NGP27b, NGP28b, or NGP30b as antigen, and comparing the reactivity of *L. major* vs. *L. tropica* sera.

Parameter	NGP27b	NGP28b	NGP30b
Area under ROC curve	**0.9757**	0.928	0.8951
Std. Error	**0.01408**	0.03232	0.0402
95% confidence interval	**0.9481-1.000**	0.8646-0.9913	0.8163-0.9739
P value	**<0.0001**	<0.0001	<0.0001
Controls (*L. tropica*), n	**15**	15	15
Patients (*L. major*), n	**81**	81	81

2.4 CONCLUSIONS

A combination of synthetic carbohydrate/glycoconjugate chemistry and immunological evaluation by CL-ELISA using sera from patients and a control group lead to the identification of specific diagnostic glycan-based biomarkers for distinguishing cutaneous leishmaniasis caused by *L. major* from heterologous diseases, and from *L. tropica* infection. The novel oligosaccharide derivatives synthesized here are terminal partial structures and potential glycotopes of known cell-surface glycoinositolphospholipids (GIPL-2 and GIPL-3) abundantly expressed in *L. major*, but absent or much less abundant in *L. tropica*. The mercaptopropyl glycosides of Gal$p$α1,3Gal$f$β (**G27**), Gal$p$α1,6Gal$p$α1,3Gal$f$β (**G28**), and Gal$p$α1,3Gal$f$β1,3Manα (**G30**), corresponding to the terminal di- and trisaccharide moieties of GIPL-2 (**G27**, **G30**) and GIPL-3 (**G28**) present in *L. major,* were efficiently synthesized using a protecting group strategy that relied predominantly on easy-to-handle acyl, acetal, and silyl protecting groups. The 4,6-*O*-DTBS group of Gal$p$ played two central roles in this work: *i*) It allowed for stereoselective α-galactosylation;[72-74] and *ii*) we discovered that it undergoes a novel regioselective ring-opening reaction producing a new Gal acceptor in a single step suitable for glycosylation at position 6 explored in the synthesis of **G28**.

The mercapto groups of saccharides **G27**, **G28**, and **G30** allowed for the convenient conjugation to maleimide-derivatized BSA producing NGPs used as antigens in CL-ELISA.

The two neoglycoproteins, **NGP27b** and **NGP30b**, both derived from GIPL-2, proved particularly useful, because they displayed 100% specificity for the distinction of *L. major* from *L. tropica* infections, and heterologous diseases, respectively. Therefore, sera of patients with skin lesions that are suspicious for cutaneous leishmaniasis can be subjected to two consecutive CL-ELISA tests, which will diagnose an *L. major* infection with a very high level of confidence. An accurate species-specific diagnosis is important for informing best treatment options, which is especially relevant in areas of population displacement in the Middle East, and in European countries with large number of refugees originated from areas where *L. major* and *L. tropica* are endemic.

2.5 EXPERIMENTAL SECTION

2.5.1 General Information

All chemicals were purchased as reagent grade from Thermo Fisher Scientific, Sigma-Aldrich or Acros Organic and used without further purification. The ACS grade solvents used for reactions were obtained from Thermo Fisher Scientific and they were distilled from the appropriate drying agents. Molecular sieves (3 Å and 4 Å) were purchased from Alfa Aesar and Fisher Scientific, respectively, and activated under high vacuum and heat prior to use. Reactions were performed under an Ar atmosphere, strictly anhydrous conditions and monitored by TLC on silica gel 60 F254 plates from EMD Millipore or Dynamic Adsorbents, Inc. Spots were detected under UV light (254 nm) and/or by charring with 4% sulfuric acid in ethanol. The purification of the compounds was performed by flash column chromatography on silica gel (40-60 µm) from Fisher

38

Chemical, and the ratio between silica and crude product ranged from 50:1 to 120:1 (dry w/w). ^{1}H and ^{13}C NMR spectra were recorded on a Bruker Avance III HD 400 MHz NMR spectrometer at 400 and 101 MHz or on a JEOL 600 MHz NMR spectrometer at 600 and 150 MHz, respectively. Chemical shifts (in ppm) were determined relative to tetramethylsilane (δ 0.00 ppm). Coupling constant(s) [Hz] were measured from one-dimensional spectra. Assignments were made by standard COSY and HSQC experiments. MS of the carbohydrates derivatives was performed on a high resolution JEOL Accu Time Of Flight (TOF) mass spectrometer using an Electrospray Ionization (ESI) source. The Thiol-ene reactions were performed in a Rayonet RPR200 photochemical reactor (USA) equipped with 16 UV lamps (350 nm). Protein derivatives were measured by Matrix Assisted Laser Desorption Ionization (MALDI)-TOF MS using sinapic acid as a matrix. 96-well polystyrene Nunc MaxiSorp ELISA plates and CL-ELISA reagents were purchased from Thermo Scientific or Jackson ImmunoResearch, and luminescence was recorded on a Luminoskan Ascent, Thermo Scientific.

2.5.2 Experimental procedures and spectroscopic data of compounds

2.5.2.1 Synthesis of the Galfβ acceptor (1)
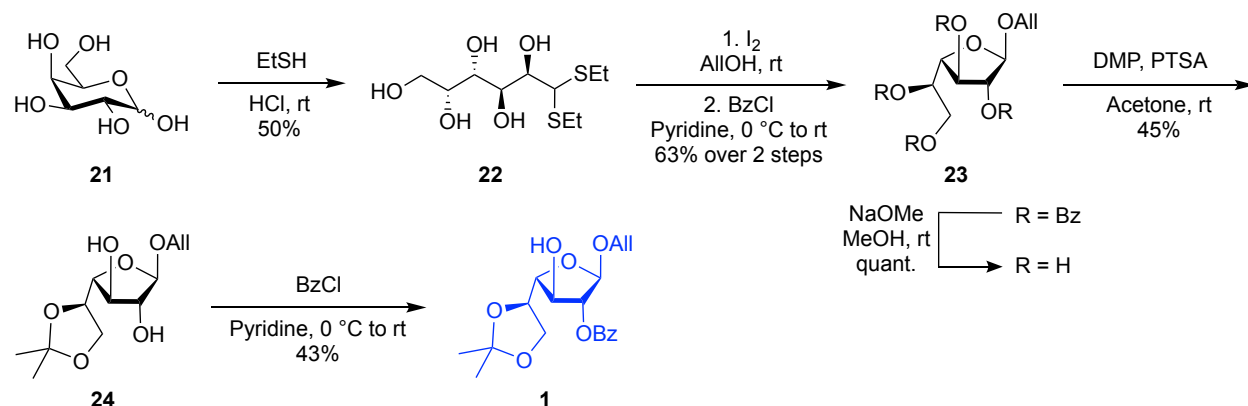
Scheme 4. Synthesis of allyl 2-O-Benzoyl-5,6-O-isopropylidene-β-D-galactofuranoside (Gal*f*β) acceptor **1**.

2.5.2.1.1 Allyl β-D-galactofuranoside (23). Dithioacetal galactose **22**[90] (1.0 g, 3.50 mmol) was dissolved in 1.5% I_2 in dry AllOH (w/v, 75 mL) under Ar and stirred overnight at rt. Excess of I_2 was quenched by the increment addition of solid $Na_2S_2O_3$ until the solution turned colorless or slightly yellow. The reaction mixture was then neutralized by the addition of $NaHCO_3$. Filtration follow by evaporation of the solvent gave the crude product allyl β-D-galactofuranoside as an amorphous light-yellow solid. Without further purification, dry pyridine (60 mL) was added to the crude mixture followed by the addition of BzCl (2.5 mL, 21.45 mmol) at 0°C. The reaction mixture was stirred under Ar overnight, poured into an ice-water mixture, and extracted with DCM (3 x 75 mL). The combined organic layers were washed with 1.0 M HCl (50 mL), brine (50 mL), dried over $MgSO_4$, filtered, concentrated and purified by flash column chromatography on silica gel (EtOAc/hexanes = 1:3) to furnish the allyl 2,3,5,6-*O*-Benzoyl β-D-galactofuranoside as a white powder (β compound; 1.4 g, 63% over two steps). R_f 0.4 (EtOAc/hexanes = 1:3). ESI-TOF HRMS: *m/z* [M+Na]+ calcd for $C_{37}H_{32}O_{10}$ 659.1893, found 659.1892. Finally, the benzoylated compound (1.2 g, 1.89 mmol), was dissolved in 60 mL of 0.25 M NaOMe under Ar, and stirred at rt overnight. Amberlyst-15 ion-exchange resin was added and stirred until pH 7, followed by filtration through Celite and concentration to give **23** as a white solid (415 mg, quant.). R_f 0.37 (DCM/MeOH = 6:1). ^{1}H NMR (400 MHz, MeOD, 300K) δ 0.75-1.65 (m, 3H, -O*H*); 2.50-2.79 (m, 1H, -O*H*); 3.56-3.76 (m, 4H, H-4, H-5, H-6a,b); 3.87-4.04 (m, 3H, Ha, H-2, H-3); 4.20 (dd, *J* = 13.1, 5.0 Hz, 1H, Ha); 4.90 (s, 1H, H*f*-1); 5.15 (d, *J* = 10.5, 1H, H-c); 5.29 (d, *J* = 17.2, 1H, H-c); 5.87-6.00 (m, 1H, H-b) ppm. ^{13}C NMR (101 MHz, MeOD, 300K) δ 64.6 (*C*-6); 69.5 (*C*-a); 72.5; 78.9; 83.5; 84.4; 108.7 (*Cf*-1); 117.2 (C-c); 135.9 (C-b) ppm. ESI-TOF HRMS: *m/z* [M+Na]+ calcd for $C_9H_{16}O_6$ 243.0845, found 243.1199.

2.5.2.1.2 Allyl 5,6-*O*-isopropylidene-β-D-galactofuranoside (24). To a solution of allyl β-D-galactofuranoside **23** (333 mg, 1.51 mmol) in 24 mL of wet acetone, DMP (1.7 mL, 13.8 mmol) and PTSA (50 mg, 0.30 mmol) were added and stirred overnight at rt. Next day, the solution was neutralized with Et_3N, concentrated and purified by flash column chromatography on silica gel (DCM/MeOH = 15:1) to yield the desired compound **24** as a colorless oil (180 mg, 45%). R_f 0.31 (DCM/MeOH = 15:1). ^{1}H NMR (400 MHz, CDCl₃, 300K) δ 1.40 (s, 3H, C*H₃*); 1.43 (s, 3H, C*H₃*); 3.00 (d, *J* = 11.7 Hz, 1H, -O*H*); 3.95-4.16 (m, 7H, -O*H*, H-a, H-6a,b); 4.24 (ddt, *J* = 12.9, 5.2, 1.5, 1.5 Hz, 1H, H-a); 4.32-4.41 (m, 1H); 5.08 (s, 1H, H*f*-1); 5.21 (dq, *J* = 10.4, 1.5 Hz, 1H, H-c); 5.28

40

(dq, J = 17.2, 1.5 Hz, 1H, H-c); 5.82-5.96 (m, 1H, H-b) ppm. ^{13}C NMR (101 MHz, CDCl$_3$, 300K) δ 25.5 (CH$_3$); 25.6 (CH$_3$); 65.7 (C-6); 68.2 (C-a); 75.7; 78.2; 78.6; 85.6; 107.8 (Cf-1); 110.2 (Cq-*isop*.); 117.7 (C-c); 133.6 (C-b) ppm. ESI-TOF HRMS: m/z [M+Na]$^+$ calcd for C$_{12}$H$_{20}$O$_6$ 283.1158, found 283.1130.

2.5.2.1.3 Allyl 2-*O*-Benzoyl-5,6-*O*-isopropylidene-β-D-galactofuranoside (1). To a solution of allyl 5,6-*O*-isopropylidene-β-D-galactofuranoside **24** (180 mg, 0.69 mmol) in pyridine/DCM (0.7 mL/7.0 mL) was added BzCl (105 μL, 0.90 mmol) dropwise at 0 °C, and the resulting mixture was warmed gradually to room temperature. The reaction was stirred for 3 h at the same temperature, at the end of which time TLC indicated it was finished. The reaction was quenched with MeOH, diluted with DCM (50 mL), and then the mixture was washed with water (25 mL) and brine (25 mL). The organic layer was separated and dried over anhydrous MgSO$_4$, filtered, and concentrated. The residue was purified by column chromatography (EtOAc/hexanes = 1:3) to afford the Gal*f*β acceptor **1** (108 mg, 43%) as colorless syrup. R$_f$ 0.33 (EtOAc/hexanes = 1:3). ^{1}H NMR (400 MHz, CDCl$_3$, 300K) δ 1.39 (s, 3H, CH_3); 1.46 (s, 3H, CH_3); 3.25 (d, J = 5.20 Hz, 1H, OH); 3.97 (dd, J = 8.44, 6.72 Hz, 1H, H-6a,b); 4.03 (td, $^3J_{3\text{-OH}}$ = 5.2, $^3J_{2,3}$ = 2.7 Hz, 1H, H-3); 4.06-4.15 (m, 3H, H*f*-6a,b, H-a, H-5); 4.24-4.36 (m, 2H, H-a, H-4); 5.10 (dd, $^3J_{2,3}$ = 2.7, $^3J_{1,2}$ = 1.1 Hz, 1H, H-2); 5.23 (dq, J = 10.39, 1.39 Hz, 1H, H-c); 5.30-5.37 (m, 2H, H*f*-1, H-c); 5.87-6.00 (m, 1H, H-b); 7.43-7.50 (m, 2H, arom.); 7.57-7.64 (m, 1H, arom.); 8.00-8.06 (m, 2H, arom.) ppm. ^{13}C NMR (101 MHz, CDCl$_3$, 300K) δ 25.4 (CH$_3$); 26.5 (CH$_3$); 65.5 (C-6); 68.5 (C-a); 76.1 (C-4); 77.7 (C-3); 84.1 (C-5); 86.2 (C-2); 104.5 (Cf-1); 109.9 (Cq-*isop*.); 117.7 (C-c); 128.6 (C-arom.); 129.0 (Cq, arom.); 129.8 (C-arom.); 133.6 (C-b); 133.7 (C-arom.); 166.8 (C=O) ppm. ESI-TOF HRMS: m/z [M+Na]$^+$ calcd for C$_{19}$H$_{24}$O$_7$ 387.1420, found 387.1346.

2.5.2.2 Synthesis of the Manpα acceptor (8)
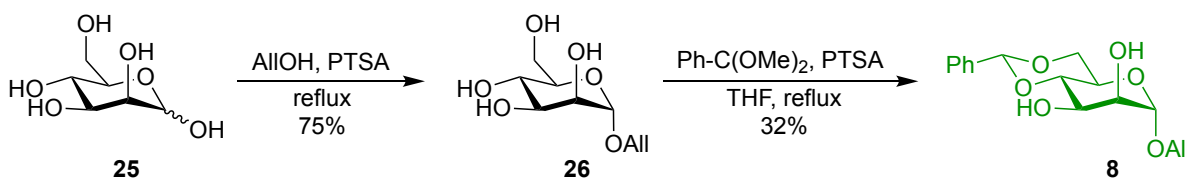
Scheme 5. Synthesis of allyl 4,6-*O*-benzylidene-α-D-mannopyranoside (Man*p*α) acceptor **8**.

2.5.2.2.1 Allyl 4,6-*O*-benzylidene-α-D-mannopyranoside (8). To a solution of the allyl glycoside **26**[91] (1.0 g, 4.54 mmol, 1.0 equiv) in dry THF (37 mL), Ph-C(OMe)$_2$ (1.36 mL, 9.06 mmol, 2.0 equiv) and PTSA (11 mg, 0.064 mmol, 0.014 equiv) were added. The mixture was stirred and refluxed for 3 h. TLC (DCM/MeOH = 6:1) indicated that the reaction was completed. The mixture was neutralized and washed with NaHCO$_3$ and extracted with EtOAc. The organic layer was dried with MgSO$_4$, filtered and concentrated. The residue was purified by column chromatography on silica gel (EtOAc/Hexanes = 2:3) to give the desired compound **8** (450 mg, 32%), as a white powder. R$_f$ 0.33 (EtOAc/Hexanes = 2:3). ^{1}H NMR (400 MHz, CDCl$_3$, 300K) δ 2.92 (br.s., 1H, OH); 3.66-4.35 (m, 8H, Ha, H-2, H-3, H-4, H-5, H-6a,b); 4.87 (s, 1H, H-1); 5.16-5.37 (m, 2H, Hc); 5.55 (s, 1H, OC*H*Ph); 5.83-5.96 (m, 1H, H-b); 7.31-7.41 (m, 3H, arom.); 7.43-7.53 (m, 2H, arom.) ppm. ESI-TOF HRMS: *m/z* [M+Na]$^+$ calcd for C$_{16}$H$_{20}$O$_6$ 331.1158, found 331.1159. ^{13}C-NMR spectra matched the ones previously described for this compound.[91]

2.5.2.3 Synthesis of the Galfβ donor (2)
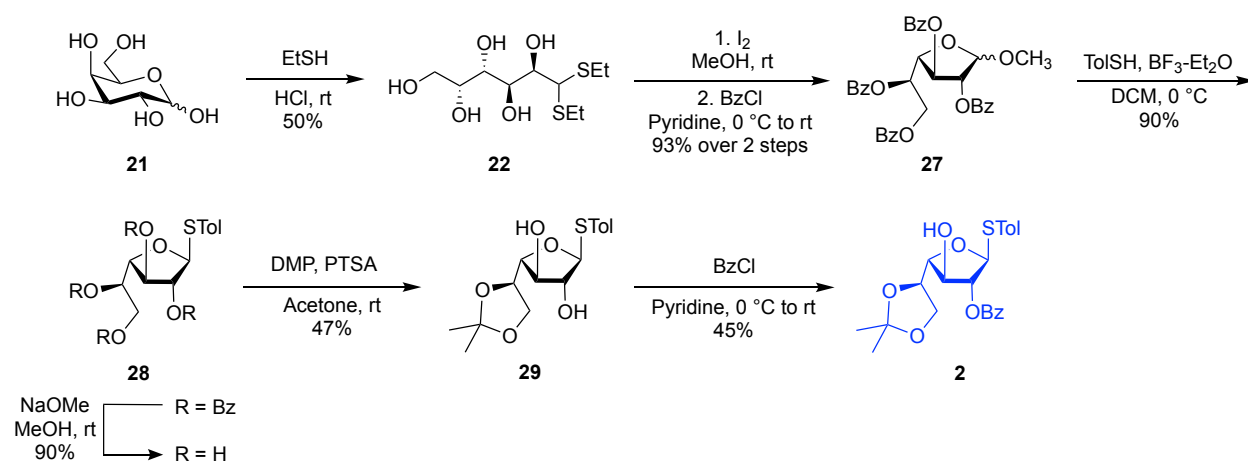
Scheme 6. Synthesis of allyl 2-*O*-Benzoyl-5,6-*O*-isopropylidene-β-D-galactofuranoside (Gal*f*β) donor **2**.

2.5.2.3.1 *p*-Tolyl 2-*O*-Benzoyl-5,6-*O*-isopropylidene-1-thio-β-D-galactofuranoside (2). To a solution of **29**[78] (178 mg, 0.55 mmol, 1.0 equiv) in pyridine/DCM (0.7 mL/7.0 mL) was added BzCl (80 μL, 0.69 mmol, 1.3 equiv) dropwise at 0 °C, and the resulting mixture was warmed gradually to room temperature. The reaction was stirred for 9 h at the same temperature, at the end

of which time TLC indicated it was finished. The reaction was quenched with MeOH, diluted with DCM, and then the mixture was washed with water and brine. The organic layer was separated and dried over anhydrous $MgSO_4$, filtered, and concentrated. The residue was purified by column chromatography (EtOAc/Hexanes = 1:3) to afford compound **2** (105 mg, 45%) as colorless syrup. R_f 0.31 (EtOAc/Hexanes = 1:3). ^{1}H NMR (400 MHz, $CDCl_3$) δ 1.37 (s, 3H, CH_3); 1.43 (s, 3H, CH_3); 2.34 (s, 3H, arom.CH_3); 3.52 (d, J = 2.6 Hz, 1H); 3.98-4.15 (m, 2H); 4.19-4.26 (m, 2H); 4.31-4.36 (m, 1H); 5.08 (t, J = 3.7 Hz, 1H); 5.64 (d, J = 3.8 Hz, 1H); 7.07-7.19 (m, 2H, arom.); 7.39-7.52 (m, 4H, arom.); 7.56-7.66 (m, 1H, arom.); 7.96-8.09 (m, 2H, arom.) ppm. ESI-TOF HRMS: m/z [M+Na]$^+$ calcd for $C_{23}H_{26}O_6S$ 453.1348, found 453.1345. ^{13}C-NMR spectra matched the ones previously described for this compound.[79]

2.5.2.4 Synthesis of the Galpα donor (3)
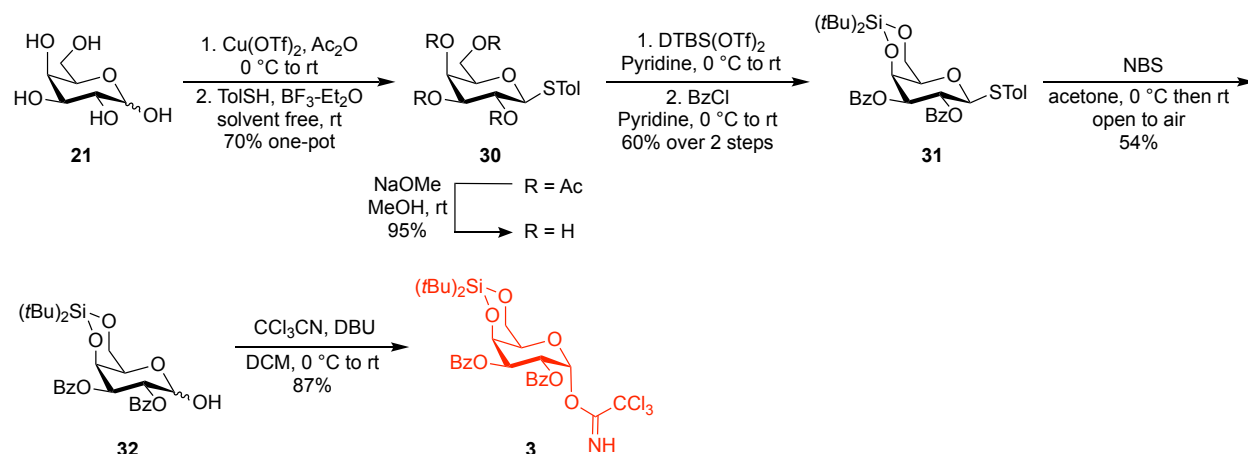
Scheme 7. Synthesis of 2,3-Di-*O*-benzoyl-4,6-*O*-di-*tert*-butylsilylene-α-D-galactopyranosyl trichloroacetimidate (Gal*p*α) donor **3**.

2.5.2.4.1   **2,3-Di-*O*-benzoyl-4,6-*O*-di-*tert*-butylsilylene-α-D-galactopyranosyl trichloroacetimidate (3)**. To a solution of the mixture α,β-hydrolyzed sugar **32** (123 mg, 0.23 mmol, 1 equiv) in DCM (6 mL), CCl_3CN (0.47 mL, 4.69 mmol, 20 equiv) and DBU (42 μL, 0.28 mmol, 1.2 equiv) were consecutively added at 0 °C and stirred at rt for 15 min. Then, the residue was concentrated and purified by flash column chromatography on silica gel (EtOAc/Hexanes =

3:1) to yield **3** (135 mg, 87%), as a white powder. R_f 0.60 (EtOAc/Hexanes = 3:1). ^{1}H NMR (400 MHz, CDCl$_3$, 300K) δ 0.98 (s, 9H, *t*Bu); 1.15 (s, 9H, *t*Bu); 4.17 (s, 1H, *H*-5); 4.32 (dd, J = 4.8, 1.9 Hz, 2H, H-6a,b); 5.01 (d, $^3J_{3,4}$ = 3.0 Hz, 1H, *H*-4); 5.69 (dd, $^3J_{2,3}$ = 10.6, $^3J_{3,4}$ = 3.0 Hz, 1H, *H*-3); 6.04 (dd, $^3J_{2,3}$ = 10.6, $^3J_{1,2}$ = 3.6 Hz, 1H, *H*-2); 6.79 (d, $^3J_{1,2}$ = 3.6 Hz, 1H, *H*-1); 7.32-7.44 (m, 4H, arom.); 7.47-7.57 (m, 2H, arom.); 7.94-8.08 (m, 4H, arom.); 8.56 (s, 1H, -N*H*) ppm. ESI-TOF HRMS: *m/z* [M+Na]$^+$ calcd for C$_{30}$H$_{36}$Cl$_3$NO$_8$S 694.1173, found 694.1167. ^{13}C-NMR spectra matched the ones previously described for this compound.[72]

2.5.2.5 Synthesis of the NGP27b [Gal*p*α1,3Gal*f*β-linker-BSA]
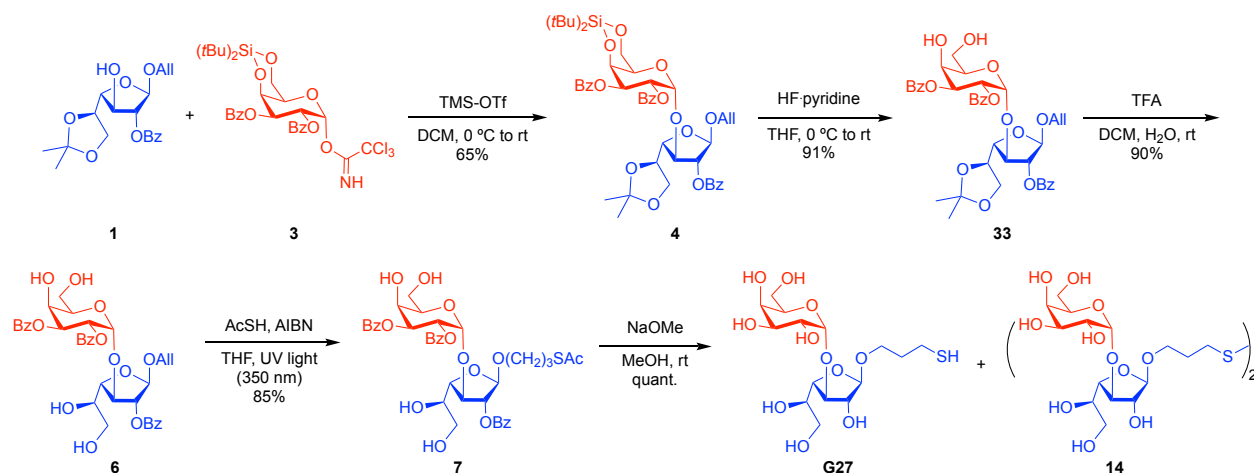
Scheme 8. Synthesis of the mercaptopropyl disaccharide **G27**.

2.5.2.5.1 Allyl 2,3-di-*O*-benzoyl-4,6-*O*-di-*tert*-butylsilylene-α-D-galactopyranosyl-(1→3)-2-*O*-benzoyl-5,6-*O*-isopropylidene-β-D-galactofuranoside (4). To a solution of Gal*f* acceptor **1** (150 mg, 0.41 mmol) and Gal*p* donor **3** (373 mg, 0.56 mmol) in anhydrous DCM (54 mL), freshly activated MS 4Å was added and stirred under Ar for 1 h at rt. Then, the solution was cool down to 0°C and TMS-OTf (22 μL, 0.12 mmol) was added dropwise. The solution was gradually brought to rt and after 1 h, the reaction mixture was quenched by addition of Et$_3$N, filtered, and washed with water and brine. The organic layers were dried over MgSO$_4$, concentrated, and purified by flash column chromatography on silica gel (EtOAc/hexanes = 1:4) to give **4** (234 mg, 65%), as a light-yellow solid. R_f 0.37 (EtOAc/hexanes = 1:4). ^{1}H NMR (400 MHz, CDCl$_3$, 300K) δ 0.95 (s,

9H, *t*Bu); 1.08 (s, 9H, *t*Bu); 1.22 (s, 3H, C*H*$_3$); 1.35 (s, 3H, C*H*$_3$); 3.70-3.87 (m, 2H, H*f*-6a,b); 4.00-4.07 (m, 1H, H-a), 4.11-4.34 (m, 7H, H-a, H*p*-5, H*p*-6a,b, H*f*-3, H*f*-4, H*f*-5); 4.90 (d, $^3J_{3,4}$ = 2.91 Hz, 1H, H*p*-4); 5.15-5.23 (m, 2H, H*f*-1, H-c); 5.32 (dd, *J* = 17.24, 1.71 Hz, 1H, H-c); 5.45 (d, $^3J_{1,2}$ = 0.98 Hz, 1H, H*f*-2); 5.48 (d, $^3J_{1,2}$ = 3.8 Hz, 1H, H*p*-1); 5.61 (dd, $^3J_{2,3}$ = 10.6, $^3J_{3,4}$ = 2.9 Hz, 1H, H*p*-3); 5.77 (dd, $^3J_{2,3}$ = 10.6, $^3J_{1,2}$ = 3.8 Hz, 1H, H*p*-2); 5.82-5.95 (m, 1H, H-b); 7.35-7.64 (m, 9H, arom.); 7.99-8.05 (m, 6H, arom.) ppm. ^{13}C NMR (101 MHz, CDCl$_3$, 300K) δ 20.7 (*C*q-*t*Bu); 23.2 (*C*q-*t*Bu); 24.8 (*C*H$_3$); 26.0 (*C*H$_3$); 27.2 (*t*Bu); 27.5 (*t*Bu); 65.3 (C*f*-6); 66.9 (C*p*-6); 67.6; 67.9 (C-a); 68.4 (C*p*-2); 71.0 (C*p*-3); 71.1 (C*p*-4); 74.4; 81.9 (C*f*-2); 82.5; 83.3; 97.0 (C*p*-1); 104.9 (C*f*-1); 109.8 (*C*q-*isop*.)*;* 117.4 (C-c); 128.3 (*C*-arom.); 128.4 (*C*-arom.); 128.5 (*C*-arom.); 129.2 (*C*q, arom.); 129.4 (*C*q, arom.); 129.7 (*C*-arom.); 129.8 x 2 (*C*-arom.); 129.9 (*C*q, arom.); 133.1 (*C*-arom.); 133.3 (*C*-arom.); 133.5 (*C*-arom.); 133.8 (C-b); 165.3 (*C*=O); 166.0 (*C*=O); 166.2 (*C*=O) ppm. ESI-TOF HRMS: *m/z* [M+Na]$^+$ calcd for C$_{47}$H$_{58}$O$_{14}$Si 897.3494, found 897.3494.

2.5.2.5.2 Allyl 2,3-di-*O*-benzoyl-α-D-galactopyranosyl-(1→3)-2-*O*-benzoyl-5,6-*O*-isopropylidene-β-D-galactofuranoside (33). Fully protected disaccharide **4** (180 mg, 0.21 mmol) was dissolved in a mixture ratio (**1:100** HF-Pyr/dry THF) (360 μL/36 mL) in a plastic conical tube and stirred for 30 min at 0°C and then 30 min at rt under Ar. The reaction mixture was cooled down again to 0°C and quenched with saturated NaHCO$_3$. Then, diluted and extracted with EtOAc, washed with water and brine, dried over MgSO$_4$, concentrated and purified by column chromatography in silica gel to give **33** (137 mg, 91%) as a white powder. R$_f$ 0.37 (EtOAc/hexanes = 1:1). ^{1}H NMR (400 MHz, CDCl$_3$, 300K) δ 1.20 (s, 3H, C*H*$_3$); 1.32 (s, 3H, C*H*$_3$); 2.84 (br. s., 1H, O*H*); 3.07 (br. s., 1H, O*H*); 3.70-3.85 (m, 2H, H*f*-6a,b); 3.89-4.20 (m, 6H, H-a, H*p*-6a,b, H*p*-5, H*f*-4, H*f*-5); 4.25 (ddt, *J* = 13.08, 4.98, 1.54, 1.54 Hz, 1H, H-a); 4.38 (t, $^3J_{3,4}$ = 4.58, 1H, H*f*-3); 4.49 (s, 1H, H*p*-4); 5.19-5.25 (m, 2H, H*f*-1, H-c); 5.35 (dq, *J* = 17.2, 1.6 Hz, 1H, H-c); 5.54 (d, $^3J_{1,2}$ = 2.6 Hz, 1H, H*p*-1); 5.62 (d, *J* = 1.1 Hz, 1H, H*f*-2); 5.71 (dd, *J* = 2.1, 0.9 Hz, 2H, H*p*-2, H*p*-3); 5.86-5.98 (m, 1H, H-b); 7.34-7.40 (m, 4H, arom.); 7.41-7.47 (m, 2H, arom.); 7.49-7.54 (m, 2H, arom.); 7.56-7.63 (m, 1H, arom.); 7.96-8.05 (m, 6H, arom.) ppm. ^{13}C NMR (101 MHz, CDCl$_3$, 300K) δ 25.0 (*C*H$_3$); 26.1 (*C*H$_3$); 63.3 (C*p*-6); 65.3 (C*f*-6); 67.9 (C-a); 68.7 (C*p*-2); 69.6 (C*p*-4); 70.3 (C*f*-3); 71.0 (C*p*-3); 74.9; 81.5 (C*f*-2); 83.4; 84.2; 97.7 (C*p*-1); 104.9 (C*f*-1); 109.8 (*C*q-*isop*.); 117.5 (C-c); 128.4 x 2 (*C*-arom.); 128.5 (*C*-arom.); 129.0 (*C*q, arom.); 129.2 (*C*q, arom.); 129.3 (*C*q, arom.); 129.7 (*C*-arom.); 129.8 (*C*-arom.); 133.4 (*C*-arom.); 133.6 (*C*-arom.); 133.7 (C-b);

165.6 (*C*=O); 165.8 (*C*=O); 165.9 (*C*=O) ppm. ESI-TOF HRMS: *m/z* [M+Na]$^+$ calcd for C$_{39}$H$_{42}$O$_{14}$ 757.2472, found 757.2470.

2.5.2.5.3 Allyl 2,3-di-*O*-benzoyl-α-D-galactopyranosyl-(1→3)-2-*O*-benzoyl-β-D-galactofuranoside (6). To a solution of desilylated disaccharide **33** (110 mg, 0.15 mmol) in 15 mL DCM, water and TFA (1.5 mL) were consecutively added and stirred vigorously at rt for 15 min. After disappearance of starting material, the resulting solution was co-evaporated with 10 mL ethanol twice under reduced pressure at <40 °C (bath). The residue was then dried on full vacuum pump and applied to column chromatography in (DCM/MeOH = 20:1) to afford **6** (94 mg, 90%) as a yellow solid. R$_f$ 0.27 (DCM/MeOH = 20:1). ^{1}H NMR (400 MHz, CDCl$_3$, 300K) δ 3.40-3.58 (m, 2H, H*f*-6a,b); 3.60-3.68 (m, 1H, H*f*-5); 3.83-3.97 (m, 2H, H*p*-6a,b); 3.98-4.06 (m, 1H, H-a); 4.09-4.20 (m, 2H, H-a, H*p*-5); 4.33 (t, $^3J_{3,4}$ = 4.6, 1H, H*f*-3); 4.39 (d, $^3J_{3,4}$ = 4.6 Hz, 1H, H*f*-4); 4.47 (s, 1H, H*p*-4); 5.13-5.21 (m, 2H, H*f*-1, H-c); 5.26-5.35 (m, 1H, H-c); 5.51 (d, $^3J_{1,2}$ = 1.3 Hz, 1H, H*f*-2); 5.58 (d, $^3J_{1,2}$ = 2.2 Hz, 1H, H*p*-1); 5.65-5.74 (m, 2H, H*p*-2, H*p*-3); 5.79-5.93 (m, 1H, H-b); 7.32-7.44 (m, 6H, arom.); 7.46-7.58 (m, 3H, arom.); 7.91-8.05 (m, 6H, arom.) ppm. ^{13}C NMR (101 MHz, CDCl$_3$, 300K) δ 63.1 (C*p*-6); 63.9 (C*f*-6); 68.0 (C-a); 69.0; 69.5 (C*p*-4); 70.4 (C*f*-3); 70.6 (C*f*-5); 70.9; 81.9 (C*f*-2); 83.0 (C*f*-4); 83.6 (C*p*-5); 97.2 (C*p*-1); 104.9 (C*f*-1); 117.6 (C-c); 128.3 (*C*-arom.); 128.4 (*C*-arom.); 128.5 (*C*-arom.); 129.0 (*C*q, arom.); 129.1 (*C*q, arom.); 129.4 (*C*q, arom.); 129.7 (*C*-arom.); 129.8 x 2 (*C*-arom.); 133.3 (*C*-arom.); 133.5 (*C*-arom.); 133.6 x 2 (C-b, *C*-arom.); 165.8 (*C*=O); 165.9 (*C*=O); 166.2 (*C*=O) ppm. ESI-TOF HRMS: *m/z* [M+Na]$^+$ calcd for C$_{36}$H$_{38}$O$_{14}$ 717.2159, found 717.2158.

2.5.2.5.4 (Acetylthio)propyl 2,3-di-*O*-benzoyl-α-D-galactopyranosyl-(1→3)-2-*O*-benzoyl-β-D-galactofuranoside (7). To a solution of **6** (37 mg, 0.053 mmol) and AIBN (9 mg, 0.055 mmol) in 8.5 mL dry THF, thiolacetic acid (26 µL, 0.36 mmol) was added and stirred under Ar at rt for 6 h in the Rayonet UV reactor. The reaction mixture was co-evaporated with toluene and concentrated. The crude product was purified by flash chromatography (DCM/MeOH = 15:1) to give **7** (35 mg, 85%) as a white solid. R$_f$ 0.37 (DCM/MeOH = 15:1). ^{1}H NMR (400 MHz, CDCl$_3$, 300K) δ 1.84 (dq, $^3J_{a,b}$ = 14.3, $^3J_{b,c}$ = 7.1 Hz, 2H, H-b); 2.02 (br. s., 1H, O*H*); 2.30 (s, 3H, C*H*$_3$); 2.83 (br. s., 1H, O*H*); 2.94 (t, $^3J_{b,c}$ = 7.1 Hz, 2H, H-c); 3.26 (br. s., 1H, O*H*); 3.40-3.76 (m, 6H, O*H*, H-a, H*f*-5, H*f*-6a,b); 3.84-4.02 (m, 2H, H*p*-6a,b); 4.13 (dd, *J* = 5.2, 3.7 Hz, 1H, H*p*-5); 4.29-4.40

(m, 2H, Hf-3, Hf-4); 4.49 (s, 1H, Hp-4); 5.12 (s, 1H, Hf-1); 5.48 (d, $^3J_{1,2}$ = 1.10 Hz, 1H, Hf-2); 5.58 (d, $^3J_{1,2}$ = 3.06 Hz, 1H, Hp-1); 5.63-5.75 (m, 2H, Hp-2, Hp-3); 7.31-7.45 (m, 6H, arom.); 7.46-7.60 (m, 3H, arom.); 7.91-8.06 (m, 6H, arom.) ppm. ^{13}C NMR (101 MHz, CDCl$_3$, 300K) δ 25.9 (C-c); 29.4 (C-b); 30.6 (*C*H$_3$); 63.0 (Cp-6); 63.9 (Cf-6); 65.9 (C-a); 69.0; 69.4 (Cp-4); 70.4 (Cf-3); 70.6 (Cf-5); 70.9; 81.8 (Cf-2); 83.3 (Cf-4); 83.5 (Cp-5); 97.5 (Cp-1); 105.9 (Cf-1); 128.3 (*C*-arom.); 128.4 (*C*-arom.); 128.5 (*C*-arom.); 129.0 (*C*q, arom.); 129.1 (*C*q, arom.); 129.4 (*C*q, arom.); 129.7 (*C*-arom.); 129.8 (*C*-arom.); 133.3 (*C*-arom.); 133.5 (*C*-arom.); 133.6 (*C*-arom.); 165.7 (*C*=O); 165.8 (*C*=O); 166.1 (*C*=O); 196.1 (*C*=O) ppm. ESI-TOF HRMS: *m/z* [M+Na]$^+$ calcd for C$_{38}$H$_{42}$O$_{15}$S 793.2142, found 793.2147.

2.5.2.5.5 Thiopropyl α-D-galactopyranosyl-(1→3)-β-D-galactofuranoside (G27). The acyl-protected disaccharide **7** (35 mg, 0.045 mmol) was dissolved in 3 mL of anhydrous 0.25 M NaOMe, and stirred for 2 hours under Ar. The solution was then neutralized with Amberlyst-15, filtered through Celite, concentrated and finally dissolved in water and lyophilized. Initially, the unprotected mercaptopropyl trisaccharide **G27** is produced, which oxidizes by handling on air within hours to the disulfide **14** (19 mg, quant.) as an off-white solid. *R*$_f$ 0.25 (*i*PrOH/H$_2$O = 5:1 w/ 3 drops AcOH). ^{1}H NMR (600 MHz, D$_2$O, 300K) δ 1.95 (q, $^3J_{b,c;\,a,b}$ = 6.36 Hz, 2H, H-b); 2.78 (t, $^3J_{b,c}$ = 7.04 Hz, 2H, H-c); 3.59-3.82 (m, 9H, Hf-5, Hp-3, Hp-2, Hp-6$_{a,b}$, H-a, Hf-6$_{a,b}$); 3.94 (dd, ^3J = 3.12, ^3J = 0.91 Hz, 1H, Hp-4); 3.96-4.02 (m, 2H, Hf-3, Hp-5); 4.11 (dd, ^3J = 6.1, ^3J = 4.0 Hz, 1H, Hf-4); 4.22 (dd, $^3J_{2,3}$ = 2.9, $^3J_{1,2}$ = 1.5 Hz, 1H, Hf-2); 4.97 (d, $^3J_{1,2}$ = 1.5, 1H, Hf-1); 4.99 (d, $^3J_{1,2}$ = 3.80 Hz, 1H, Hp-1) ppm. ^{13}C NMR (150 MHz, CDCl$_3$, 300K) δ 28.5 (C-b); 35.0 (C-c); 61.3 (Cp-6); 63.0 (Cf-6); 66.4 (C-a); 68.5 (Cp-2); 69.4 (Cp-3, Cp-4); 71.1(Cf-5); 71.6 (Cp-5); 79.5 (Cf-2); 82.3 (Cf-4); 85.2 (Cf-3); 100.1 (Cp-1); 107.8 (Cf-1) ppm. ESI-TOF HRMS: *m/z* [M+Na]$^+$ calcd for C$_{15}$H$_{28}$O$_{11}$S 439.1250, found 439.1198; for C$_{30}$H$_{54}$O$_{22}$S$_2$ 853.2446, found 853.2331.

2.5.2.5.6 Synthesis of the NGP27b [Gal$p$α1,3Gal$f$β -linker-BSA]. MALDI-TOF MS: *m/z* for BSA [M+H]$^+$ 66120; for NGP27b [M+H]$^+$ 84536.
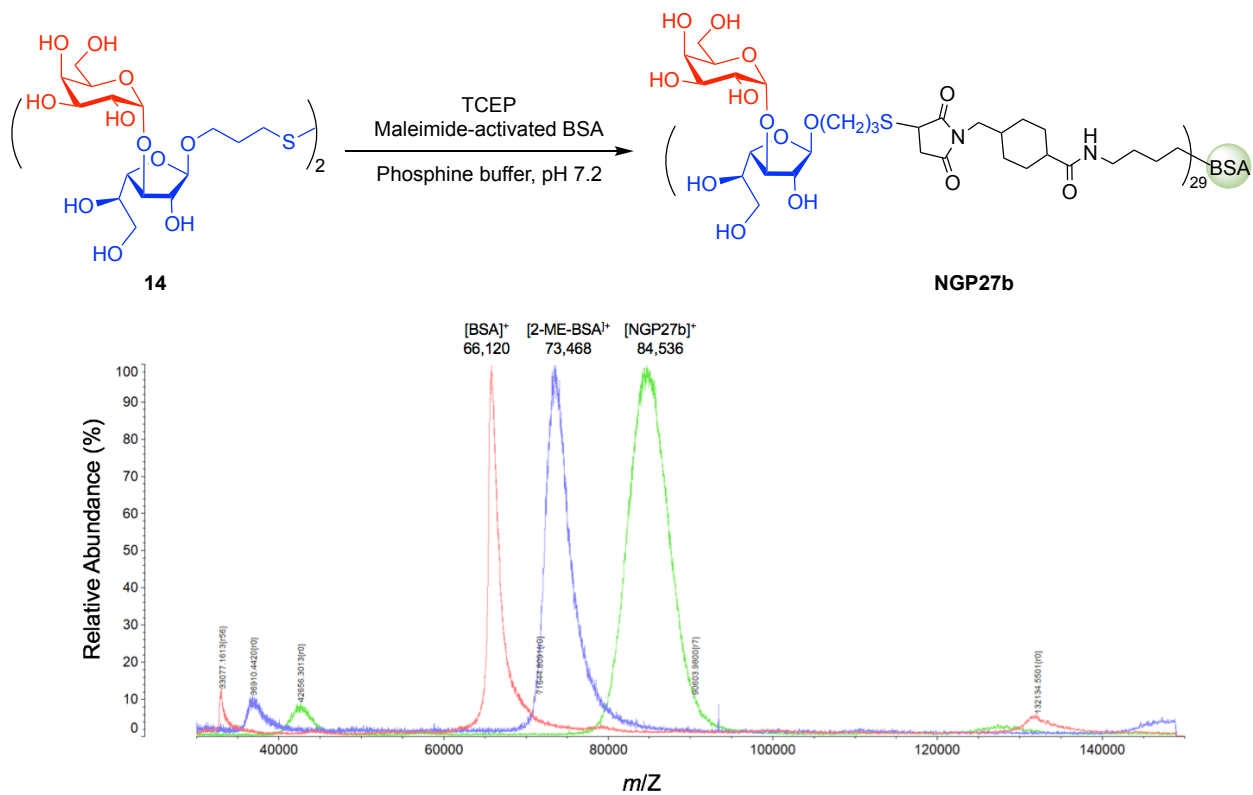
Figure 18. (Top) Schematic representation of conjugation of **G27** to BSA. (Bottom) MALDI-TOF mass spectra of **NGP27b** [Galα*p*1,3Galβ*f*-linker-BSA] overlaid with pure BSA and 2-ME-linker-BSA.

2.5.2.6 Synthesis of the NGP28b [*Galpα1,6Galpα1,3Galfβ*-linker-BSA]
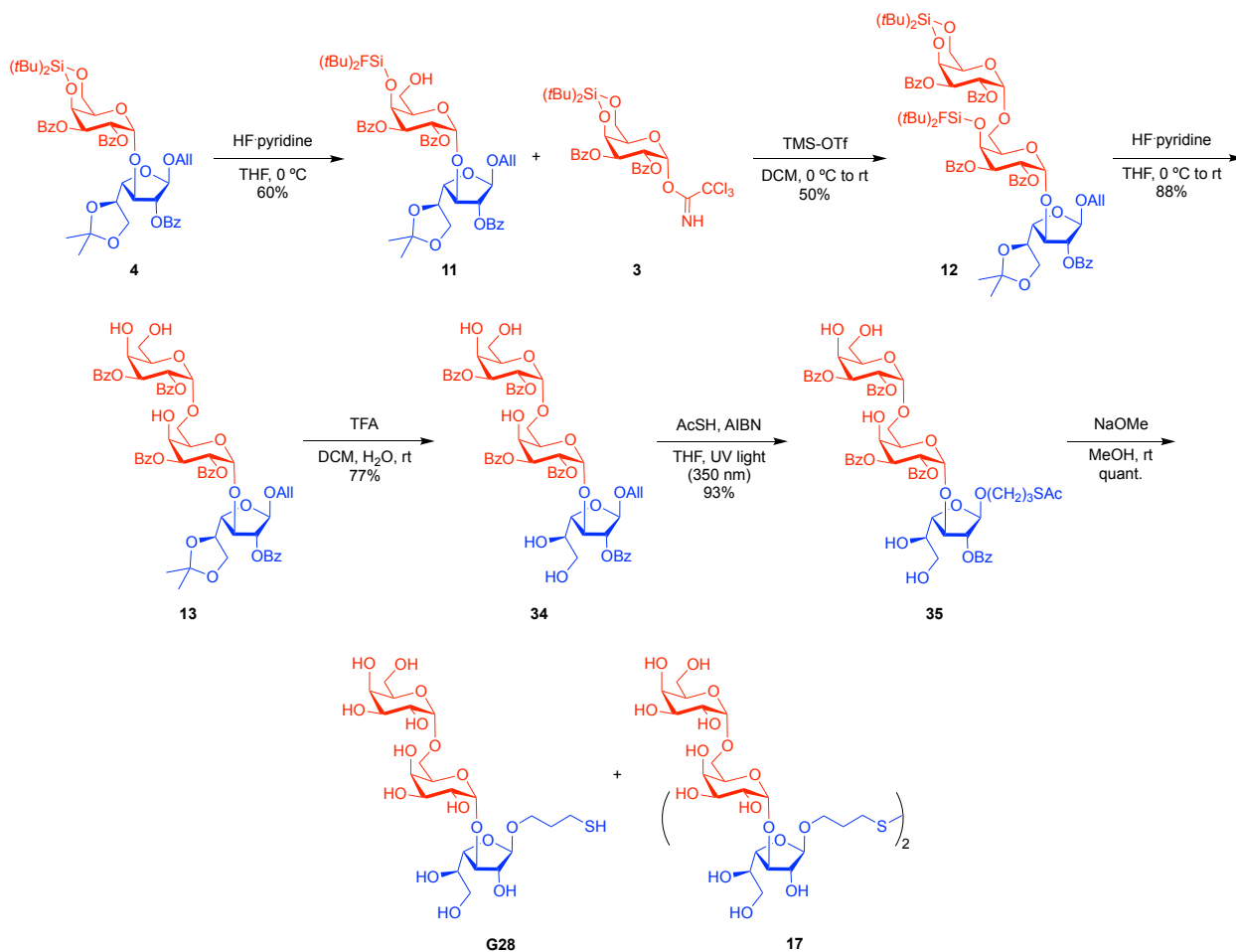
Scheme 9. Synthesis of the mercaptopropyl trisaccharide **G28**.

2.5.2.6.1 Allyl 2,3-di-*O*-benzoyl-4-*O*-di-*tert*-butylsilylenefluorine-α-D-galactopyranosyl-(1→3)-2-*O*-benzoyl-5,6-*O*-isopropylidene-β-D-galactofuranoside (11). The fully protected disaccharide **4** (300 mg, 0.34 mmol) was dissolved in 50 mL of anhydrous THF in a plastic conical tube and cooled 0°C. Next, 100 µL of HF-Pyr (70%) was added and stirred for 2 h at 0°C under Ar. The reaction mixture was then quenched with saturated NaHCO$_3$ solution, extracted with EtOAc 5x, washed with water, brine and dried over MgSO$_4$. The residue was purified by flash chromatography on silica gel (EtOAc/hexanes = 1:4) to furnish the selective desilylated disaccharide **11** (180 mg, 60%) as a white powder. R_f 0.24 (EtOAc/hexanes = 1:4). ^{1}H NMR (400

MHz, CDCl$_3$, 300K) δ 1.00 (s, 9H, *t*Bu); 1.02 (s, 9H, *t*Bu); 1.21 (s, 3H, C*H*$_3$); 1.30 (s, 3H, C*H*$_3$); 2.74 (dd, *J* = 8.6, 4.6 Hz, 1H, O*H*); 3.68-3.87 (m, 3H, H*f*-6a,b, H*p*-6a,b); 3.91-4.00 (m, 1H, H*p*-6a,b); 4.04-4.22 (m, 4H, H-a, H*f*-3, H*f*-4, H*f*-5); 4.23-4.31 (m, 1H, H-a); 4.41 (dd, *J* = 7.90, 4.50 Hz, 1H, H*p*-5); 4.89 (d, $^3J_{3,4}$ = 2.3 Hz, 1H, H*p*-4); 5.19-5.28 (m, 2H, m, 2H, H*f*-1, H-c); 5.32-5.42 (m, 1H, H-c); 5.49 (d, $^3J_{1,2}$ = 3.8 Hz, 1H, H*p*-1); 5.64-5.79 (m, 3H, H*f*-2, H*p*-2, H*p*-3); 5.86-6.00 (m, 1H, H-b); 7.32-7.39 (m, 4H, arom.); 7.41-7.53 (m, 4H, arom.); 7.56-7.63 (m, 1H, arom.); 7.93-8.05 (m, 6H, arom.) ppm. ^{13}C NMR (101 MHz, CDCl$_3$, 300K) δ 20.4 (*C*q-*t*Bu); 20.6 (*C*q-*t*Bu); 25.0 (*C*H$_3$); 26.1 (*C*H$_3$); 27.1 (*t*Bu); 27.2 (*t*Bu); 62.4 (C*p*-6); 65.3 (C*f*-6); 67.8 (C-a); 68.4 (C*p*-2); 71.2 (C*p*-3); 71.4 (C*p*-4); 72.4 (C*p*-5); 75.0; 81.4 (C*f*-2); 83.8; 84.3; 97.9 (C*p*-1); 104.9 (C*f*-1); 109.8 (*C*q-isop.); 117.6 (C-c); 128.2 (*C*-arom.); 128.4 (*C*-arom.); 128.5 (*C*-arom.); 129.1 (*C*q, arom.); 129.3 (*C*q, arom.); 129.5 (*C*q, arom.); 129.7 (*C*-arom.); 129.8 (*C*-arom.); 129.9 x 2 (*C*-arom.); 133.2 (*C*-arom.); 133.3 (*C*-arom.); 133.6 (*C*-arom.); 133.7 (C-b); 165.7 (*C*=O), 165.9 (*C*=O), 166.5 (*C*=O) ppm. ESI-TOF HRMS: *m/z* [M+Na]$^+$ calcd for C$_{47}$H$_{59}$FO$_{14}$Si 917.3556, found: 917.3560.

2.5.2.6.2 Allyl 2,3-di-*O*-benzoyl-4,6-*O*-di-*tert*-butylsilylene-α-D-galactopyranosyl-(1→6)-2,3-di-*O*-benzoyl-4,6-*O*-di-*tert*-butylsilylene-α-D-galactopyranosyl-(1→3)-2-*O*-benzoyl-5,6-*O*-isopropylidene-β-D-galactofuranoside (12).

To a solution of disaccharide acceptor **11** (180 mg, 0.20 mmol) and 4,6-di-*O*-*tert*butylsilyl-2,3-di-*O*-benzoyl-α-D-galactopyranosyl trichloroacetimidate donor **3** (180 mg, 0.27 mmol) in anhydrous DCM (24 mL), freshly activated and crushed 4Å molecular sieves was added and stirred under Ar for 1 h at rt. Then, the solution was cooled down at 0°C, TMS-OTf (11 μL, 0.060 mmol) was added dropwise, and gradually brought it to room temperature and stirred for 1.5 h. To quench the reaction, Et$_3$N was added and stirred. The solution was diluted with DCM, extracted with water and brine solution, dried over MgSO$_4$, filtered, concentrated and purified by column chromatography on silica gel (EtOAc/hexanes = 1:4) to give **12** (132 mg, 50%), as a light-yellow solid. R$_f$ 0.47 (EtOAc/hexanes = 1:3). ^{1}H NMR (400 MHz, CDCl$_3$, 300K) δ 0.83 (s, 9H, *t*Bu); 0.89 (s, 9H, *t*Bu); 0.92 (s, 9H, *t*Bu); 1.13 (s, 9H, *t*Bu); 1.20 (s, 3H, C*H*$_3$); 1.28 (s, 3H, C*H*$_3$); 3.61-3.86 (m, 3H, H*f*-6a,b, H*p*-6a,b); 3.95-4.01 (m, 1H, H*p*-6a,b); 4.02-4.05 (m, 1H, H*f*-4); 4.08-4.39 (m, 8H, H-a, H*p*'-6a,b, H*f*-3, H*f*-5, H*p*'-4, H*p*'-5); 4.51-4.61 (m, 1H, H*p*-5); 4.79-4.84 (m, 1H, H*p*-4); 5.12-5.17 (m, 1H, H-c); 5.27 (d, $^3J_{1,2}$

= 3.4 Hz, 1H, H*p'*-1); 5.31-5.41 (m, 2H, H*f*-1, H-c); 5.51 (s, 1H, H*p*-1); 5.54-5.61 (m, 2H, H*p*-3, H*f*-2); 5.71-5.86 (m, 3H, H*p*-2, H*p'*-2, H*p'*-3); 5.87-6.00 (m, 1H, H-b); 7.28-7.41 (m, 10H, arom.); 7.42-7.56 (m, 5H, arom.); 7.90-8.03 (m, 10H, arom.) ppm. ^{13}C NMR (101 MHz, CDCl$_3$, 300K) δ 20.3 (*C*q-*t*Bu); 20.5 (*C*q-*t*Bu); 20.7 (*C*q-*t*Bu); 23.2 (*C*q-*t*Bu); 25.1 (*C*H$_3$); 26.2 (*C*H$_3$); 26.8 (*t*Bu); 27.0 (*t*Bu); 27.3 (*t*Bu); 27.5 (*t*Bu); 65.4 (C*p*-6); 65.5 (C*f*-6); 67.1; 67.1 (CH$_2$, C*p'*-6); 67.7 (C-a); 68.4 (C*p*-2); 68.6; 70.2 (C*p*-5); 71.0 (C*p*-3); 71.2 (C*p*-4); 71.5; 75.4; 77.2; 81.0 (C*f*-2); 83.9; 85.0 (C*f*-4); 96.5 (C*p'*-1); 98.3 (C*p*-1); 105.0 (C*f*-1); 109.8 (*C*q-*isop*.); 116.9 (C-c); 128.2 x 2 (*C*-arom.); 128.3 (*C*-arom.); 128.4 x 2 (*C*-arom.); 129.2 (*C*q, arom.); 129.3 (*C*q, arom.); 129.5 (*C*q, arom.); 129.6 (*C*-arom.); 129.7 (*C*q, arom.); 129.7 (*C*-arom.); 129.8 (*C*-arom.); 129.9 x 2 (*C*-arom.); 130.0 (*C*q, arom.); 132.8 (*C*-arom.); 133.0 (*C*-arom.); 133.1 (*C*-arom.); 133.2 (*C*-arom.); 133.4 (*C*-arom.); 134.1 (C-b); 165.5 (*C*=O), 165.7 (*C*=O), 165.9 (*C*=O), 166.2 (*C*=O), 166.3 (*C*=O) ppm. ESI-TOF HRMS: *m/z* [M+Na]$^+$ calcd for C$_{75}$H$_{93}$FO$_{21}$Si$_2$ 1427.5630, found: 1427.5625.

2.5.2.6.3 Allyl 2,3-di-*O*-benzoyl-α-D-galactopyranosyl-(1→6)-2,3-di-*O*-benzoyl-α-D-galactopyranosyl-(1→3)-2-*O*-benzoyl-5,6-*O*-isopropylidene-β-D-galactofuranoside (13).

The fully protected trisaccharide **12** (39 mg, 0.028 mmol) was dissolved in 8.0 mL of anhydrous THF in a plastic conical tube and cooled 0°C. Then, 80 μL of HF-Pyr (70%) was added and stirred for 30 min. at 0°C and 30 min. at rt under Ar. The reaction mixture was cooled again to 0°C and quenched with saturated a NaHCO$_3$ solution. Finally, the mixture was extracted with EtOAc x5, washed with water and brine, dried over MgSO$_4$, concentrated, and purified by PTLC on silica gel (DCM/MeOH = 20:1) to furnish the desilylated trisaccharide **13** (27 mg, 88%) as a white powder. R$_f$ 0.36 (DCM/MeOH = 15:1). ^{1}H NMR (400 MHz, CDCl$_3$, 300K) δ 1.18 (s, 3H, C*H$_3$*); 1.29 (s, 3H, C*H$_3$*); 3.67-3.89 (m, 3H, H*f*-6a,b, H*p*-6a,b); 3.92-4.21 (m, 8H, H-a, H*p*-6a,b, H*p'*-6a,b, H*p*-4, H*f*-3, H*f*-4, H*f*-5,); 4.24-4.31 (m, 1H, H-a); 4.34 (m, 1H, H*p'*-4); 4.43 (m, 1H, H*p'*-5); 4.48-4.57 (m, 1H, H*p*-5); 5.19 (dd, *J* = 10.4, 1.5 Hz, 1H, H-c); 5.25 (s, 1H, H*f*-1); 5.30-5.38 (m, 1H, H-c); 5.40 (d, *J* = 2.9 Hz, 1H, H*p'*-1); 5.43 (d, *J* = 3.8 Hz, 1H, H*p*-1); 5.49-5.56 (m, 2H, H*p*-3, H*f*-2); 5.60-5.73 (m, 3H, H*p*-2, H*p'*-2, H*p'*-3); 5.84-6.00 (m, 1H, H-b); 7.17-7.25 (m, 3H, arom.); 7.32-7.61 (m, 12H, arom.); 7.87-8.07 (m, 10H, arom.) ppm. ^{13}C NMR (101 MHz, CDCl$_3$, 300K) δ 25.0 (*C*H$_3$); 26.2 (*C*H$_3$); 63.1 (C*p'*-6); 65.3 (C*f*-6); 66.8 (C*p*-6); 67.9 (C-a); 68.1; 68.7; 68.8 (C*p*-5); 68.8; 69.5; 69.6; 70.6; 71.0; 74.9; 81.5 (C*f*-2); 83.0; 84.4; 97.5 (C*p'*-1); 97.9 (C*p*-1); 105.0 (C*f*-1); 109.8 (*C*q-*isop*.); 117.3 (C-c); 128.3 (*C*-arom.); 128.4 (*C*-arom.); 128.6 (*C*-arom.); 129.1 (*C*q,

arom.); 129.2 x 2 (*C*q, arom.); 129.3 (*C*q, arom.); 129.4 (*C*q, arom.); 129.6 (*C*-arom.); 129.7 (*C*-arom.); 129.8 (*C*-arom.); 133.1 (*C*-arom.); 133.2 (*C*-arom.); 133.3 (*C*-arom.); 133.6 (*C*-arom.); 133.9 (C-b); 165.4 (*C*=O); 165.6 (*C*=O); 165.7 (*C*=O); 165.8 (*C*=O); 165.9 (*C*=O) ppm. ESI-TOF HRMS: *m/z* [M+Na]$^+$ calcd for $C_{59}H_{60}O_{21}$ 1127.3525, found: 1127.3524.

2.5.2.6.4 Allyl 2,3-di-*O*-benzoyl-α-D-galactopyranosyl-(1→6)-2,3-di-*O*-benzoyl-α-D-galactopyranosyl-(1→3)-2-*O*-benzoyl-β-D-galactofuranoside (34).

To a solution of trisaccharide **13** (27 mg, 0.024 mmol) in DCM (3.0 mL), H$_2$O (300 μL) and TFA (300 μL) were consecutively added, and the mixture was vigorously stirred at rt for 15 min. After disappearance of starting material based on TLC, the resulting solution was twice co-evaporated with EtOH (10 mL). The residue was then further dried under vacuum and purified by PTLC on silica gel (DCM/MeOH = 15:1) to afford the partially deprotected **34** (20 mg, 77%) as a yellow syrup. R$_f$ 0.30 (DCM/MeOH = 15:1). ^{1}H NMR (400 MHz, MeOD, 300K) δ 3.46-3.61 (m, 2H, H*f*-6a,b); 3.63-3.69 (m, 1H); 3.72-3.90 (m, 3H, H*p*-6a,b, H*p*'-6a,b); 3.98-4.12 (m, 2H, H-a, H*p*'-6a,b); 4.20-4.33 (m, 5H, H-a,); 4.37-4.40 (m, 1H); 4.57-4.66 (m, 1H); 5.07-5.14 (m, 1H, H-c); 5.26-5.38 (m, 3H, H-c, H*f*-1, H*p*'-1); 5.55 (br.s., 1H, H*p*-1); 5.60-5.71 (m, 5H, H*f*-2, H*p*-2, H*p*-3, H*p*'-2, H*p*'-3); 5.84-5.98 (m, 1H, H-b); 7.25-7.43 (m, 11H, arom.); 7.48-7.57 (m, 4H, arom.); 7.87-7.98 (m, 8H, arom.); 8.04-8.09 (m, 2H, arom.) ppm. ^{13}C NMR (101 MHz, MeOD, 300K) δ 62.6 (C*p*'-6); 64.4 (C*f*-6); 67.7 (C*p*-6); 68.8; 69.0 (C-a); 69.3; 70.5; 70.7; 71.1; 72.2; 72.7; 72.9; 73.0; 83.0; 85.0; 85.4; 98.5 (C*p*'-1); 99.4 (C*p*-1); 106.6 (C*f*-1); 117.4 (C-c); 129.5 (*C*H, arom.); 129.6 (*C*H, arom.); 129.71 x 2 (*C*H, arom.); 129.8 (*C*H, arom.); 130.8 x 2 (*C*H, arom.); 130.9 x 2 (*C*H, arom.); 131.0 (*C*q, arom.); 131.1 (*C*q, arom.); 131.2 (*C*q, arom.); 131.3 (*C*q, arom.); 135.7 134.4 (*C*-arom.); 134.5 (*C*-arom.); 134.6 (*C*-arom.); 134.7 x 2 (*C*-arom.); (C-b); 167.3 (*C*=O); 167.4 (*C*=O); 167.5 x 2 (*C*=O); 167.6 (*C*=O) ppm. ESI-TOF HRMS: *m/z* [M+Na]$^+$ calcd for $C_{56}H_{56}O_{21}$ 1087.3212, found: 1087.3202.

2.5.2.6.5 (Acetylthio)propyl 2,3-di-*O*-benzoyl-α-D-galactopyranosyl-(1→6)-2,3-di-*O*-benzoyl-α-D-galactopyranosyl-(1→3)-2-*O*-benzoyl-β-D-galactofuranoside (35).

To a solution of allyl trisaccharide **34** (12 mg, 0.011 mmol) and AIBN (2.5 mg, 0.015 mmol) in anhydrous THF (3 mL) under Ar, thioacetic acid (6 μL, 0.08 mmol) was added, and the mixture was stirred under

water cooling (~ 25 °C) for 12 h in a Rayonet UV reactor equipped with 350 nm lamps. The solution was then co-evaporated with toluene and concentrated to near dryness. The crude product was purified by PTLC on silica gel (DCM/MeOH = 10:1) to afford the acyl-protected trisaccharide **35** (12 mg, 93%) as a white solid. R_f 0.30 (DCM/MeOH = 10:1). ^{1}H NMR (400 MHz, MeOD, 300K) δ 1.72-1.90 (m, 2H, H-b); 2.20 (s, 3H, CH_3); 2.90-2.98 (m, 2H, H-c); 3.46-3.59 (m, 2H, Hf-6a,b); 3.63-3.67 (m, 1H); 3.72-3.92 (m, 4H); 4.04-4.12 (m, 1H); 4.24-4.38 (m, 5H); 4.59 (s, 1H); 4.66-4.72 (m, 1H); 5.31 (d, $^3J_{1,2}$ = 2.57 Hz, 1H, Hp'-1); 5.36 (s, 1H, Hf-1); 5.57 (d, $^3J_{1,2}$ = 2.20 Hz, 1H, Hp-1); 5.61-5.75 (m, 5H, Hf-2, Hp-2, Hp-3, Hp'-2, Hp'-3); 7.26-7.46 (m, 11H, arom.); 7.48-7.57 (m, 4H, arom.); 7.85-7.99 (m, 8H, arom.); 8.04-8.09 (m, 2H, arom.) ppm. ^{13}C NMR (101 MHz, MeOD, 300K) δ 27.3 (C-c); 30.7 (CH$_3$); 31.1 (C-b); 62.7 (Cp'-6); 64.5 (Cf-6); 66.7 (Cp-6); 67.88 (C-a); 69.1; 69.3; 70.6; 71.0; 71.2; 72.1; 72.6; 72.9; 73.1; 82.5; 85.4; 85.9; 98.3 (Cp'-1); 99.6 (Cp-1); 107.1 (Cf-1); 129.5 (C-arom.); 129.6 (C-arom.); 129.7 x 2 (C-arom.); 129.8 (C-arom.); 130.8 (C-arom.); 130.9 (C-arom.); 131.0 (Cq, arom.); 131.1 (Cq, arom.); 131.2 (Cq, arom.); 131.3 x 2 (Cq, arom.); 134.4 (C-arom.); 134.5 (C-arom.); 134.6 x 2 (C-arom.); 134.7 (C-arom.); 167.3 (C=O); 167.4 (C=O); 167.5 (C=O); 167.6 (C=O); 167.7 (C=O); 197.6 (C=O) ppm. ESI-TOF HRMS: m/z [M+Na]$^+$ calcd for C$_{58}$H$_{60}$O$_{22}$S 1163.3195, found: 1163.3194.

2.5.2.6.6 Thiopropyl α-D-galactopyranosyl-(1→6)-α-D-galactopyranosyl-(1→3)-β-D-galactofuranoside (G28). The acyl-protected trisaccharide **35** (20 mg, 0.018) was dissolved in 3.0 mL of anhydrous 0.25 M NaOMe, and stirred for 2 hours under Ar. The solution was then neutralized with Amberlyst-15, filtered through Celite, concentrated and finally dissolved in water and lyophilized. Initially, the unprotected mercaptopropyl trisaccharide **G28** is produced, which oxidizes by handling on air within hours to the disulfide **17** (10 mg, quant.) as an off-white solid. R_f 0.25 (iPrOH/H$_2$O = 5:1 w/3 drops AcOH). ESI-TOF HRMS: m/z [M+Na]$^+$ calcd for C$_{21}$H$_{38}$O$_{16}$S for C$_{42}$H$_{74}$O$_{32}$S$_2$ 1177.3502, found 1177.3664.

2.5.2.6.7 Synthesis of the NGP28b [Gal$p$α1,6Gal$p$α1,3Gal$f$β-linker-BSA]. MALDI-TOF MS: m/z for BSA [M+H]$^+$ 66120; for NGP2B [M+H]$^+$ 85874.
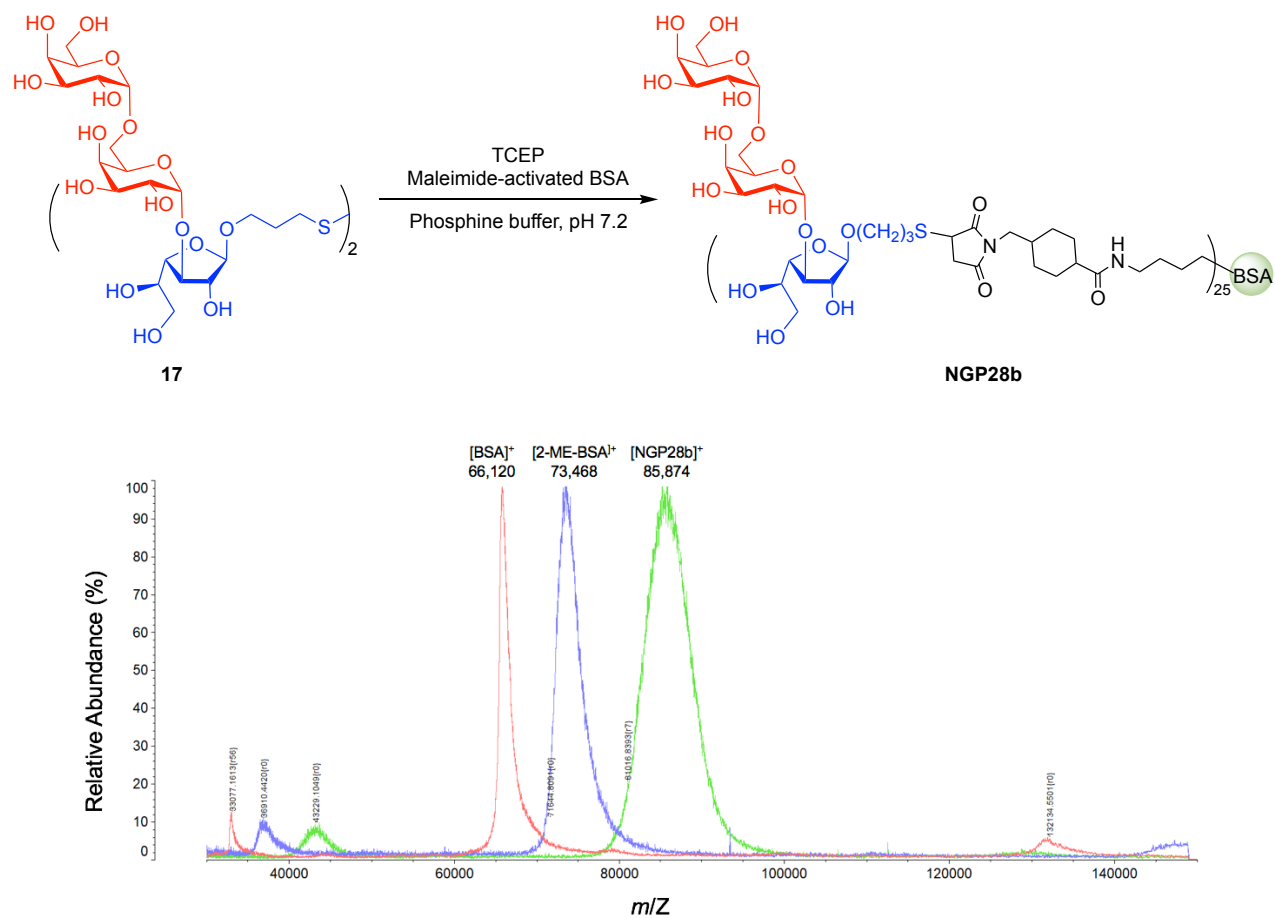
Figure 19. (Top) Schematic representation of conjugation of **G28** to BSA. (Bottom) MALDI-TOF mass spectra of **NGP28b** [Galαp1,6Galαp1,3Galβf-linker-BSA] overlaid with pure BSA and 2-ME-linker-BSA.
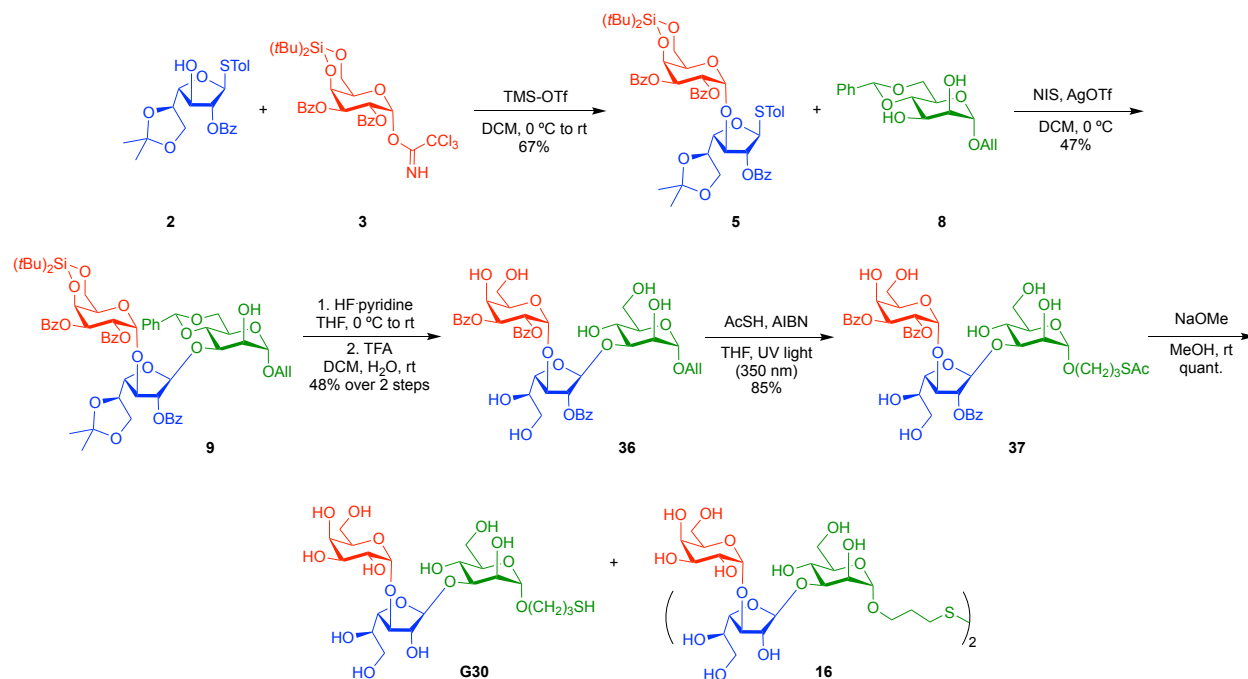
Scheme 10. Synthesis of the mercaptopropyl trisaccharide **G30**.

2.5.2.7.1 *p*-Tolyl 2,3-di-*O*-benzoyl-4,6-*O*-di-*tert*-butylsilylene-α-D-galactopyranosyl-(1→3)-2-*O*-Benzoyl-5,6-*O*-isopropylidene-1-thio-β-D-galactofuranoside (5).

To a solution of Gal*f* acceptor **2** (520 mg, 1.21 mmol) and Gal*p* donor **3** (1.11 g, 1.65 mmol) in anhydrous DCM (186 mL), freshly activated MS 4Å was added and stirred under Ar for 1 h at rt. Then, the solution was cool down to 0°C and TMS-OTf (77.0 μL, 0.43 mmol) was added dropwise. The solution was gradually brought to rt and after 1 h, the reaction mixture was quenched by addition of Et$_3$N, filtered, and washed with water and brine. The organic layers were dried over MgSO$_4$, concentrated, and purified by flash column chromatography on silica gel (EtOAc/Hexanes = 1:5) to give the disaccharide donor **5** as a yellow powder (756 mg, 67%). R$_f$ = 0.30 (EtOAc/Hexanes = 1:5). ^{1}H NMR (400 MHz, CDCl$_3$) δ 0.96 (s, 9H, *t*Bu); 1.06 (s, 9H, *t*Bu); 1.19 (s, 3H, C*H$_3$*); 1.36 (s, 3H, C*H$_3$*); 2.32 (s, 3H, arom.C*H$_3$*); 3.81 (d, *J* = 6.6 Hz, 2H, H*f*-6a,b); 4.12-4.23 (m, 3H, H*p*-5, H*f*-5, H*p*-6a,b); 4.27-4.38 (m, 3H, H*f*-3, H*f*-4, H*p*-6a,b); 4.93 (d, $^3J_{3,4}$ = 3.0 Hz, 1H, H*p*-4); 5.49 (d, $^3J_{1,2}$ = 3.79 Hz, 1H, H*p*-1); 5.53-5.59 (m, 2H, H*f*-1, H*f*-2); 5.63 (dd, $^3J_{2,3}$ = 10.6, $^3J_{3,4}$ = 3.0 Hz, 1H, H*p*-3); 5.80 (dd, $^3J_{2,3}$ = 10.6, $^3J_{1,2}$ = 3.8 Hz, 1H, H*p*-2); 7.10 (d, *J* = 8.2 Hz, 2H, arom.); 7.31-

7.64 (m, 11H, arom.); 7.99-8.14 (m, 6H, arom.) ppm. ^{13}C NMR (101 MHz, CDCl$_3$, 300K) δ 20.7 (*C*q-*t*Bu); 21.1 (arom.*C*H$_3$); 23.2 (*C*q-*t*Bu); 24.7 (*C*H$_3$); 25.9 (*C*H$_3$); 27.2 (*t*Bu); 27.5 (*t*Bu); 65.2 (C*f*-6); 66.8 (C*p*-6); 67.8 (C*p*-5); 68.3 (C*p*-2); 71.0 (C*p*-3); 71.1 (C*p*-4); 73.7 (C*f*-5); 81.5; 82.2 (C*f*-2); 82.5; 91.0 (C*f*-1); 96.6 (C*p*-1); 109.8 (*C*q-*isop*.); 128.3 (*C*-arom.); 128.4 (*C*-arom.); 128.6 (*C*-arom.); 129.1 (*C*q, arom.); 129.4 (*C*q, arom.); 129.7 x 2 (*C*-arom.); 129.8 (*C*-arom.); 129.9 x 2 (*C*q, arom.); 130.0 (*C*-arom.); 132.8 (*C*-arom.); 133.1 (*C*-arom.); 133.3 (*C*-arom.); 133.6 (*C*-arom.); 137.9 (*C*q); 165.3 (*C*=O); 166.0 (*C*=O); 166.2 (*C*=O) ppm. ESI-TOF HRMS: *m/z* [M+Na]$^+$ calcd for C$_{51}$H$_{60}$O$_{13}$SSi 963.3422, found 963.3489.

2.5.2.7.2 Allyl 2,3-di-*O*-benzoyl-4,6-*O*-di-*tert*-butylsilylene-α-D-galactopyranosyl-(1→3)-2-*O*-Benzoyl-5,6-*O*-isopropylidene-β-D-galactofuranosyl-(1→3)-4,6-*O*-benzylidene-α-D-mannopyranoside (9).

To a solution of Man*p* acceptor **8** (429 mg, 1.39 mmol) and disaccharide donor **5** (414 mg, 0.44 mmol) in anhydrous DCM (78 mL), NIS (248 mg, 1.10 mmol) and AgOTf (7.0 mg, 0.027 mmol) were added consecutively at 0 °C. After 45 min, the reaction mixture was quenched by addition of Et$_3$N, filtered, and washed with a saturated solution of Na$_2$S$_2$O$_3$ and brine. The organic layers were dried over MgSO$_4$, concentrated, and purified by column chromatography on silica gel (EtOAc/Hexanes = 1:3) to give the desired fully protected trisaccharide **9** (231 mg, 47%), as a light-yellow powder. R$_f$ 0.27 (EtOAc/Hexanes = 1:3). ^{1}H NMR (400 MHz, CDCl$_3$, 300K) δ 0.94 (s, 9H, *t*Bu); 1.06 (s, 12H, *t*Bu, C*H*$_3$); 1.30 (s, 3H, C*H*$_3$); 3.21 (s, 1H); 3.32-3.40(m, 1H, H*f*-6a,b); 3.59 (dd, *J* = 8.4, 6.5 Hz, 1H, H*f*-6a,b); 3.71-3.90 (m, 3H, H*m*-6a,b); 3.92-4.26 (m, 10H, Ha, H*p*-6a,b, H*m*-6a,b); 4.32 (dd, *J* = 7.2, 3.4 Hz, 1H, H*f*-3); 4.84 (d, $^3J_{3,4}$ = 2.8 Hz, 1H, H*p*-4); 4.97 (d, *J* = 1.1 Hz, 1H, H*m*-1); 5.15-5.24 (m, 3H, H*f*-1, H-c, H*f*-2); 5.29 (dq, *J* = 17.2, 1.5 Hz, 1H, H-c); 5.38 (s, 1H, OC*H*Ph); 5.49 (d, $^3J_{1,2}$ = 3.7 Hz, 1H, H*p*-1); 5.61 (dd, $^3J_{2,3}$ = 10.6, $^3J_{3,4}$ = 2.8 Hz, 1H, H*p*-3); 5.76 (dd, $^3J_{2,3}$ = 10.6, $^3J_{1,2}$ = 3.7 Hz, 1H, H*p*-2); 5.82-5.94 (m, 1H, H-b); 7.23-7.30 (m, 3H, arom.); 7.32-7.64(m, 11H, arom.); 7.95-8.07 (m, 6H, arom.) ppm. ^{13}C NMR (101 MHz, CDCl$_3$, 300K) δ 20.7 (*C*q-*t*Bu); 23.2 (*C*q-*t*Bu); 24.8 (*C*H$_3$); 25.9 (*C*H$_3$); 27.2 (*t*Bu); 27.4 (*t*Bu); 63.7; 64.9 (C*f*-6); 66.7 (C*p*-6); 67.8; 68.2 (C-a); 68.5 (C*p*-2); 68.7 (C*m*-6); 69.0; 70.6 (C*p*-3); 71.2 (C*p*-4); 73.0; 73.6; 76.6; 79.8; 81.2 (C*f*-3); 83.9 (C*f*-2); 97.2 (C*p*-1); 99.3 (C*m*-1); 101.6 (OC*H*Ph); 103.1 (C*f*-1); 109.5 (*C*q-*isop*.); 117.9 (C-c); 126.1 (*C*-arom.); 128.1 (*C*-arom.); 128.4 (*C*-arom.); 128.6 (*C*-arom.); 128.7 (*C*-arom.); 128.8 (*C*q, arom.); 129.3 (*C*q, arom.); 129.7 (*C*-arom.); 129.8 (*C*-arom.); 129.9 (*C*-arom.); 133.1 (*C*-arom.); 133.4 (*C*-arom.); 133.5 (C-b); 133.7 (*C*-arom.);

56

137.6 (Cq); 166.0 (*C*=O); 166.1 (*C*=O); 166.3 (*C*=O) ppm. ESI-TOF HRMS: *m/z* [M+Na]+ calcd for $C_{60}H_{72}O_{19}Si$ 1147.4335, found 1147.4332.

2.5.2.7.3   Allyl   2,3-di-*O*-benzoyl-α-D-galactopyranosyl-(1→3)-2-*O*-Benzoyl-β-D-galactofuranosyl-(1→3)-α-D-mannopyranoside (36). The fully protected trisaccharide **9** (60 mg, 0.053 mmol) was dissolved in a mixture ratio (1:100 HF·Pyridine/dry THF) (120 μL/12 mL) in a plastic conical tube and stirred for 30 min at 0°C and 30 min at rt under Ar. The reaction mixture was cooled down again to 0°C and quenched with saturated NaHCO₃. Then, the resulting solution was diluted and extracted with EtOAc, washed with water and brine, dried over MgSO₄, and concentrated to yield the desilylated trisaccharide as a light-yellow oil. R*f* 0.16 (EtOAc/Hexanes 1:1). Without further purification, to a solution of the resulted trisaccharide (60 mg, 0.06 mmol) in DCM (9.0 mL), H₂O (900 μL) and TFA (900 μL) were consecutively added, and the mixture was vigorously stirred at rt for 20 min. After disappearance of starting material based on TLC, the resulting solution was co-evaporated with EtOH (10 mL) twice. The residue was then further dried under vacuum and purified by PTLC on silica gel (DCM/MeOH = 10:1) to afford the partially deprotected trisaccharide **36** (22 mg, 48%) as a light-yellow syrup. R*f* 0.33 (DCM/MeOH = 10:1). ¹H NMR (400 MHz, MeOD, 300K) δ 3.49-3.70 (m, 5H); 3.71-3.97 (m, 6H); 3.99-4.10 (m, 2H, H-a); 4.23 (dd, *J* = 13.0, 5.0 Hz, 1H, H-a); 4.34-4.41 (m, 2H, H*p*-4); 4.44-4.50 (m, 2H, H*p*-5); 5.17 (d, *J* = 10.4 Hz, 1H H-c); 5.26-5.38 (m, 2H, H*f*-1, H-c); 5.55 (d, $^{3}J_{1,2}$ = 3.8 Hz, 1H, H*p*-1); 5.59-5.75 (m, 3H, H*p*-2, H*p*-3, H*f*-2); 5.87-5.99 (m, 1H, H-b); 7.35-7.44 (m, 4H, arom.); 7.46- 7.58 (m, 4H, arom.); 7.59-7.67 (m, 1H, arom.); 7.98 (t, *J* = 8.7 Hz, 4H, arom.); 8.08 (d, *J* = 7.7 Hz, 2H, arom.) ppm. Missing one H-1, because is right there under the MeOH peak. ¹³C NMR (101 MHz, MeOD, 300K) δ 62.2 (CH₂); 63.2 (CH₂); 64.5 (CH₂); 67.0; 68.9; 69.1; 69.0 (C-a); 70.5; 72.3; 72.7; 73.0; 75.1; 78.2; 83.8; 84.0 (C*f*-2); 85.4 (C*p*-5); 99.6 (C*p*-1); 100.6 (C*m*-1); 105.0 (C*f*-1); 117.7 (C-c); 129.6 (*C*-arom.); 129.7 (*C*-arom.); 129.8 (*C*-arom.); 130.8 (*C*q, arom.); 130.9 (*C*-arom.); 131.0 (*C*q, arom.); 131.1 (*C*-arom.); 131.2 (*C*q, arom.); 134.6 (*C*-arom.); 134.7 (*C*-arom.); 134.8 (*C*-arom.); 135.5 (C-b); 167.6 (*C*=O); 167.7 (*C*=O) ppm. ESI-TOF HRMS: *m/z* [M+Na]+ calcd for $C_{42}H_{48}O_{19}$ 879.2687, found 879.2897.

2.5.2.7.4 (Acetylthio)propyl 2,3-di-*O*-benzoyl-α-D-galactopyranosyl-(1→3)-2-*O*-Benzoyl-β-D-galactofuranosyl-(1→3)-α-D-mannopyranoside (37). To a solution of **36** (22 mg, 0.026 mmol) and AIBN (6.3 mg, 0.038 mmol) in anhydrous THF (6 mL), AcSH (18 μL, 0.25 mmol) was added and stirred under argon for 5 min. The solution was then placed in a Rayonet UV reactor (350 nm) stirred for 12 h under water cooling (~rt). The solution was concentrated by two co-evaporations with toluene, and purified by PTLC on silica gel (DCM/MeOH = 10:1) to give the acyl-protected trisaccharide **37** as a white powder (20.5 mg, 85%). R_f = 0.32 (DCM/MeOH = 10:1). ^{1}H NMR (400 MHz, MeOD, 300K) δ 1.81-1.91 (m, 2H, H-b); 2.29 (s, 3H, CH_3); 2.85-3.06 (m, 2H, H-c); 3.43-3.96 (m, 12H); 4.07 (br. s., 1H, Hm-2); 4.34-4.41 (m, 2H, Hp-4); 4.44-4.50 (m, 2H, Hp-5); 4.59 (s, 1H); 4.81 (s, 1H, Hm-1); 5.36 (s, 1H, Hf-1); 5.49 (s, 2H); 5.55 (d, $^3J_{1,2}$ = 3.7 Hz, 1H, Hp-1); 5.59-5.75 (m, 3H, Hp-2, Hp-3, Hf-2); 7.35-7.45 (m, 4H, arom.); 7.46-7.58 (m, 4H, arom.); 7.59-7.68 (m, 1H, arom.); 7.97 (t, J = 8.7 Hz, 4H, arom.); 8.08 (d, J = 7.6 Hz, 2H, arom.) ppm. ^{13}C NMR (101 MHz, MeOD, 300K) δ 27.0 (C-c); 30.6 (CH_3); 30.8 (C-b); 62.2 (CH_2); 63.2 (CH_2); 64.6 (CH_2); 67.0; 67.2 (C-a); 68.9; 69.1; 70.5; 72.3; 72.8; 73.0; 75.1; 78.4; 83.8; 84.0; 85.3; 99.6 (Cp-1); 101.5 (Cm-1); 105.1 (Cf-1); 129.6 (*C*-arom.); 129.7 (*C*-arom.); 129.8 (*C*-arom.); 130.8 (*C*q, arom.); 130.9 (*C*-arom.); 131.0 (*C*q, arom.); 131.1 (*C*-arom.); 131.2 (*C*q, arom.); 134.6 (*C*-arom.); 134.7 (*C*-arom.); 134.8 (*C*-arom.); 167.6 (*C*=O); 167.7 (*C*=O); 197.6 (*C*=O) ppm. ESI-TOF HRMS: m/z [M+Na]$^+$ calcd for $C_{44}H_{52}O_{20}S$ 955.2670, found 955.2994.

2.5.2.7.5 Thiopropyl α-D-galactopyranosyl-(1→3)-β-D-galactofuranosyl-(1→3)-α-D-mannopyranoside (G30). The acyl-protected trisaccharide **37** (20 mg, 0.021) was dissolved in 3.0 mL of 0.25 M NaOMe, and stirred for 2 h under Ar. The solution was then neutralized with Amberlyst-15, filtered through Celite, concentrated and finally dissolved in water and lyophilized. Initially, the unprotected mercaptopropyl trisaccharide **G30** was produced, which oxidizes by handling on air within hours to the disulfide **16** (12 mg, quant.) as an off-white solid. R_f 0.25 (*i*PrOH/H_2O = 5:1 w/3 drops AcOH). ESI-TOF HRMS: m/z [M+Na]$^+$ calcd for $C_{21}H_{38}O_{16}S$ for $C_{42}H_{74}O_{32}S_2$ 1177.3502, found 1177.3508.

2.5.2.7.6 Synthesis of the NGP30b [Gal*p*α1,3Gal*f*β1,3Man*p*α-linker-BSA]. MALDI-TOF MS: m/z for BSA [M+H]$^+$ 66120; for NGP30B [M+H]$^+$ 88196.
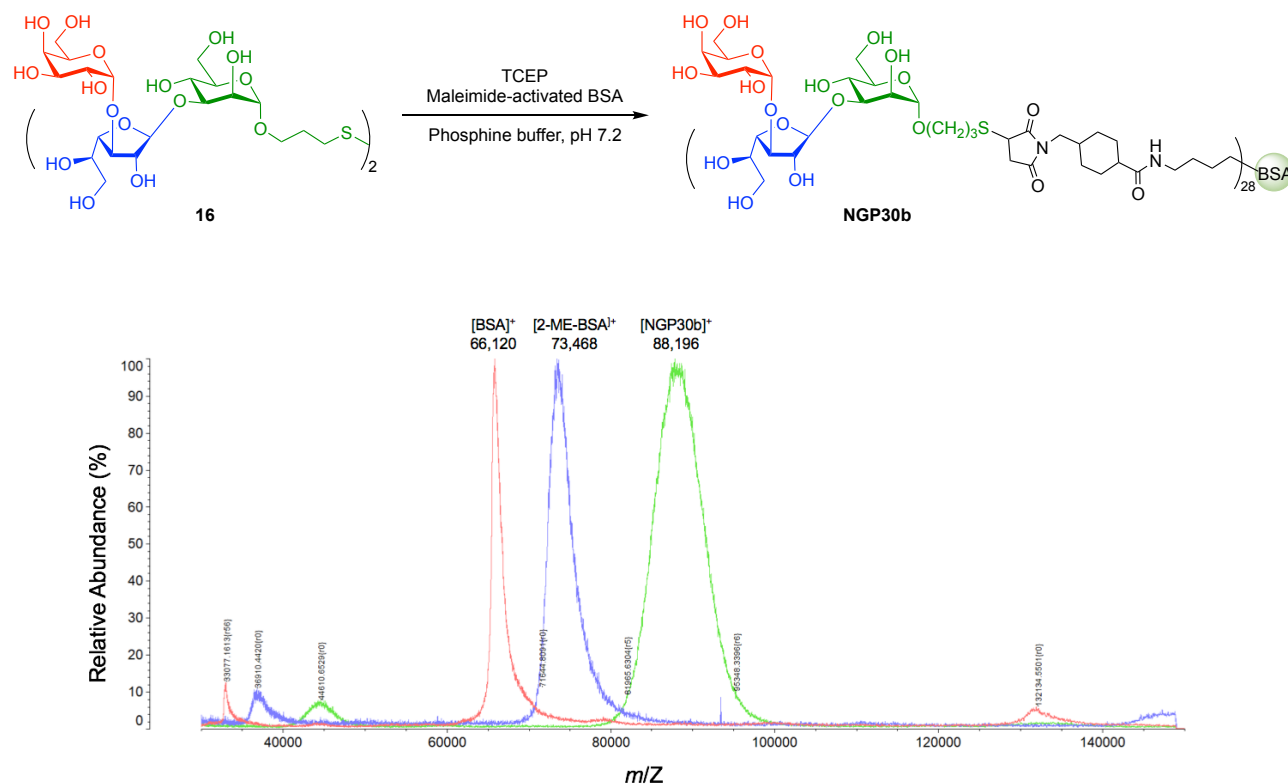
Figure 20. (Top) Schematic representation of conjugation of **G30** to BSA. (Bottom) MALDI-TOF mass spectra of **NGP30b** [Gal*p*α1,3Gal*f*β1,3Man*p*α-linker-BSA] overlaid with pure BSA and 2-ME-linker-BSA.

2.5.3 Biological data

2.5.3.1 Cohort description

All patient samples were collected by collaborators. The KSA samples were collected chiefly by Dr. Waleed Al-Salem, Mr. Yasser Al-Raey and the Saudi Ministry of Health in collaboration with other colleagues at LSTM. Molecular analysis of the samples was performed by Dr. Waleed Al-Salem and Mr. Yasser Al-Raey.

The collection was conducted at two sites, one in Al-Ahsa, and the other in Asir (**Table 5**). Individuals with suspected CL were referred to the clinic and diagnosed first by dermatological examination and microscopy analysis, and then by PCR. Briefly, lesion aspirates were taken for

59

culture and microscopy confirmation of parasites, as were swabs for *ITS*1-PCR RFLP

identification of *Leishmania* species. Serum samples were also collected at the same time. Where

possible, patient samples were collected before any treatment had commenced. Where secondary

infection was present (fungal or bacterial), antibiotics or antifungals were prescribed first, before

assignation of either intralesional or intramuscular sodium stibogluconate (Pentostam®). Where

patients returned to the clinic for subsequent treatment, additional samples were collected. Blood

type, gender, lesion number, nationality and age were recorded.

Table 7. Description of the cohort evaluated in this study.

Characteristics	*L. major* (n = 56) *	*L. tropica* (n = 15)
Gender	Male = 54 Female = 1 Missing = 1	Male = 7 Female = 8
Age[†]	33 (16 - 67)	20 (10-58)
Province	Al Ahsa = 54 Asir = 1 Missing = 1	Asir = 15
Lesion Number	1-5 = 42 6-11 = 10 12+ = 3 Missing = 1	1 = 13 2-5 = 2
Appearance of Lesion	Nodular = 13 Nodular/Ulcer = 8 Papular = 11 Scar = 3 Ulcerative = 14 Missing = 4 Mixed = 3 ◊	Nodular = 2 Nodular/Ulcer = 5 Papular = 3 Scar = 4 Ulcerative =1
Nationality	Bangladesh = 5 Egypt = 13 Filipino = 3 India = 17 Nepal = 5 Pakistan = 4 Saudi = 4	Bangladesh = 1 Saudi = 14

60

	Other = 5 [□]	
	A = 17	A = 7
	B = 14	AB = 1
Blood Type	AB = 4	O = 7
	O = 14	
	Missing = 7	

∗ 1st visit (n = 56), 2nd visit (n = 33), 3rd visit (n= 15)

[†] Median age with range in brackets

[•] Papular + one other lesion type (n =4)

[◊] Three or more lesion types

[□] Yemen/Lebanon/Bedouin-Saudi (n= 1), Sudan (n = 2)

2.5.3.2 CL-ELISA Protocol

Levels of *Leishmania* anti-α-Gal IgG antibodies in human sera was determined essentially as previously described.[44, 70] The antibodies and concentrations varied between assays (see **Table 6** for details), but the overall imunoassay steps remained the same. Briefly, white 96-well plates (Nunc) were coated with the appropriate NGP in 0.2 M carbonate: bicarbonate buffer (pH 9.6) at 4°C, overnight, at concentrations determined through titration experiments. The plates were blocked with 200 µL/well 1% BSA-PBS (PBS-B), and serially incubated with antibodies; all incubations were performed at 37 °C for 1 h. Plates were washed between incubations, three times with PBS-T. The luminescence was developed with SuperSignal™ ELISA Pico Chemiluminescent Substrate (ThermoFisher, 37070) diluted 1:1:8 in 0.2 M carbonate-bicarbonate buffer. Controls for each NGP/sera pool combination were included in triplicate on each plate; antigen negative, primary negative, secondary negative, and HRP negative control. The average RLU was taken for these controls and subtracted from the average of the unknown sample replicates to control for nonspecific/background signal from the reagents.

61

The cutoff of each immunoassay microplate was determined using the method described by Frey et al.[92]. Briefly, we first defined the upper prediction limit, expressed as the standard deviation (SD) multiplied by a factor (SD*f*), calculated based on the Student *t*-distribution, according to the number of negative controls (NC) in each plate and a confidence level $(1 - \alpha)$ of 95%. Therefore, cutoff value was calculated as the NC RLU mean + SD*f*. Since in the titer of each ELISA was defined as the ratio of the tested serum's RLU value to the cutoff value. A serum sample was considered positive when its titer was equal to or higher than 1.000 and negative when the titer was lower than 1.000.

Table 8. Parameters used for the CL-ELISA assays.

Reagent		Details
NGP		KM27/30/BME 50 ng/well
		KM28 12.5 ng/well
Antibody	1°	1:800
	2°	Goat anti-Human IgG (H+L) Biotin conjugate
		Thermo Fisher Scientific
		cat# 31770
		1:10,000
	3°	Pierce™ High Sensitivity NeutrAvidin™-HRP
		Thermo Fisher Scientific
		cat# 31030
		1:5000

2.6 FURTHER RESEARCH AND INFORMATION

2.6.1 Benzoate byproduct (20)

Below, is the spectroscopic characterization of the benzoate byproduct **20** formed in the glycosylation reaction between the disaccharide acceptor **11** and the monosaccharide donor **3** to formed the fully protected trisaccharide **12**.
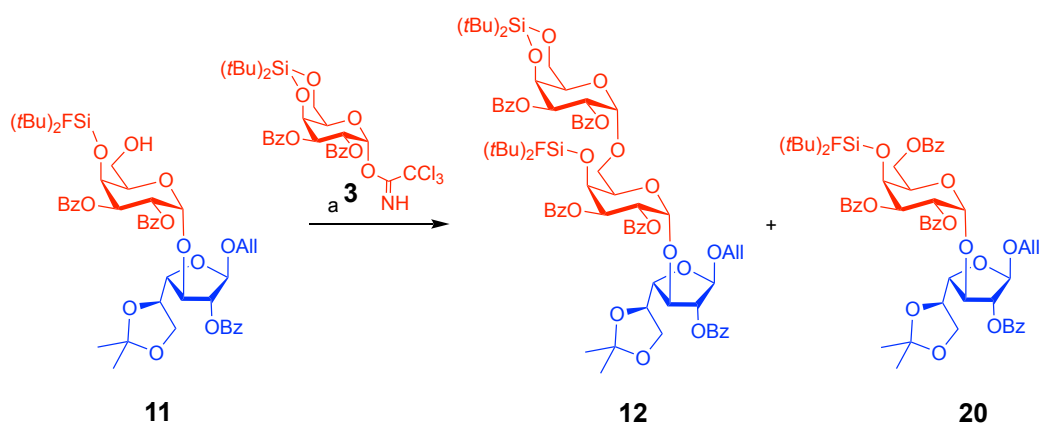
Scheme 11. Byproduct formed in the synthesis of the fully protected trisaccharide **12**.

Allyl 2,3-di-*O*-benzoyl-4-*O*-di-*tert*-butylsilylenefluorine-6-*O*-benzoyl-α-D-galactopyranosyl-(1→3)-2-*O*-benzoyl-5,6-*O*-isopropylidene-β-D-galactofuranoside (20). The compound was purified by flash chromatography on silica gel (EtOAc/hexanes = 1:4) to furnish the benzoate byproduct **20** (30%) as a light-yellow powder. R_f 0.50 (EtOAc/hexanes = 1:3). ^{1}H NMR (400 MHz, CDCl$_3$, 300K) δ 1.00 (s, 9H, *t*Bu); 1.01 (s, 9H, *t*Bu); 1.22 (s, 3H, C*H*$_3$); 1.32 (s, 3H, C*H*$_3$); 3.71-3.77 (m, 1H); 3.80-3.86 (m, 1H); 3.93 (dd, *J* = 12.8, 6.1 Hz, 1H, H-a); 4.10-4.23 (m, 4H, H-a); 4.44-4.53 (m, 1H); 4.67-4.72 (m, 2H); 5.00-5.11 (m, 3H, H-c, H*f*-1); 5.25 (d, *J* = 17.0 Hz, 1H, H-c); 5.57-5.62 (m, 2H, H*p*-1); 5.74-5.85 (m, 3H, H-b); 7.27-7.57 (m, 12H, arom.); 7.91-8.05 (m, 8H, arom.) ppm. ^{13}C NMR (101 MHz, CDCl$_3$, 300K) δ 20.4 (*C*q-*t*Bu); 20.6 (*C*q-*t*Bu); 25.0 (*C*H$_3$); 26.1 (*C*H$_3$); 27.1 (*t*Bu); 27.2 (*t*Bu); 63.0 (C-6); 65.4 (C-6); 68.0 (C-a); 68.2; 69.4; 71.0; 71.5; 75.0; 81.2; 83.1; 84.1; 96.9 (*C*p-1); 104.8 (*C*f-1); 109.9 (*C*q-*isop.*); 117.5 (C-c); 128.2 (*C*-arom.); 128.3 (*C*-arom.); 128.4 (*C*-arom.); 128.5 (*C*-arom.); 129.2 (*C*q, arom.); 129.3 (*C*q, arom.); 129.4 (*C*q, arom.); 129.6 (*C*-arom.); 129.7 (*C*-arom.); 129.8 (*C*q, arom.); 130.0 (*C*-arom.); 132.9 (*C*-arom.);

63

133.2 (*C*-arom.); 133.3 (*C*-arom.); 133.4 (*C*-arom.); 133.8 (C-b); 165.2 (*C*=O), 165.9 (*C*=O), 166.0 (*C*=O), 166.5 (*C*=O) ppm. ESI-TOF HRMS: *m/z* [M+Na]$^+$ calcd for $C_{54}H_{63}FO_{15}Si$ 1021.3818, found: 1021.3804.

2.6.2 Alternative Disaccharide acceptor (10)

Scheme 12. shows an alternative synthetic route for the synthesis of the fully protected trisaccharide **12**. The main difference is the use of the disaccharide **10** as an acceptor molecule in the glycosylation reaction with Kiso donor **3** to obtained the fully protected trisaccharide **12**. Even tough, the disaccharide **10** has two free hydroxyls at positions -4 and -6, the reaction is regioselective towards the primary hydroxyl -6. A comparison of the compounds after removal of the silylidene group **13** was done using the compound obtained in the synthetic route showed in **Scheme 1**.
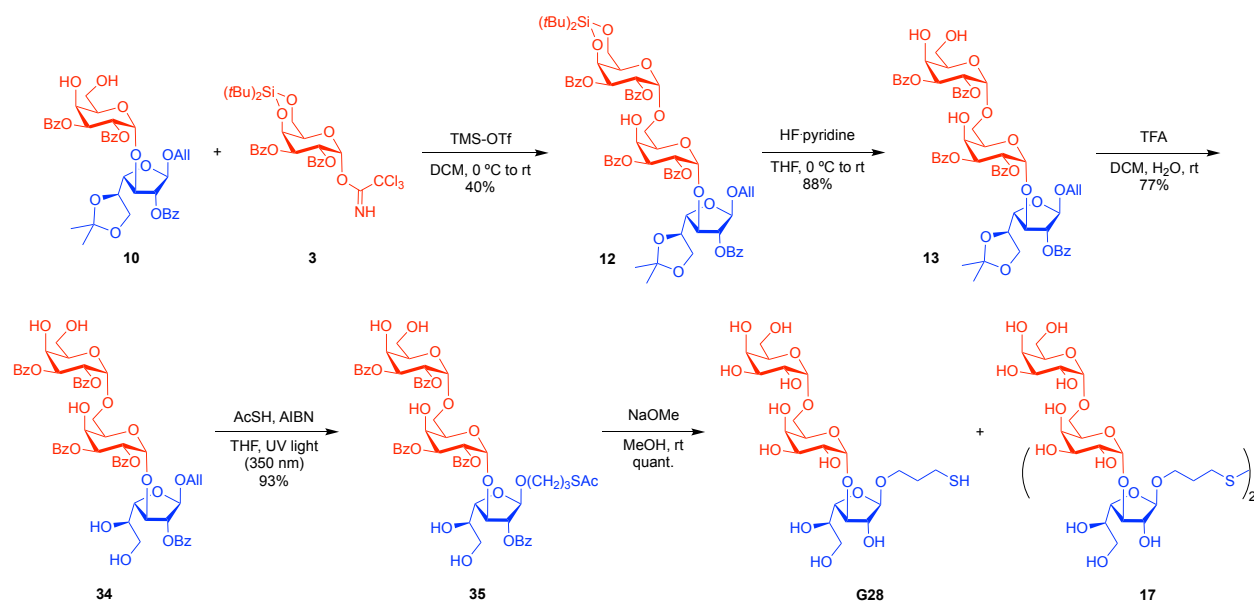
Scheme 12. Alternative synthetic route for the preparation of the mercaptopropyl trisaccharide **G28**.

2.6.3 First approach for the synthesis of the trisaccharide Gal$p$α1,6Gal$p$α1,3Gal$f$β (G28)

The first approach for the synthesis of the trisaccharide Gal$p$α1,6Gal$p$α1,3Gal$f$β (3) derived from GIPL-3 of *L. major* was done trying to build the molecule from the nonreducing to the reducing end as shown in **Scheme 13**. The synthesis was straightforward with good yields for almost every step in the reaction sequence. Unfortunately, the glycosylation of acceptor **38** with trichloroacetimidate donor **3** resulted predominantly in the undesired β-Gal configuration, as was confirmed for a $^3J_{1,2}$ coupling constant of 6.8 Hz. This result is reasonable due to the presence of a OBz group at position 2, which is a neighboring group participating substituent, that form a cyclic oxonium intermediate blocking the bottom face of the donor. Even though the Kiso donor **3** also has an OBz group at position 2, the DTBS group at position 4,6 prevents formation of a β-glycoside almost completely, leading to the α-glycoside with great stereoselectivity[72]. This result shows that a bulky glycoside at position 6 and a bulky silly group at position 4 cannot replace the DTBS with respect to its α-selectivity. However, trisaccharide **44** with the undesirable β-configuration is a useful compound for the study of the importance of the configuration of the Gal$p$-Gal$f$ glycosidic bond for molecular recognition by antibodies.
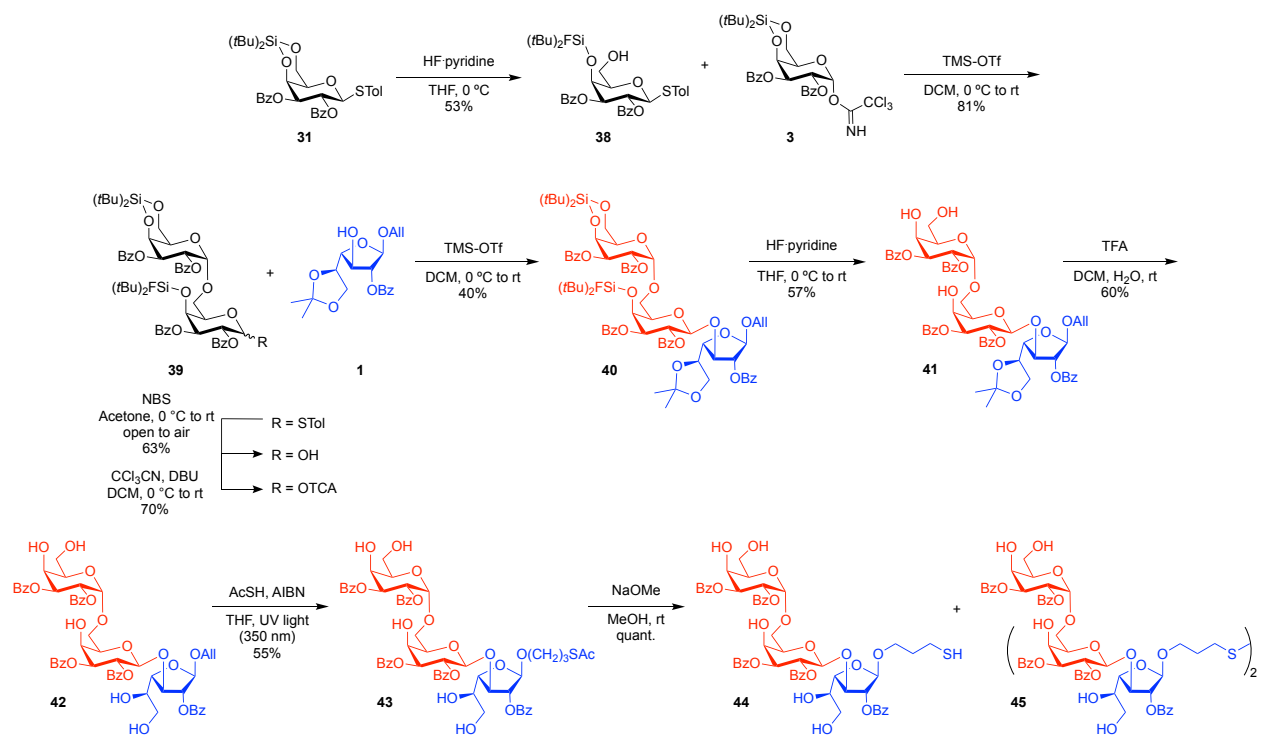
Scheme 13. Synthesis of mercaptopropyl trisaccharide **44**.

Chapter 3: Discovery of Glycan BMKs for New World CL by Reversed Immunoglycomics

3.1 ABSTRACT

The role of the LPG of *Leishmania* parasites in innate immune system has been extensively studied. However, information about the role of the GIPLs is limited, especially with respect to the New World species of *Leishmania*. GIPLs are low molecular weight glycoconjugates covering the parasite surface, highly abundant in the amastigote form of the disease. Critical aspects of their structure and functions are still unknown in the interaction with the vertebrate host. In this study, we evaluated the role of those molecules in two medically important South American species *L. braziliensis* and *T. cruzi*, causative agents of CL and CD, respectively.

Here, we present a reversed immunoglycomics approach, in which glycan BMKs for *L. braziliensis* and *T. Cruzi* infection are discovered by interrogating a synthetic glycoarray containing an α-galactopyranose- and β-galactofuranose-containing oligosaccharides of the terminal glycan portions of type-2 GIPLs, which are galactose rich GIPLs present in *Leishmania* glycocalix. The glycans were chemically synthesize using orthogonal protecting groups strategies, ranging from Galβ*f*1,3Manα to more complex Galα*p*1,3Galβ*f*1,3Manα molecules. Conjugation of the synthetic glycans to BSA afforded NGPs, and their immunological evaluation by CL-ELISA using patient sera from patients from two endemic regions, Bolivia and Argentina revealed glycan BMKs for *L. braziliensis* and *T. Cruzi* infection. This work provides important insights into the molecular structures of glycan BMKs for *L. braziliensis* infection in humans.

Finally, trying to expand the study and understand the antibody response in terms on structure-activity relationship, two tetrasaccharides Gal*p*α1,6Gal*p*α1,3Gal*f*β1,3Man*p*α and Gal*f*β1,3Man*p*α1,2-[Gal*f*β1,3Man*p*α] which are present in *Leishmania* and *T. cruzi* GIPLs, respectively were synthesized.

3.2 INTRODUCTION

CD, also known as American trypanosomiasis and different forms of leishmaniasis are infectious, vector-borne diseases caused by the protozoan parasites *T. cruzi* and *Leishmania spp.*, respectively. Collectively, these diseases affect millions of people worldwide, mostly those who live in poverty and remote areas of certain parts of the world. It is estimate that less than 1% of infected people have access to diagnosis and treatment[25]. When left untreated, CD in the chronic phase and cutaneous leishmaniasis, caused by *Leishmania Braziliensis* may eventually lead to permanent disability. In order to treat a patient with CD or leishmaniasis, first the disease needs to be unfailingly diagnosed, not relying exclusively on dermatological examinations or speculations based on clinical symptoms, how it is normally done in developing countries where the proper diagnostic tools are often not available. Furthermore, the impact of both diseases is not limited to the rural areas in which vectorborne transmission occurs. In the U.S. alone there has been a dramatic increase in the prevalence of CD in blood blanks, in part due to increasing migration of asymptomatic individuals from endemic regions being the most affected country accounting for three-fourths of all cases[93]. Thus, there is a pressing necessity for the development of more reliable, affordable, and robust diagnostic tool for both CD and leishmaniasis. Moreover, there is urgent need for new and reliable biomarkers (BMKs) for the follow-up of the treatment of these diseases and for active and passive surveillance in elimination settings.

3.3 RESULTS AND DISCUSSION

3.3.1 Synthesis of NGP29b, NGP31b, and NGP32b

3.3.1.1 Synthesis of the NGP29B [Galfβ1,3Manpα-linker-BSA]

For the synthesis of mercaptopropyl disaccharide **G29**, terminal moiety of GIPL-1 found in *L. major*, fully benzoylated β-thiogalactofuranoside Gal*f*β **28** was used as a donor and the benzylidene protected mannose Man*p*α **8** as an acceptor. The glycosylation reaction between **28** and **8** was carried in dry conditions using *N*-iodosuccinimide and silver triflate to do the activation of the STol yielding the desired disaccharide **46** (70%) with exclusive β-stereoselectivity. Followed, the benzylidene acetal protecting group was cleaved to give the partially deprotected sugar **47** with 53% yield. Then, radical addition of AcSH **48** (79%) followed by saponification gave the fully deprotected disaccharide **G29** and its disulfide **49** quantitative (**Scheme 14**).
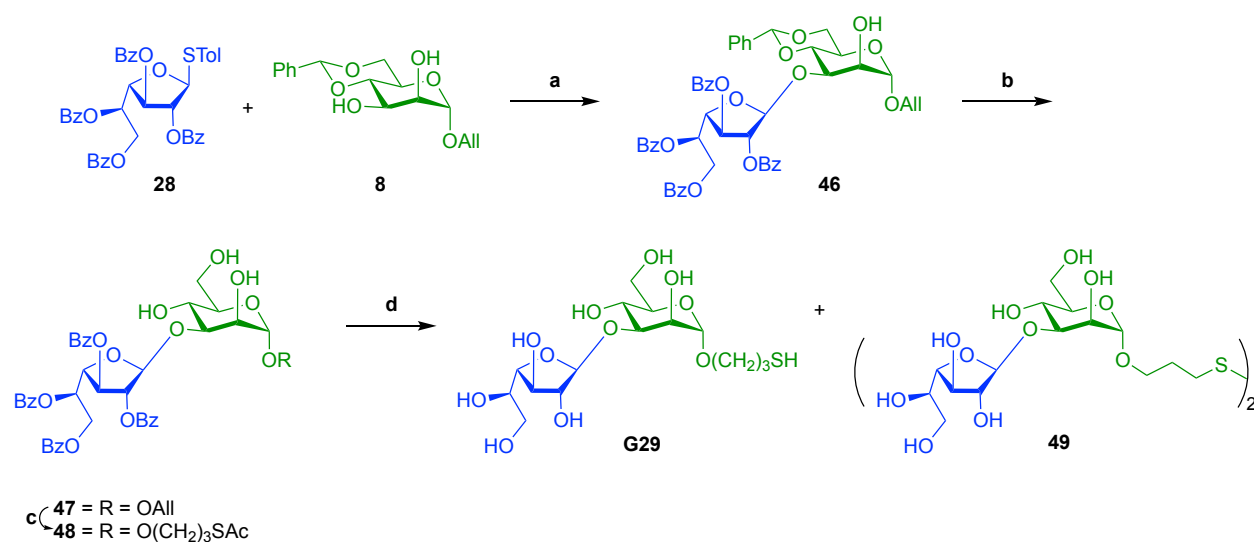
Scheme 14. Synthesis of mercaptopropyl disaccharide **G29**.

a: NIS, AgOTf, DCM, 0 °C then r.t., 3 h, molecular sieves 4 Å (70%); b: TFA/H$_2$0/DCM 1:1:10, r.t., 15 min (53%); c: AcSH, AIBN, THF, UV light (350 nm), 6 h (79%) and d: NaOMe, MeOH, r.t., 2 h (quant.).
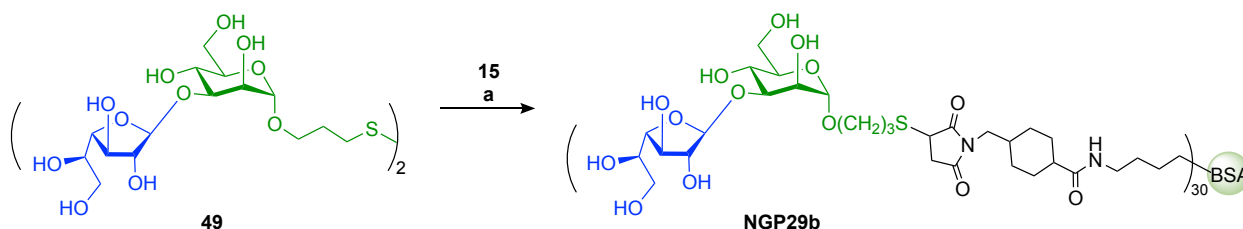
Scheme 15. Conjugation of glycan and maleimide derivatized BSA **15** to produce **NGP29b**. **a**) TCEP·HCl, phosphate buffer pH 7.2, rt, 2 h. The average number of glycans per BSA molecule was determined by MALDI-TOF.

3.3.1.2 Synthesis of G31 [Galpα1,6Galpα1,3Galfβ1,3Manpα]

The first methodology for the synthesis of the tetrasaccharide Galpα1,6Galpα1,3Galfβ1,3Manpα, GIPL-3 extended glycan, started using the fully protected trisaccharide **9** as acceptor molecule upon reaction with HF-Pyridine to get **50**. Once this compound was isolated, purified and characterized, the next reaction was the glycosylation among **50** and the Kiso donor **3**. The reaction was successful and the desired tetrasaccharide **51** was obtained with 47% yield. Since all the starting materials were consumed, we look into byproduct formation and after analysis we discovered that the reaction also produces a byproduct with the 5-OH free due to Silylidene migration **52**, benzoate formation in the acceptor molecule **53** via the same mechanism described in **Figure 2**, and also some hydrolysis of the donor molecule **54**. The reaction was optimized changing equivalents of promoter, starting materials, concentration, etc., but the results were about the same, see **Scheme 16**.
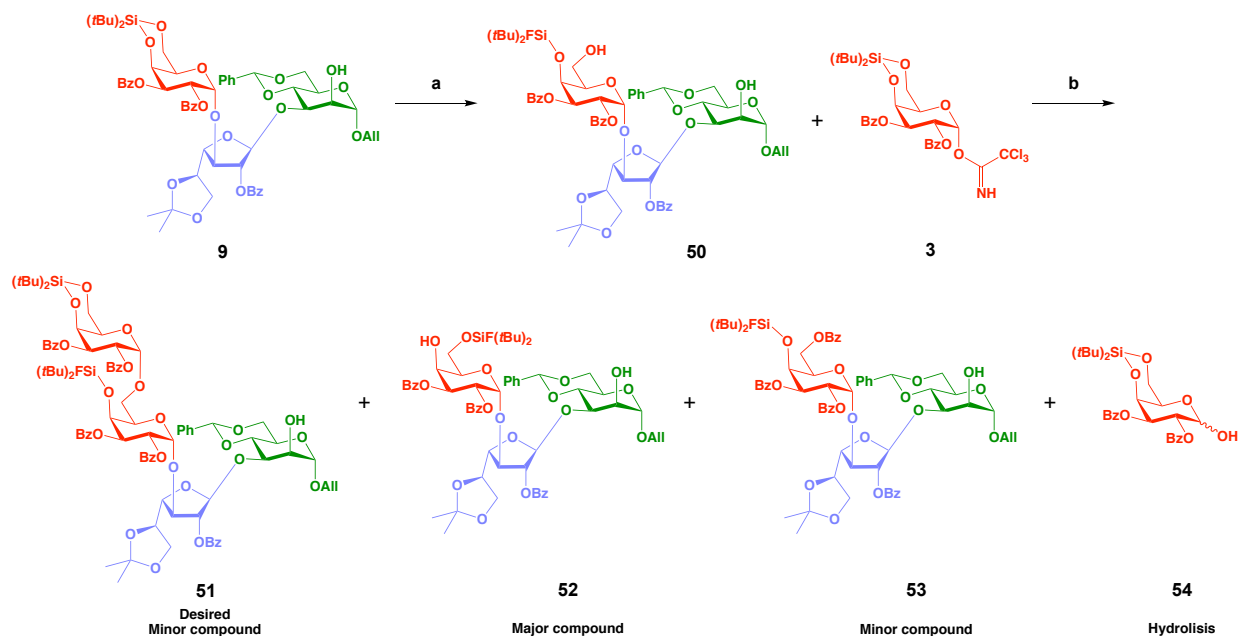
Scheme 16. First approach for the synthesis of the mercaptopropyl tetrasaccharide **G31**.
a: HF-Pyridine, THF, 0 °C, 30 min (65%); b: TMS-OTf, DCM, 0 °C then r.t., 50 min (47%).

Motivated to develop a better synthetic route, our next attempt is shown in **Scheme 17**. For that, we used the disaccharide donor **5** upon removal of the silylidene protecting group. This new acceptor **55** with two free hydroxyls at positions -4 and -6 was then submitted to glycosylation reaction with the Kiso donor **3**, getting regioselective the trisaccharide **56** at the -6 position, with exclusively α-stereoselectivety and 40% yield. After purification and characterization, a following glycosylation of **56** with mannose acceptor Man*p*α **8** was done using NIS and AgOTf to get the desired tetrasaccharide **57** as a unique compound in the reaction. The %yield for this reaction still need to be optimized.
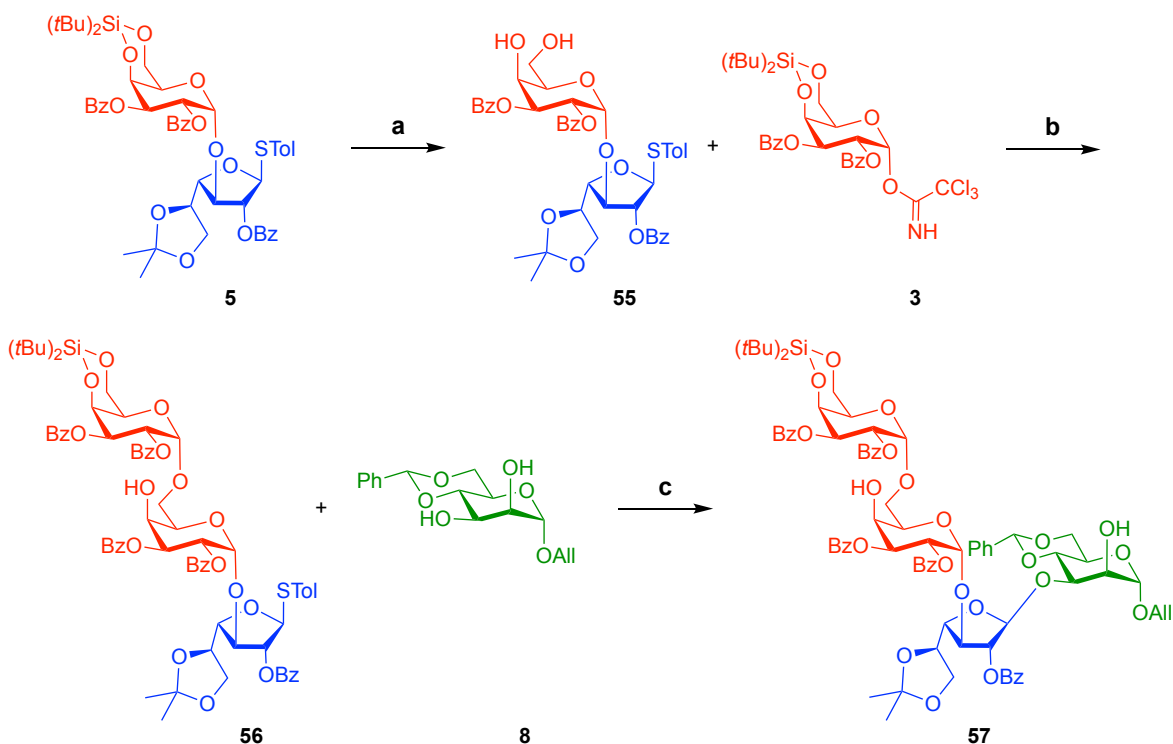
Scheme 17. Synthesis of the mercaptopropyl tetrasaccharide **G31**.

a: HF-Pyridine, THF, 0 °C to r.t., 1 h (72%); b: TMS-OTf, DCM, 0 °C then r.t., 50 min (40%); c: NIS, AgOTf, DCM, 0 °C then r.t., 1 h, molecular sieves 4 Å (47%).

3.3.1.3 Synthesis of G32 (Galfβ1,3Manpα1,2-[Galfβ1,3Manpα])

For the synthesis of the tetrasaccharide (Galfβ1,3Manpα1,2-[Galfβ1,3Manpα]), GIPL present in the cell surface of *T. cruzi*, we used as starting material the terminal glycan of GIPL-1 **46**. Then, it was fully protected by an acetylation reaction to get the sugar **58**, which was converted later in the disaccharide donor **60**. For that, first the disaccharide was reduced to the hemiacetal **59** as an α,β mixture, and finally the tricholoroacetimidate was installed. Lastly, with donor **60** and acceptor **46** a glycosylation reaction was optimized and the desired tetrasaccharide Galfβ1,3Manpα1,2-[Galfβ1,3Manpα] fully protected **61** was successfully obtained (**Scheme 18**).
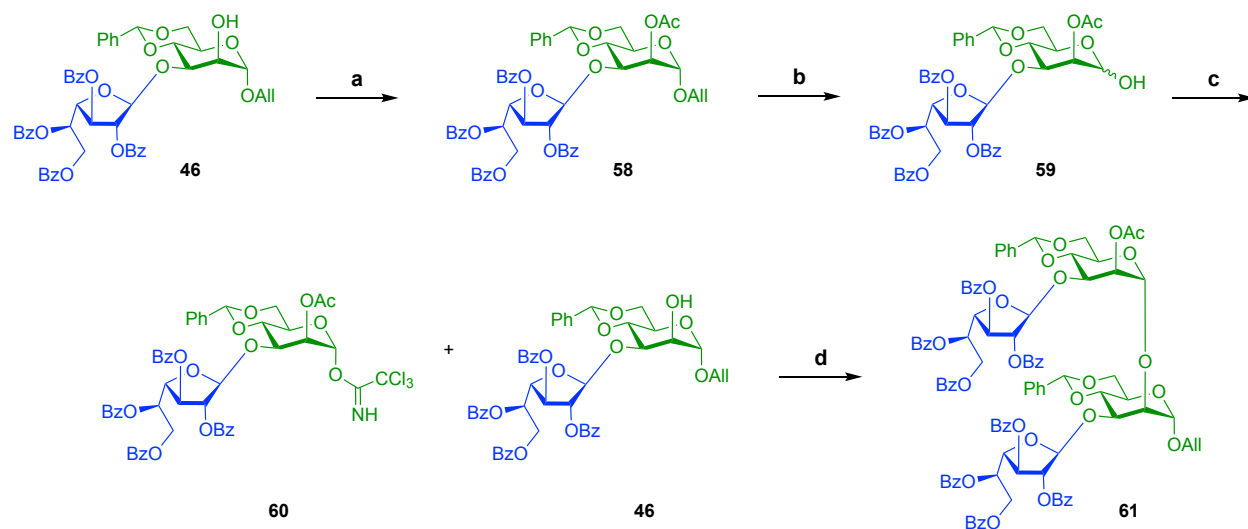
Scheme 18. Synthesis of the mercaptopropyl tetrasaccharide **G32**.

a: Ac_2O, DMAP, Pyridine, 0 °C to r.t., 3 h (82%); b: $PdCl_2$, MeOH, r.t., 3 h (80%); c: CCl_3CN, DBU, DCM, 0 °C then r.t., 15 min (87%); d: BF_3OEt_2, DCM, 0 °C then r.t., (40%).

3.3.2 CL-ELISAs of NGP27-30b, NGP24b, and NGP5b as potential BMKs for New World CL caused by *L. Braziliensis* and CD

3.3.2.1 Sera pools
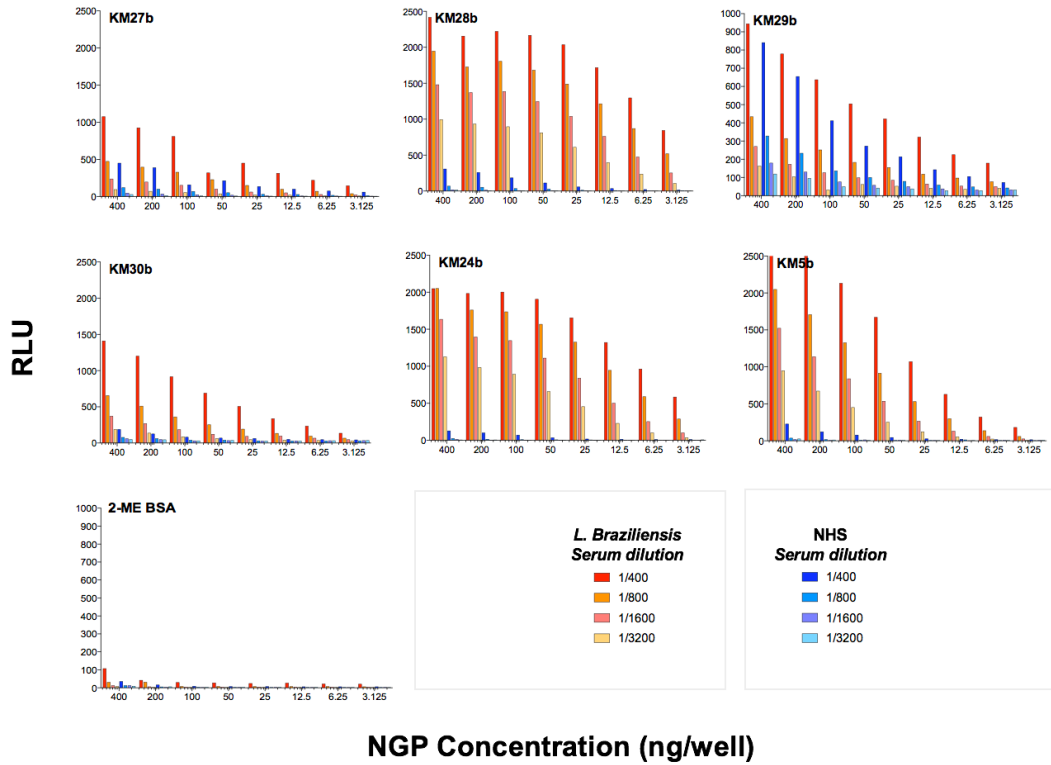
Figure 21. Cross-titrations with pools of patient sera with active *L. Braziliensis*, or pooled sera of healthy individuals from Bolivia.
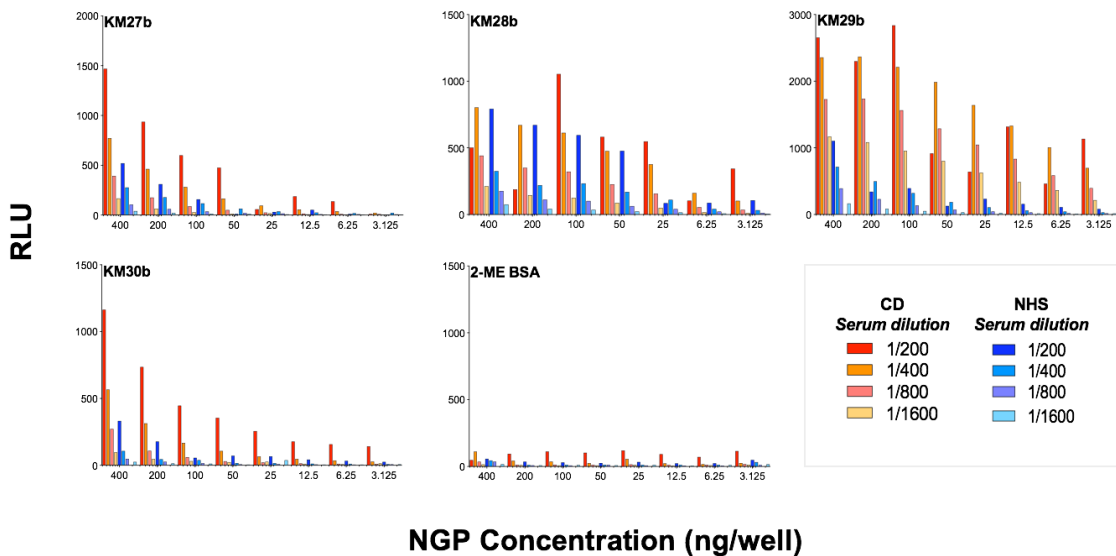
Figure 22. Cross-titrations with pools of patient sera with active CD, or pooled sera of healthy individuals from Bolivia.

3.3.2.2 Individual sera
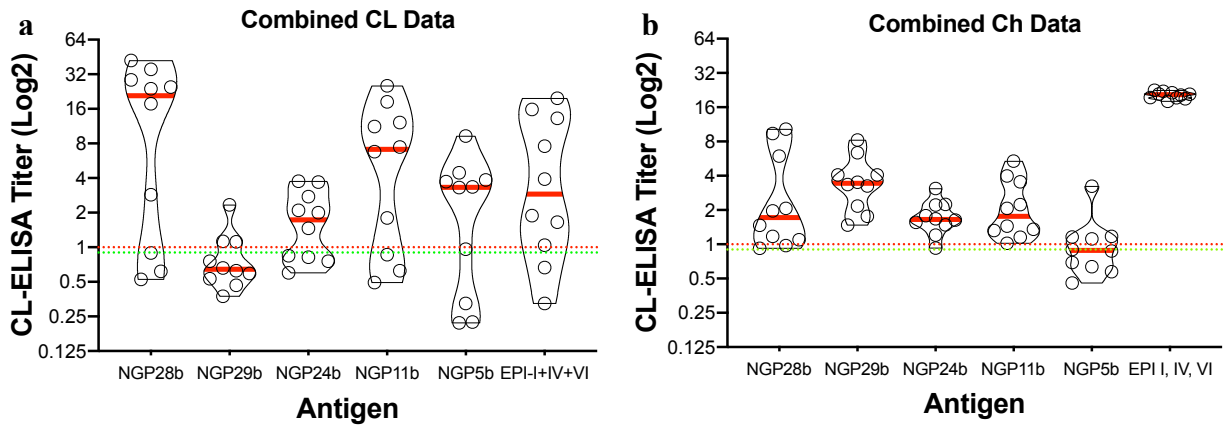
Figure 23. Bolivia CL and CD panel data.

CL sera (n = 10):   Patients from Bolivia infected with *L. braziliensis*.
Ch sera (n = 10):   Patients from Bolivia infected with *T. cruzi*
EPI-I+IV+VI: An epimastigote lysate mix with several strains (6, 2, and 4, respectively) from each genotype (I, IV, and VI, respectively).
We are using this lysate to cover the specificities of the Chagas conventional serology. Since epimastigotes have little to none α-Gal epitopes, we are not measuring anti-α-Gal Abs with this antigen mix, but could be measuring anti-β-Gal*f* Abs, which could be cross reacting with CL sera. In that regard, interestingly, these CL sera showed much lower cross-reactivity with NGP29b, which showed to be very reactive with Chagas sera.

As shown in **Figure 23 a** and **b** the best reactivity against CL and CD was observed for the NGP28b and NGP29b, respectively. Then, a new CL-ELISA assay was done using both NGPs and CL sera patient from Salta (Argentina) and Bolivia (**Figure 23**).

75

www.manaraa.com
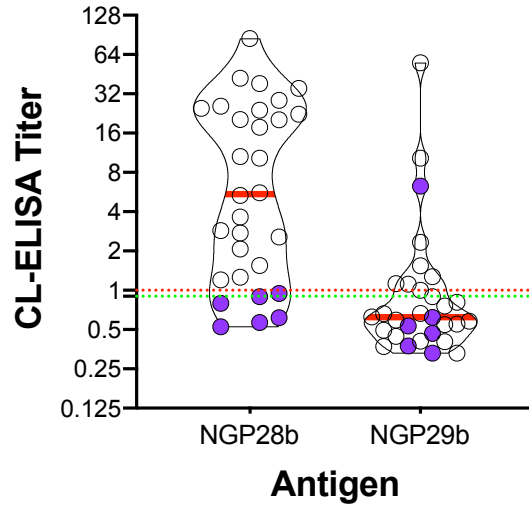
Figure 24. CL patient sera from Salta (Argentina) and Bolivia.

🟣 Sera negative or inconclusive

N = 30 CL patients

NGP28b	**NGP29b**
Positive = 24/30 (80%)	Positive = 8/30 (27%)
Negative = 5/30 (17%)	Negative = 21/30 (70%)
Inconclusive = 1/30 (3%)	Inconclusive = 1/30 (3%)

3.4 CONCLUSIONS

In this chapter, we successfully synthesized the NGP29b [Gal$f$β1,3Man$p$α-linker-BSA], that contains the terminal glycan of GIPL1, present in the glycocalix of *Leishmania* parasites. Furthermore, we developed and optimized two synthetic routes for the synthesis of larger oligosaccharides, G31 [Gal$p$α1,6Gal$p$α1,3Gal$f$β1,3Man$p$α] and G32 (Gal$f$β1,3Man$p$α1,2-[Gal$f$β1,3Man$p$α]), which are terminal tetrasaccharides present in the GIPLs of *Leishmania* parasites and *T. cruzi*, respectively. The preliminary biological results from the screening of the terminal glycans of type-2 GIPLs from the cell surface of *L. major* (NGPs 27b - NGPs30b), and also some glycoconjugates present in *T. Cruzi* (NGPs 5b, 11b, and 24b) with CL and CD sera from

76

Boliva and Argentina, showed that NGP28b [Gal*p*α1,6Gal*p*α1,3Gal*f*β-linker-BSA] has a strong IgG Abs response with *L. braziliensis* sera, while NGP29b [Gal*f*β1,3Man*p*α-linker-BSA] has a strong IgG Abs response with *T. cruzi* sera. From this data, we postulate the NGP28b and NGP29b as immunodominant glycotopes for diagnosis of new world CL and CD, respectively. Finally, our results strongly support that *L. braziliensis* is one of the New World *Leishmania* species that expresses GIPLs or other glycoconjugates with similar glycotopes to those found in *L. major*.

3.5 EXPERIMENTAL SECTION

3.5.2 Experimental procedures and spectroscopic data of compounds

3.5.2.1 Synthesis of the donor Galfβ (28)
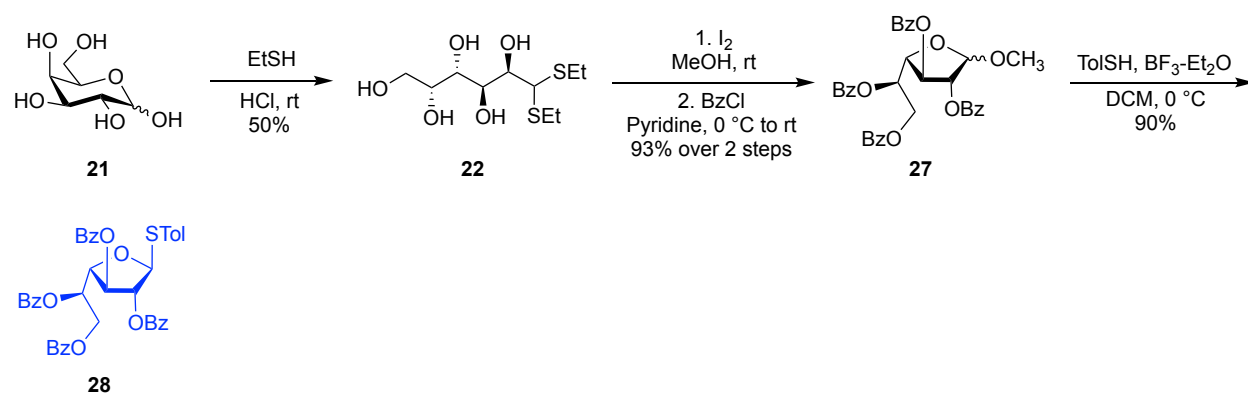
Scheme 19. Synthesis of *p*-Tolyl 2,3,5,6-tetra-*O*-benzoyl-1-thio-β-D-galactofuranoside **28**.

p-**Tolyl 2,3,5,6-tetra-*O*-benzoyl-1-thio-β-D-galactofuranoside (28)**. Methyl glycoside **27**[78] (880 mg, 1.44 mmol) was dissolved in dry DCM (16 mL) at 0 °C and *p*-thiocresol (240 mg, 1.93 mmol) was then added. The reaction mixture was stirred for 20 min and BF$_3$·OEt$_2$ (4.0 mL, 32.4 mmol) was added dropwise and stirred for 1 h at 0 °C. The reaction mixture was neutralized with Et$_3$N and diluted with DCM. The organic layer was then washed successively with a saturated aqueous solution of NaHCO$_3$, water and brine. The organic layers were combined, concentrated and the crude product was purified by flash column chromatography (EtOAc/Hexanes/ 1:5) to give

77

the *per*-benzoylated sugar **28** (909 mg, 90%) as an amorphous white solid. R$_f$ 0.38 (EtOAc/Hexanes/ 1:4). ^{1}H NMR (600 MHz, CDCl$_3$, 300K) δ 2.31 (s, 3H, arom.C*H*$_3$); 4.67-4.79 (m, 2H, *H*-6a,b); 4.95 (t, *J* = 5.50 Hz, 1H, *H*-4); 5.65 (s, 1H, *H*-2); 5.68-5.72 (m, 1H, *H*-3); 5.77 (s, 1H, *H*-1); 6.08-6.14 (m, 1H, *H*-5); 7.03-7.10 (m, 2H, arom.); 7.27-7.40 (m, 6H, arom.); 7.42-7.48 (m, 4H, arom.); 7.49-7.55 (m, 3H, arom.); 7.57-7.62 (m, 1H, arom.); 7.88 (d, *J* = 8.3 Hz, 2H, arom.); 7.97 (d, *J* = 7.6 Hz, 2H, arom.); 8.07 (t, *J* = 9.3 Hz, 4H, arom.) ppm. ESI-TOF HRMS: *m/z* [M+Na] calcd for C$_{41}$H$_{34}$O$_9$S 725.1821, found 725.1801. ^{13}C-NMR spectra matched the ones previously described for this compound.[78]

3.5.2.2 Synthesis of the NGP29B [Galfβ1,3Manpα-linker-BSA]
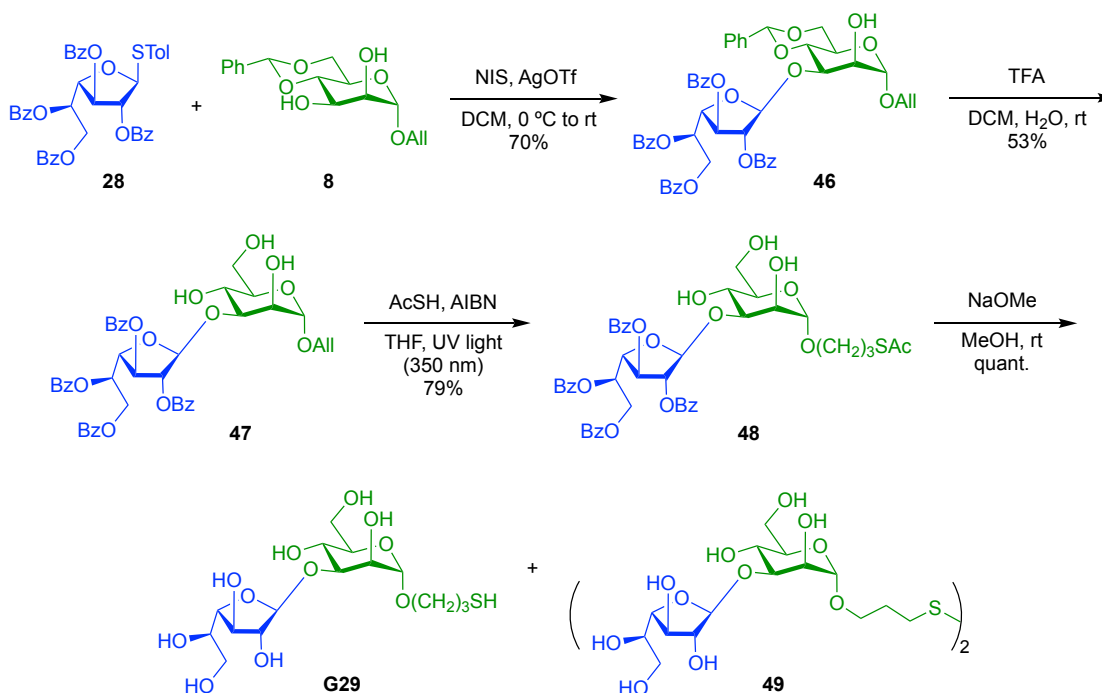
Scheme 20. Synthesis of the mercaptopropyl disaccharide **G29**.

3.5.2.2.1 Allyl 2,3,5,6-tetra-*O*-benzoyl-β-D-galactofuranosyl-(1→3)-4,6-*O*-benzylidene-α-D-mannopyranoside (46). A solution of Man*p*α acceptor **8** (215 mg, 0.70 mmol) and Gal*f* donor **28** (151 mg, 0.22 mmol) in anhydrous DCM (25 mL) with freshly activated MS 4Å was stirred under Ar for 30 min at 0°C. Then, NIS (121 mg, 0.54 mmol) and AgOTf (3.3 mg, 0.013 mmol) were added to the flask, which was kept stirring at 0 °C for 15 min, and gradually brought to room

temperature. After 3 h at rt, the reaction mixture was quenched by addition of Et$_3$N, filtered, and washed with a saturated solution of Na$_2$S$_2$O$_3$ and brine. The organic layers were dried over MgSO$_4$, concentrated, and purified by column chromatography on silica gel (EtOAc/Hexanes = 2:3) to afford **46** (133 mg, 70%), as a light-yellow oil. R$_f$ 0.37 (EtOAc/Hexanes = 2:3). ^{1}H NMR (400 MHz, CDCl$_3$, 300K) δ 2.94 (s, 1H, -O*H*); 3.78-4.37 (m, 9H, H-a, H*f*-6a,b, H*m*-6a,b); 4.57 (dd, *J* = 12.1, 8.4 Hz, 1H, H-a); 4.74 (dd, *J* = 5.6, 3.1 Hz, 1H); 5.00 (d, *J* = 1.1 Hz, 1H, H*m*-1); 5.23 (dd, *J* = 10.3, 1.4 Hz, 1H, H-c); 5.27-5.35 (m, 1H, H-c); 5.43 (d, *J* = 1.5 Hz, 1H); 5.44 (s, 1H, H*f*-1); 5.50 (s, 1H, OC*H*Ph); 5.56 (dd, *J* = 5.5, 0.9 Hz, 1H); 5.85-5.99 (m, 2H, H-b); 7.13-7.25 (m, 4H, arom.); 7.28-7.64 (m, 13H, arom.); 7.82 (dd, *J* = 8.3, 1.2 Hz, 2H, arom.); 7.92-7.97 (m, 2H, arom.); 8.02 (ddd, *J* = 11.2, 8.4, 1.2 Hz, 4H, arom.) ppm. ^{13}C NMR (101 MHz, CDCl$_3$, 300K) δ 63.7; 64.2 (C-a); 68.3 (CH$_2$); 68.7; 68.9 (CH$_2$); 70.1; 71.9; 76.8; 77.2; 81.3; 82.5; 99.2 (C*m*-1); 102.1 (OC*H*Ph); 102.5 (C*f*-1); 118.1(C-c); 125.9 (*C*-arom.); 128.3 x 2 (*C*-arom.); 128.4 x 2 (*C*-arom.); 128.5 (*C*-arom.); 128.6 (*C*q, arom.); 129.0 (*C*q, arom.); 129.1 (*C*-arom.); 129.5 (*C*q, arom.); 129.6 (*C*q, arom.); 129.7 (*C*-arom.); 129.8 (*C*-arom.); 129.9 (*C*-arom.); 130.0 (*C*-arom.); 132.9 (*C*-arom.); 133.1 (*C*-arom.); 133.4 (*C*-arom.); 133.5 (*C*-arom.); 133.6 (C-b); 137.3 (*C*q, arom.); 165.5 (C=O); 165.7 (C=O); 165.9 (C=O); 166.0 (C=O) ppm. ESI-TOF HRMS: *m/z* [M+Na]$^+$ calcd for C$_{50}$H$_{46}$O$_{15}$ 909.2734, found 909.2706.

3.5.2.2.2 Allyl 2,3,5,6-tetra-*O*-benzoyl-β-D-galactofuranosyl-(1→3)-α-D-mannopyranoside (47).

Fully protected disaccharide **46** (94 mg, 0.11 mmol) was dissolved in DCM (15 mL). While stirring at rt, H$_2$O (1.5 mL) and TFA (1.5 mL) were sequentially added, and the reaction proceeded for 20 min. After the starting material was observed to disappear on TLC, the resulting solution was co-evaporated with EtOH (10 mL) twice. The solution was concentrated, dried under vacuum pressure, and purified by PTLC (DCM/MeOH = 15:1) to yield **47** (45 mg, 53%) as a beige powder. R$_f$ 0.37 (DCM/MeOH = 15:1). ^{1}H NMR (400 MHz, CDCl$_3$, 300K) δ 2.31 (br. s., 1H, -O*H*); 2.94 (br. s., 1H, -O*H*); 3.21 (br. s., 1H, -O*H*); 3.61-3.72 (m, 1H); 3.80-4.21 (m, 7H); 4.9-4.83 (m, 2H); 4.90 (dd, *J* = 5.7, 3.8 Hz, 1H); 4.93 (d, *J* = 1.2 Hz, 1H, H*m*-1); 5.19 (dd, *J* = 10.3, 1.3 Hz, 1H, H-c); 5.27 (dd, *J* = 17.2, 1.5 Hz, 1H, H-c); 5.47 (s, 1H, H*f*-1); 5.50 (d, *J* = 1.6 Hz, 1H); 5.72 (dd, *J* = 5.7, 2.0 Hz, 1H); 5.79-5.92 (m, 1H, H-b); 5.92-5.99 (m, 1H); 7.28-7.46 (m, 8H, arom.); 7.49-7.61 (m, 4H, arom.); 7.88-7.94 (m, 2H, arom.); 7.96-8.04 (m, 4H, arom.); 8.05-8.12 (m, 2H, arom.) ppm. ^{13}C NMR (101 MHz, CDCl$_3$, 300K) δ 62.6 (CH$_2$); 63.1 (CH$_2$); 66.3; 68.2 (CH$_2$); 68.5; 70.2;

79

71.9; 77.0; 78.9; 81.2; 83.0; 98.6 (C*m*-1); 104.4 (C*f*-1); 117.9(C-c); 128.4 (*C*-arom.); 128.5 x 2 (*C*-arom.); 128.6 (*C*-arom.); 128.7 (*C*q, arom.); 129.3 (*C*q, arom.); 129.4 (*C*q, arom.); 129.7 (*C*-arom.); 129.8 (*C*-arom.); 129.9 (*C*-arom.); 130.0 (*C*-arom.); 133.2 (*C*-arom.); 133.4 (*C*-arom.); 133.5 (*C*-arom.); 133.7 (C-b); 165.6 (C=O); 165.7 (C=O); 166.1 (C=O); 166.3 (C=O) ppm. ESI-TOF HRMS: *m/z* [M+Na]$^+$ calcd for $C_{43}H_{42}O_{15}$ 821.2421, found 821.2452.

3.5.2.2.3 (Acetylthio)propyl 2,3,5,6-tetra-*O*-benzoyl-β-D-galactofuranosyl-(1→3)-α-D-mannopyranoside (48).

To a solution of **47** (45 mg, 0.056 mmol) and AIBN (10 mg, 0.061 mmol) in anhydrous THF (9.0 mL), AcSH (28 μL, 0.40 mmol) was added and stirred under Ar for 5 min. The solution was then placed in a Rayonet UV reactor with cooling water and stirred continuously for 6 h. The solution was concentrated by two co-evaporations with toluene, and purified by PTLC (DCM/MeOH = 20:1) to yield **48** (39 mg, 79%) as a yellow oil. R$_f$ 0.30 (DCM/MeOH = 20:1). ^{1}H NMR (400 MHz, CDCl$_3$, 300K) δ 1.82 (quin, *J* = 6.6 Hz, 2H); 2.30 (s, 3H, C*H$_3$*); 2.91 (t, *J* = 7.0 Hz, 2H); 3.20 (br. s., 1H); 3.28-3.45 (m, 2H); 3.56-3.75 (m, 3H); 3.85 (d, *J* = 3.4 Hz, 2H); 3.92-4.10 (m, 3H); 4.70-4.82 (m, 2H); 4.85 (s, 1H, *H*-1-Man); 4.93 (dd, *J* = 5.6, 3.6 Hz, 1H); 5.49 (s, 1H, *H*-1-Gal*f*); 5.50-5.56 (m, 1H); 5.72 (dd, *J* = 5.7, 1.5 Hz, 1H); 5.93-6.03 (m, 1H); 7.28-7.45 (m, 8H, arom.); 7.49-7.59 (m, 4H, arom.); 7.90 (d, *J* = 7.3 Hz, 2H, arom.); 7.95-8.04 (m, 4H, arom.); 8.08 (d, *J* = 7.5 Hz, 2H, arom.). ^{13}C NMR (101 MHz, CDCl$_3$, 300K) δ 25.8 (*C*H$_2$); 29.2 (*C*H$_2$); 30.6 (*C*H$_3$); 62.4 (*C*H$_2$); 63.1 (*C*H$_2$); 65.9 (*C*H$_2$); 66.0 (*C*H); 68.3 (*C*H); 70.1 (*C*H); 71.9 (*C*H); 77.2 (*C*H); 78.6 (*C*H); 81.0 (*C*H); 82.9 (*C*H); 99.5 (*C*-1-Man); 104.2 (*C*-1-Gal*f*); 128.3 (*C*H, arom.); 128.4 x 2 (*C*H, arom.); 128.5 x 2 (*C*, arom.); 128.7 (*C*, arom.); 129.3 (*C*, arom.); 129.4 (*C*, arom.); 129.7 (*C*H, arom.); 129.8 x 2 (*C*H, arom.); 129.9 (*C*H, arom.); 133.1 (*C*H, arom.); 133.3 (*C*H, arom.); 133.5 (*C*H, arom.); 133.6 (*C*H, arom.); 165.5 (C=O); 165.6 (C=O); 166.0 (C=O); 166.2 (C=O); 195.8 (C=O-CH$_3$) ppm. ESI-TOF HRMS: *m/z* [M+Na]$^+$ for $C_{45}H_{46}O_{16}S$ 897.2404, found 897.2718.

3.5.2.2.4 Thiopropyl β-D-galactofuranosyl-(1→3)-α-D-mannopyranoside (G29).

To a flask containing **48** (29 mg, 0.033 mmol), 3 mL of 0.5M NaOMe was added under Ar, and stirred at rt for 2 h. HRMS showed full removal of the protecting groups, and all material was present as a mixture of thiol and disulfide. Amberlyst-15 ion-exchange resin was added and stirred until pH of 7, followed by filtration through Celite and concentrated by lyophilization to give **49** as a white

powder (14 mg, quant.). R_f 0.33 (EtOAc/EtOH/H$_2$O/NH$_3$ 7:3:1:0.5). ESI-TOF HRMS: m/z [M+Na]$^+$calcd for C$_{15}$H$_{28}$O$_{11}$S 439.1250, found 439.1214; for C$_{30}$H$_{54}$O$_{22}$S$_2$ 853.2446, found 853.2366.

3.5.2.2.5 Synthesis of the NGP29B [Gal*f*β1,3Man*p*α-linker-BSA]. MALDI-TOF MS: m/z for BSA [M+H]$^+$ 66120; for NGP29b [M+H]$^+$ 85160.
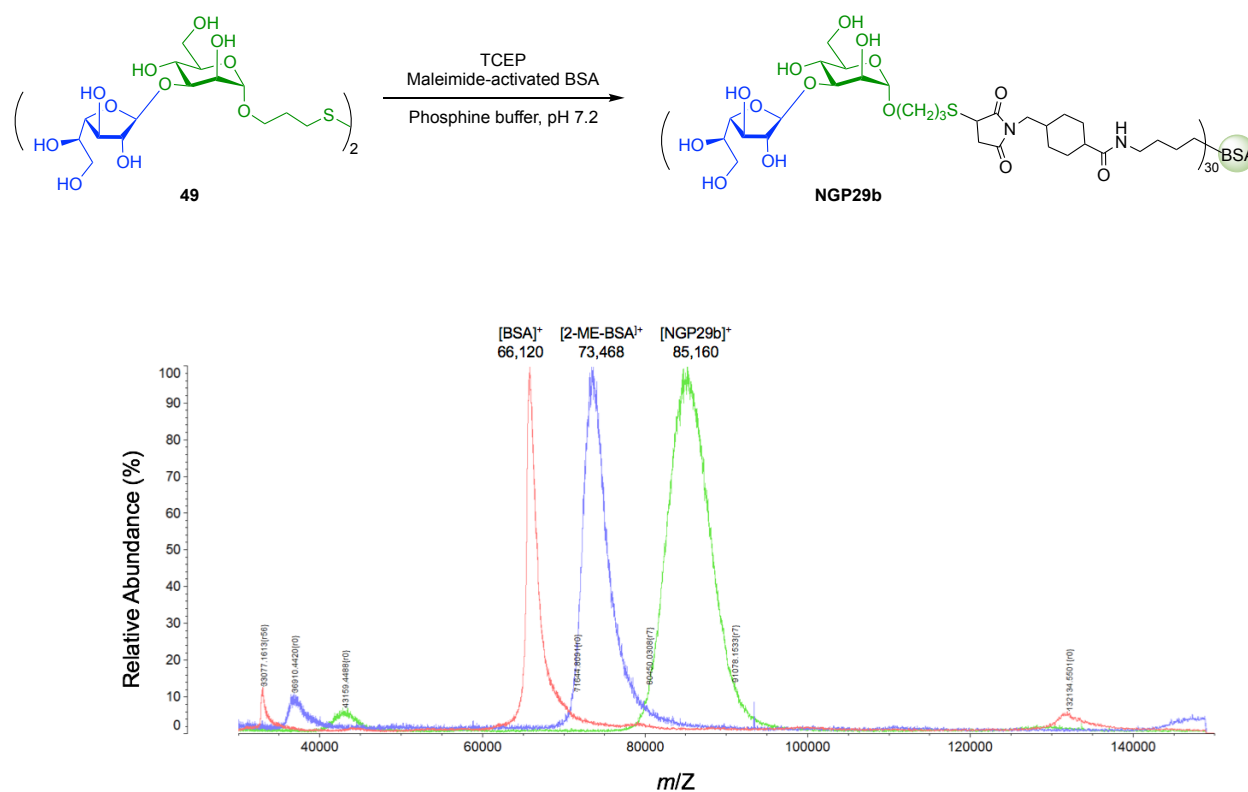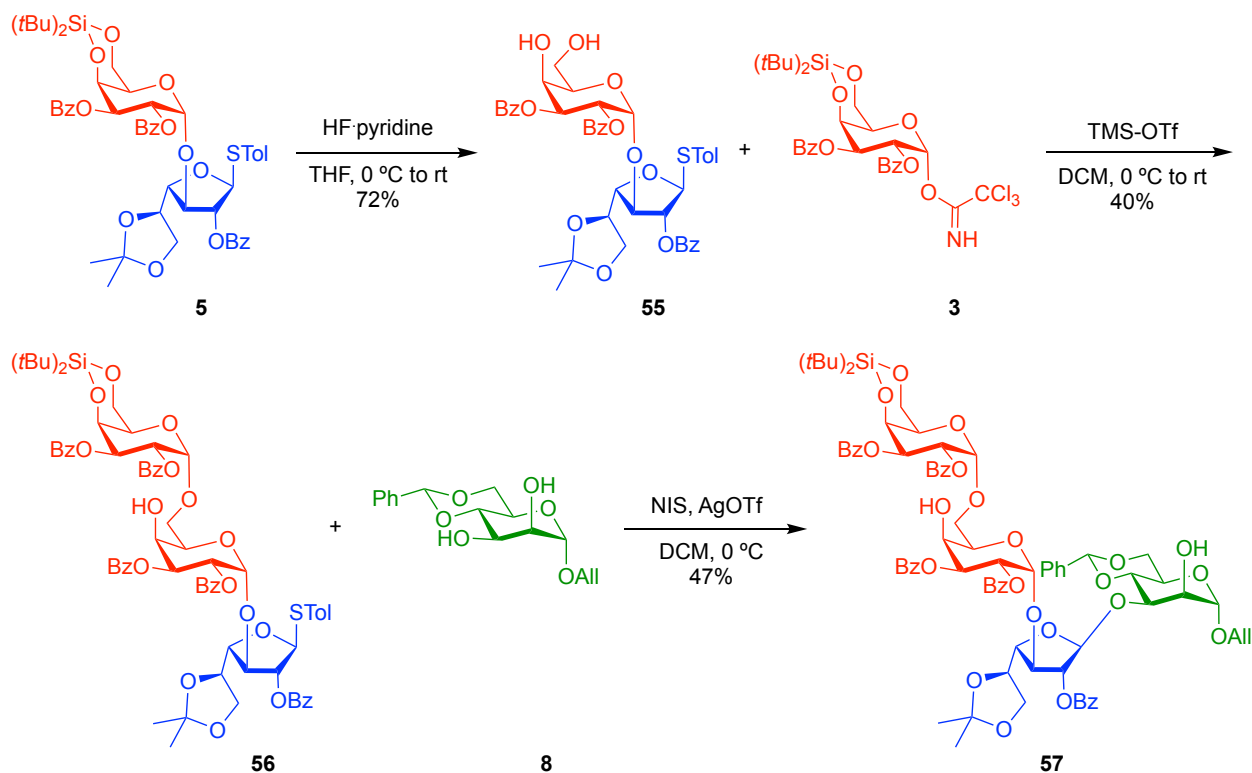

Figure 25. (Top) Schematic representation of conjugation of **G29** to BSA. (Bottom) MALDI-TOF mass spectra of **NGP29b** [Gal*f*β1,3Man*p*α-linker-BSA] overlaid with pure BSA and 2-ME-linker-BSA.

81

Scheme 21. Synthesis of the mercaptopropyl tetrasaccharide **G31**.

3.5.2.3.1 *p*-Tolyl 2,3-di-*O*-benzoyl-4,6-hidroxyl-α-D-galactopyranosy-(1→3)-2-*O*-Benzoyl-5,6-*O*-isopropylidene-1-thio-β-D-galactofuranoside (55). Fully protected disaccharide **5** (200 mg, 0.21 mmol) was dissolved in a mixture ratio (**1:100** HF-Pyr/dry THF) (400 μL/40 mL) in a plastic conical tube and stirred for 30 min at 0°C and then 30 min at rt under Ar. The reaction mixture was cooled down again to 0°C and quenched with saturated NaHCO$_3$. Then, diluted and extracted with EtOAc, washed with water and brine, dried over MgSO$_4$, concentrated and purified by column chromatography in silica gel to give **55** (122 mg, 72%) as a white powder. R$_f$ 0.37 (EtOAc/hexanes = 1:1). ^{1}H NMR (400 MHz, CDCl$_3$) δ 1.15 (s, 3H, CH_3); 1.31 (s, 3H, CH_3); 2.33 (s, 3H, arom.CH_3); 3.75-3.86 (m, 2H, Hf-6a,b); 3.88-4.04 (m, 2H, Hp-6a,b); 4.16 (dd, J = 6.7, J = 4.3 Hz, 1H, Hf-5); 4.29 (dd, J = 5.3, J = 1.5 Hz, 1H, Hp-5); 4.33-4.41 (m, 2H, Hf-3, Hf-4); 4.52 (s, 1H, Hp-4); 5.29 (solvent CH_2Cl$_2$); 5.52 (br. s., 1H, Hp-1); 5.58 (d, $^3J_{1,2}$ = 1.3 Hz, 1H, Hf-1); 5.67 (t, J = 2.0 Hz, 1H, Hf-2); 5.73 (br. s., 2H, Hp-2, Hp-3); 7.11 (d, J = 7.9 Hz, 2H, arom.); 7.32-7.62

(m, 11H, arom.); 7.97-8.09 (m, 6H, arom.) ppm. ^{13}C NMR (101 MHz, CDCl$_3$, 300K) δ 21.1 (arom.CH_3); 24.8 (CH_3); 26.0 (CH_3); 53.4 (solvent CH_2Cl_2); 63.2 (Cp-6); 65.2 (Cf-6); 68.5 (Cp-2); 69.5 (Cp-4); 70.6; 71.0 (Cp-3); 74.1 (Cf-5); 82.0 (Cf-2); 82.2; 83.2 (Cp-5); 91.1 (Cf-1); 97.4 (Cp-1); 109.7 (Cq-$isop$.); 128.4 (C-arom.); 128.5 (C-arom.); 128.9 (Cq, arom.); 129.2 (Cq, arom.); 129.3 (Cq, arom.); 129.7 (Cq, arom.); 129.7 (C-arom.); 129.8 x 3 (C-arom.); 132.8 (C-arom.); 133.2 (C-arom.); 133.3 (C-arom.); 133.7 (C-arom.); 137.9 (Cq); 165.6 (C=O); 165.8 (C=O); 165.9 (C=O) ppm. ESI-TOF HRMS: m/z [M+Na]$^+$ calcd for C$_{43}$H$_{44}$O$_{13}$S 800.2503, found 757.2470.

3.5.2.3.2 *p*-Tolyl 2,3-di-*O*-benzoyl-4,6-*O*-di-*tert*-butylsilylene-α-D-galactopyranosyl-(1→6)-2,3-di-*O*-benzosyl-4-hidroxyl-α-D-galactopyranosyl-(1→3)-2-*O*-Benzoyl-5,6-*O*-isopropylidene-1-thio-β-D-galactofuranoside (56).

To a solution of disaccharide acceptor **55** (107 mg, 0.13 mmol) and Gal*p* donor **3** (120 mg, 0.18 mmol) in anhydrous DCM (18 mL), freshly activated MS 4Å was added and stirred under Ar for 1 h at rt. Then, the solution was cool down to 0°C and TMS-OTf (6.5 μL, 0.036 mmol) was added dropwise. The solution was gradually brought to rt and after 1 h, the reaction mixture was quenched by addition of Et$_3$N, filtered, and washed with water and brine. The organic layers were dried over MgSO$_4$, concentrated, and purified by flash column chromatography on silica gel (EtOAc/Hexanes = 1:3) to give the trisaccharide **56** as a beige powder (70 mg, 40%). R$_f$ = 0.30 (EtOAc/Hexanes = 1:3). ^{1}H NMR (400 MHz, CDCl$_3$) δ 0.91 (s, 9H, *t*Bu); 1.12 (s, 12H, *t*Bu, CH_3); 1.26 (s, 3H, CH_3); 2.30 (s, 3H, arom.CH_3); 3.72-3.80 (m, 3H); 4.03-4.16 (m, 3H); 4.20 (d, J = 5.0 Hz, 1H); 4.30 (br. s., 2H); 4.37-4.43 (m, 2H); 4.50-4.56 (m, 1H); 4.79 (d, J = 2.8 Hz, 1H); 5.33 (d, J = 3.5 Hz, 1H); 5.48 (d, J = 3.8 Hz, 1H); 5.54-5.65 (m, 2H); 5.67-5.77 (m, 4H); 7.04 (d, J = 8.1 Hz, 2H, arom.); 7.08-7.15 (m, 2H, arom.); 7.20 (d, J = 7.3 Hz, 1H, arom.); 7.31-7.57 (m, 15H, arom.); 7.93-8.03 (m, 9H, arom.) ppm. ^{13}C NMR (101 MHz, CDCl$_3$, 300K) δ 20.7 (Cq-*t*Bu); 21.1 (arom.CH_3); 23.2 (Cq-*t*Bu); 24.8 (CH_3); 26.0 (CH_3); 27.2 (*t*Bu); 27.4 (*t*Bu); 65.2 (CH_2); 67.0 (CH_2); 67.1 (CH); 67.3 (CH_2); 68.4 (CH); 68.5 (CH); 68.6 (CH); 69.2 (CH); 70.1 (CH); 71.0 (CH); 71.1 (CH); 74.1 (CH); 81.9 (CH); 82.4 (CH); 84.1 (CH); 91.4 (CH); 91.8 (Cq); 97.3 (CH); 97.6 (CH); 109.7 (Cq-*isop*.); 128.2 (C-arom.); 128.3 (C-arom.); 128.4 (C-arom.); 128.5 (C-arom.); 128.6 (C-arom.); 129.0 (Cq, arom.); 129.1 (Cq, arom.); 129.2 (Cq, arom.); 129.3 (Cq, arom.); 129.6 x 2 (C-arom.); 129.7 x 2 (C-arom.); 129.8 x 2 (C-arom.); 132.8 (C-arom.); 132.9 (C-arom.); 133.0 (C-arom.); 133.1 (C-arom.); 133.3 (C-arom.); 133.5 (C-arom.); 137.9 (Cq); 163.5 (Cq); 165.4 (C=O); 165.5 (C=O); 165.8 (C=O); 165.9 (C=O);

166.0 (C=O) ppm. ESI-TOF HRMS: m/z [M+Na]$^+$ calcd for $C_{71}H_{78}O_{20}SSi$ 1333.4474, found 1333.4535.

3.5.2.3.3 Allyl 2,3-di-O-benzoyl-4,6-O-di-$tert$-butylsilylene-α-D-galactopyranosyl-(1$\rightarrow$6)-2,3-di-O-benzoyl-4-hidroxyl-α-D-galactopyranosyl-(1$\rightarrow$3)-2-O-Benzoyl-5,6-O-isopropylidene-β-D-galactofuranosyl-(1$\rightarrow$3)-4,6-O-benzylidene-α-D-mannopyranoside (57).

To a solution of Man$p$ acceptor **8** (10 mg, 32 μmol) and trisaccharide donor **56** (10 mg, 7.6 μmol) in anhydrous DCM (2 mL), NIS (4.3 mg, 19.1 μmol) and AgOTf (0.12 mg, 0.47 μmol) were added consecutively at 0 °C. After 1 h, the reaction mixture was quenched by addition of Et$_3$N, filtered, and washed with a saturated solution of Na$_2$S$_2$O$_3$ and brine. The organic layers were dried over MgSO$_4$, concentrated, and purified by PTLC on silica gel (EtOAc/Hexanes = 1:3) to give the desired fully protected tetrasaccharide **57** (5.5 mg, 47%), as a light-yellow oil. R$_f$ 0.27 (EtOAc/Hexanes = 1:3). ^{1}H NMR (400 MHz, CDCl$_3$) δ 0.89 (s, 9H, tBu); 1.06 (s, 3H, CH_3); 1.10 (s, 9H, tBu); 1.15 (s, 3H, CH_3); 2.05 (d, J = 3.4, 1H); 3.36-3.43 (m, 1H); 3.44-3.51 (m, 1H); 3.61-3.92 (m, 7H); 3.96-4.09 (m, 4H); 4.18-4.46 (m, 9H); 4.99 (d, J = 8.2 Hz, 1H); 5.25 (dd, J = 10.4, J = 1.3 Hz, 1H); 5.35 (dd, J = 17.2, J = 1.6 Hz, 1H); 5.40-5.46 (m, 1H); 5.53 (d, J = 3.3, 1H); 5.56-5.69 (m, 4H); 5.84 (d, J = 5.1, 2H); 5.87-5.99 (m, 2H); 7.19-7.25 (m, 4H, arom.); 7.27-7.45 (m, 11H, arom.); 7.49-7.58 (m, 5H, arom.); 7.77-7.85 (m, 4H, arom.); 7.87-7.91 (m, 2H, arom.); 7.93-7.98 (m, 4H, arom.) ppm. ^{13}C NMR (101 MHz, CDCl$_3$, 300K) δ 20.7 (Cq-tBu); 23.2 (Cq-tBu); 25.1 (CH$_3$); 26.0 (CH$_3$); 27.2 (tBu); 27.5 (tBu); 29.7 (CH$_2$); 63.8 (CH); 65.3 (CH$_2$); 67.0 (CH$_2$); 67.3 (CH); 67.4 (CH$_2$); 68.2 (CH$_2$); 68.4 (CH); 68.8 (CH); 69.0 (CH); 69.3 (CH); 70.7 (CH); 71.2 (CH); 72.0 (CH); 72.1 (CH); 74.9 (CH); 77.2 (CH); 77.5 (CH); 79.8 (CH); 83.2 (CH); 84.8 (CH); 96.1 (CH, C-1); 97.8 (CH, C-1); 99.7 (CH, C-1); 102.1 (CH, C-1); 102.5 (CH, C-1); 109.4 (Cq-$isop$.); 117.1 (C-c); 126.5 (C-arom.); 128.1 (C-arom.); 128.2 (C-arom.); 128.3 (C-arom.); 128.4 x 2 (C-arom.); 128.5 (C-arom.); 128.7 (C-arom.); 128.9 (Cq, arom.); 129.1 (Cq, arom.); 129.2 (Cq, arom.); 129.6 (C-arom.); 129.7 x 2 (C-arom.); 129.8 (C-arom.); 129.9 (Cq, arom.); 130.0 (Cq, arom.); 132.8 (C-arom.); 133.1 (C-arom.); 133.4 (C-arom.); 133.5 (C-arom.); 133.9 (C-arom.); 138.2 (Cq, arom.); 165.4 (C=O); 165.7 (C=O); 165.8 (C=O); 166.0 (C=O); 166.9 (C=O) ppm. ESI-TOF HRMS: m/z [M+Na]$^+$ calcd for $C_{80}H_{90}O_{26}Si$ 1517.5387, found 1517.5383.
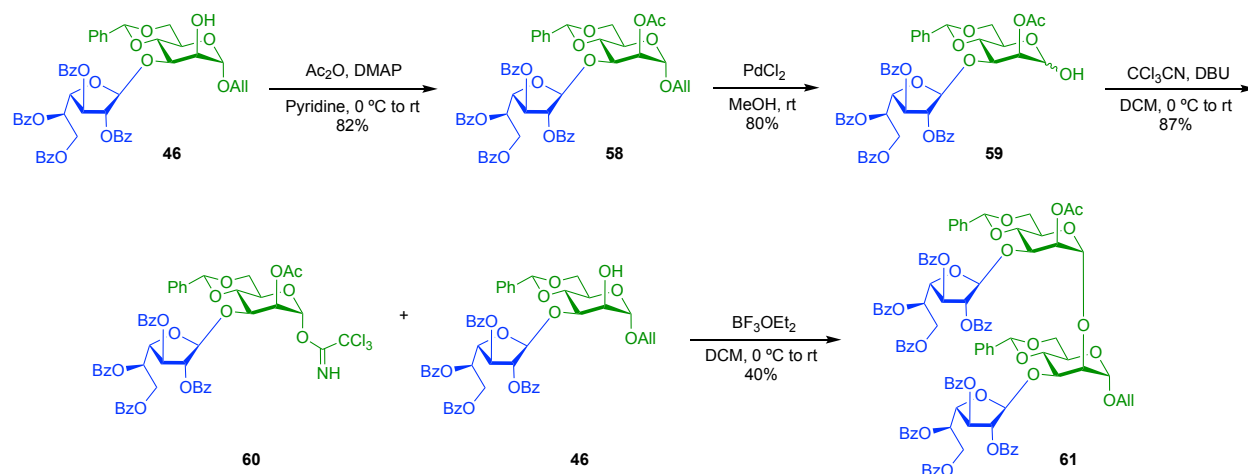
Scheme 22. Synthesis of the mercaptopropyl tetrasaccharide **G32**.

3.5.2.4.1 Allyl 2,3,5,6-tetra-*O*-benzoyl-β-D-galactofuranosyl-(1→3)-2-acetyl-4,6-*O*-benzylidene-α-D-mannopyranoside (58). To a solution of disaccharide **46** (717 mg, 0.81 mmol) in dry pyridine (48 mL) at 0°C, acetic anhydride (4.0 mL) and DMAP (40 mg) were added. The mixture was stirred at 0°C for 30 min, allowed to warm to rt and stirred for 3 h. The mixture was washed with water and extracted with EtOAc. The organic layers were dried over MgSO$_4$, concentrated, and purified by column chromatography on silica gel (EtOAc/Hexanes = 1:3) to afford **58** (616 mg, 82%), as a light-yellow powder. R$_f$ 0.57 (EtOAc/Hexanes = 2:3). ^{1}H NMR (400 MHz, CDCl$_3$, 300K) δ 2.21 (s, 3H, -COC*H*$_3$); 3.80-3.88 (m, 1H); 3.90-4.05 (m, 3H); 4.19 (ddt, *J* = 12.8, 5.2, 1.5, 1.5 Hz, 1H); 4.25-4.35 (m, 2H); 4.45 (dd, *J* = 9.7, 3.7 Hz, 1H); 4.62 (dd, *J* = 12.0, 8.2 Hz, 1H); 4.71 (dd, *J* = 5.3, 3.0 Hz, 1H); 4.87 (d, *J* = 1.5 Hz, 1H); 5.23 (dq, *J* = 10.3, 1.3 Hz, 1H); 5.31 (dq, *J* = 17.2, 1.5 Hz, 1H); 5.40-5.45 (m, 3H); 5.48 (d, *J* = 5.4 Hz, 1H); 5.53 (s, 1H); 5.83-5.97 (m, 2H, H-b); 7.12-7.25 (m, 6H, arom.); 7.29-7.38 (m, 6H, arom.); 7.43-7.57 (m, 4H, arom.); 7.82-7.88 (m, 2H, arom.); 7.92-7.98 (m, 4H, arom.); 7.99-8.04 (m, 2H, arom.) ppm. ^{13}C NMR (101 MHz, CDCl$_3$, 300K) δ 20.9 (CH$_3$); 63.8; 63.9 (CH$_2$); 68.4 (CH$_2$); 68.6; 68.7 (CH$_2$); 69.1; 70.0; 77.2; 77.7; 81.4; 81.6; 97.8; 101.9; 102.2; 118.3 (C-c); 125.8 (*C*-arom.); 128.2 (*C*-arom.); 128.3 x 4 (*C*-arom.); 128.9 (*C*q, arom.); 129.0 (*C*q, arom.); 129.1 (*C*-arom.); 129.5 (*C*q, arom.); 129.6 (*C*q, arom.); 129.7 (*C*-arom.); 129.8 (*C*-arom.); 129.9 (*C*-arom.); 130.0 (*C*-arom.);

85

132.9 (*C*-arom.); 133.1 (*C*-arom.); 133.2 (*C*-arom.); 133.3 (C-b); 137.1 (*C*q, arom.); 165.1 (C=O); 165.4 (C=O); 165.6 (C=O); 166.0 (C=O); 170.1 (C=O) ppm. ESI-TOF HRMS: *m/z* [M+Na]⁺ calcd for $C_{52}H_{48}O_{16}$ 951.2840, found 951.2842.

3.5.2.4.2 Hydroxyl 2,3,5,6-tetra-*O*-benzoyl-β-D-galactofuranosyl-(1→3)-2-acetyl-4,6-*O*-benzylidene-α-D-mannopyranoside (59). To a solution of fully protected disaccharide **58** (571 mg, 0.62 mmol) in dry MeOH (48 mL), PdCl₂ (72 mg) was added. The mixture was stirred at rt for 3 h. The mixture was filtered through celite, while washed with MeOH. The filtrate was evaporated under vacuum and purified by column chromatography on silica gel (EtOAc/Hexanes = 2:3) to afford **59** (437 mg, 80%), as a light-yellow powder. R$_f$ 0.30 (EtOAc/Hexanes = 2:3). ¹H NMR (400 MHz, CDCl₃, 300K) δ 2.21 (s, 3H, -COC*H*₃); 3.14 (d, J = 4.0 Hz, 1H); 3.77-3.86 (m, 1H); 3.97-4.06 (m, 1H); 4.08-4.20 (m, 1H); 4.26 (dd, *J* = 10.1, 4.8 Hz, 1H); 4.34 (dd, *J* = 11.9, 3.7 Hz, 1H); 4.50 (dd, *J* = 10.0, 3.7 Hz, 1H); 4.61 (dd, *J* = 11.9, 8.1 Hz, 1H); 4.71 (dd, *J* = 5.4, 2.9 Hz, 1H); 5.24 (dd, *J* = 3.8, 1.1 Hz, 1H); 5.39-5.55 (m, 5H); 5.93 (dt, *J* = 7.8, 3.3 Hz, 1H); 7.10-7.19 (m, 3H, arom.); 7.27-7.40 (m, 10H, arom.); 7.43-7.58 (m, 4H, arom.); 7.85 (dd, *J* = 8.3, 1.2 Hz, 2H, arom.); 7.92-7.98 (m, 4H, arom.); 7.99-8.05 (m, 2H, arom.) ppm. ¹³C NMR (101 MHz, CDCl₃, 300K) δ 20.9 (CH₃); 63.8; 63.9 (CH₂); 68.7; 68.8 (CH₂); 68.9; 70.0; 77.1; 77.8; 81.4; 81.7; 93.7; 101.9; 102.2; 125.9 (*C*-arom.); 128.2 (*C*-arom.); 128.3 (*C*-arom.); 128.9 (*C*q, arom.); 129.0 (*C*q, arom.); 129.1 (*C*-arom.); 129.5 (*C*q, arom.); 129.6 (*C*q, arom.); 129.7 (*C*-arom.); 129.8 (*C*-arom.); 129.9 (*C*-arom.); 130.0 (*C*-arom.); 133.0 (*C*-arom.); 133.1 (*C*-arom.); 133.2 (*C*-arom.); 133.4 (*C*-arom.); 137.1 (*C*q, arom.); 165.2 (C=O); 165.5 (C=O); 165.7 (C=O); 166.1 (C=O); 170.2 (C=O) ppm. ESI-TOF HRMS: *m/z* [M+Na]⁺ calcd for $C_{49}H_{44}O_{16}$ 911.2527, found 911.2520.

3.5.2.4.3 2,3,5,6-tetra-*O*-benzoyl-β-D-galactofuranosyl-(1→3)-2-acetyl-4,6-*O*-benzylidene-α-D-mannopyranoside trichloroacetimidate (60). To a solution of the mixture α,β-hydrolyzed disaccharide **59** (421 mg, 0.47 mmol) in dry DCM (24 mL), CCl₃CN (1.0 mL, ~20 equiv) and DBU (0.1 mL, ~1.4 equiv) were consecutively added at 0 °C and stirred at rt for 15 min. Then, the residue was concentrated and purified by flash column chromatography on silica gel (EtOAc/Hexanes = 1:2) to yield **60** (425 mg, 87%), as a light-yellow powder. R$_f$ 0.40 (EtOAc/Hexanes = 1:2). ¹H NMR (400 MHz, CDCl₃, 300K) δ 2.25 (s, 3H, -COC*H*₃); 3.81-3.93

(m, 1H); 4.03-4.19 (m, 2H); 4.24-4.40 (m, 2H); 4.52 (dd, J = 9.5, 3.7 Hz, 1H); 4.64 (dd, J = 11.7, 8.0 Hz, 1H); 4.77 (dd, J = 5.1, 3.4 Hz, 1H); 5.44-5.48 (m, 2H); 5.52 (d, J = 5.4 Hz, 1H); 5.56-5.64 (m, 2H); 5.97 (dt, J = 7.7, 3.8 Hz, 1H); 6.26 (s, 1H); 7.09-7.20 (m, 3H, arom.); 7.22-7.40 (m, 10H, arom.); 7.42-7.58 (m, 4H, arom.); 7.87 (d, J = 7.8 Hz, 2H, arom.); 7.95 (t, J = 8.6 Hz, 4H, arom.); 8.02 (d, J = 7.8 Hz, 2H, arom.); 8.74 (s, -NH) ppm. ^{13}C NMR (101 MHz, CDCl$_3$, 300K) δ 20.7 (CH$_3$); 63.4 (CH$_2$); 66.3; 66.9; 68.4 (CH$_2$); 68.9; 69.9; 76.4; 77.2; 77.6; 81.5; 81.8; 90.5 (Cq); 95.7; 101.9; 102.3; 125.8 (C-arom.); 128.2 (C-arom.); 128.4 x 3 (C-arom.); 128.9 (Cq, arom.); 129.0 (Cq, arom.); 129.1 (C-arom.); 129.4 (Cq, arom.); 129.5 (Cq, arom.); 129.7 (C-arom.); 129.8 (C-arom.); 129.9 (C-arom.); 133.0 (C-arom.); 133.1 (C-arom.); 133.3 (C-arom.); 133.4 (C-arom.); 136.8 (Cq, arom.); 160.1 (C=N); 165.1 (C=O); 165.5 (C=O); 165.6 (C=O); 165.9 (C=O); 169.8 (C=O) ppm. ESI-TOF HRMS: m/z [M+Na]$^+$ calcd for C$_{51}$H$_{44}$Cl$_3$NO$_{16}$ 1054.1623, found 1054.1650.

3.5.2.4.4 Allyl 2,3,5,6-tetra-*O*-benzoyl-β-D-galactofuranosyl-(1→3)-2-acetyl-4,6-*O*-benzylidene-α-D-mannopyranoside-(1→2)-[2,3,5,6-tetra-*O*-benzoyl-β-D-galactofuranosyl-(1→3)-4,6-*O*-benzylidene-α D-mannopyranoside] (61).

A solution of disaccharide acceptor **46** (25 mg, 0.03 mmol) and disaccharide donor **60** (43 mg, 0.04 mmol) in anhydrous DCM (6 mL) with freshly activated MS 4Å was stirred under Ar for 30 min at 0°C. Then, BF$_3$OEt$_2$ (2.0 μL, 0.54 mmol) was added to the flask, which was kept stirring at 0 °C for 15 min, and gradually brought to room temperature. After 30 min at rt, the reaction mixture was quenched by addition of Et$_3$N, filtered, and washed with a saturated solution of Na$_2$S$_2$O$_3$ and brine. The organic layers were dried over MgSO$_4$, concentrated, and purified by column chromatography on silica gel (EtOAc/Hexanes = 2:3) to afford **61** (20 mg, 40%), as a light-yellow oil. R$_f$ 0.53 (EtOAc/Hexanes = 2:3). ^{1}H NMR (400 MHz, CDCl$_3$, 300K) δ 2.12 (s, 3H); 3.85-3.94 (m, 3H); 3.97-4.41 (m, 11H + 2H from EtOAc); 4.49-4.56 (m, 2H); 4.64 (dd, J = 5.4, 2.7 Hz, 1H); 4.71 (dd, J = 11.7, 8.2 Hz, 1H); 4.77 (dd, J = 5.2, 3.4 Hz, 1H); 4.84 (d, J = 1.0, 1H); 5.23-5.36 (m, 5H); 5.44 (s, 1H); 5.49 (d, J = 5.5, 1H); 5.51-5.57 (m, 3H); 5.59 (s, 1H); 5.80 (dd, J = 3.6, 1.2 Hz, 1H); 5.85-5.97 (m, 2H); 6.01 (dt, J = 7.7, 3.8 Hz, 1H); 7.15-7.25 (m, 12H, arom.); 7.28-7.39 (m, 15H, arom.); 7.45-7.56 (m, 7H, arom.); 7.74-7.84 (m, 4H, arom.); 7.92-7.99 (m, 6H, arom.); 8.00-8.08 (m, 6H, arom.) ppm. ^{13}C NMR (101 MHz, CDCl$_3$, 300K) δ 14.2 (CH); 20.8 (CH$_3$); 21.1 (CH); 29.7 (CH); 60.4 (CH$_2$); 63.6 (CH$_2$); 64.1 (CH); 64.3 (CH); 64.4 (CH$_2$); 67.8 (CH); 68.1 (CH$_2$); 68.7 (CH$_2$); 69.2 (CH); 70.1 (CH); 70.2 (CH);

71.4 (CH); 75.1 (CH); 76.8 (CH); 77.2 x 2 (CH); 77.5 (CH); 77.7 (CH); 81.5 (CH); 81.6 (CH); 81.7 (CH); 82.4 (CH); 99.0 (CH); 101.4 (CH); 101.9 (CH); 102.0 (CH); 102.4 (CH); 102.5 (CH); 117.9 (CH_2); 125.8 (*C*-arom.); 126.0 (*C*-arom.); 128.1 (*C*-arom.); 128.2 (*C*-arom.); 128.3 (*C*-arom.); 128.8 (*C*q, arom.); 128.9 (*C*q, arom.); 129.0 (*C*-arom.); 129.1 (*C*q, arom.); 129.2 (*C*q, arom.); 129.5 (*C*q, arom.); 129.6 (*C*q, arom.); 129.7 x 2 (*C*-arom.); 129.8 x 2 (*C*-arom.); 129.9 x 3 (*C*-arom.); 130.0 (*C*-arom.); 132.8 (*C*-arom.); 132.9 (*C*-arom.); 133.0 (*C*-arom.); 133.1 (*C*-arom.); 133.2 (*C*-arom.); 133.3 x 2 (*C*-arom.); 133.4 x 2 (*C*-arom.). 137.1 (*C*q, arom.); 137.3 (*C*q, arom.); 165.1 (C=O); 165.5 (C=O); 165.6 (C=O); 165.7 (C=O); 165.9 (C=O); 166.0 (C=O); 169.9 (C=O). ESI-TOF HRMS: *m/z* $[M+Na]^+$ calcd for $C_{99}H_{88}O_{30}$ 1779.5258, found 1779.5445.

Chapter 4: Discovery of an Galpα(1,6)[Galpα(1,2)]Galpβ-containing neoglycoprotein as a synthetic biomarker for CD

4.1 ABSTRACT

CD is caused by the protozoan parasite *T. cruzi,* and it affects 6-7 million people worldwide. Chemotherapeutic intervention is effective for the most part, but is associated with significant adverse effects. The development of safer drugs is hampered by the difficulty of determining drug efficacies *in vivo* due to the lack of a clinical *T. cruzi*-specific biomarker. The mammal-dwelling trypomastigote form of *T. cruzi* expresses heavily glycosylated glycosylphosphatidylinositol mucins (tGPI-MUC), whose *O*-glycans are predominantly branched, and often contain terminal α-Gal*p* moieties. Since such α-Gal containing glycans are absent in humans, they are highly immunogenic, causing high titers of anti-α-Gal Abs in all CD patients. In search for a specific α-Gal-based biomarker we show the synthesis of neoglycoprotein NGP11b, consisting of BSA decorated with multiple copies of the branched trisaccharide Galpα(1,6)[Galpα(1,2)]Galpβ. When subjected to CL-ELISA using CD patient sera and NHS of healthy individuals, NGP11b shows strong differential antibody reactivities similar to tGPI-MUC. Likewise, NGP11b has a considerably stronger antibody reactivity with sera from *T. cruzi*-infected 1,3 α-Gal Transferase knock-out mice when compared to sera of healthy mice. Notably, NGP11b shows a greater specificity than tGPI-MUC with a clear CD positive/negative boundary. Lastly, CD patients show a remarkable reduction in anti-α-Gal antibody reactivity to NGP11b after only one year post chemotherapy. Our data suggest that Galpα(1,6)[Galpα(1,2)]Galpβ may be an immunodominant partial structure of terminal *T. cruzi* glycans or a mimic thereof, and that NGP11b is suitable as a diagnostic biomarker for CD and for drug efficacy assessment in patients.

4.2 INTRODUCTION

American trypanosomiasis, commonly known as CD, is a neglected tropical disease (NTD) caused by the protozoan parasite *T. cruzi.* Historically limited to Latin America, CD has spread beyond its geographical boundaries due to global migration, and currently affects 6-7 million people worldwide.[94-96] An estimated 300,000 infected individuals reside within the United States posing a threat for transmission.[23] *T. cruzi* transmission occurs by several routes including insect-vector transmission by Triatominae species (commonly known as kissing bugs) and other non-vectorial mechanisms, which include blood transfusion, transplantation, consumption of contaminated foods and fluids, and vertical transmission from mother to infant.[95, 97-99]

Clinical manifestations of CD can be broken down into two distinct phases, i.e., the acute phase and the chronic phase. The acute phase is characterized by the presence of mild, nonspecific symptoms which include fever and malaise,[98] while the chronic phase is characterized by a broad spectrum of clinical outcomes, which range from complete lack of symptoms, to severe disease or even death.[97, 100] An estimated 20-30% individuals with chronic CD will develop cardiomyopathy, which can lead to cardiac failure and sudden death, while others can experience development of gastrointestinal complications including megacolon, or megaesophagus.[96, 97, 101]

T. cruzi exhibits a complex life cycle separated into mammalian dwelling stages and vector dwelling stages.[102] Inside the triatomine insect vector, replicative non-infective epimastigotes (Epis) reside in the midgut, eventually migrating to the insect's hindgut and differentiating to the infectious metacyclic trypomastigotes (Metas) induced by nutritional stress. After taking a bloodmeal, the triatomine will release Meta forms in the feces which can infect the host through the wound site or the mucosa. Inside host cells, Metas differentiate into replicative non-infective intracellular amastigotes (ICAs) which multiply by binary fission into the cytoplasm. ICAs

90

eventually differentiate into mammalian tissue cell-derived trypomastigotes (TCTs) that burst out of the host cell, allowing the parasite to invade surrounding cells, or gain access to the bloodstream.

Currently, only two drugs are available for the treatment of CD: nifurtimox (NFX) and benznidazole (BNZ). While these drugs are both effective in the acute phase, they are less effective in the chronic phase.[95, 103] Moreover, these drugs are highly toxic resulting in 20-30% of patients terminating treatment.[103, 104] Furthermore, patients take approximately 10-20 years to exhibit negative seroconversion with conventional serology (CS) making assessment of chemotherapeutic efficacy problematic. As the number of circulating parasites decreases due to chemotherapy, polymerase chain reaction, which is considered the gold standard for diagnosis, reaches its detection limit, and is therefore only of limited utility for drug efficacy assessments in patients. The lack of specific BMKs for CD poses a major burden on the development and assessment of novel antitrypanosomal drugs.[105] Poor prognostic perspectives from CS do not support widespread treatment of chronic CD, resulting in only 1% of patients undergoing treatment.[106]

T. cruzi has a complex cell surface that contains various types of glycoconjugates linked to the plasma membrane through glycosylphosphatidylinositol (GPI)-anchors. They include major families of GPI-anchored mucins (GPI-MUC), mucin-associated surface proteins (MASP), trans-sialidases (TS), and protein-free glycoinositolphospholipids (GIPLs).[36, 38, 107] GPI-MUC are the most abundant glycoconjugates decorating the parasite surface, consisting of 2×10^6 copies per parasite, expressed by 863 genes.[38] Many *O*-glycans found on the GPI-anchored mucins of TCTs (tGPI-MUC) contain terminal nonreducing α-Gal*p* residues. Only one tGPI-MUC *O*-glycan has been fully characterized to date, i.e. the linear trisaccharide, Gal*p*α1,3Gal*p*β1,4GlcNAc*p*α, which makes up approximately 10% of all *O*-glycans in tGPI-MUC.[12] Most of the remaining 90% are believed to be branched at the reducing α-GlcNAc terminus, however, their exact structures remain

91

uncharacterized.[12] These α-Gal-containing glycans are highly immunogenic to humans, due to their absence on human cells as a result of the inactivation of the α1,3-galactosyltransferase (α1,3-GalT) gene millions of years ago in ancestral primates.[12, 41, 108] Patients with CD produce substantial amounts of lytic, protective anti-α-Gal Abs against α-Gal epitopes found on tGPI-MUC. These anti-α-Gal Abs are the major protective Abs in both acute and chronic CD,[12, 29, 42, 43] and are present in the sera of CD patients from different endemic (Brazil, Argentina, Chile, Bolivia, Mexico, Venezuela) and non-endemic countries (Spain, United States), signifying that these epitopes are universally expressed in different strains, and genotypes of *T. cruzi*.[2, 29, 42, 109, 110] Unlike protein Abs, carbohydrate specific Abs disappear from circulation soon, i.e. within a few years, after elimination of the parasite from the infected host[29] suggesting that α-Gal-containing glycotopes of tGPI-MUC may not only be highly specific BMKs for accurate diagnosis, but could be instrumental in the early assessment of post-chemotherapeutic outcomes as antigens in CL-ELISA.[15, 29, 109, 111] On account of that, synthetic NGPs based on terminal, non-reducing α-Gal residues found in tGPI-MUC,[15, 17, 112] exhibit a promising approach for CD diagnosis that could also provide a more rapid and specific test and avoid very demanding long-term patient follow-up as observed in the CS tests.

Here we describe the synthesis of neoglycoprotein **NGP11b**, consisting of BSA decorated with multiple copies of the putative tGPI-MUC-derived glycotope Gal*p*α1,6[Gal*p*α1,2]Gal*f*β, and the assessment of its suitability as a biomarker for CD diagnosis, and its potential for the monitoring of disease clearance after chemotherapy. The capability of NGP11b to serve as a diagnostic biomarker in patients and to confirm experimental *T. cruzi* infection in a mouse model, was assessed by CL-ELISA using sera of CD patients, and sera of *T. cruzi*-infected 1,3α-transferase knockout mice, respectively. The antibody reactivities of *T. cruzi*-positive and *T. cruzi*-

negative sera to NGP11b and a preparation of tGPI-MUC from the *T. cruzi colombiana* strain were compared. In addition, we show a first preliminary assessment of NGP11b as a biomarker in the monitoring of anti-α-Gal antibody levels in patients who have undergone treatment with BNZ.

4.3 RESULTS AND DISCUSSION

4.3.1 Synthesis of NGP11b

The synthetic strategy to generate the mercaptopropyl glycoside of Gal*p*α1,6[Gal*p*α1,2]Gal*p*β **G11** with two nonreducing α-Gal moieties and its conjugation to commercially available maleimide-derivatized BSA is presented. Structural analysis of tGPI-MUC glycans of *T. cruzi* and preliminary interrogations of an α-Gal-containing glycoarray by CL-ELISA using chronic CD patient sera suggest that this branched glycan could be a terminal partial structure of glycans expressed in the tGPI-MUC of *T. cruzi*.[15, 17, 113]

The neoglycoprotein NGP11b was prepared by the synthetic strategy depicted in **Scheme 23**, and consisted of the following steps: (a) a double glycosylation of the partially protected acceptor **62** using the stereoselective introduction of α-Gal moieties with Kiso's α-Gal donor **3** equipped with a 4,6-*O*-di-*tert*-butyl silylidene group and trimethylsilyl trifluoromethanesulfonate (TMSOTf) activation to furnish the fully protected trisaccharide **63** in 72% yield; (b) the removal of the silylidene group using hydrofluoric acid-pyridine (HF-Py) complex in 90% yield **64**, followed by hydrolysis of the isopropylidene group with TFA/H_2O/DCM in 96% yield **65**; (c) the installation of a mercaptopropyl group at the reducing end of the glycan by radical addition of thioacetic acid (AcSH) to the allyl glycoside **65** in the presence of azobisisobutyronitrile (AIBN) in dry THF under UV-light illumination to afford thioester **66** in 76% yield; (d) the complete deacylation of thioester **66** using Zemplén conditions affording the target trisaccharide **G11**

quantitatively, which oxidizes to the disulfide **67** within approximately 1h, unless oxygen is strictly excluded; and (e) the conjugation of glycan **G11** (obtained by reduction of disulfide **67** with tris(2-carboxyethyl)phosphine hydrochloride) (TCEP·HCl) *in situ*, to commercial maleimide-derivatized BSA. The intermediates **63-66**, and the disulfide **67** were fully characterized by thin layer chromatography, optical rotation, ^{1}H and ^{13}C nuclear magnetic resonance (NMR) spectroscopy, and high-resolution electrospray ionization-time of flight (HR ESI-TOF) mass spectrometry. The average number of conjugated glycans per BSA molecule, i.e. Gal*p*α(1,6)[Gal*p*α(1,2)]Gal*p*β units/BSA, was determined by MALDI-TOF mass spectrometry. The average number of glycans per BSA molecule was calculated by subtracting the average mass of the commercial maleimide-derivatized BSA from the average mass of NGP11b, **Figure 26**.
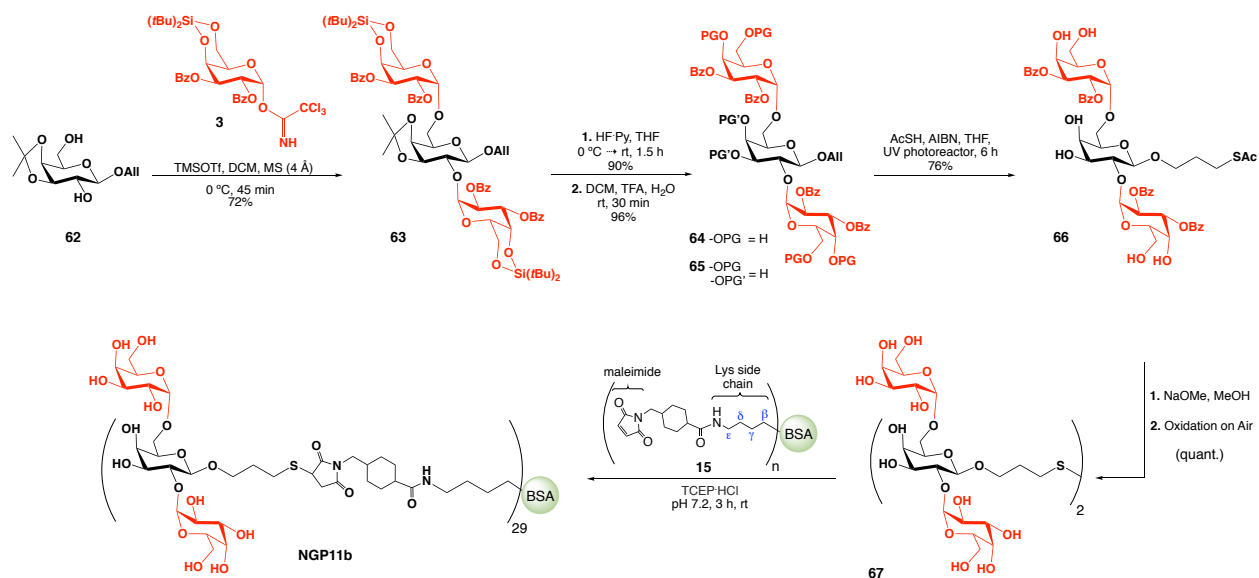
Scheme 23. Synthesis of the trisaccharide 3-thiopropyl α-D-galactosyl-(1→2)-[α-D-galactosyl (1→6)]-β-D-galactoside **G11** and its conjugation to maleimide derivatized BSA to afford **NGP11b**.
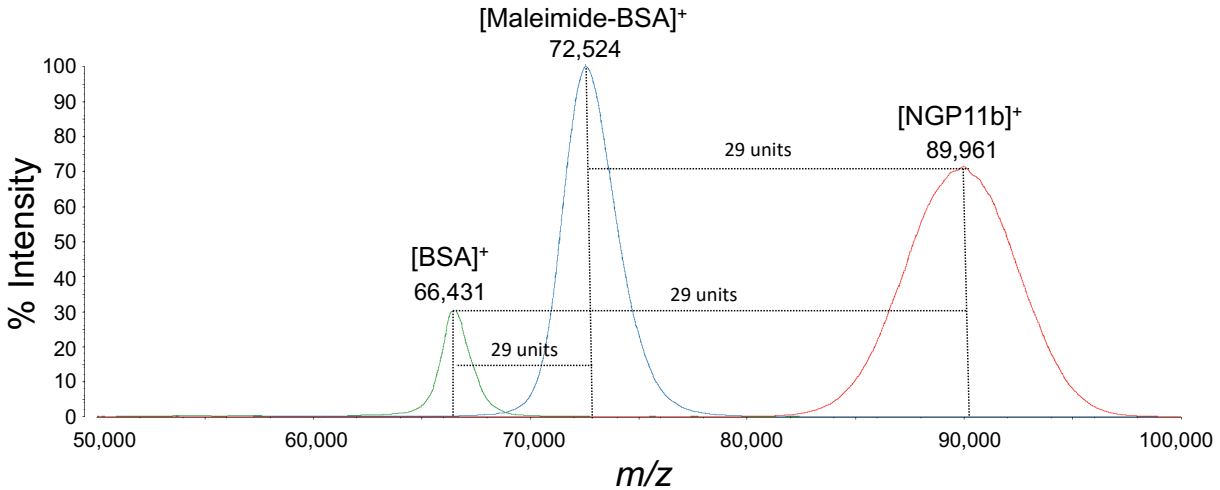
Figure 26. Overlaid MALDI-TOF MS spectra of BSA, Maleimide-BSA, and NGP11b.

4.3.2 Evaluation of NGP11b as a biomarker for CD by CL-ELISA

With NGP11b in hand, its suitability as a diagnostic biomarker was assessed and compared to a tGPI-MUC preparation from the *T. cruzi colombiana* strain.[15] Purified tGPI-MUC and NGP11b were immobilized in 96-well polystyrene Nunc Maxisorp ELISA plates and antibody-binding responses were measured via CL-ELISA using pooled sera from 10 chronic CD patients (ChHSP) and 10 healthy donors (NHSP). In order to optimize the CL-ELISA conditions for maximum specificity and sensitivity, cross-titrations with various dilutions of pooled sera and different quantities of immobilized antigen were performed. As shown in **Figure 27a**. and **2b**., both tGPI-MUC and NGP11b clearly display high differential immunoreactivities between ChHSP and NHSP. The reactivity of NHSP was considerably lower than ChHSP at all titration points, indicating that natural anti-α-Gal Abs from healthy individuals react poorly with tGPI-MUC and NGP11b, while anti-α-Gal Abs from CD patients maintain strong reactivities in a dose-dependent manner. For example, at a sera dilution of 1: 400 and 50 ng of immobilized NGP11b, a differential antibody reactivity of a factor of 11 (ChSP vs. NHSP) is observed in **Figure 27b**., while

maintaining a robust sensitivity. tGPI-MUC displays even greater differentials, presumably due to the presence of many structurally different epitopes within this antigen. For example, at a sera dilution of 1:400 and 50 ng of immobilized tGPI-MUC, a differential antibody reactivity of a factor of 28 is noted.

NGP11b was also evaluated for its ability to detect murine anti-α-Gal Abs by titrating pooled sera from 10 C57Bl/6 α-GalT-KO mice infected with *T. cruzi* (ChMSP) and 10 healthy C57Bl/6 α-GalT-KO mice (NMSP) as shown in **Figure 27c**. The reactivity of ChMSP maintained an average of 23 times higher than NMSP at all sera dilution points suggesting that only murine anti-α-Gal Abs raised during *T. cruzi* infection recognize and bind strongly to NGP11b, in contrast to poor recognition of natural anti-α-Gal Abs from healthy mice. This high differential immunoreativity ascertains that NGP11b can be applied as a biomarker in laboratories that use 1,3α-GalT KO mice as a CD model.

In order to evaluate the specificity of ChHSP to terminal α-Gal*p* residues, both antigens, tGPI-MUC and NGP11b, were treated with green coffee bean α-galactosidase (α-Galase), an exoglycosidase that catalyzes the hydrolysis of terminal, non-reducing α1,3; α1,4; and α1,6-linked galactose from oligosaccharides. We rationalized that a reduction of the immunoreactivity of ChHSP following Galase treatment would corroborate the α-Gal specificity of Abs present in ChHSP. Indeed, CL-ELISA results show that treatment of tGPI-MUC and NGP11b with α-Galase reduces the immunoreactivity of ChHSP by 49.5% and 59.6%, respectively as shown in **Figure 27d**. These results strongly suggest that practically half of the antibody reactivity of ChHSP toward tGPI-MUC can be attributed specifically to the recognition of terminal, non-reducing α1,3; α1,4; and/or α1,6-linked Gal, and nearly 60% of the antibody reactivity of ChHSP towards NGP11b is a consequence of specific binding to the α1,6-linked Gal residue. The remaining antibody

96

reactivity observed after hydrolytic cleavage of the α1,6-linked Gal residue of NGP11b could indicate that the α1,2-linked Gal is also specifically recognized. Alternatively, it may point to cross-reactivity of the same Abs with the newly generated disaccharide Gal$p$α(1,2)Gal$p$β. It is not surprising that the reduction of antibody reactivity after α-Galase treatment in case of tGPI-MUC is somewhat less pronounced, because tGPI-MUC is likely to contain other carbohydrate, peptide and/or glycopeptide epitopes which may be independently recognized by different Abs present in ChHSP.

The ability for NGP11b to accurately designate sera from individual CD patients as positive, and not cross-react with sera from healthy donors, is essential for its usefulness as a diagnostic biomarker. To further assess the sensitivity and specificity of NGP11b as a diagnostic biomarker for CD, it was put to a test by measuring antibody-binding responses of individual sera from 70 patients with confirmed CD and 27 healthy donors by CL-ELISA, and by comparing to tGPI-MUC, **Figure 27e**. When NGP11b was used as an antigen in CL-ELISA, CD patients and healthy individuals fell into two distinct groups on the CL-ELISA plot, with a clear boundary between the two categories of CD positive or negative. Only one CD patient lies in between and cannot be conclusively diagnosed with NGP11b as a biomarker. Thus, as a diagnostic biomarker for CD, NGP11b is 98.6% sensitive and 100% specific. In comparison, when using tGPI-MUC as an antigen, four CD patient sera (5.7%) gave false-negatives, and one was inconclusive. Thus, NGP11b shows a greater biomarker specificity than tGPI-MUC.

While NGP11b holds promise as a biomarker for CD diagnosis, another important question is whether or not it is also suitable for the assessment of chemotherapy efficacy in patients. To address this question, the anti-α-Gal antibody levels of six migrant CD patients from Latin America, who are treated in Barcelona, Spain, were determined before and after treatment with

BNZ using NGP11b as a biomarker in CL-ELISA. Our data show that even though individual patients had different anti-α-Gal antibody levels prior to chemotherapy, one year after chemotherapy, all patients showed a reduction of anti-α-Gal antibody levels by 38-50%. On average, a drop of 45% in patient titers after treatment was observed, indicating that NGP11b can follow α-Gal-specific Abs that begin to disappear from circulation soon after elimination of *T. cruzi* from the host.

Taken together, these data suggest that NGP11b can be utilized as a CD specific biomarker for diagnosis and drug efficacy assessment. NGP11b may eventually replace tGPI-MUC, which can suffer from lack of sufficient specificity, batch-to-batch inconsistencies, and require the cultivation of a large amount of infectious trypomastigotes, followed by lengthy purification processes.
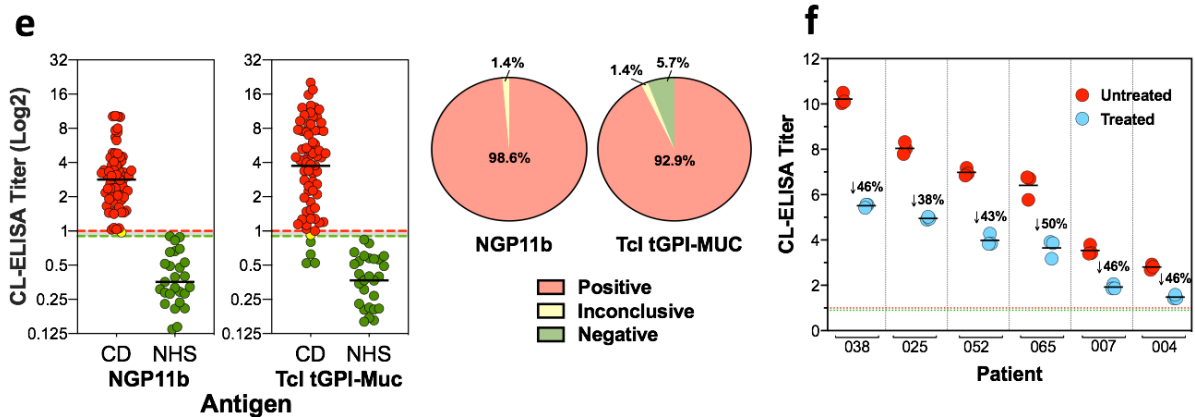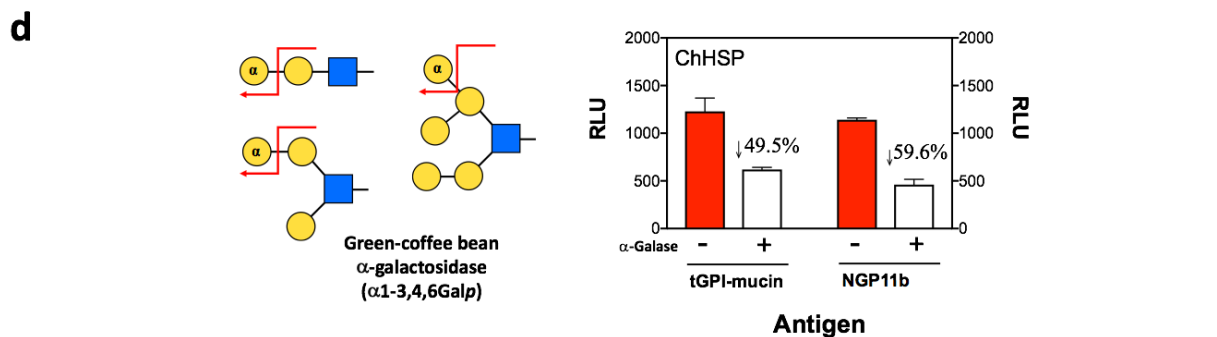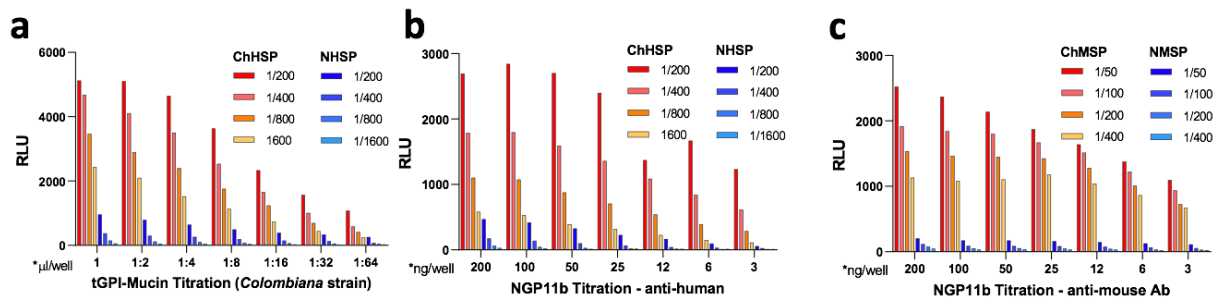
Figure 27. Immunological evaluations of NGP11b by CL-ELISA; high RLU values indicate a high antibody reactivity. **a**) Cross-titration of varying quantities of immobilized tGPI-MUC (isolated and purified from *T. cruzi colombiana*) at different serum dilutions. Chagas Human Sera Pool (ChHSP) (*n*=10) was obtained from patients with chronic CD, and Normal Human Sera Pool (NHSP) (*n*=10) was obtained from healthy donors. **b**) Cross-titration of varying quantities of immobilized NGP11b at different dilutions of ChHSP and NHSP. **c**) Cross-titration of varying quantities of immobilized NGP11b against different dilutions of murine sera pools from 1,3αGal Transferase-KO mice with *T. cruzi* infection (ChMSP) and healthy 1,3αGal Transferase-KO mice (NMSP). **d**) CL-ELISA reactivity of ChHSP with tGPI-MUC and NGP11b before and after treatment of the immobilized antigens with α-Galase. **e**) CL-ELISA titers of individual CD patients from Venezuela and Mexico and individual healthy donors with NHS from the USA against NGP11b and tGPI-MUC. **f**) Anti-α-Gal antibody reactivity of the sera of patients with Chronic Chagas Disease (CCD) against NGP11b analyzed by CL-ELISA before and after chemotherapy for monitoring the efficacy of BZN in patients. Serum samples from individual patients were tested in triplicate before BNZ treatment (Untreated-Red labels), and 24 months after drug treatment (Treated-Blue labels). Codified patients are represented by numbers (# 038, 025, 052, 065, 007, and 004). Each circle represents the determination of one technical replicate. **e-f.** The tGPI-MUC and NGP11b CL-ELISA titers were calculated according to Frey's paper.[92] RLU of sample average was divided by each particular plate cutoff, calculated as the mean value of 9 NHSP. Dotted horizontal red line: titer equal to 1.0. Green dashed line: titer equal to 0.9. Data interpretation: positive result, titer equal or greater than 1.0; inconclusive result, titer <1.0 and >0.9; negative result, titer equal or <0.9. [99.5% CI for all data collected].

4.4 CONCLUSIONS

A branched trisaccharide with two terminal, non-reducing α-Gal units (Gal*p*α(1,6)[Gal*p*α(1,2)]Gal*p*β-(CH₂)₃SH was synthesized and conjugated to BSA to produce NGP11b, which was serologically evaluated as a biomarker for CD diagnosis and for early assessment of drug efficacy in patients. Strong dose-dependent antibody responses of patient sera as well as sera of *T. cruzi*-infected 1,3α-GalT KO mice were measured by CL-ELISA, suggesting

100

that Gal$p$α(1,6)[Gal$p$α(1,2)]Gal$p$β may be an immunodominant partial structure of terminal *T. cruzi* glycans or a mimic thereof. We have shown that the majority of the antibody reactivities toward NGP11b observed in CD patient sera can be attributed specifically to the recognition of terminal, non-reducing α-Gal residues. On the other hand, sera of healthy individuals show poor antibody reactivity with NGP11b.

Using a large cohort of 97 individual sera from CD patients and healthy donors, we demonstrated that NGP11b can place *T. cruzi* positive and *T. cruzi* negative sera into two distinct groups by CL-ELISA. Only one single serum fell between the two groups and was therefore inconclusive. Based on these results, NGP11b has an accuracy of 98.6% in distinguishing *T. cruzi* positive sera from the sera of healthy individuals. In contrast, when tGPI-MUC is used as a biomarker with the same cohort, the accuracy was only at 92.1%, as four sera of CD patients appeared negative, and one was inconclusive. This result shows that NGP11b has the potential to replace tGPI-MUC as a biomarker for CD in serological assays. We have also demonstrated for the first time that a synthetic *T. cruzi* trypomastigote resembling glycan can be used for the early assessment of parasiticidal drug efficacy in CD patients.

In summary, our results corroborate the antigenicity and specificity of the α-Gal epitopes in NGP11b. Due to significant differential antibody reactivities between sera of CD patients and healthy individuals, NGP11b is suitable as a diagnostic CD biomarker, and also shows potential for CD follow-up after chemotherapeutic intervention. Current efforts are focused on the discovery and immunological evaluation of carbohydrate-based BMKs that produce even larger antibody reactivity differentials, between *T. cruzi* positive and negative sera, and to extend drug efficacy studies to longer time periods.

4.5 EXPERIMENTAL SECTION

4.5.1 General Information

All chemicals were purchased as reagent grade and used without further purification from Thermo Fisher Scientific, Sigma-Aldrich or Acros Organic. The ACS grade solvents used for reactions were obtained from Thermo Fisher Scientific and if necessary further dried following standard procedures. Molecular sieves (MS 3 and 4 Å) were purchased from Alfa Aesar or Fisher Scientific, respectively, and activated under high vacuum and heat prior to use. Reactions were performed under an argon (Ar) atmosphere, strictly anhydrous conditions and monitored by thin-layer chromatography (TLC) on silica gel 60 F254 plates from EMD Millipore or Dynamic Adsorbents, Inc. Spots were detected under UV light and/or by charring with 2% sulfuric acid in ethanol. The purification of the compounds was performed by column chromatography on silica gel (40-60 μm) from Fisher Chemical, and the ratio between silica and crude product ranged from 50:1 to 200:1 (dry w/w). Optical rotation measurements were obtained on an ATAGO AP300 automatic polarimeter. ^{1}H and ^{13}C NMR spectra were recorded on a Bruker Avance III HD 400 MHz NMR spectrometer at 400 and 101 MHz, respectively. Chemical shifts (in ppm) were determined relative to tetramethylsilane (δ 0.00 ppm). Coupling constant(s) [Hz] were measured from one-dimensional spectra. Mass spectrometry (MS) of the carbohydrates derivatives was performed on a high resolution JEOL Accu Time Of Flight (TOF) mass spectrometer using an Electrospray Ionization (ESI) source. Protein derivatives were measured by Matrix Assisted Laser Desorption Ionization (MALDI)-TOF MS. The Thiol-ene reaction was performed in a Rayonet RPR200 photochemical reactor (USA) equipped with 16 UV lamps (350 nm).

4.5.2 CL-ELISA of tGPI-MUC and NGP11b

tGPI-MUC were extracted and purified as described by the Almeida group.[12, 15] CL-ELISA was performed as described[15, 114] to assess the specificity of IgG from patients infected with CD against NGP11b in comparison to purified tGPI-MUC. The antigens were immobilized to Nunc MaxiSorp polystyrene microplates for 16 h at 4 °C in Carbonate-Bicarbonate Buffer (CBB), 200 mM, pH 9.6. After antigen loading, the plates were blocked with 200 μL per well Phosphate-Buffered Saline (PBS) containing 1% BSA, (**PBS-B**) and incubated for 1 h at 37 °C. The plates were then washed three times with 200 μL of PBS containing 0.05% Tween 20 detergent (**PBS-T**). Pools of human sera, or individual patient sera were analyzed in triplicate at a dilution of 1:200-1:1600 and 1:800, respectively, in PBS-B, and 0.05% **PBS-TB**. The plates were incubated for 1 h at 37 °C followed by washing three times with 200 μL of PBS-T. 50 μL of Biotinylated goat Anti-human IgG Abs, diluted at 1:10,000 in PBS-TB was added to each well and incubated for 1 h at 37 °C. After washing three times with 200 μL of PBS-T, 50 μL of High sensitivity Neutravidin-Horseradish Peroxidase (**NA-HRP**) diluted in PBS-TB was added at 1:5,000 dilution. The plates were incubated again for 1 h at 37 °C. After a final round of washing with PBS-T, the plates were developed with 50 μL of the substrate Super Signal ELISA Pico Stable Peroxide Solution and Super Signal ELISA Pico Luminol Enhancer; and CBB/0.1% BSA in a 1:1:8 ratio (v/v/v) and relative luminescent units (RLU) were measured using a Luminoskan Accent Luminometer. The titers were calculated by dividing the average of patient RLU values by the cutoff of each plate, which was determined by utilizing the standard deviation multiplier at 99.5%. The Confidence Interval (**CI**) for 9 true negative sera was calculated as described by Frey et al (CI 99.5% 9 controls = 3.537).[92]

4.5.3 α-Galactosidase treatment of tGPI-MUC and NGP11b

To confirm the specificity of ChHSP IgG Abs reacting strongly against tGPI-MUC and NGP11b, the antigens were treated with α-Galase prior to performing CL-ELISA as described.[15] Briefly, 25 ng of NGP11b, and 2.83 ng of tGPI-MUC were immobilized per well on a Nunc MaxiSorp polystyrene microplate for 16 h at 37 °C. The plates were blocked with 200 µL of PBS-B, followed by treatment with 0.5 units of α-Galase per well in ice cold 100 mM potassium phosphate buffer at pH 6.5 for 16 h at 37 °C. The CL-ELISA was then processed as described in the section above.

4.5.4 Conjugation of the glycan to maleimide-derivatized BSA

The kit for the conjugation of the thiol containing glycan **G11** to BSA (Imject™ Maleimide-Activated BSA, 77116 cat. number), was purchased from Thermo Fisher Scientific and the conjugation procedure followed was similar to the ones described by the manufacturer and previously published.[15]

Tris(2-carboxyethyl)phosphine hydrochloride (TCEP·HCl, 0.8 mg, 2.8 µmol) was dissolved in 250 µL of conjugation buffer provided in the kit (83 mM sodium phosphate buffer, 0.1 M EDTA, 0.9 M sodium chloride, 0.02% sodium azide, pH 7.2). The TCEP·HCl solution was added to a 1.5 mL micro-centrifuge tube that contained sugar-disulfide **67** (2.7 mg, 2.4 µmol), and the mixture was agitated in a shaker for 30 min to furnish sugar-thiol **G11**. An aliquot of 10 µL (0.11 mg of **G11**) was set aside for the colorimetric determination of the thiol concentration. The maleimide-activated BSA (2 mg, 15-25 moles of maleimide/mole BSA) was reconstituted with 200 µL of ultrapure water to produce a 10 mg/mL solution. The trisaccharide solution was added to the

104

reconstituted BSA and incubated at RT for 2-3 h in a shaker. After that time, 18.3 μL (which would correspond to the same quantity of **G11** if not conjugation had occurred) were removed from the conjugation mixture to determine the concentration of unreacted thiol. This aliquot was diluted to 2.75 mL with reaction buffer (0.1 M sodium phosphate, pH 8.0, containing 1 mM EDTA), combined with 50 μL of Ellman's reagent [5,5'dithiobis-(2-nitrobenzoic acid) = DTNB] solution (4 mg DTNB in 1 mL of reaction buffer), and reacted for 15 min at RT. With a UV Vis spectrophotometer, the absorbance at 412 nm was measured. The thiol concentration was determined using the molar extinction coefficient of 2-nitro-5-thiobenzoic acid (TNB, $\varepsilon = 14,150$ M^{-1} cm^{-1}), and the amount of sugar conjugated, typically 2.0 μmol, was calculated.

The conjugation mixture was diluted with ultrapure water to a volume of 1 mL and desalted using an Amicon Ultra 3K centrifugal filter and was centrifuged for 20 min at $4,000 \times g$, RT. The mixture was washed with 1 mL of ultrapure water three times following the same procedure. The tube with the filtrate was then removed, and 500 μL of ultrapure water was added to the NGP11b solution remaining in the filter. Since, a small amount of aggregation can occur, the solution/suspension was transferred onto a 2 mL ZebaTM spin desalting column (7K MWCO) provided in the kit that was previously washed with 1 mL of ultrapure pure water 4 times by centrifuged at $1,000 \times g$ for 2 min, RT. This procedure removed all salts and aggregated protein. The filtrated was lyophilized and can be stored at -50 ºC for at least 6 months. In our hands, this combination of filtration and size exclusion chromatography avoids or minimizes aggregation of the NGP. To determine the NGP11b quantity, a solution of 1-2 mg of it in 1-3 mL of ultrapure water was prepared, and the concentration was determined with a Pierce BCA Protein Assay Reagent kit using a spectrophotometer at a detection wavelength of 562 nm.

4.5.5 Matrix Assisted Laser Desorption Ionization Time-Of-Flight Mass Spectrometry (MALDI-TOF MS)

To determine the mass of BSA and NGP11b, 1 μL of BSA (125 μg/mL) was combined into a 1.5 mL micro-centrifuge tube with 1 μL NGP11b (670 μg/mL) and 2 μL of matrix (10 mg/mL sinapinic acid, 50% acetonitrile, 0.1% TFA). Two microliters of the combined sample:matrix was spotted onto a 48-well steel MALDI plate and allowed to crystallize at room temperature for approximately 20 minutes. The mass spectra were acquired using a SHIMADZU MALDI-8020 mass spectrometer set to linear mode with dithering at a scan range of 10,000 to 100,000 m/z. Data acquisition included a laser power of 110, laser rep. rate (Hz) 50, accumulated shots 5, blast shots 2, profiles at 200, pulse extraction set to 66431, and a blanking mass of 15000. Spectra were processed by Threshold Apex set at constant Threshold, Gaussian smoothing, smoothing filter width 200 and peak width 2. BSA standard was used for calibration and internal references set at $[BSA+H]^+$ = 66431 with a 5ppm mass tolerance.

4.5.6 Experimental procedures and spectroscopic data of compounds
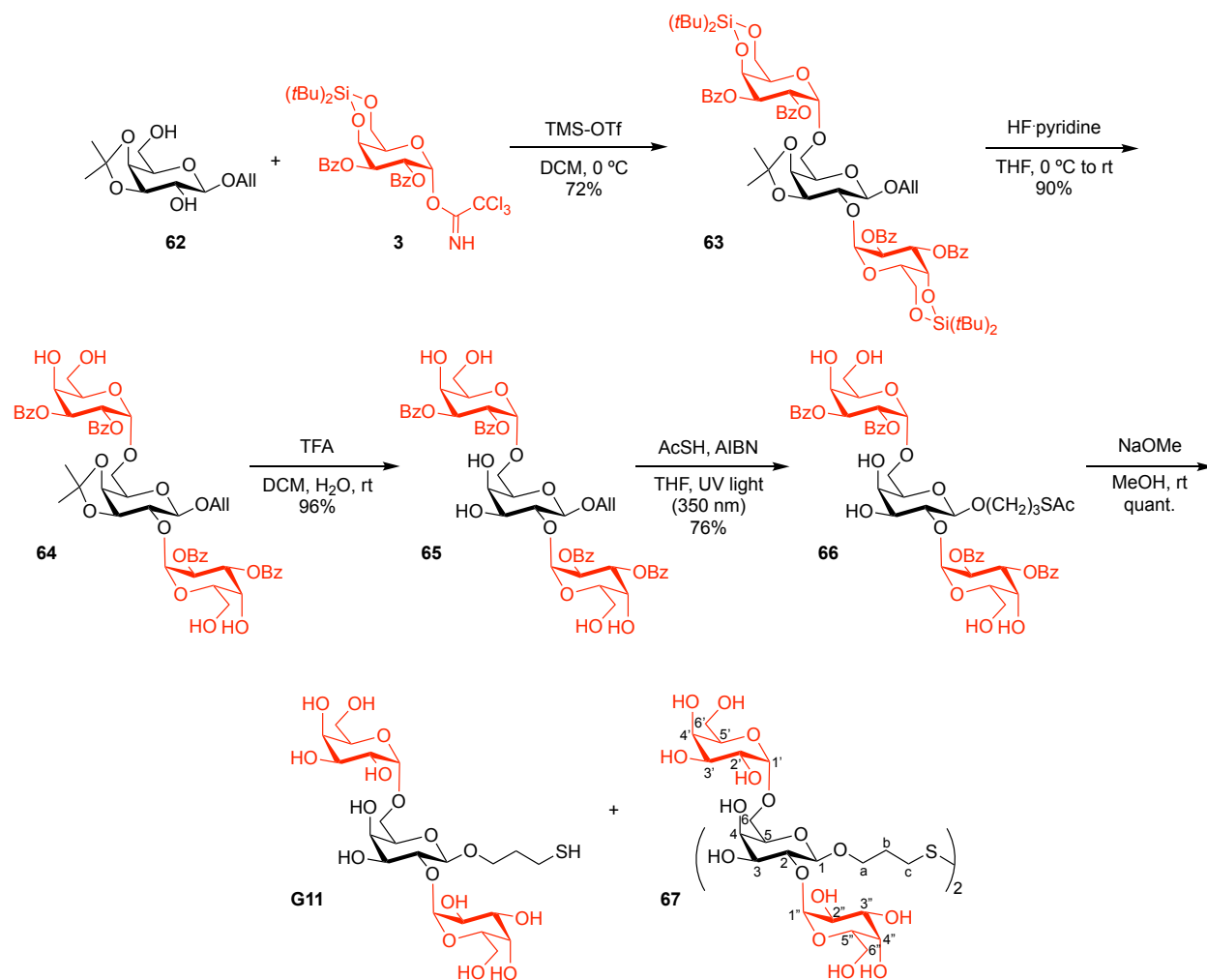
Scheme 24. Synthesis of the branched trisaccharide **G11**.

4.5.6.1 **Allyl** **2,3-di-*O*-benzoyl-4,6-*O*-di-*tert*-butylsilyl-α-D-galactosyl-(1→2)-[2,3-di-*O*-benzoyl-4,6-*O*-di-*tert*-butylsilylidene-α-D-galactosyl-(1→6)]-3,4-*O*-isopropylidene-β-D-galactoside (63)**: To a solution of the known galactoside acceptor **62**[115] (165 mg, 0.63 mmol) and trichloroacetimidate donor **3**[73, 116] (896 mg, 1.34 mmol) in anhydrous DCM (12 mL) freshly activated and crushed molecular sieves (4 Å) were added and the mixture was stirred under Ar for 1 h at 0 °C. Then, TMS-OTf (12 μL, 66 μmol) was added dropwise, the reaction mixture was continuously stirred for 45 min at 0 °C, and finally quenched with Et₃N (250 μL, 1.79 mmol). The mixture was diluted with DCM, the molecular sieves was filtered off, and the mixture was washed

with water and brine. The organic layers were dried over MgSO$_4$, concentrated, and purified by flash column chromatography on silica gel (EtOAc/hexanes = 1:6) to afford the fully protected trisaccharide **63** (584 mg, 72%) as a white powder. R_f 0.28 (EtOAc/hexanes = 1:4). $[\alpha]_D^{26}$ +65.9 (c = 0.08 in CH$_2$Cl$_2$). ^{1}H NMR (400 MHz, CDCl$_3$, 300K) δ 8.04-7.93 (m, 8H, arom.), 7.60-7.46 (m, 4H, arom), 7.45-7.31 (m, 8H, arom.), 5.79-5.70 (m, 2H), 5.67-5.56 (m, 3H), 5.49 (m, 1H, OCH$_2$C*H*=CH$_2$), 5.33 (d, *J* = 3.2 Hz, 1H), 4.95 (d, *J* = 17.1 Hz, 1H), 4.89-4.75 (m, 3H), 4.35-3.90 (m, 11H), 3.85-3.83 (m, 1H), 3.76-3.62 (m, 2H), 3.59-3.52 (m, 1H), 1.43 (s, 3H, CC*H*$_3$), 1.12 (s, 18H, 2 × *t*Bu-Si), 1.07 (s, 3H, CC*H*$_3$), 0.96 (s, 18H, 2 × *t*Bu-Si) ppm. ^{13}C NMR (101 MHz, CDCl$_3$, 300K) δ 166.2, 166.0, 165.7, 133.3, 133.2, 133.1, 133.0, 130.0, 129.8, 129.8, 129.7, 129.6, 129.5, 128.4, 128.3, 117.9, 117.7, 110.0, 101.3 (C-1), 96.4 (C-1), 96.1 (C-1), 78.0, 75.7, 73.6, 71.5, 71.3, 70.8, 70.7, 70.2, 68.7, 68.5, 67.0, 66.9, 66.7, 66.6, 28.0, 27.5, 27.3, 27.2, 26.1, 23.3, 23.2, 20.8, 20.7 ppm. ESI-TOF HRMS m/z calcd for C$_{68}$H$_{88}$O$_{20}$Si$_2$ [M+Na]$^+$: 1303.5305, found: 1303.5257.

4.5.6.2 Allyl 2,3-di-*O*-benzoyl-α-D-galactosyl-(1→2)-[2,3-di-*O*-benzoyl-α-D-galactosyl-(1→6)]-3,4-*O*-isopropylidene-β-D-galactoside (64):

The fully protected trisaccharide **63** (120 mg, 0.09 mmol) was dissolved in 12 mL of anhydrous THF in a plastic conical tube and cooled 0°C. Then, 120 μL of HF-Pyr (70%) was added and the solution was stirred for 30 min. at 0°C and 1 h at RT under Ar. The reaction mixture was cooled again to 0°C and quenched with saturated a NaHCO$_3$ solution. Finally, the mixture was extracted with EtOAc, washed with water and brine, dried over MgSO$_4$, concentrated, and purified by flash column chromatography on silica gel (EtOAc/hexanes = 4:1) to furnish the desilylated trisaccharide **64** (85 mg, 90%) as a white powder. R_f 0.26 (EtOAc/hexanes = 4:1). $[\alpha]_D^{26}$ +162.7 (c = 0.14 in CH$_2$Cl$_2$). ^{1}H NMR (400 MHz, CDCl$_3$, 300K) δ 8.03-7.93 (m, 8H, arom.), 7.55-7.43 (m, 4H, arom), 7.41-7.29 (m, 8H, arom.), 5.77-5.60 (m, 5H), 5.48 (m, 1H, OCH$_2$C*H*=CH$_2$), 5.36 (s, 1H), 4.96 (dd, *J* = 17.2, 1.3 Hz, 1H), 4.88 (d, *J* = 10.4 Hz, 1H), 4.45 (d, *J* = 11.6 Hz, 2H), 4.31 (t, *J* = 3.6 Hz, 1H), 4.17 (d, *J* = 8.4 Hz, 1H), 4.15-4.04 (m, 3H), 4.01-3.89 (m, 6H), 3.89-3.83 (m, 1H), 3.74 (dd, *J* = 9.9, 5.8 Hz, 1H), 3.64-3.50 (m, 2H), 3.40-3.26 (m, 2H, -OH), 2.86-2.76 (m, 1H, -OH), 1.45 (s, 3H, CC*H*$_3$), 1.06 (s, 3H, CC*H*$_3$), 0.91-0.79 (m, 1H, -OH) ppm. ^{13}C NMR (101 MHz, CDCl$_3$, 300K) δ 166.1, 166.0, 165.8, 133.5, 133.4, 133.3, 129.9, 129.8, 129.7, 129.6, 129.5, 129.4, 128.6, 128.5, 117.8, 110.3, 101.3 (C-1), 96.8 (C-1), 96.7 (C-1), 78.1, 77.4, 73.5, 71.4, 71.0, 70.9, 70.4, 70.2, 69.8, 69.3, 69.0, 68.6, 66.6,

63.8, 63.2, 28.1, 26.1 ppm. ESI-TOF HRMS m/z calcd for $C_{52}H_{56}O_{20}$ [M+Na]$^+$: 1023.3263, found: 1023.3252.

4.5.6.3 Allyl 2,3-di-*O*-benzoyl-α-D-galactosyl-(1→2)-[2,3-di-*O*-benzoyl-α-D-galactosyl-(1→6)]-β-D-galactoside (65):

To a solution of trisaccharide **64** (260 mg, 0.26 mmol) in DCM (8 mL), H_2O (1.0 mL) and TFA (1.0 mL) were consecutively added, and the mixture was vigorously stirred at RT for 30 min. After disappearance of starting material based on TLC, the resulting solution was co-evaporated with EtOH (10 mL) twice. The residue was then further dried under *vacuum* and purified by flash column chromatography on silica gel (DCM/MeOH = 9:1) to afford the partially deprotected **65** (240 mg, 96%) as a colorless syrup. R$_f$ 0.33 (DCM/MeOH = 9:1). $[\alpha]_D^{26}$ +215.6 (c = 0.05 in CH_2Cl_2). ^{1}H NMR (400 MHz, MeOD, 300K) δ 8.02-7.86 (m, 8H, arom.), 7.55-7.46 (m, 4H, arom), 7.45-7.29 (m, 8H, arom.), 5.72-5.61 (m, 5H), 5.55 (m, 1H, OCH$_2$C*H*=CH$_2$), 5.31 (d, *J* = 3.2 Hz, 1H), 4.94 (dd, *J* = 17.4, 1.5 Hz, 1H), 4.86-4.79 (m, 1H), 4.61 (t, *J* = 6.0 Hz, 1H), 4.37-4.27 (m, 3H), 4.10 (t, *J* = 6.0 Hz, 1H), 4.02-3.91 (m, 2H), 3.85-3.69 (m, 9H), 3.52 (dd, *J* = 12.5, 5.9 Hz, 1H) ppm. ^{13}C NMR (101 MHz, MeOD, 300K) δ 166.1, 166.0, 165.8, 133.7, 133.2, 133.1, 133.0, 129.7, 129.6, 129.5, 129.4, 129.3, 129.2, 128.2, 128.1, 116.1, 102.6 (C-1), 96.2 (C-1), 96.1 (C-1), 75.6, 72.8, 72.2, 71.3, 71.0, 70.32, 69.7, 69.5, 69.2, 69.0, 67.7, 67.5, 66.4, 61.1, 61.0 ppm. ESI-TOF HRMS m/z calcd for $C_{49}H_{52}O_{20}$ [M+Na]$^+$: 983.2950, found: 983.2975.

4.5.6.4 3-(Acetylthio)propyl 2,3-di-*O*-benzoyl-α-D-galactosyl-(1→2)-[2,3-di-*O*-benzoyl-α-D-galactosyl-(1→6)]-β-D-galactoside (66):

To a solution of allyl trisaccharide **65** (230 mg, 0.24 mmol) and AIBN (20 mg, 0.12 mmol) in anhydrous THF (3 mL) under Ar, thioacetic acid (43 μL, 0.60 mmol) was added, and the mixture was stirred under water cooling (~ 25°C) for 6 h in a Rayonet UV reactor equipped with 350 nm lamps. The solution was then co-evaporated with toluene and concentrated to near dryness. The crude product was purified by flash column chromatography on silica gel (CHCl$_3$/MeOH = 14:1) to afford the acyl-protected trisaccharide **66** (188 mg, 76%) as a white solid. R$_f$ 0.33 (CHCl$_3$/MeOH = 7:1). $[\alpha]_D^{26}$ +100.1 (c = 0.07 in MeOH). ^{1}H NMR (400 MHz, MeOD, 300K) δ 8.02-7.85 (m, 8H, arom.), 7.62-7.29 (m, 12H, arom), 5.72-5.57 (m, 5H), 5.49 (s, 1H), 5.31 (d, *J* = 2.4 Hz, 1H), 4.65-4.58 (m, 1H), 4.37-4.28 (m, 2H), 4.23 (d, *J* = 7.0 Hz, 1H), 4.13-3.90 (m, 3H), 3.86-3.64 (m, 9H), 3.59-3.50 (m, 1H), 2.95-2.83 (m, 1H), 2.72-2.55 (m, 2H), 2.23 (s, 3H) ppm. ^{13}C NMR (101 MHz, MeOD, 300K) δ 195.9, 166.1, 166.0,

165.8, 133.2, 133.1, 133.0, 129.7, 129.6, 129.5, 129.3, 129.2, 128.3, 128.2, 128.1, 103.5 (C-1), 96.1 (C-1), 96.0 (C-1), 75.6, 72.8, 72.1, 71.3, 71.0, 70.2, 69.6, 69.3, 69.1, 67.7, 67.7, 67.6, 66.3, 61.0, 29.3, 25.3 ppm. ESI-TOF HRMS m/z calcd for $C_{51}H_{56}O_{21}S$ $[M+Na]^+$: 1059.2932, found: 1059.2925.

4.5.6.5 3-Thiopropyl α-D-galactosyl-(1→2)-[α-D-galactosyl-(1→6)]-β-D-galactoside (G11):

The acyl-protected trisaccharide **66** (188 mg, 0.18 mmol) was dissolved in 20 mL of anhydrous 0.25 M NaOMe, and stirred for 2 hours under Ar. The solution was then neutralized with Amberlyst-15, filtered through Celite, concentrated and finally dissolved in water and lyophilized. Initially, the unprotected mercaptopropyl trisaccharide **G11** is produced, which oxidizes by handling on air within hours to the disulfide **67** (118 mg, quant.) as an off-white solid. R_f 0.25 (*i*PrOH/H_2O = 5:1 w/ 3 drops AcOH). $[\alpha]_D^{26}$ 61.6 (c = 0.03 in H_2O). ^{1}H NMR (600 MHz, D_2O, 300 K) δ 5.35 (d, 1H, J = 4.0 Hz, H-1''), 4.94 (d, 1H, J = 3.5 Hz, H-1'), 4.52 (d, 1H, J = 7.9 Hz, H-1), 4.23 (m, 1H, H-5''), 3.96 (m, 2H, H-4'', H-6''$_a$), 3.95 (m, 2H, H-3', H-6'$_a$), 3.94 (m, 2H, H-5', H-a), 3.93 (m, 1H, H-4), 3.88 (m, 1H, H-6$_a$), 3.85 (m, 2H, H-5, H-3''), 3.82 (m, 1H, H-4'), 3.80 (m, 1H, H-2'), 3.76 (m, 2H, H-2'', H-a), 3.71 (m, 1H, H-6'$_b$), 3.70 (m, 1H, H-3), 3.69 (m, 1H, H-6''$_b$), 3.64 (m, 1H, H-6$_b$), 3.60 (t, 1H, J = 8.8 Hz, H-2), 2.80 (t, 2H, J = 7.0 Hz, H-c), 2.01 (m, 2H, H-b) ppm. ^{13}C NMR (101 MHz, D_2O, 300K) δ 103.4 (C-1), 98.3 (C-1'), 98.1 (C-1''), 75.1 (CH-2), 74.7 (CH-5), 71.6 (CH-3), 71.1 (CH-5'), 70.7 (CH-5''), 69.6 (CH-4'), 69.4 (CH-4, CH-3''), 69.3 (CH-4''), 69.2 (CH-3'), 68.8 (CH_2-a), 68.4 (CH-2'), 68.3 (CH-2''), 66.4 (CH_2-6$_{a, b}$), 61.3 (CH_2-6'$_{a, b}$), 61.0 (CH_2-6''$_{a, b}$), 34.4 (CH_2-c), 28.5 (CH_2-b) ppm. ESI-TOF HRMS m/z calcd for $C_{42}H_{74}O_{32}S_2$ $[M+Na]^+$: 1177.3502, found: 1177.3310.

5.1 SYNTHESIS OF **GAL***P*α**(1,3)GAL***P*β**(1,4)GLCNAC**α**-CONTAINING NEOGLYCOPROTEIN AND ITS**

IMMUNOLOGICAL EVALUATION IN THE CONTEXT OF CHAGAS DISEASE

5.1.1 Synthesis of the NGP24b [Gal*p*α(1,3)Gal*p*β(1,4)GlcNacα-linker-BSA]

The goal of this side project was to synthesize sufficient quantities of NGP24b, which had previously been synthesized by former PhD student Nathaniel Schocker, to study its suitability as a BMK for follow-up of Chagas disease after chemotherapy.

The target mercaptopropyl trisaccharide **G24** was synthesized as follow: an elevated temperature glycosylation[117] between the know allyl GlcNAc acceptor **68**[118] and a large excess of the acetylated tricholoroacetimidate α-Gal donor **69** (prepared under similar conditions of **Scheme 7**) give the disaccharide Gal*p*β(1,4)GlcNAcα **70** in high yield 70%[75]. Saponification gave the deacetylated disaccharide **71**, then *p*-methoxybenzylation at position 3 of the galactose residue via its tin acetal gave **72**, followed by benzoylation of the remaining hydroxyls afforded **73**. Oxidative cleavage of *p*-methoxybenzyl (PMB) with DDQ furnished the Galβ(1,4)GlcNAcα acceptor **74**. This new disaccharide acceptor **74** was glycosylated with the known di-*tert*-butylsilylidene equipped αGal trichloroacetimidate donor **3** [72], using TMS-OTf catalysis to give trisaccharide **75** (being fully characterized for the first time). Then, the di-*tert*-butylsilylidene group was cleaved with a large excess of 70% HF-pyr to give **76**, followed by radical addition using AcSH and AIBN under UV light yielding **77**. Finally, a saponification was done it to get the desired epitote **G24** ready for conjugation to a carrier protein (**Figure 28**).
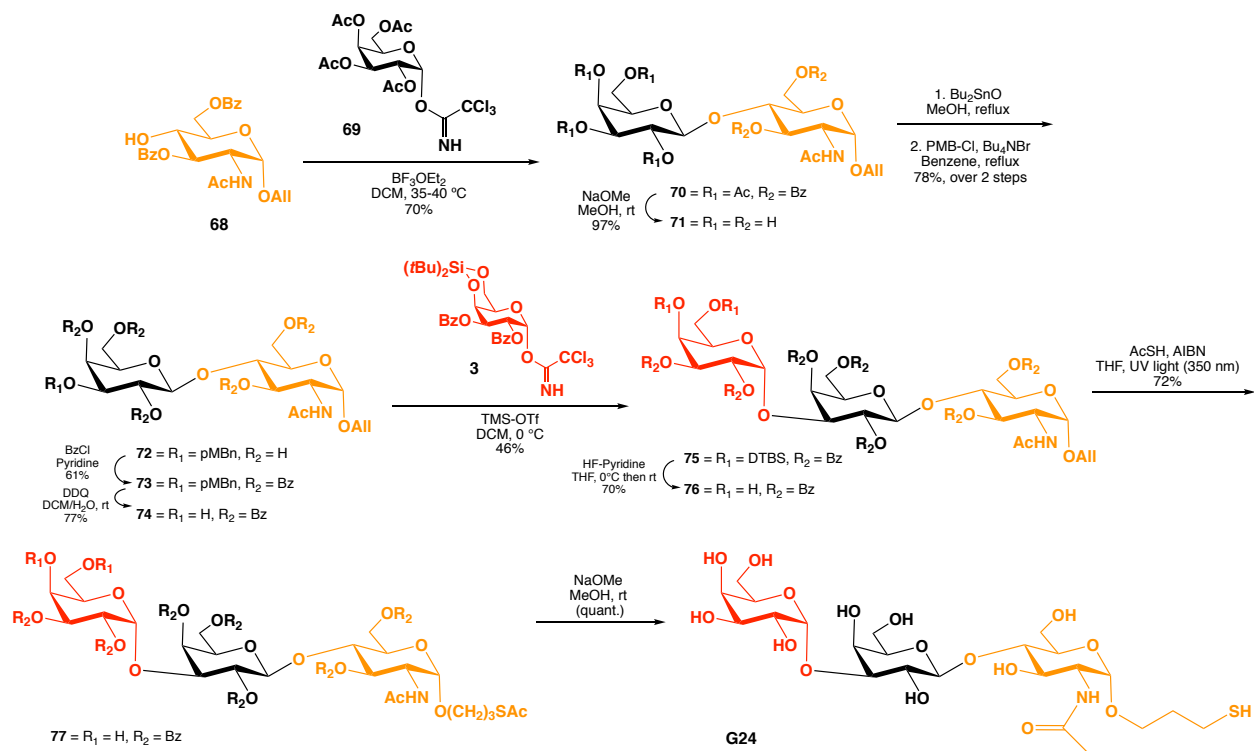
Scheme 25. Synthesis of the mercaptopropyl tetrasaccharide **G24**.
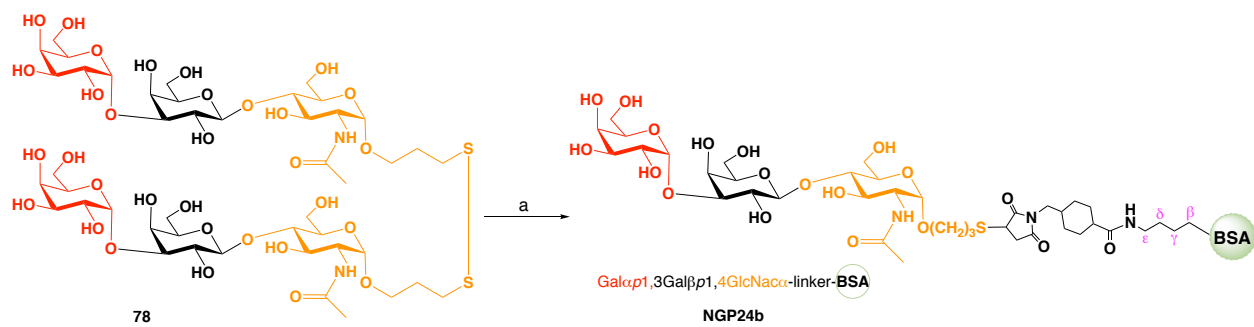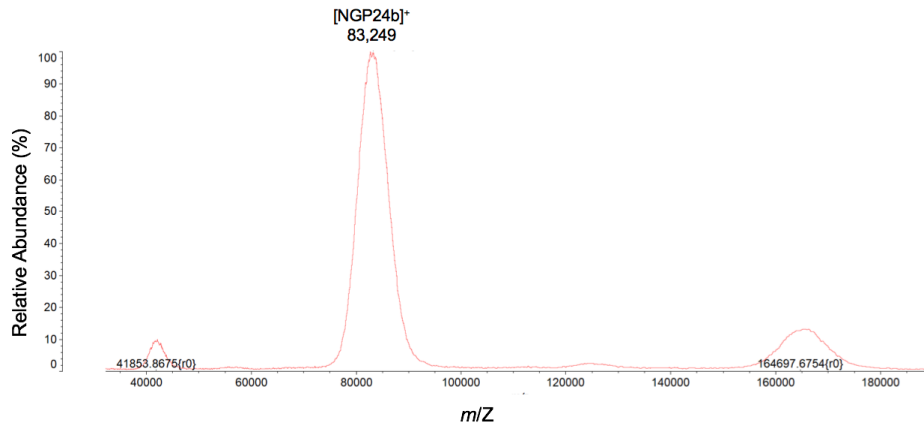
Figure 28. (Top) Schematic representation of conjugation of **G24** to BSA. a: TCEP, phosphine buffer pH 7.2 and maleimide-activated BSA. (Bottom) MALDI-TOF mass spectra of Galα(1,3)Galβ(1,4)GlcNacα-linker-**BSA** (NGP24b).

5.1.2 Biological data of the NGP24b
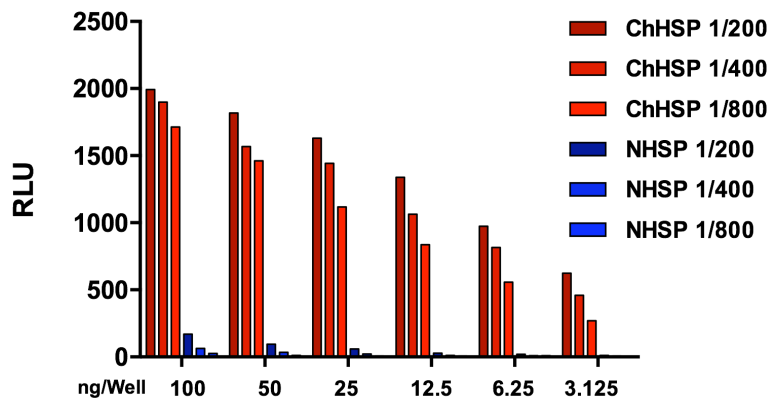
Figure 29. Cross-titration of KM24b with NHS and **Chagasic human serum pools (CHSP)**.

This titration was done to analyze the best difference factor between sera dilutions (ChHSP vs. NHSP) and amount (ng) of the antigen (mercaptopropyl trisaccharide sugar conjugated to BSA (KM24b)]. From **Figure 29**, could be concluded that 25 ng or even less material as 12.5 ng of antigen with 1/800 serum dilution per well can work with a great differential between CHSP and NHSP. These results will be applied for the further CL-ELISA assays.

113
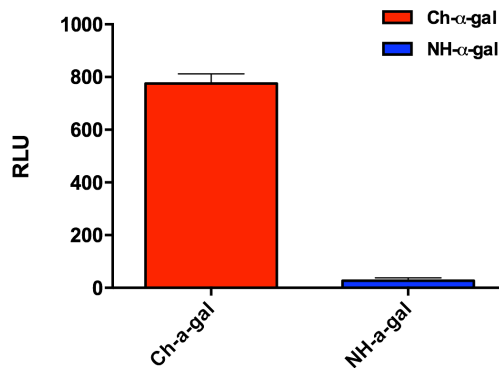
Figure 30. Reactivity of KM24b against anti-α-Gal Abs.

As shown in **Figure 30**, CL-ELISA revealed that Gal*p*α(1,3)Gal*p*β(1,4)GlcNAcα-BSA (KM24b) display a huge binding to purified anti-α-Gal Abs from CCD patients, with very little binding to anti-α-Gal Abs from sera of healthy individuals (NHS anti-α-Gal). The results highlight the importance of the epitope for recognition by Chagas anti-α-Gal Abs, which can be useful for diagnosis and follow up after chemotherapy of CD.

114
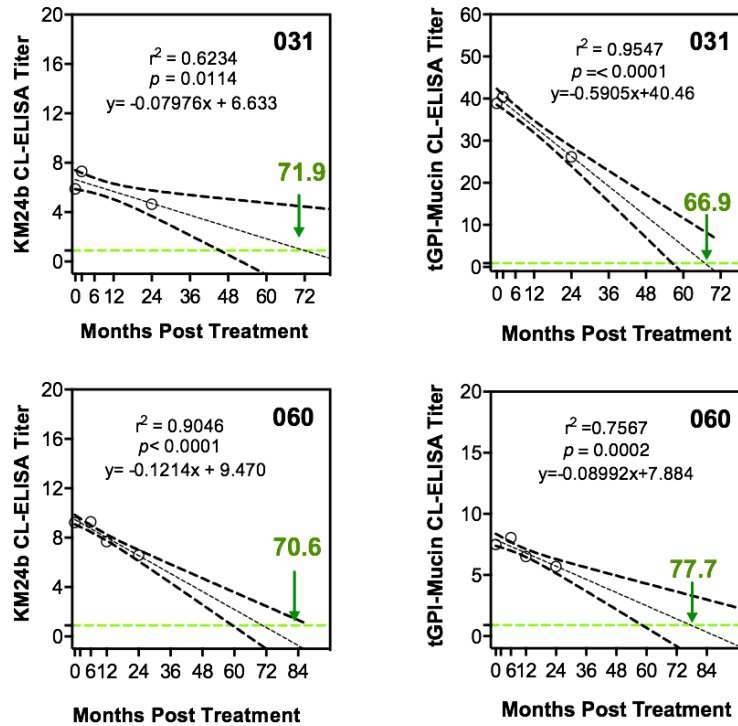
Figure 31. Synthetic α-Gal-NGP KM24b as a BMK for follow-up of Chagas Chemotherapy.

Figure 31 shows the follow-up of Chagas chemotherapy for two patients from Spain and Bolivia, 031 and 060 respectively. The progression of the chemotherapy after months of treatment was done by CL-ELISA using KM24b as an antigen on the left side and pure isolated *t*GPI-Mucin on the right side. How it can be analyzed, the results from the synthetic NGP24b after 3, 6, 12 and 24 months of treatment is following the same lineal pattern as expected based on the calculations with good r^2 and p values ($p < 0.05$) and similar to the isolated *t*GPI mucin. However, it is important to follow the patients after 48 or 60 months to add points to the graph and have a better conclusion.
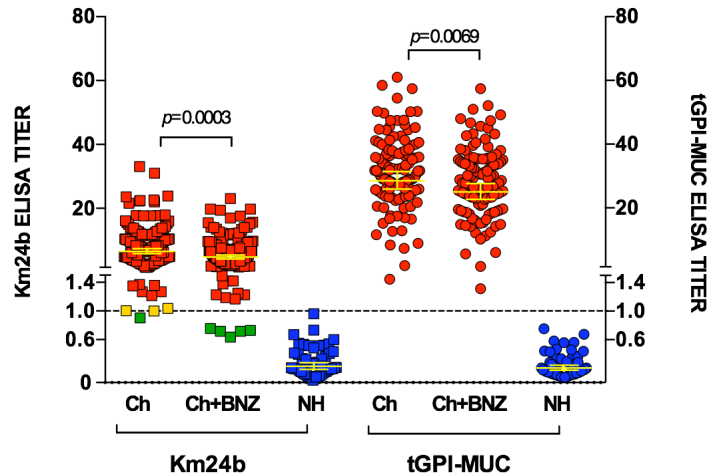
Figure 32. Synthetic α-Gal-NGP KM24b as a BMK for diagnosis of Chagas Chemotherapy and comparison with a tGPI-MUC preparation.

As shown in **Figure 32**, titration evaluate the role of KM24b as a BMK for the diagnosis of CD. CL-ELISA was performed using sera of CD patients confirmed by PCR, sera of patients under treatment with benznidazole and normal human sera. The cutoff at 1.0 was used to show that patients have been cured or have never been exposed to ChD. The result from the figure indicates a very significant shift in KM24b $p = 0.0003$ between Ch and Ch+BNZ better than in tGPI-MUC $p = 0.0069$. However, with NGP24b there are also some inconclusive results (yellow), and some false negative results (green). The tGPI-MUC control does not show inconclusive or false negative results.

The results above indicate that it is possible to use NGP24b for the diagnosis and follow-up chemotherapy of CD.
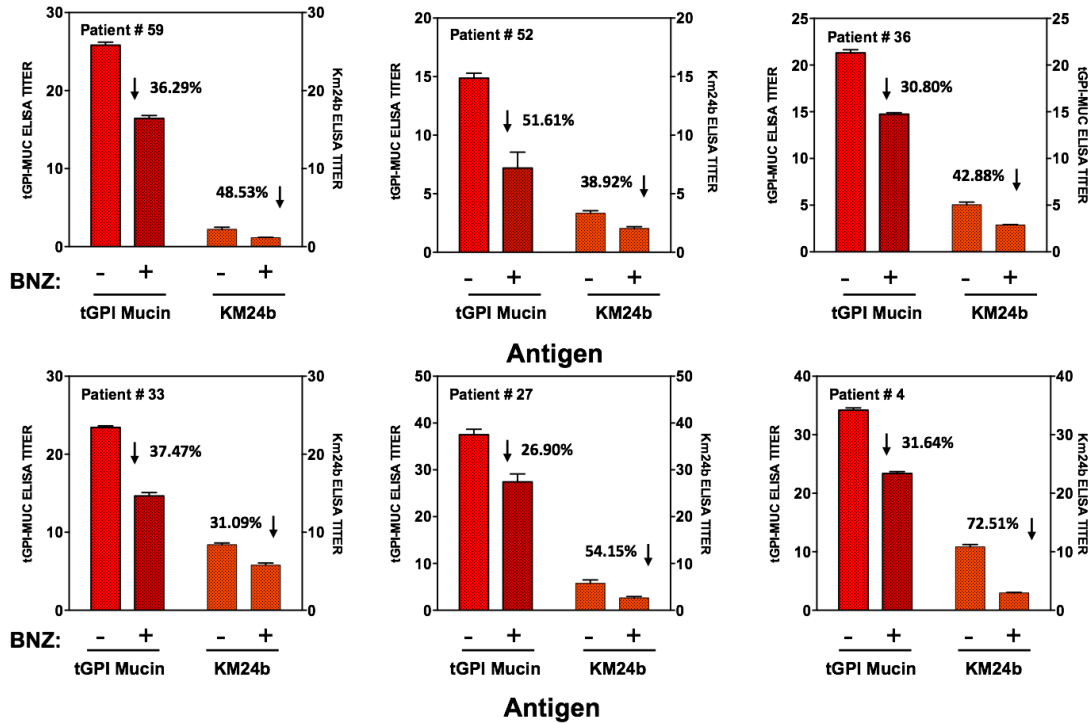
Figure 33. Reactivity of Biomarcha Serum against KM24b compared to *t*GPI-mucins pre-and post-chemotherapy.

The last titration was done with specific serum of patients as indicated by numbers, to compare reactivity of the antigens KM24 and purified *t*GPI mucin before and after-treatment. The analysis from the **Figure 33** indicates the highest antibody response in patients without BNZ treatment for either antigen *t*GPI mucin or KM24b, being higher in all cases for *t*GPI which is normally expected. The percentage differences for KM24b ranking from 31.09% to 72.51% are significant to consider this NGP as a good immunodominant glycotopes.

The synthetic route was successfully achieved with good yields for every single step, as well as the conjugation to BSA. NGP24b gave excellent differential reactivities when comparing CD patients and healthy individuals, that it was suitable for follow-up studies after chemotherapy, and that extrapolation suggest that seroconversion will occur within 66.9-77.7 months.

117

5.2 OPTIMIZATION OF GLYCOPROTEIN FORMATION WITH HSA

The protocol for the optimization of the glycoprotein formation with HSA, consisted on three main steps: (*i*) verification of the deprotected sugar by MS (**Figure 34**); (*ii*) modification of the ratios between sugar and bifunctional linker Sulfo-SMCC during the conjugation step (**Figure 35**); and (*iii*) MALDI-TOF to calculate the ratios between sugar units and linker-BSA conjugate (**Figure 36**).
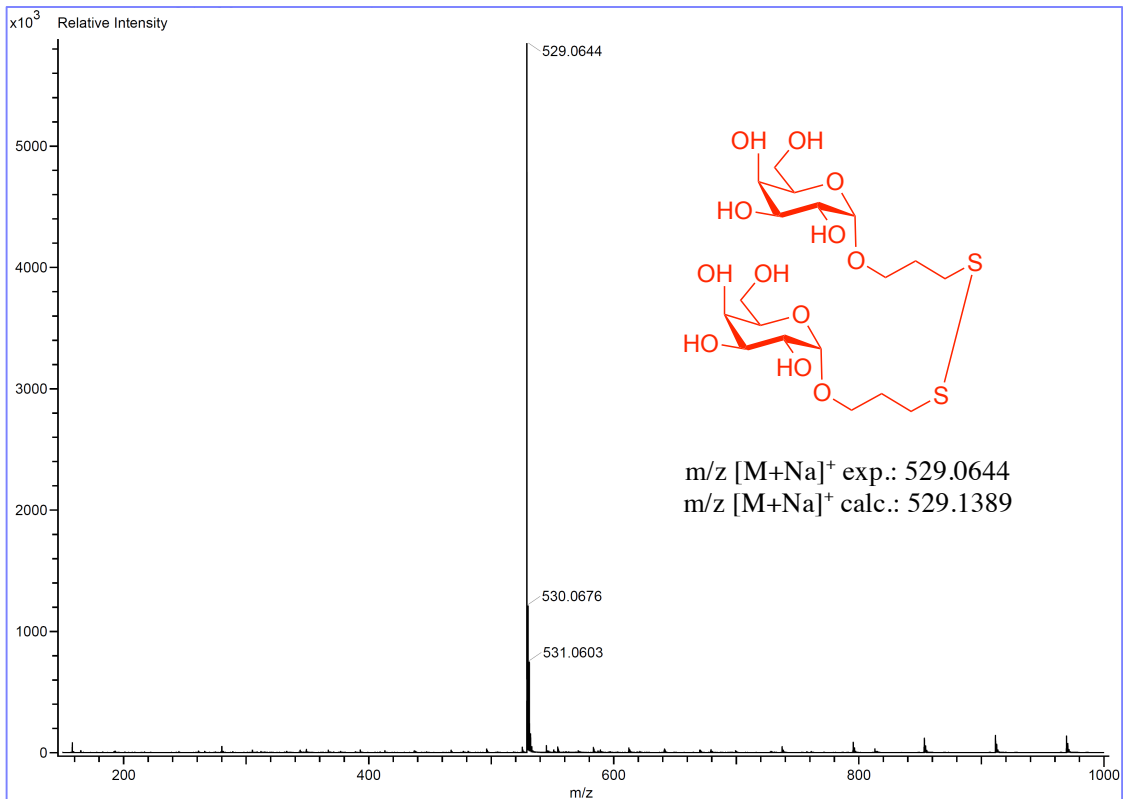
Figure 34. MS of KM3 fully deprotected.
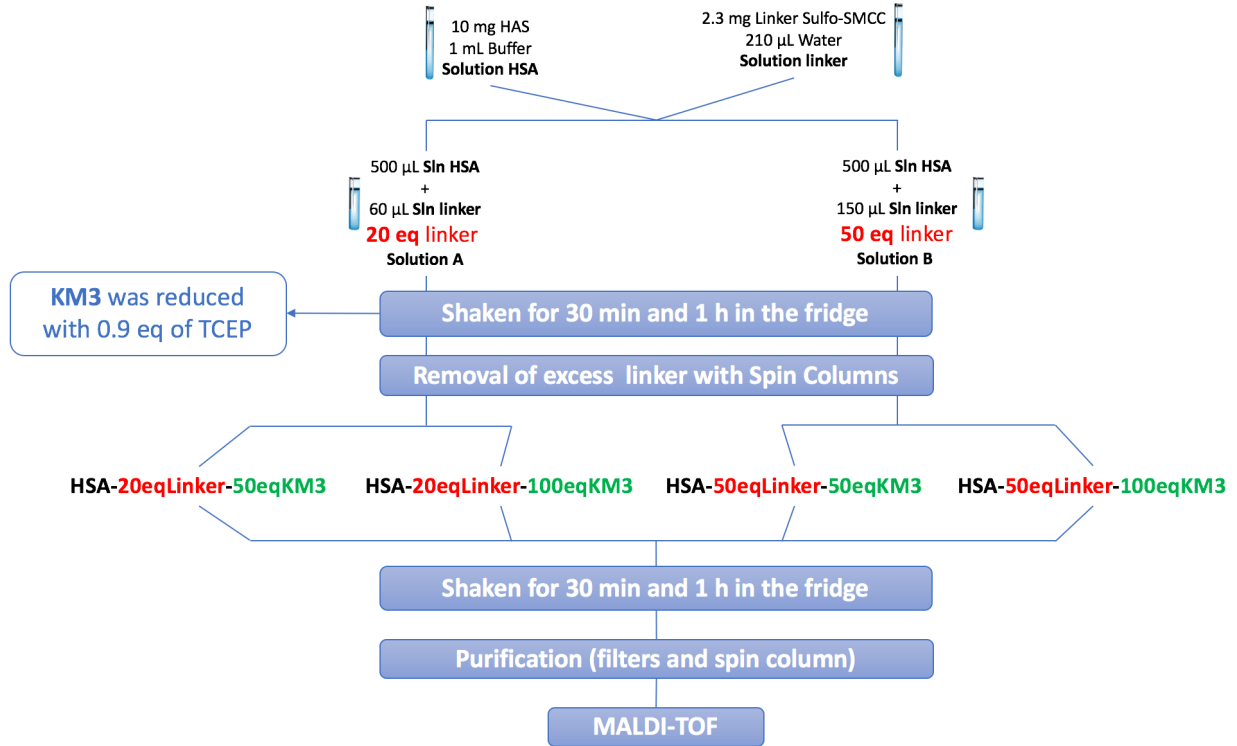
Figure 35. KM3-SulfoLinker-HSA Conjugation – Protocol.
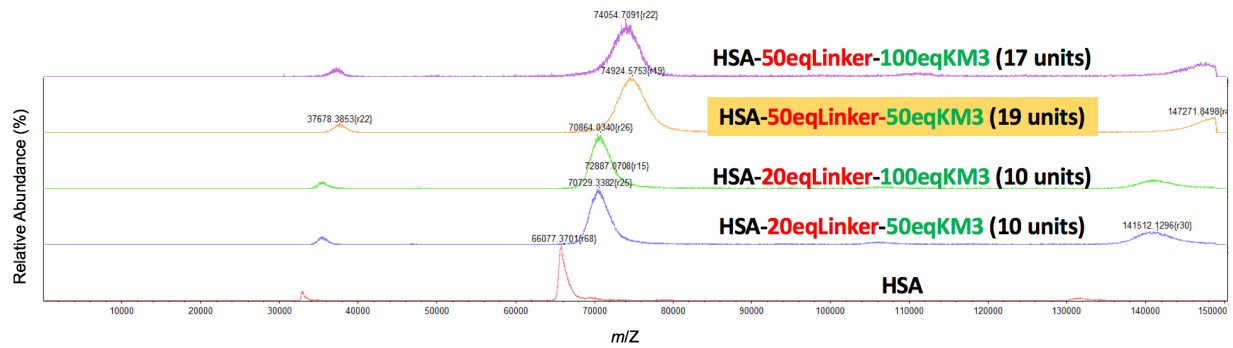
Figure 36. KM3-SulfoLinker-HSA – MALDI-TOF.

5.3 SYNTHETIC NEOGLYCOPROTEINS

Finally, **Table 7** summarizes the glycoconjugates synthesized, purified and characterized during these years of graduate research. The glycans used in the conjugations were synthesized by me or by former students in Dr. Michael's group. Those glycoconjugates were sent to our collaborators showing interesting CL-ELISA results which were published in three journals in which I am a coauthor[15, 70, 114].

Table 9. Summary of the all glycans synthesized by me, or synthesized by other students and purified/characterized/conjugated by me.

Glycoconjugates				
Sugar code*	Chemical structure	To BSA	To HSA	To Agarose beads
2-ME	2-mercaptoethanol	x	x	
G3	Galα	x	x	
G5	Galpα(1,6)Galpβ	x		x
G9	Galpα(1,3)Galpβ	x		x
G11	Galpα(1,6)[Galpα(1,2)]Galpβ	x	x	
G15	Cysteine (Cys)	x	x	x
G19	Galfβ(1,4)GlcNAcα	x		
G20	Galfβ(1,4)[Galpβ1,6]GlcNAcα	x		
G24	Galpα(1,3)Galpβ(1,4)GlcNacα	x	x	x
G27	Galpα1,3Galfβ	x		
G28	Galpα1,6Galpα1,3Galfβ	x		
G29	Galfβ1,3Manpα	x		
G30	Galpα1,6Galfβ1,3Manpα	x		
G31	Galpα1,6Galpα1,3Galfβ1,3Manpα**			
G32	(Galfβ1,3Manpα1,2-[Galfβ1,3Manpα])**			

*MS spectra were taken before protein conjugation.

** The synthetic routes for the synthesis of the tetrasaccharides were optimized and they were obtained as the fully protected compounds. Deprotections need to be done, as well as the conjugation to the carrier proteins.

References

[1]   M. J. McConville, M. A. Ferguson, *Biochem J* **1993**, *294 (Pt 2)*, 305-324.

[2]   I. C. Almeida, G. M. Krautz, A. U. Krettli, L. R. Travassos, *J Clin Lab Anal* **1993**, *7*, 307-316.

[3]   A. Varki, R. D. Cummings, J. D. Esko, P. Stanley, G. W. Hart, M. Aebi, A. G. Darvill, T. Kinoshita, N. H. Packer, J. H. Prestegard, R. L. Schnaar, P. H. Seeberger, **2015**.

[4]   P. M. Rudd, T. Elliott, P. Cresswell, I. A. Wilson, R. A. Dwek, *Science* **2001**, *291*, 2370-2376; C. R. Bertozzi, L. L. Kiessling, *Science* **2001**, *291*, 2357-2364; H. E. Murrey, L. C. Hsieh-Wilson, *Chem Rev* **2008**, *108*, 1708-1731.

[5]   T. J. Boltje, T. Buskas, G. J. Boons, *Nat Chem* **2009**, *1*, 611-622.

[6]   H. Geyer, R. Geyer, *Biochim Biophys Acta* **2006**, *1764*, 1853-1869.

[7]   J. Guo, X. S. Ye, *Molecules* **2010**, *15*, 7235-7265.

[8]   Y. Wu, D. C. Xiong, S. C. Chen, Y. S. Wang, X. S. Ye, *Nat Commun* **2017**, *8*, 14851.

[9]   J. T. Smoot, A. V. Demchenko, *Adv Carbohydr Chem Biochem* **2009**, *62*, 161-250; A. A. Joseph, A. Pardo-Vargas, P. H. Seeberger, *J Am Chem Soc* **2020**, *142*, 8561-8564.

[10] L. Krasnova, C. H. Wong, *J Am Chem Soc* **2019**, *141*, 3735-3754.

[11] S. Neelamegham, K. Aoki-Kinoshita, E. Bolton, M. Frank, F. Lisacek, T. Lütteke, N. O'Boyle, N. H. Packer, P. Stanley, P. Toukach, A. Varki, R. J. Woods, S. D. Group, *Glycobiology* **2019**, *29*, 620-624.

[12] I. C. Almeida, M. A. Ferguson, S. Schenkman, L. R. Travassos, *Biochem J* **1994**, *304 (Pt 3)*, 793-802.

[13] C. A. Buscaglia, V. A. Campo, J. M. Di Noia, A. C. Torrecilhas, C. R. De Marchi, M. A. Ferguson, A. C. Frasch, I. C. Almeida, *J Biol Chem* **2004**, *279*, 15860-15869.

[14] A. Acosta-Serrano, C. Hutchinson, E. S. Nakayasu, I. C. Almeida, M. Carrington, in *Trypanosomes: After the genome* (Eds.: J. D. Barry, J. C. Mottram, R. McCulloch, A. Acosta-Serrano), Horizon Scientific Press, Norwich, UK, **2007**, pp. 319-337.

[15] U. Ortega-Rodriguez, S. Portillo, R. A. Ashmus, J. A. Duran, N. S. Schocker, E. Iniguez, A. L. Montoya, B. G. Zepeda, J. J. Olivas, N. H. Karimi, J. Alonso-Padilla, L. Izquierdo, M. J. Pinazo, B. A. de Noya, O. Noya, R. A. Maldonado, F. Torrico, J. Gascon, K. Michael, I. C. Almeida, *Methods Mol Biol* **2019**, *1955*, 287-308.

[16] G. T. Hermanson, in *Bioconjugate Techniques, Vol. 2nd edition* (Ed.: A. Press), New York, **2008**.

[17] R. A. Ashmus, N. S. Schocker, Y. Cordero-Mendoza, A. F. Marques, E. Y. Monroy, A. Pardo, L. Izquierdo, M. Gállego, J. Gascon, I. C. Almeida, K. Michael, *Org Biomol Chem* **2013**, *11*, 5579-5583.

[18] N. S. Schocker, S. Portillo, R. A. Ashmus, C. R. N. Brito, I. E. Silva, Y. Cordero-Mendoza, A. F. Marques, E. Y. Monroy, A. Pardo, L. Izquierdo, M. Gállego, J. Gascon, I. C. Almeida, K. Michael, in *Coupling and Decoupling of Diverse Molecular Units in Glycosciences* (Eds.: Z. J. Witczak, R. Bielski), Springer International Publishing AG, Cham, Switzerland, **2018**, pp. 195-211.

[19] A. Descoteaux, S. J. Turco, *Biochim Biophys Acta* **1999**, *1455*, 341-352.

[20] Y. Cabezas, L. Legentil, F. Robert-Gangneux, F. Daligault, S. Belaz, C. Nugier-Chauvin, S. Tranchimand, C. Tellier, J. P. Gangneux, V. Ferrières, *Org Biomol Chem* **2015**, *13*, 8393-8404.

121

[21]   M. Z. Handler, P. A. Patel, R. Kapila, Y. Al-Qubati, R. A. Schwartz, *J Am Acad Dermatol* **2015**, *73*, 911-926; 927-918.

[22]   R. Reithinger, J. C. Dujardin, H. Louzir, C. Pirmez, B. Alexander, S. Brooker, *Lancet Infect Dis* **2007**, *7*, 581-596.

[23]   J. Gascon, C. Bern, M. J. Pinazo, *Acta Trop* **2010**, *115*, 22-27.

[24]   Y. Jackson, A. Pinto, S. Pett, *Trop Med Int Health* **2014**, *19*, 212-218.

[25]   E. Chatelain, *Comput Struct Biotechnol J* **2017**, *15*, 98-103.

[26]   A. Rassi, J. A. Marin-Neto, *Lancet* **2010**, *375*, 1388-1402.

[27]   J. Rodriques Coura, S. L. de Castro, *Mem Inst Oswaldo Cruz* **2002**, *97*, 3-24.

[28]   J. C. Dias, J. R. Coura, M. A. Yasuda, *Rev Soc Bras Med Trop* **2014**, *47*, 123-125; I. Molina, F. Salvador, A. Sánchez-Montalvá, B. Treviño, N. Serre, A. Sao Avilés, B. Almirante, *Antimicrob Agents Chemother* **2015**, *59*, 6125-6131; M. J. Olivera, Z. M. Cucunubá, C. A. Álvarez, R. S. Nicholls, *Am J Trop Med Hyg* **2015**, *93*, 1224-1230.

[29]   I. C. Almeida, D. T. Covas, L. M. Soussumi, L. R. Travassos, *Transfusion* **1997**, *37*, 850-857.

[30]   C. Bern, *N Engl J Med* **2015**, *373*, 1882.

[31]   R. R. Assis, I. C. Ibraim, F. S. Noronha, S. J. Turco, R. P. Soares, *PLoS Negl Trop Dis* **2012**, *6*, e1543.

[32]   I. C. Almeida, M. A. J. Ferguson.

[33]   F. V. Toukach, A. S. Shashkov, E. Katzenellenbogen, N. A. Kocharova, A. Czarny, Y. A. Knirel, E. Romanowska, N. K. Kochetkov, *Carbohydr. Res.* **1996**, *295*, 117-126.

[34]   C. Marino, L. Baldoni, *Chembiochem* **2014**, *15*, 188-204.

[35]   E. Suzuki, A. K. Tanaka, M. S. Toledo, H. K. Takahashi, A. H. Straus, *Infect Immun* **2002**, *70*, 6592-6596.

[36]   C. A. Buscaglia, V. A. Campo, A. C. Frasch, J. M. Di Noia, *Nat Rev Microbiol* **2006**, *4*, 229-236; A. C. Frasch, *Parasitol Today* **2000**, *16*, 282-286.

[37]   M. E. Giorgi, R. M. de Lederkremer, *Carbohydr Res* **2011**, *346*, 1389-1393.

[38]   L. M. De Pablos, A. Osuna, *Infect Immun* **2012**, *80*, 2258-2264.

[39]   I. C. Almeida, M. A. J. Ferguson, S. Schenkman, L. R. Travassos, *Biochem. J.* **1994**, *304*, 793-802.

[40]   U. Galili, in *The Natural Anti-Gal Antibody as Foe Turned Friend in Medicine*, 1st ed., Elsevier - Academic Press, Cambridge, MA, United States, **2017**, pp. 1-18.

[41]   U. Galili, K. Swanson, *Proc Natl Acad Sci U S A* **1991**, *88*, 7401-7404.

[42]   I. C. Almeida, S. R. Milani, P. A. Gorin, L. R. Travassos, *Journal of immunology* **1991**, *146*, 2394-2400.

[43]   R. T. Gazzinelli, M. E. Pereira, A. Romanha, G. Gazzinelli, Z. Brener, *Parasite Immunol* **1991**, *13*, 345-356; J. L. Avila, M. Rojas, U. Galili, *J Immunol* **1989**, *142*, 2828-2834.

[44]   W. S. Al-Salem, D. M. Ferreira, N. A. Dyer, E. J. Alyamani, S. M. Balghonaim, A. Y. Al-Mehna, S. Al-Zubiany, e.-K. Ibrahim, A. M. Al Shahrani, H. Alkhuailed, M. A. Aldahan, A. M. Al Jarallh, S. S. Abdelhady, M. H. Al-Zahrani, I. C. Almeida, A. Acosta-Serrano, *Parasitology* **2014**, *141*, 1898-1903.

[45]   H. J. de Vries, S. H. Reedijk, H. D. Schallig, *Am J Clin Dermatol* **2015**, *16*, 99-109.

[46]   J. Alvar, I. D. Vélez, C. Bern, M. Herrero, P. Desjeux, J. Cano, J. Jannin, M. den Boer, W. L. C. Team, *PLoS One* **2012**, *7*, e35671.

[47]   V. Vanlerberghe, G. Diap, P. J. Guerin, F. Meheus, S. Gerstl, P. Van der Stuyft, M. Boelaert, *Trop Med Int Health* **2007**, *12*, 274-283.

122

[48]   K. Aït-Oudhia, E. Gazanion, B. Vergnes, B. Oury, D. Sereno, *Parasitol Res* **2011**, *109*, 1225-1232.

[49]   D. O. Santos, C. E. Coutinho, M. F. Madeira, C. G. Bottino, R. T. Vieira, S. B. Nascimento, A. Bernardino, S. C. Bourguignon, S. Corte-Real, R. T. Pinho, C. R. Rodrigues, H. C. Castro, *Parasitol Res* **2008**, *103*, 1-10; A. S. Nagle, S. Khare, A. B. Kumar, F. Supek, A. Buchynskyy, C. J. Mathison, N. K. Chennamaneni, N. Pendem, F. S. Buckner, M. H. Gelb, V. Molteni, *Chem Rev* **2014**, *114*, 11305-11347.

[50]   W. S. Al-Salem, C. Solórzano, G. D. Weedall, N. A. Dyer, L. Kelly-Hope, A. Casas-Sánchez, Y. Alraey, E. J. Alyamani, A. Halliday, S. M. Balghonaim, K. S. Alsohibany, Z. Alzeyadi, M. H. Alzahrani, A. M. Al-Shahrani, A. M. Assiri, Z. Memish, Á. Acosta-Serrano, *Parasit Vectors* **2019**, *12*, 195.

[51]   R. Du, P. J. Hotez, W. S. Al-Salem, A. Acosta-Serrano, *PLoS Negl Trop Dis* **2016**, *10*, e0004545; W. S. Al-Salem, D. M. Pigott, K. Subramaniam, L. R. Haines, L. Kelly-Hope, D. H. Molyneux, S. I. Hay, A. Acosta-Serrano, *Emerg Infect Dis* **2016**, *22*, 931-933; G. Muhjazi, A. F. Gabrielli, J. A. Ruiz-Postigo, H. Atta, M. Osman, H. Bashour, A. Al Tawil, H. Husseiny, R. Allahham, R. Allan, *PLoS Negl Trop Dis* **2019**, *13*, e0007827; A. Youssef, R. Harfouch, S. El Zein, Z. Alshehabi, R. Shaaban, S. S. Kanj, *Am J Trop Med Hyg* **2019**, *101*, 108-112; K. Rehman, J. Walochnik, J. Mischlinger, B. Alassil, R. Allan, M. Ramharter, *Emerg Infect Dis* **2018**, *24*, 1973-1981.

[52]   P. J. Weina, R. C. Neafie, G. Wortmann, M. Polhemus, N. E. Aronson, *Clin Infect Dis* **2004**, *39*, 1674-1680; H. Goto, J. A. Lauletta Lindoso, *Infect Dis Clin North Am* **2012**, *26*, 293-307.

[53]   H. Goto, J. A. Lindoso, *Expert Rev Anti Infect Ther* **2010**, *8*, 419-433.

[54]   M. Mohebali, A. Fotouhi, B. Hooshmand, Z. Zarei, B. Akhoundi, A. Rahnema, A. R. Razaghian, M. J. Kabir, A. Nadim, *Acta Trop* **2007**, *103*, 33-40.

[55]   P. P. van Thiel, T. Leenstra, P. A. Kager, H. J. de Vries, M. van Vugt, W. F. van der Meide, A. Bart, J. E. Zeegelaar, A. van der Sluis, H. D. Schallig, T. van Gool, W. R. Faber, P. J. de Vries, *Clin Infect Dis* **2010**, *50*, 80-83.

[56]   R. El Hajj, H. Bou Youness, L. Lachaud, P. Bastien, C. Masquefa, P. A. Bonnet, H. El Hajj, I. Khalifeh, *PLoS Negl Trop Dis* **2018**, *12*, e0006854.

[57]   T. Di Muccio, A. Scalone, A. Bruno, M. Marangi, R. Grande, O. Armignacco, L. Gradoni, M. Gramiccia, *PLoS One* **2015**, *10*, e0129418; L. Gradoni, *Euro Surveill* **2013**, *18*, 20539; G. Boecken, C. Sunderkötter, C. Bogdan, T. Weitzel, M. Fischer, A. Müller, M. Löbermann, G. Anders, E. von Stebut, M. Schunk, G. Burchard, M. Grobusch, R. Bialek, G. Harms-Zwingenberger, B. Fleischer, M. Pietras, M. Faulde, K. Erkens, G. S. o. Dermatology, G. S. o. T. Medicine, G. S. o. Chemotherapy, *J Dtsch Dermatol Ges* **2011**, *9 Suppl 8*, 1-51; T. Herremans, E. Pinelli, M. Casparie, N. Nozari, J. Roelfsema, L. Kortbeek, *Int Health* **2010**, *2*, 42-46; S. K. Söbirk, M. Inghammar, M. Collin, L. Davidsson, *Epidemiol Infect* **2018**, *146*, 1267-1274; W. Poeppl, C. Oeser, K. Grabmeier-Pfistershammer, J. Walochnik, H. Burgmann, *Travel Med Infect Dis* **2013**, *11*, 90-94.

[58]   A. Pavli, H. C. Maltezou, *Int J Infect Dis* **2010**, *14*, e1032-1039.

[59]   S. Antinori, E. Gianelli, S. Calattini, E. Longhi, M. Gramiccia, M. Corbellino, *Clin Microbiol Infect* **2005**, *11*, 343-346.

[60]   R. Manfredi, M. A. di Bari, L. Calza, F. Chiodo, *Eur J Epidemiol* **2001**, *17*, 793-795.

[61]   A. Kuna, M. Gajewski, M. Bykowska, H. Pietkiewicz, R. Olszański, P. Myjak, *Postepy Dermatol Alergol* **2019**, *36*, 104-111.

123

[62] L. M. B. de Souza, V. Thomaz Soccol, R. R. Petterle, M. D. Bates, P. A. Bates, *Parasitology* **2018**, *145*, 1938-1948; J. Saab, F. Fedda, R. Khattab, L. Yahya, A. Loya, M. Satti, A. G. Kibbi, M. A. Houreih, W. Raslan, M. El-Sabban, I. Khalifeh, *J Cutan Pathol* **2012**, *39*, 251-262.

[63] J. P. Gangneux, J. Menotti, F. Lorenzo, C. Sarfati, H. Blanche, H. Bui, F. Pratlong, Y. J. Garin, F. Derouin, *J Clin Microbiol* **2003**, *41*, 1419-1422.

[64] A. Masmoudi, W. Hariz, S. Marrekchi, M. Amouri, H. Turki, *J Dermatol Case Rep* **2013**, *7*, 31-41.

[65] P. Schneider, L. F. Schnur, C. L. Jaffe, M. A. Ferguson, M. J. McConville, *Biochem J* **1994**, *304 (Pt 2)*, 603-609.

[66] C. L. Forestier, Q. Gao, G. J. Boons, *Front Cell Infect Microbiol* **2014**, *4*, 193; A. Guha-Niyogi, D. R. Sullivan, S. J. Turco, *Glycobiology* **2001**, *11*, 45R-59R.

[67] M. J. McConville, A. Bacic, *J Biol Chem* **1989**, *264*, 757-766; G. Rosen, M. V. Londner, D. Sevlever, C. L. Greenblatt, *Mol Biochem Parasitol* **1988**, *27*, 93-99.

[68] M. J. McConville, S. W. Homans, J. E. Thomas-Oates, A. Dell, A. Bacic, *J Biol Chem* **1990**, *265*, 7385-7394.

[69] J. L. Avila, M. Rojas, A. Acosta, *J Clin Microbiol* **1991**, *29*, 2305-2312.

[70] K. S. Subramaniam, V. Austin, N. S. Schocker, A. L. Montoya, M. S. Anderson, R. A. Ashmus, M. Mesri, W. Al-Salem, I. C. Almeida, K. Michael, A. Acosta-Serrano, *Parasitology* **2018**, *145*, 1758-1764.

[71] K. Ruda, J. Lindberg, P. J. Garegg, S. Oscarson, P. Konradsson, *J. Am. Chem. Soc.* **2000**, *122*, 11067-11072; L. Gandolfi-Donadio, C. Gallo-Rodriguez, R. M. de Lederkremer, *J Org Chem* **2002**, *67*, 4430-4435.

[72] A. Imamura, A. Kimura, H. Ando, H. Ishida, M. Kiso, *Chemistry* **2006**, *12*, 8862-8870.

[73] A. Kimura, A. Imamura, H. Ando, H. Ishida, M. Kiso, *Synlett* **2006**, 2379-2382.

[74] A. Imamura, N. Matsuzawa, S. Sakai, T. Udagawa, S. Nakashima, H. Ando, H. Ishida, M. Kiso, *J Org Chem* **2016**, *81*, 9086-9104.

[75] N. S. Schocker, S. Portillo, C. R. Brito, A. F. Marques, I. C. Almeida, K. Michael, *Glycobiology* **2016**, *26*, 39-50.

[76] **Supporting Information**.

[77] Y. Bai, T. L. Lowary, *J Org Chem* **2006**, *71*, 9658-9671.

[78] G. C. Completo, T. L. Lowary, *J Org Chem* **2008**, *73*, 4513-4525.

[79] L. M. Deng, X. Liu, X. Y. Liang, J. S. Yang, *J Org Chem* **2012**, *77*, 3025-3037.

[80] C. A. Tai, S. S. Kulkarni, S. C. Hung, *J Org Chem* **2003**, *68*, 8719-8722.

[81] A. Oliveira, Universidade nova de Lisboa (Universidade nova de Lisboa), **2015**.

[82] M. J. Tilve, C. R. Cori, C. Gallo-Rodriguez, *J Org Chem* **2016**, *81*, 9585-9594.

[83] N. K. Kochetkov, A. J. Khorlin , A. F. Bochkov, *Vol. 5*, Tetrahedron Letters, **1964**, pp. 289-293.

[84] B. O. Owino, D. Matoke-Muhia, Y. Alraey, J. M. Mwangi, J. M. Ingonga, P. M. Ngumbi, A. Casas-Sanchez, A. Acosta-Serrano, D. K. Masiga, *PLoS Negl Trop Dis* **2019**, *13*, e0007712.

[85] M. Greiner, D. Pfeiffer, R. D. Smith, *Prev Vet Med* **2000**, *45*, 23-41.

[86] D. El Safadi, S. Merhabi, R. Rafei, H. Mallat, M. Hamze, A. Acosta-Serrano, *Trans R Soc Trop Med Hyg* **2019**, *113*, 471-476; R. Ozaras, H. Leblebicioglu, M. Sunbul, F. Tabak, Balkan, II, M. Yemisen, I. Sencan, R. Ozturk, *Expert Rev Anti Infect Ther* **2016**, *14*, 547-555.

[87]   P. D. Ready, *Euro Surveill* **2010**, *15*, 19505; P. Torpiano, D. Pace, *Expert Rev Anti Infect Ther* **2015**, *13*, 1123-1138.

[88]   U. Galili, *Immunology* **2013**, *140*, 1-11; B. A. Macher, U. Galili, *Biochim Biophys Acta* **2008**, *1780*, 75-88.

[89]   U. Galili, E. A. Rachmilewitz, A. Peleg, I. Flechner, *J Exp Med* **1984**, *160*, 1519-1531.

[90]   P. Norris, D. Horton, *In PreparatiVe Carbohydrate Chemistry*, Marcel Dekker: New York, **1997**.

[91]   A. Oliveira, Universidade nova de Lisboa (Universidade nova de Lisboa), **2015**.

[92]   A. Frey, J. Di Canzio, D. Zurakowski, *J Immunol Methods* **1998**, *221*, 35-41.

[93]   D. Steverding, *Parasit Vectors* **2014**, *7*, 317.

[94]   W. H. O. E. Committee, *World Health Organ Tech Rep Ser* **2002**, *905*, i-vi, 1-109, back cover; J. A. Perez-Molina, I. Molina, *Lancet* **2018**, *391*, 82-94.

[95]   F. J. Carod-Artal, J. Gascon, *Lancet Neurol* **2010**, *9*, 533-542.

[96]   J. A. Perez-Molina, F. Norman, R. Lopez-Velez, *Curr Infect Dis Rep* **2012**, *14*, 263-274; G. A. Schmunis, *Mem Inst Oswaldo Cruz* **2007**, *102 Suppl 1*, 75-85.

[97]   A. Rassi, Jr., A. Rassi, J. A. Marin-Neto, *Lancet* **2010**, *375*, 1388-1402.

[98]   C. Bern, S. Kjos, M. J. Yabsley, S. P. Montgomery, *Clin Microbiol Rev* **2011**, *24*, 655-681.

[99]   B. A. de Noya, O. N. Gonzalez, *Acta Trop* **2015**, *151*, 94-102.

[100] J. R. Coura, J. Borges-Pereira, *Acta Trop* **2010**, *115*, 5-13; M. F. Bellini, R. Silistino-Souza, M. Varella-Garcia, M. T. de Azeredo-Oliveira, A. E. Silva, *Journal of tropical   medicine* **2012**, *2012*.

[101] B. Custer, M. Agapova, R. Bruhn, R. Cusick, H. Kamel, P. Tomasulo, H. Biswas, L. Tobler, T. H. Lee, S. Caglioti, M. Busch, *Transfusion* **2012**, *52*, 1901-1911.

[102] Z. Brener, *Rev Inst Med Trop Sao Paulo* **1971**, *13*, 171-178.

[103] J. A. Urbina, *J Eukaryot Microbiol* **2015**, *62*, 149-156.

[104] R. Viotti, C. Vigliano, B. Lococo, M. G. Alvarez, M. Petti, G. Bertocchi, A. Armenti, *Expert Rev Anti Infect Ther* **2009**, *7*, 157-163.

[105] M. J. Pinazo, M. C. Thomas, J. Bua, A. Perrone, A. G. Schijman, R. J. Viotti, J. M. Ramsey, I. Ribeiro, S. Sosa-Estani, M. C. Lopez, J. Gascon, *Expert Rev Anti Infect Ther* **2014**, *12*, 479-496.

[106] I. Ribeiro, A. M. Sevcsik, F. Alves, G. Diap, R. Don, M. O. Harhay, S. Chang, B. Pecoul, *PLoS Negl Trop Dis* **2009**, *3*, e484; *Wkly Epidemiol Rec* **2015**, *90*, 33-43.

[107] A. Acosta-Serrano, I. C. Almeida, L. H. Freitas-Junior, N. Yoshida, S. Schenkman, *Mol Biochem Parasitol* **2001**, *114*, 143-150.

[108] U. Galili, *Anti-Gal in Humans and Its Antigen the α-Gal Epitope.*, 1st ed., Elsevier - Academic Press, Cambridge, MA, United States, **2017**.

[109] F. Torrico, J. Gascon, L. Ortiz, C. Alonso-Vega, M. J. Pinazo, A. Schijman, I. C. Almeida, F. Alves, N. Strub-Wourgaft, I. Ribeiro, E. S. Group, *Lancet Infect Dis* **2018**, *18*, 419-430.

[110] L. Izquierdo, A. F. Marques, M. Gallego, S. Sanz, S. Tebar, C. Riera, L. Quinto, E. Aldasoro, I. C. Almeida, J. Gascon, *Mem Inst Oswaldo Cruz* **2013**, *108*, 928-931.

[111] A. L. Andrade, C. M. Martelli, R. M. Oliveira, S. A. Silva, A. I. Aires, L. M. Soussumi, D. T. Covas, L. S. Silva, J. G. Andrade, L. R. Travassos, I. C. Almeida, *Am J Trop Med Hyg* **2004**, *71*, 594-597.

[112] N. S. Schocker, S. Portillo, C. R. N. Brito, A. F. Marques, I. C. Almeida, K. Michael, *Glycobiology* **2016**, *26*, 39-50.

125

[113] N. S. Schocker, S. Portillo, R. A. Ashmus, C. R. N. Brito, I. E. Silva, Y. C. Mendoza, A. F. Marques, E. Y. Monroy, A. Pardo, L. Izquierdo, M. Gallego, J. Gasco, I. C. Almeida, K. Michael, in *Coupling and Decoupling of Diverse Molecular Units in Glycosciences* (Ed.: B. R. e. In: Witczak Z.), Springer, Cham, **2017**

[114] E. Iniguez, N. S. Schocker, K. Subramaniam, S. Portillo, A. L. Montoya, W. S. Al-Salem, C. L. Torres, F. Rodriguez, O. C. Moreira, A. Acosta-Serrano, K. Michael, I. C. Almeida, R. A. Maldonado, *PLoS Negl Trop Dis* **2017**, *11*, e0006039.

[115] A. K. Balcerzak, S. S. Ferreira, J. F. Trant, R. N. Ben, *Bioorg. Med. Chem. Lett.* **2012**, *22*, 1719-1721.

[116] A. Imamura, A. Kimura, H. Ando, H. Ishida, M. Kiso, *Chem. Eur. J.* **2006**, *12*, 8862-8870.

[117] J. L. Hendel, J. W. Wang, T. A. Jackson, K. Hardmeier, R. De los Santos, F. I. Auzanneau, *J Org Chem* **2009**, *74*, 8321-8331.

[118] R. Danac, L. Ball, S. J. Gurr, T. Muller, A. J. Fairbanks, *Chembiochem* **2007**, *8*, 1241-1245.

Glossary

α-Gal*p*	α-galactopyranosyl
β-Gal*f*	β-galactofuranosyl
Abs	antibodies
Ac	acetyl
All	allyl
Anti-Gal	anti-αGalactosyl antibody
Ar	argon
AUC	area under the curve
BMKs	biomarkers
BNZ	benznidazole
BSA	bovine serum albumin
Bz	benzoyl
CCD	chronic Chagas disease
CD	Chagas disease
Ch anti-α-Gal	anti-α-Gal antibodies purified from sera of patients with chronic CD
ChHSP	chronic CD patients
ChMSP	mice infected with *T. cruzi*
CL	cutaneous leishmaniasis
CL-ELISA	chemiluminescent enzyme-linked immunosorbent assay
CS	conventional serology
Cys	cysteine
DBU	1,8-diazabicyclo[5.4.0]undec-7-ene
DCM	methylene dichloride
DMAP	dimethylaminopyridine
DMP	2,2-dimethoxypropane
DTBS	di-*tert*-butylsilyl (protecting group)
DTBS(OTf)$_2$	di-*tert*-butylsilyl bis(trifluoromethanesulfonate)
ESI-TOF HRMS	electrospray ionization time-of-flight high resolution mass spectra
EtOAc	ethyl acetate

127

Gal	galactose
Gal*f*	galactofuranose
Gal*p*	galactopyranose
GIPLs	glycoinositol-phospholipids
GPI	glycosyl-phosphatidylinositol
GPI-MUC	GPI-anchored mucins
h	hours
ICAs	intracellular amastigotes
IgG	Immunoglobulin G
IgM	Immunoglobulin M
KSA	the Kingdom of Saudi Arabia
Leishmania spp.	*Leishmania* species
L. braziliensis	*Leishmania braziliensis*
L. donovani	*Leishmania donovani*
L. major	*Leishmania major*
L. mexicana	*Leishmania mexicana*
L. tropica	*Leishmania tropica*
LPG	lipophosphoglycan
LPS	lipopolysaccharide
M	molarity
MALDI-TOF	matrix-assisted laser desorption ionization time-of-flight
Man	mannose
MASP	mucin-associated surface proteins
Metas	metacyclic trypomastigotes
Min	minutes
MS	molecular sieves
NBS	*N*-Bromosuccinimide
NFX	nifurtimox
NGPs	neoglycoproteins
NHS	normal human serum
NHS anti-α-Gal	anti-α-Gal antibodies from sera of healthy individuals

128

NIS	*N*-Iodosuccinimide
NMR	nuclear magnetic resonance
NMSP	healthy mice
NTD	neglected tropical disease
PTLC	preparative thin layer chromatography
PTSA	*para*-toluenesulfonic acid
quant.	quantitative
RLU	relative luminescence units
ROC Curve	receiver operating characteristic curve
rt	room temperature
*t*Bu	*tert*-butyl
TCEP	tris(2-carboxyethyl)phosphine hydrochloride
T. cruzi	*Trypanosoma cruzi*
TCTs	mammalian tissue cell-derived trypomastigotes
TFA	trifluoroacetic acid
TLC	thin-layer chromatography
THF	tetrahydrofuran
TMS-OTf	trimethylsilyl trifluoromethanesulfonate
TS	trans-sialidases
U/well	units per well
UK	United Kingdom
WHO	World Health Organization

Appendix

^{1}H NMR, 400 MHz, CDCl$_3$, compound (1)

^{13}C NMR, 100 MHz, CDCl$_3$, compound (1)

130
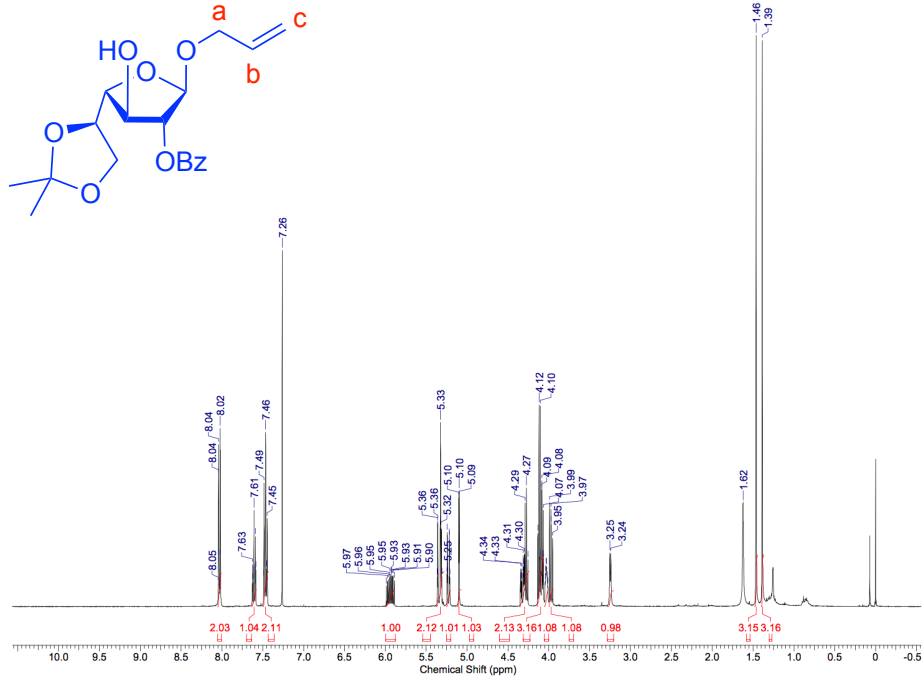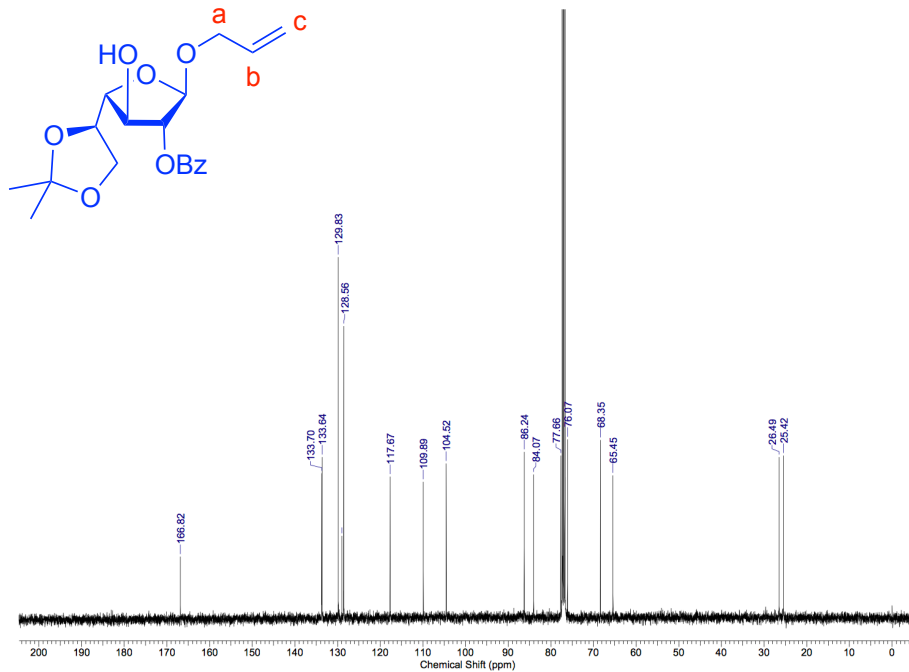
¹H NMR, 400 MHz, CDCl₃, compound (8)
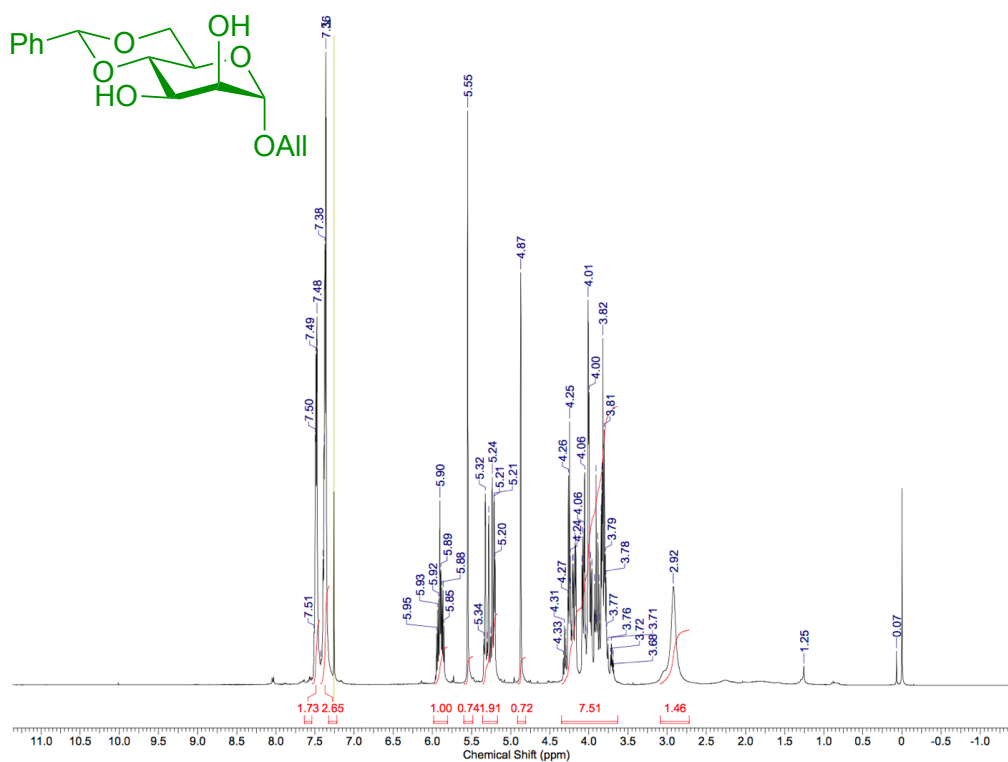
¹H NMR, 400 MHz, CDCl₃, compound (28)

131
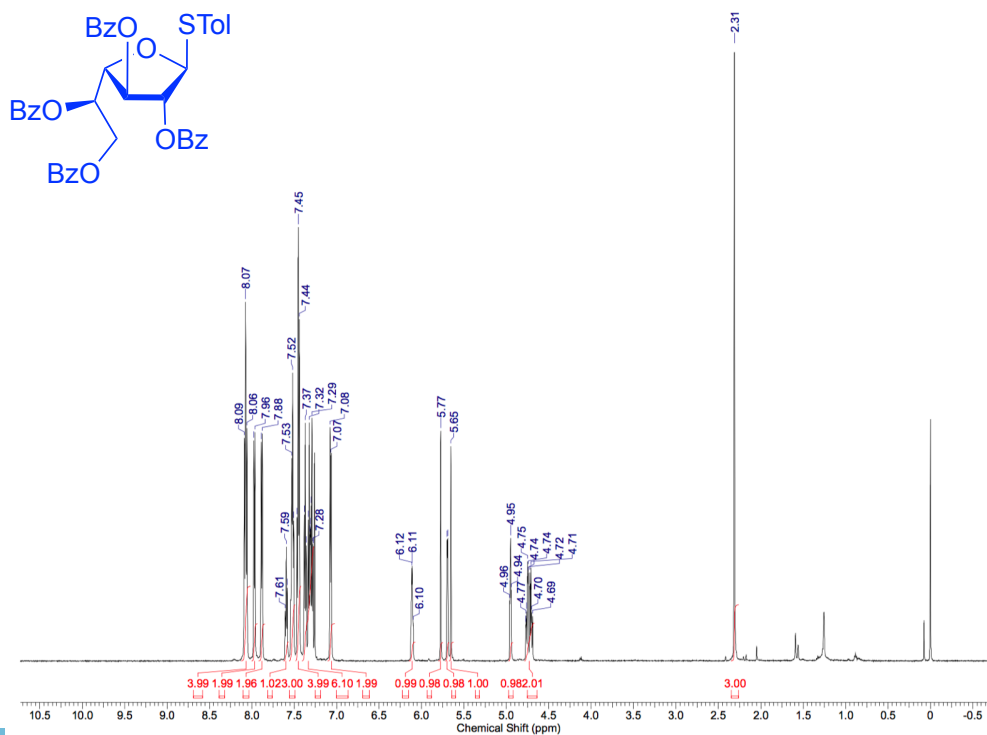
^{1}H NMR, 400 MHz, CDCl$_3$, compound (2)
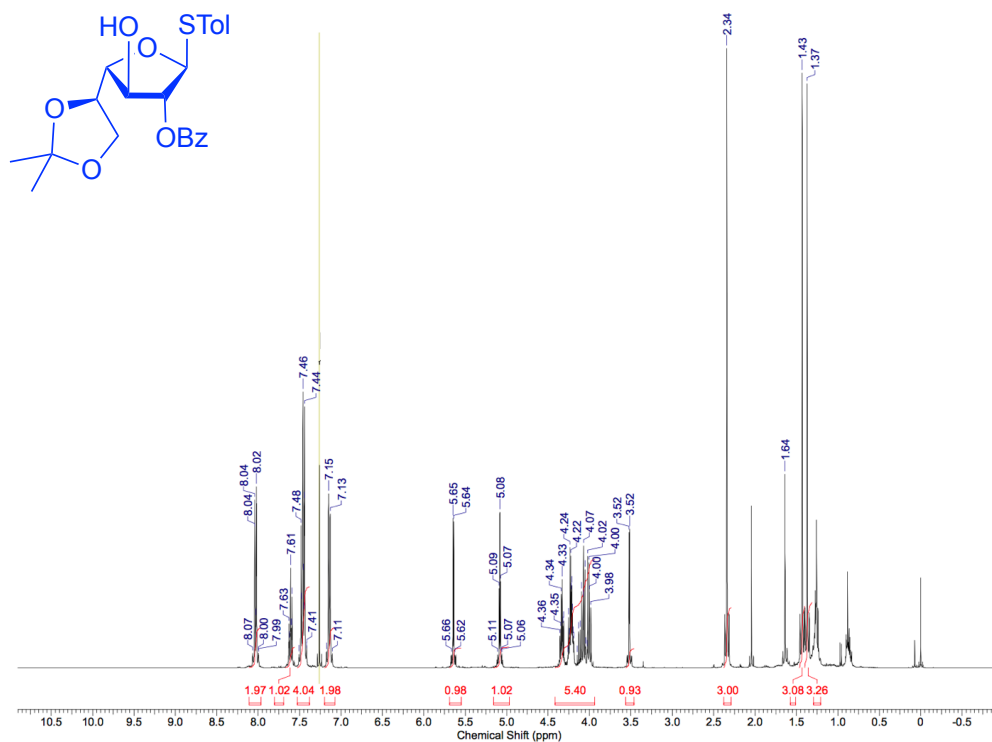
^{1}H NMR, 400 MHz, CDCl$_3$, compound (3)

132
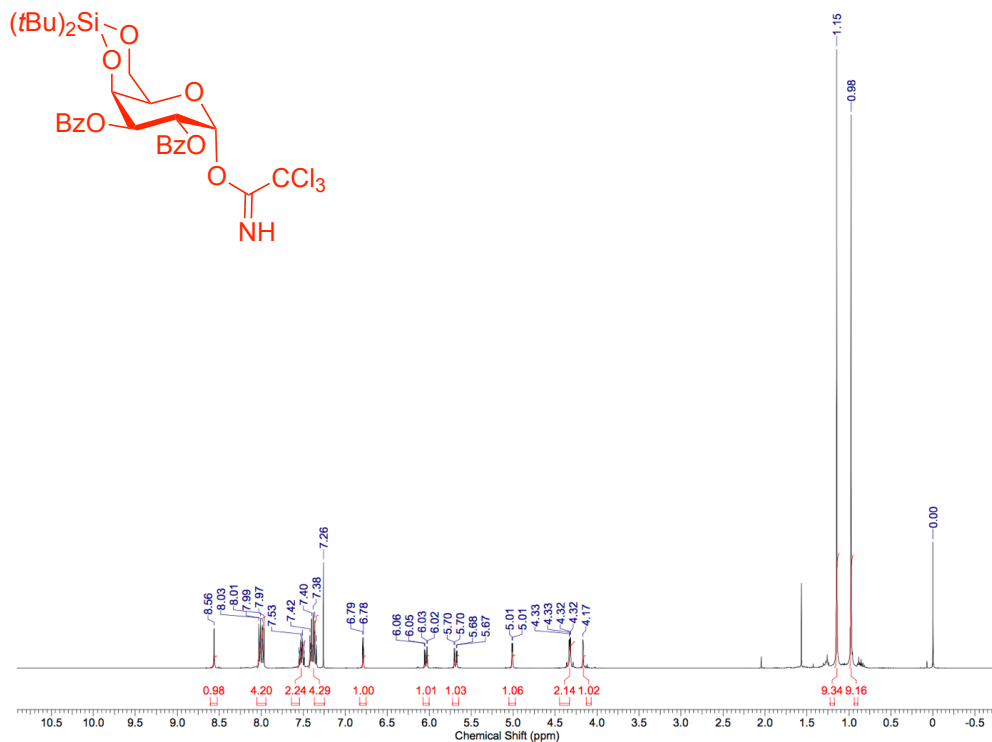
^{1}H NMR, 400 MHz, CDCl$_3$, compound (4)

^{13}C NMR, 100 MHz, CDCl$_3$, compound (4)

133
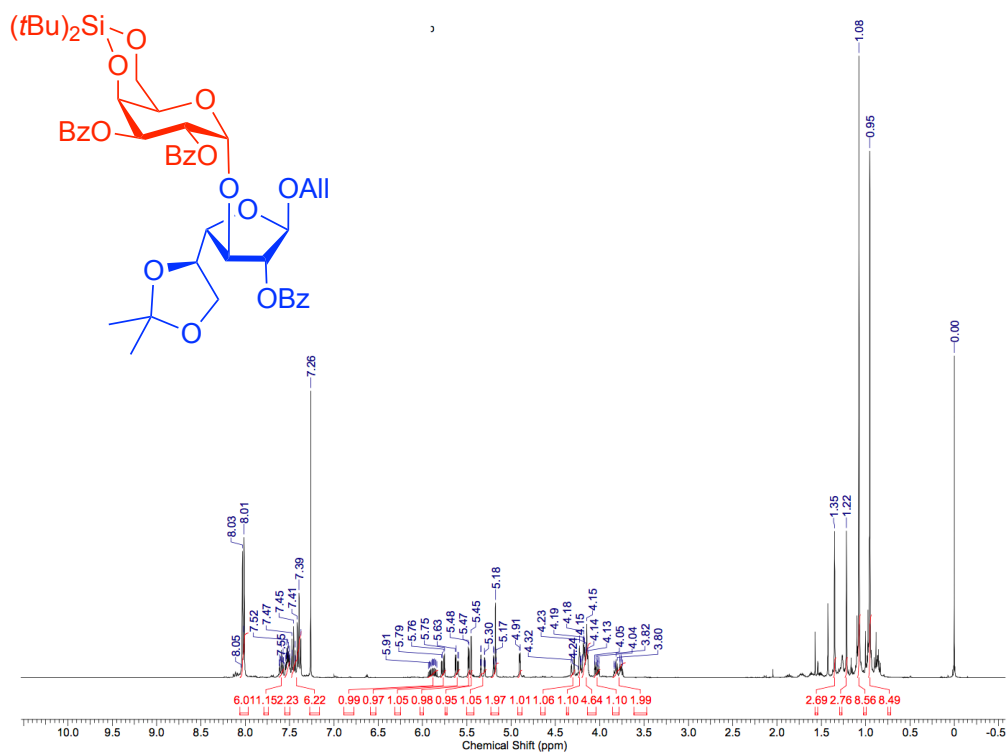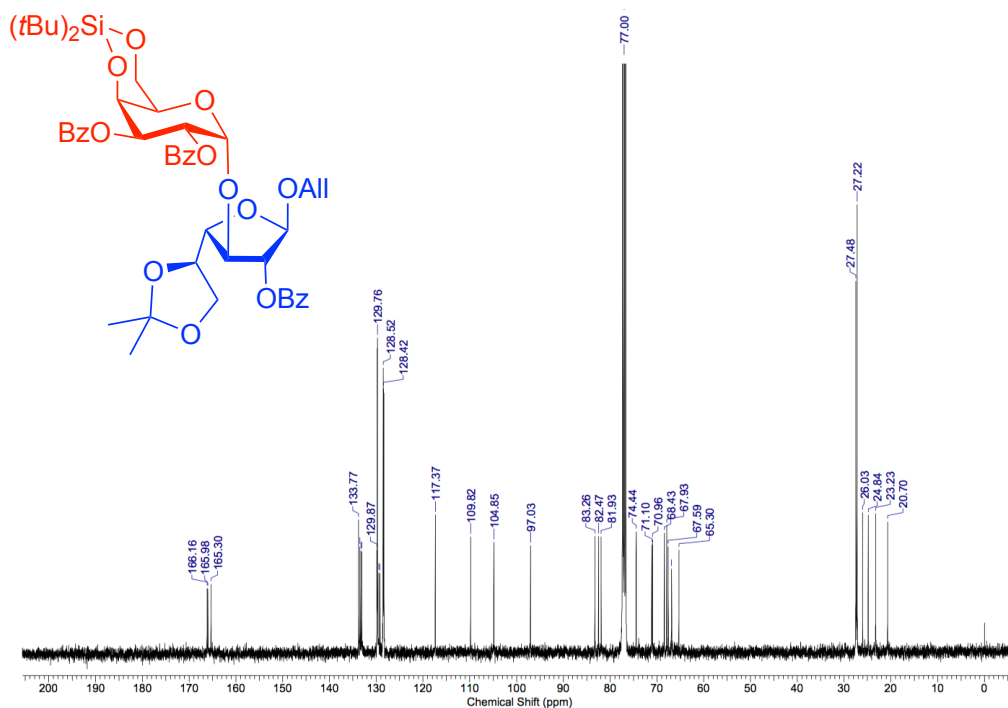
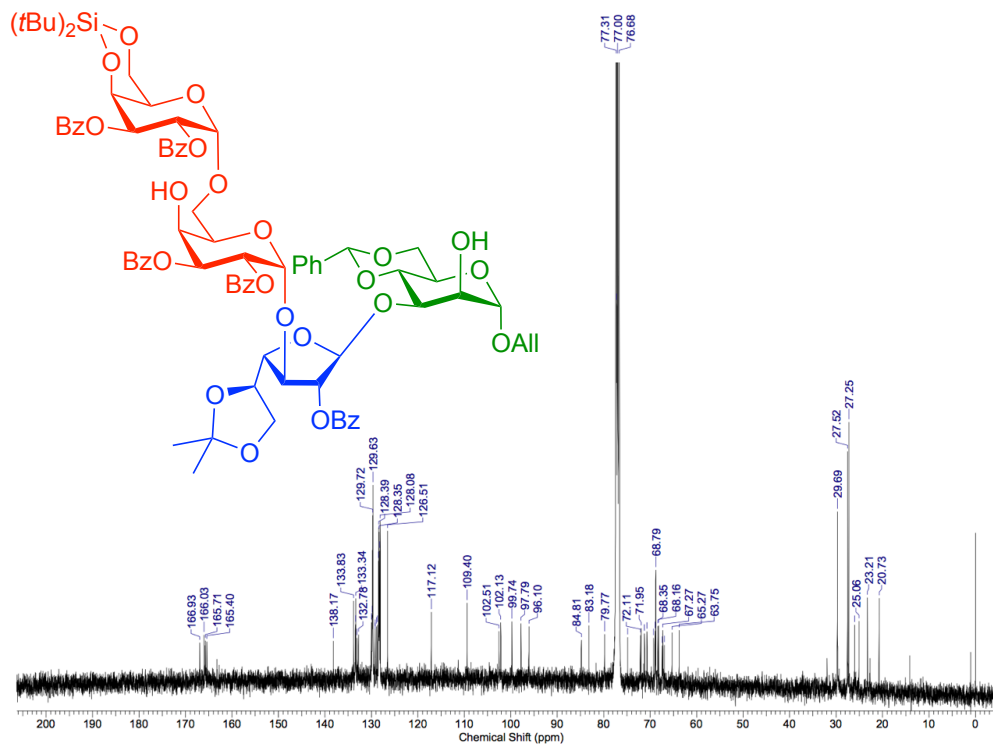**HSQC NMR, 400 MHz, CDCl₃, compound (4)**

COSY NMR, 400 MHz, CDCl₃, compound (4)

134
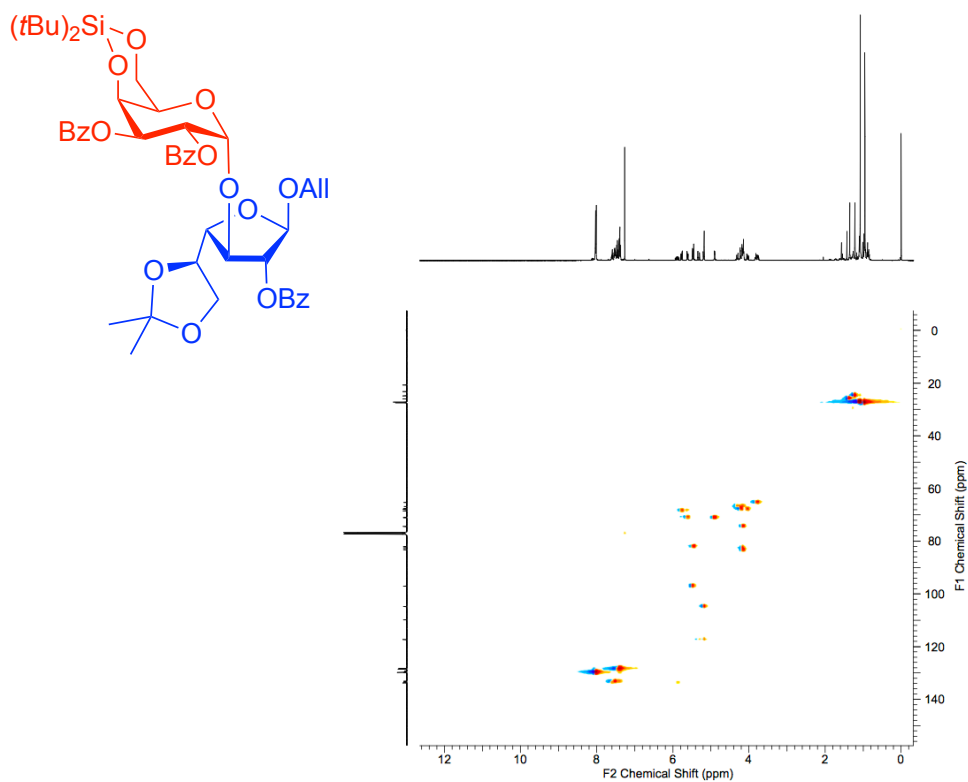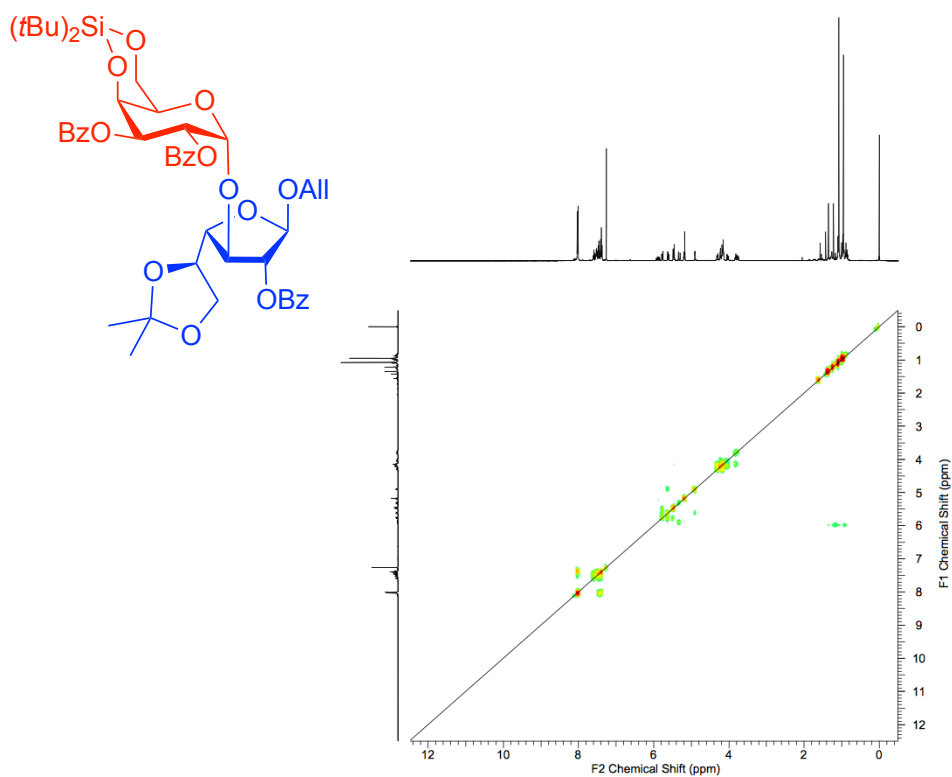
¹H NMR, 400 MHz, CDCl₃, compound (33)

¹³C NMR, 100 MHz, CDCl₃, compound (33)

135
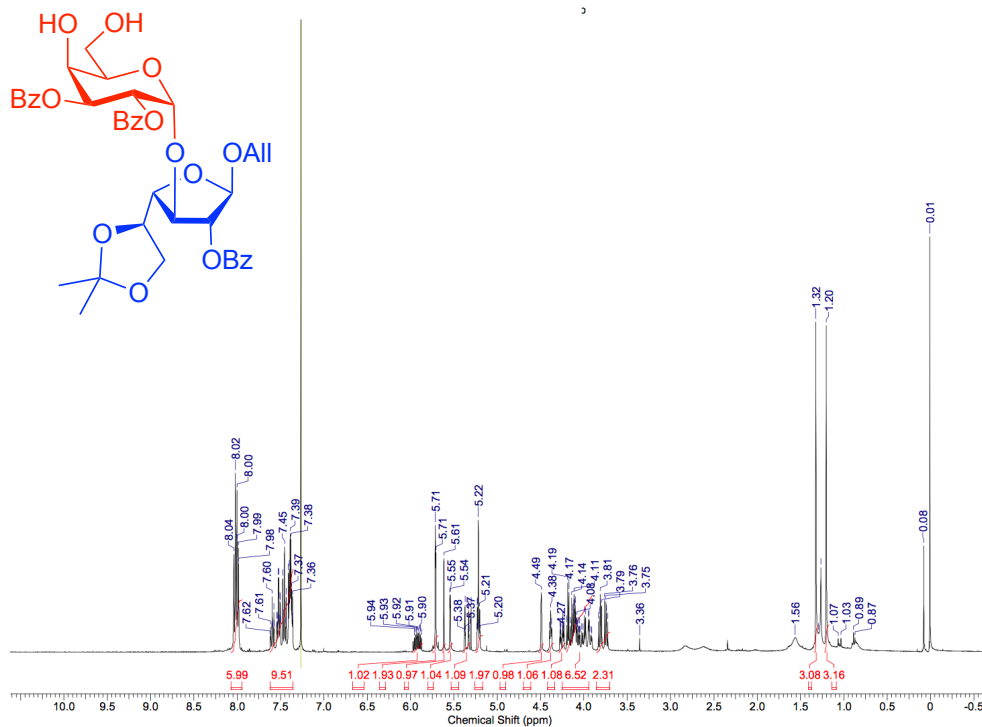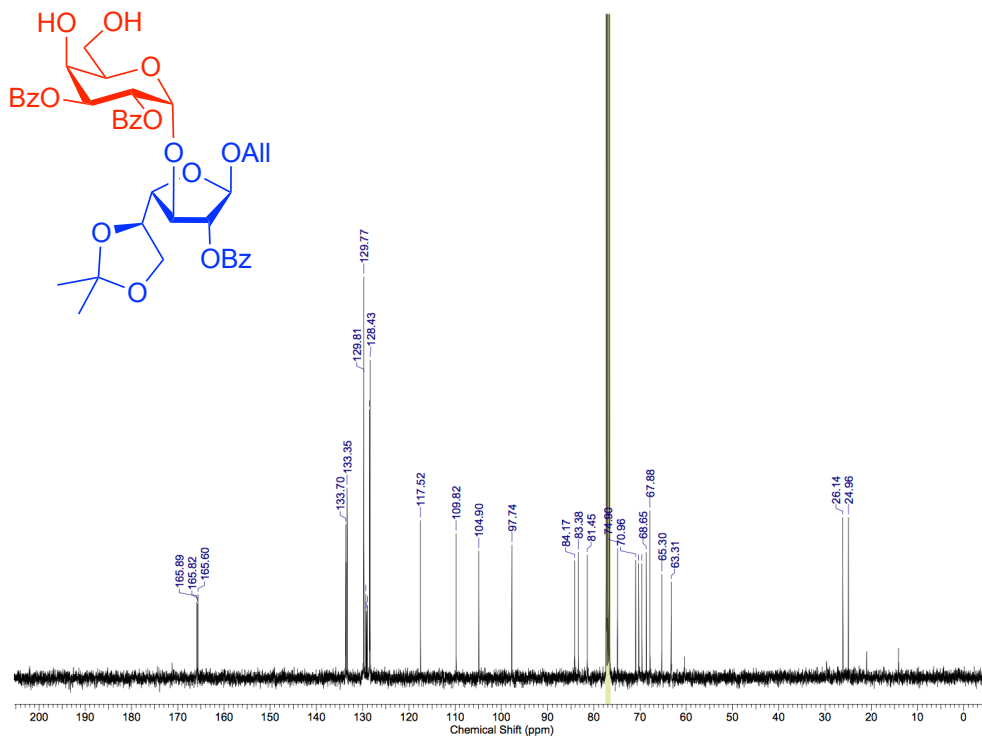
¹H NMR, 400 MHz, CDCl₃, compound (6)
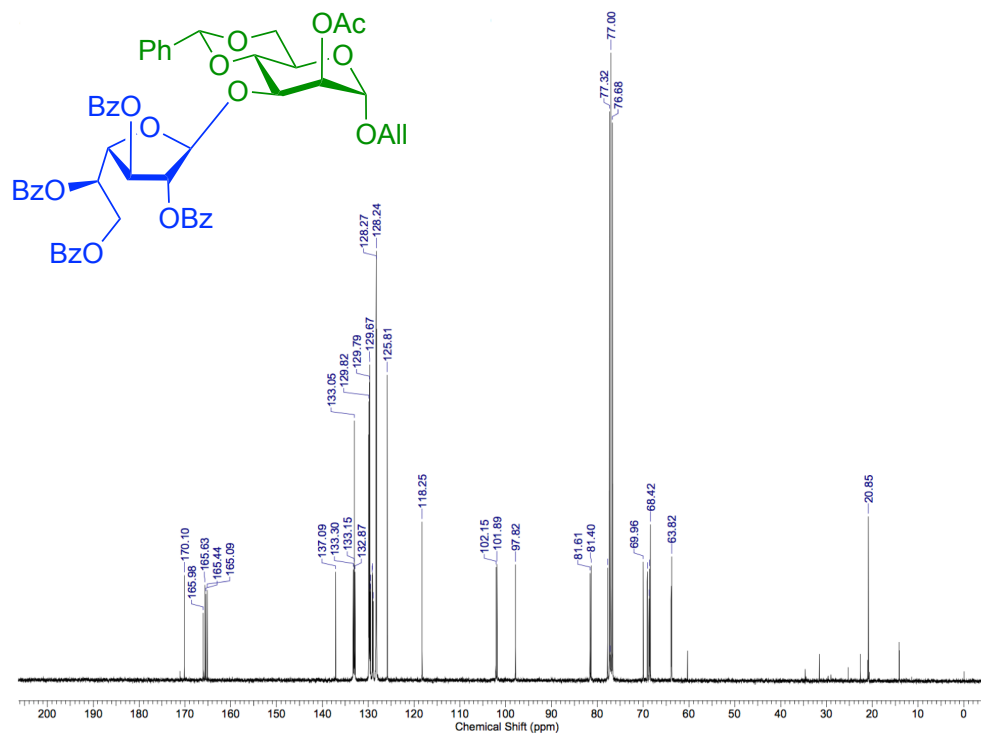

¹³C NMR, 100 MHz, CDCl₃, compound (6)

136
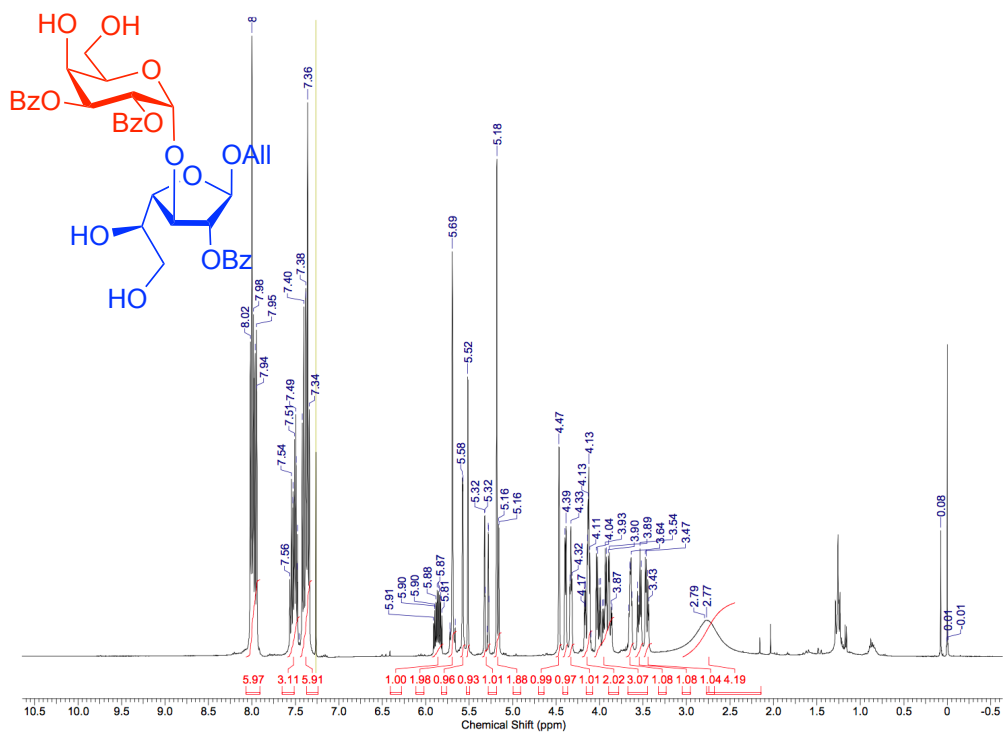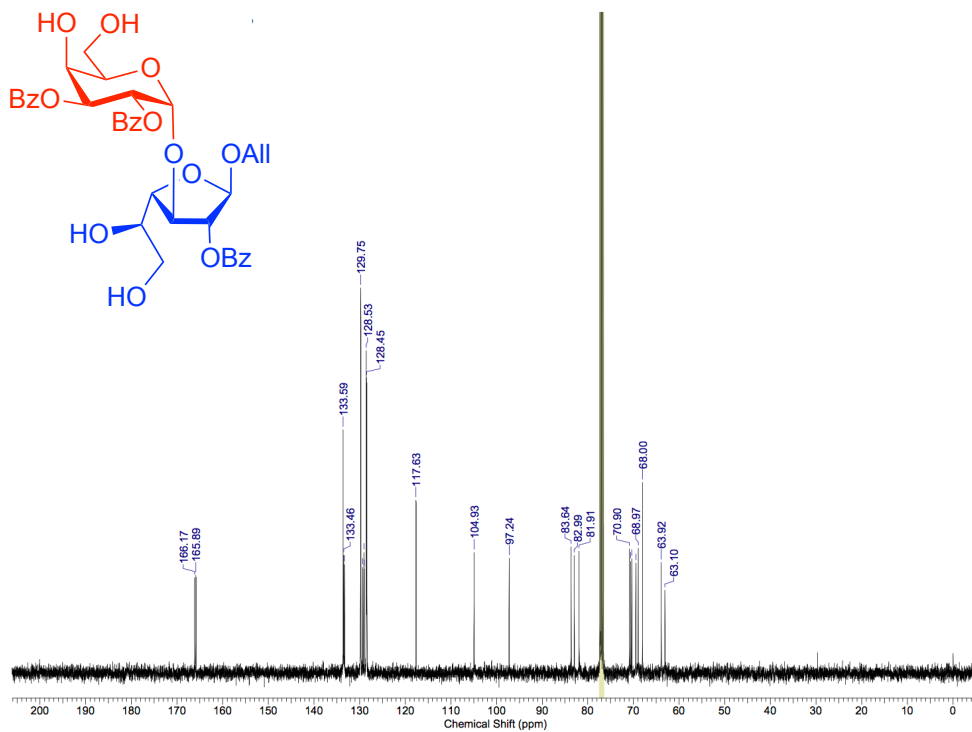
¹H NMR, 400 MHz, CDCl₃, compound (7)
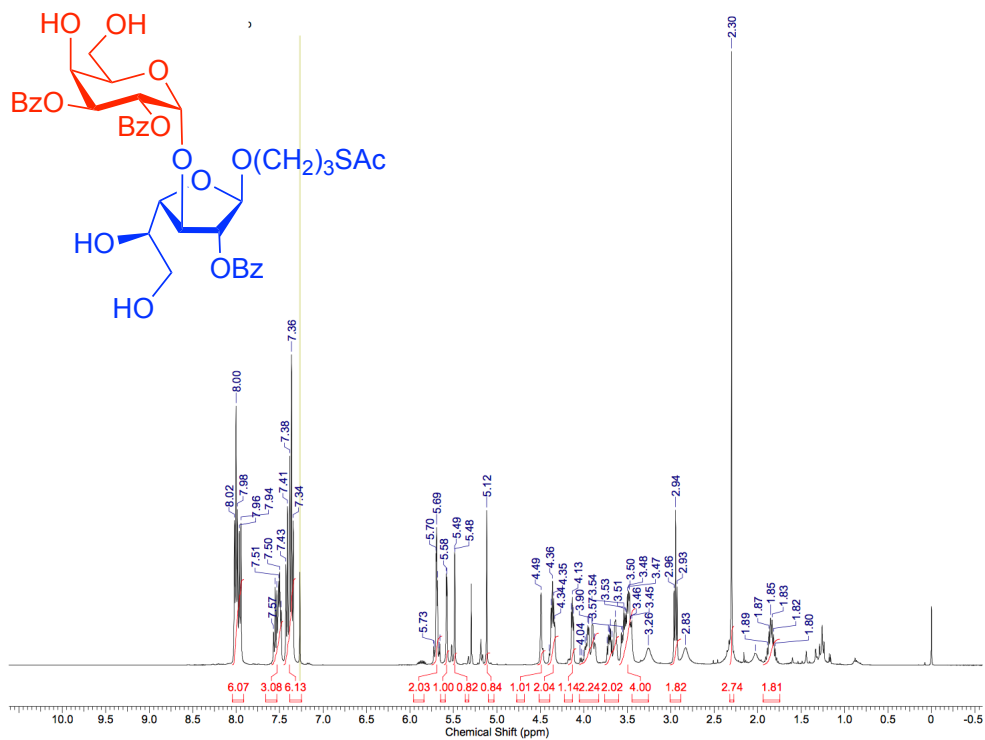
¹³C NMR, 100 MHz, CDCl₃, compound (7)
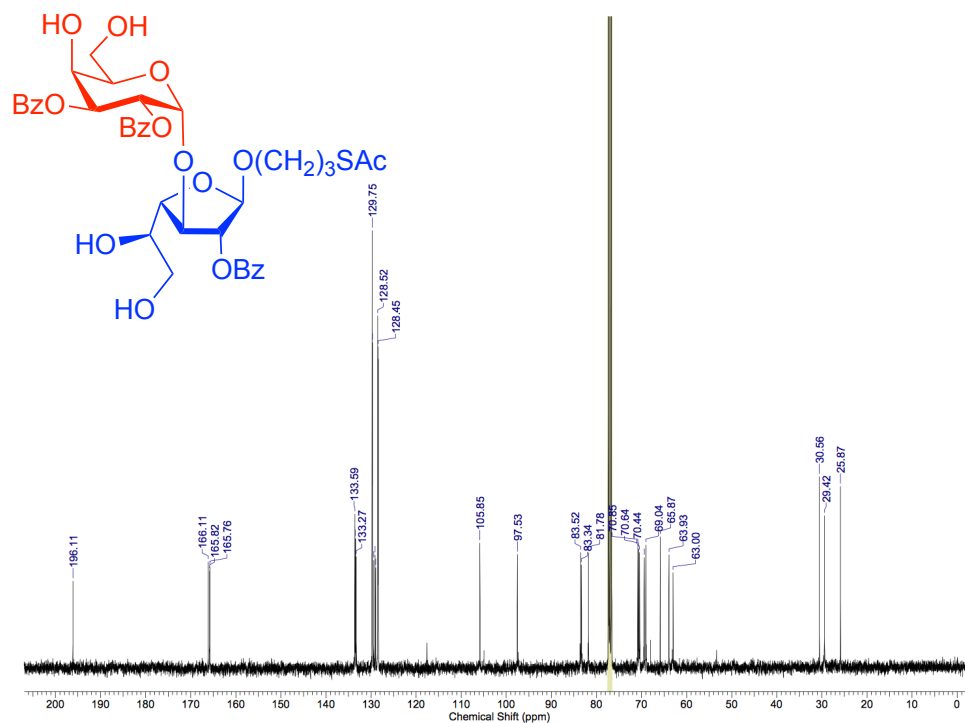
^{1}H NMR, 400 MHz, D$_2$O, compound (14)

^{13}C NMR, 100 MHz, D$_2$O, compound (14)

138
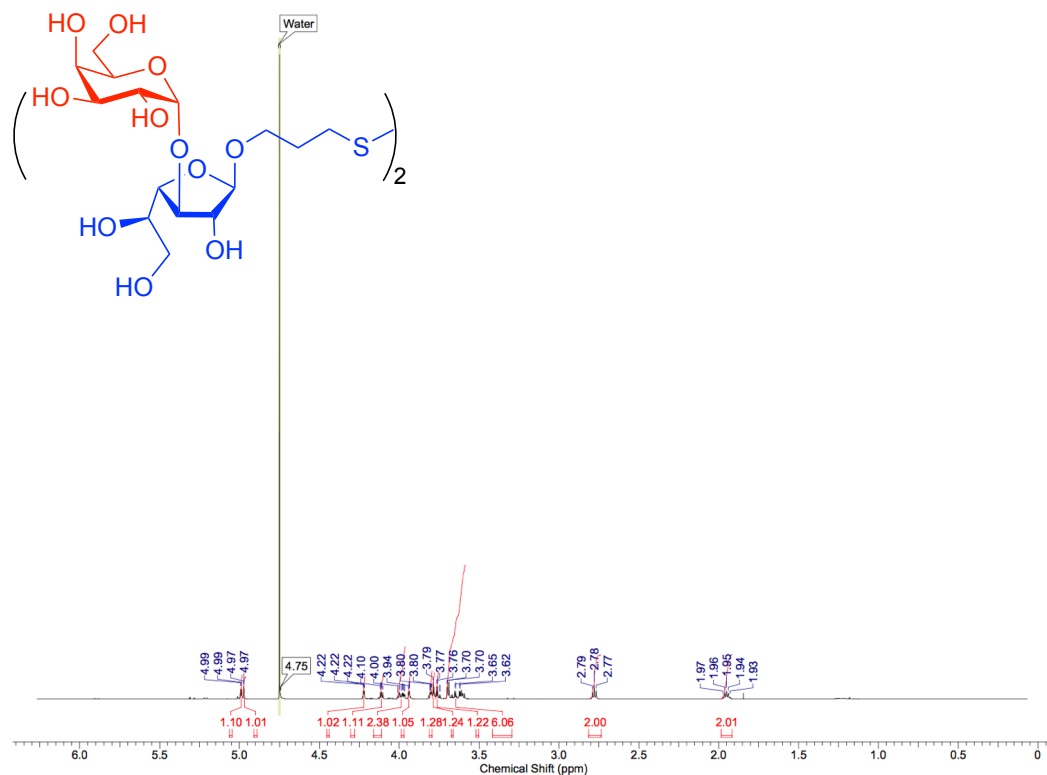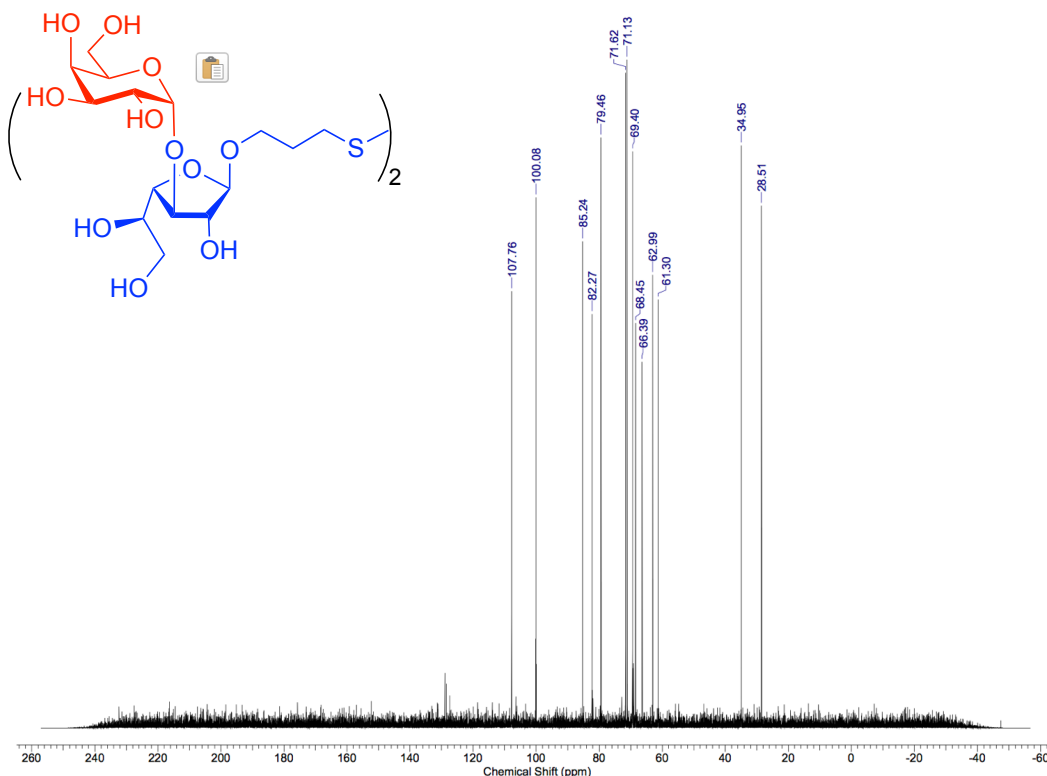
¹H NMR, 400 MHz, CDCl₃, compound (11)
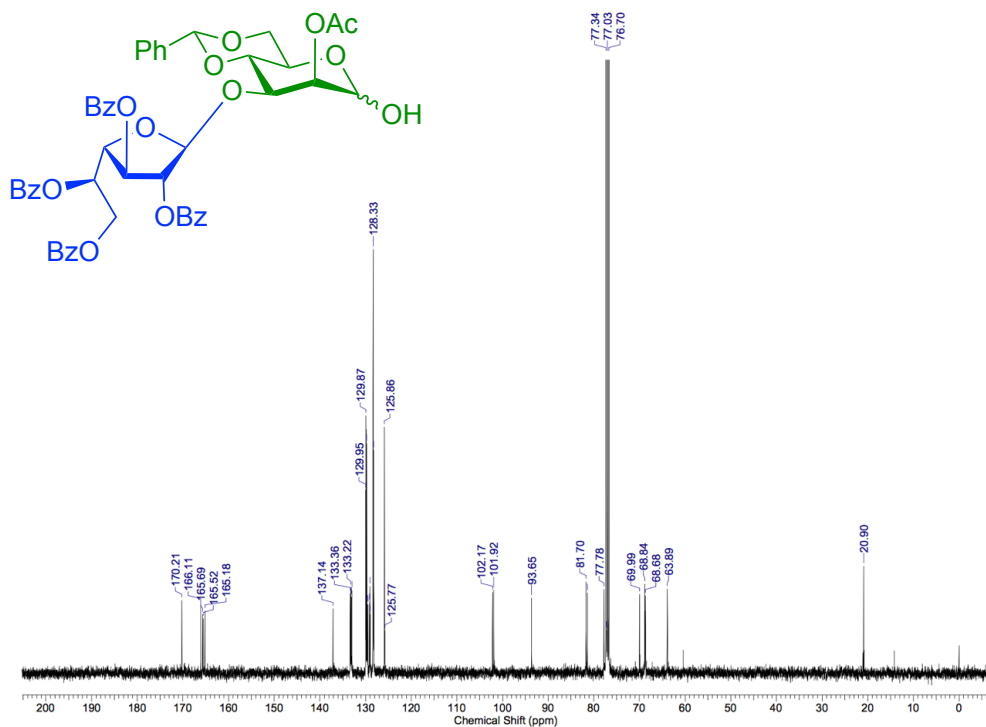

¹³C NMR, 100 MHz, CDCl₃, compound (11)
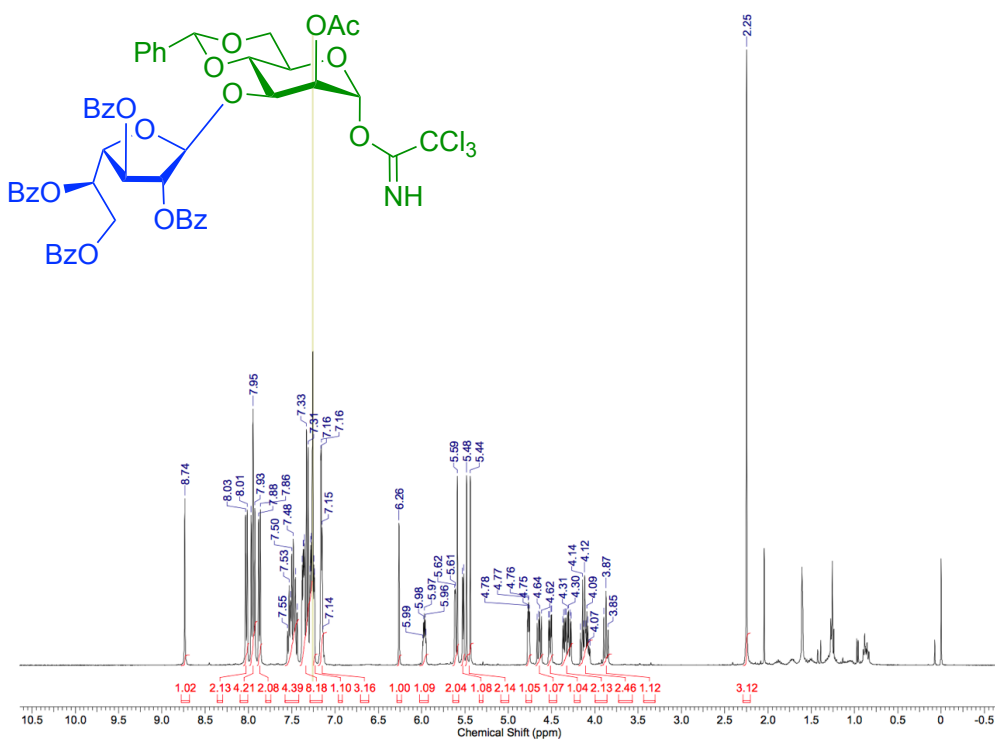

139
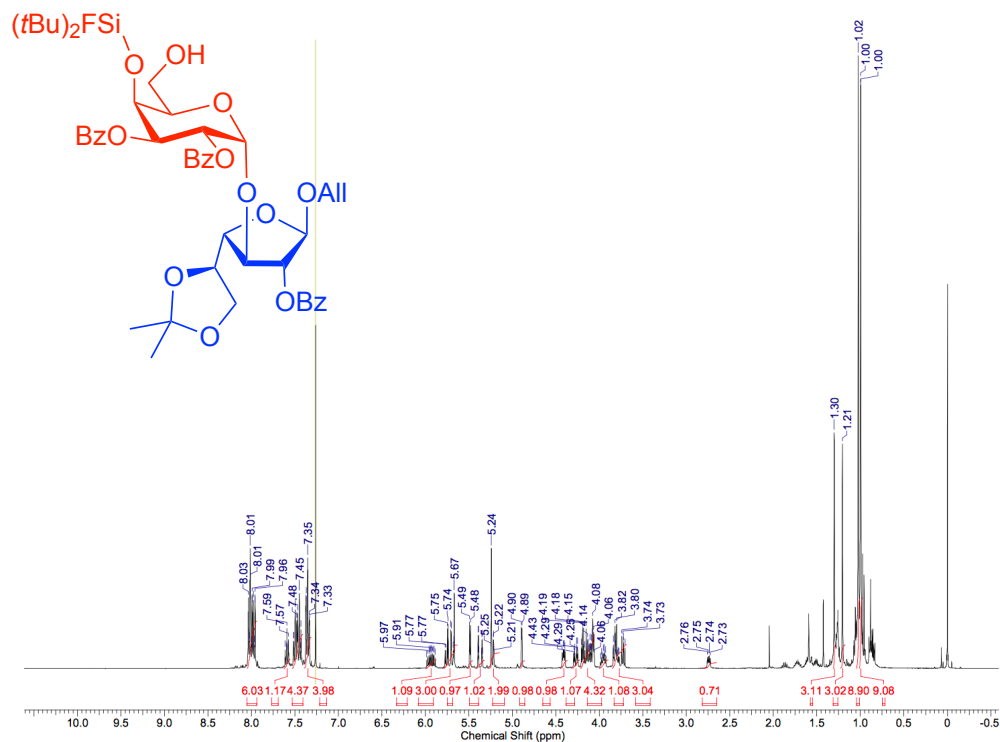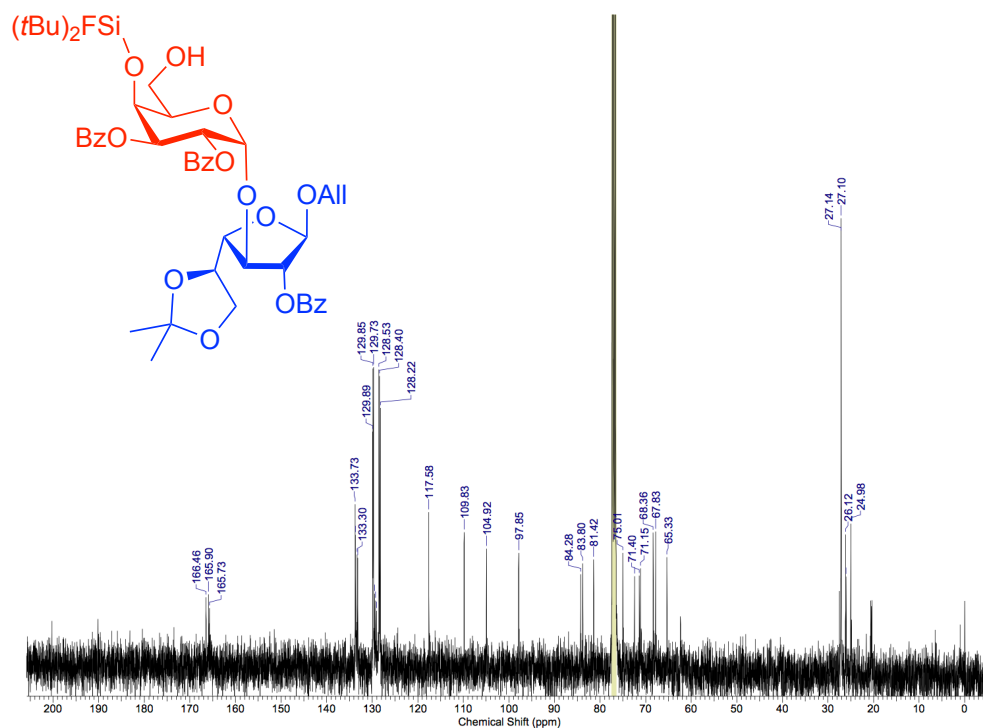
¹H NMR, 400 MHz, CDCl₃, compound (20)

¹³C NMR, 100 MHz, CDCl₃, compound (20)

140
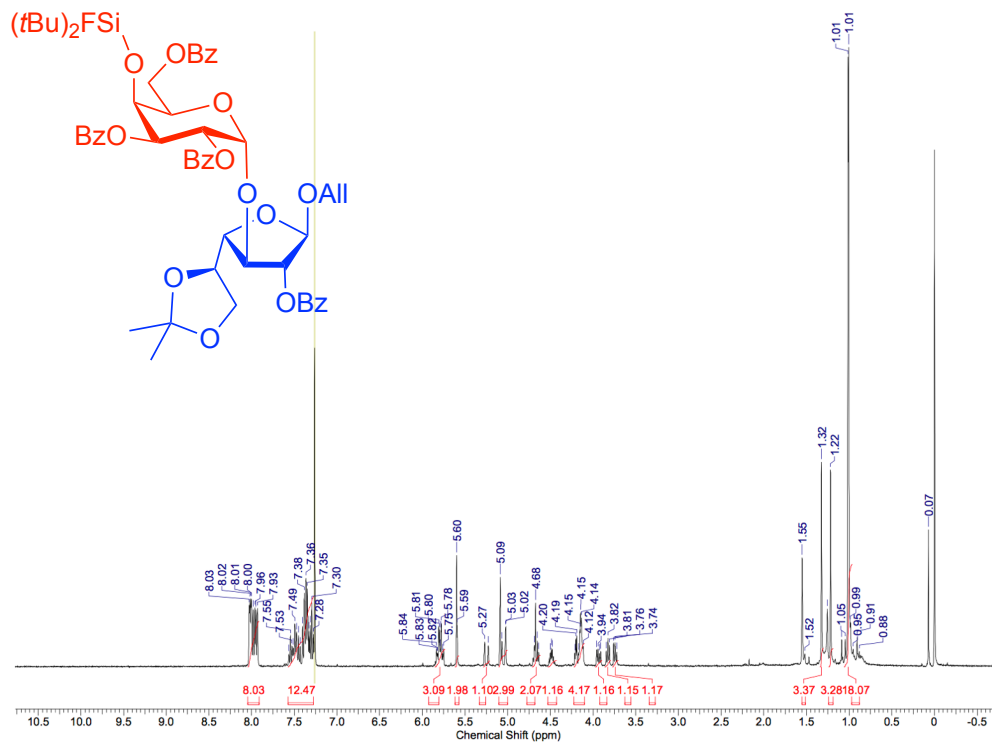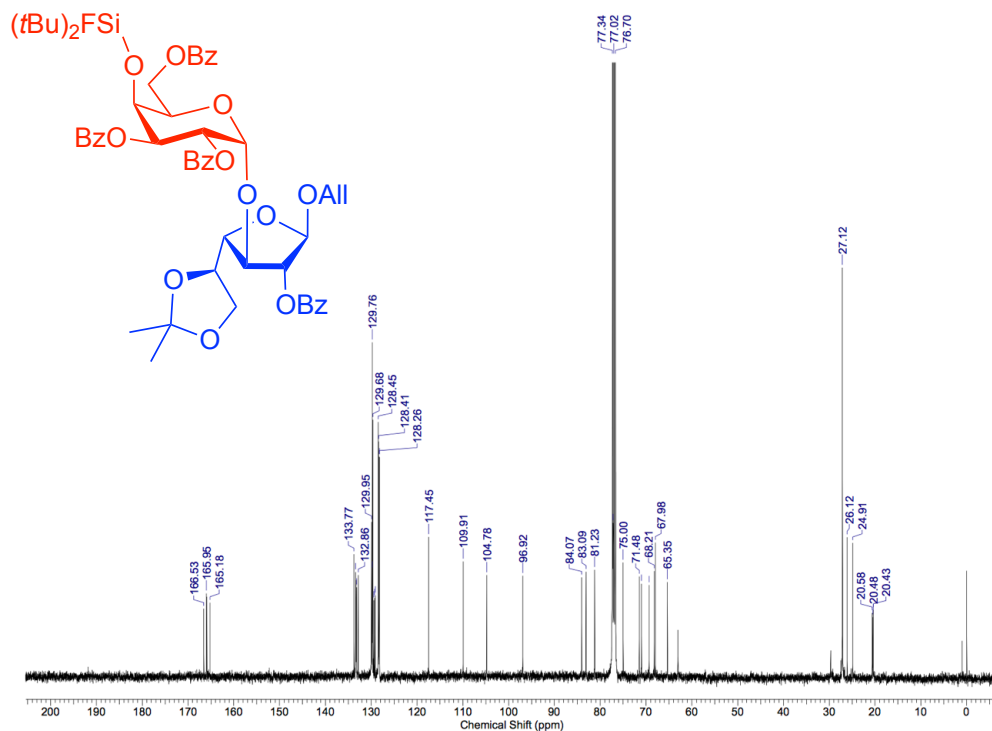
¹H NMR, 400 MHz, CDCl₃, compound (12)

¹³C NMR, 100 MHz, CDCl₃, compound (12)

141
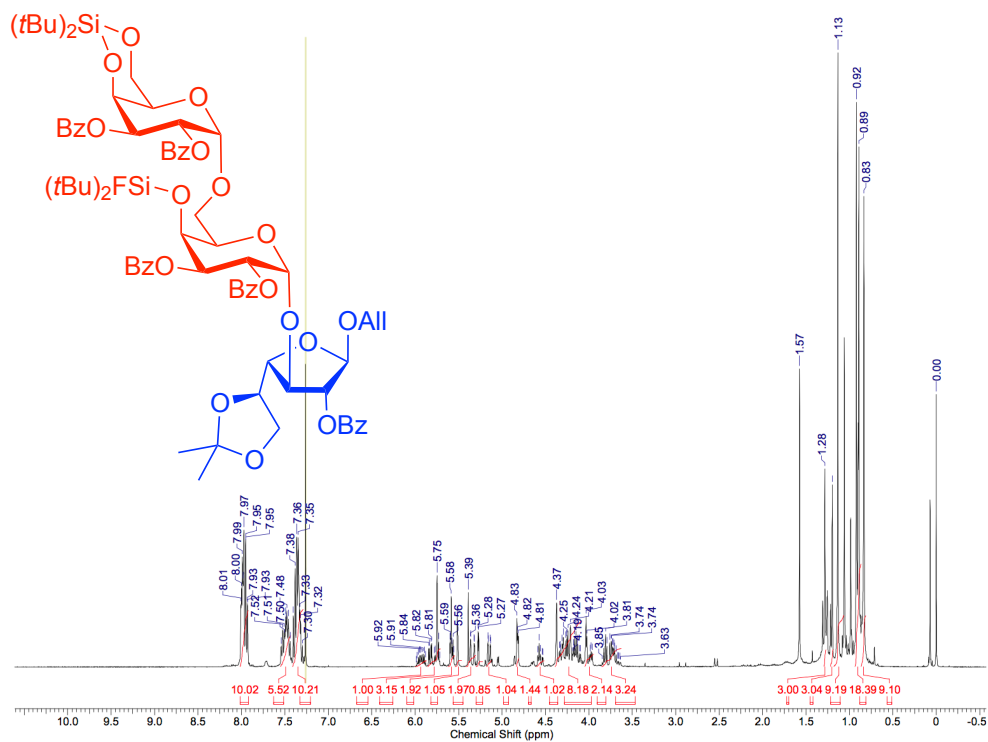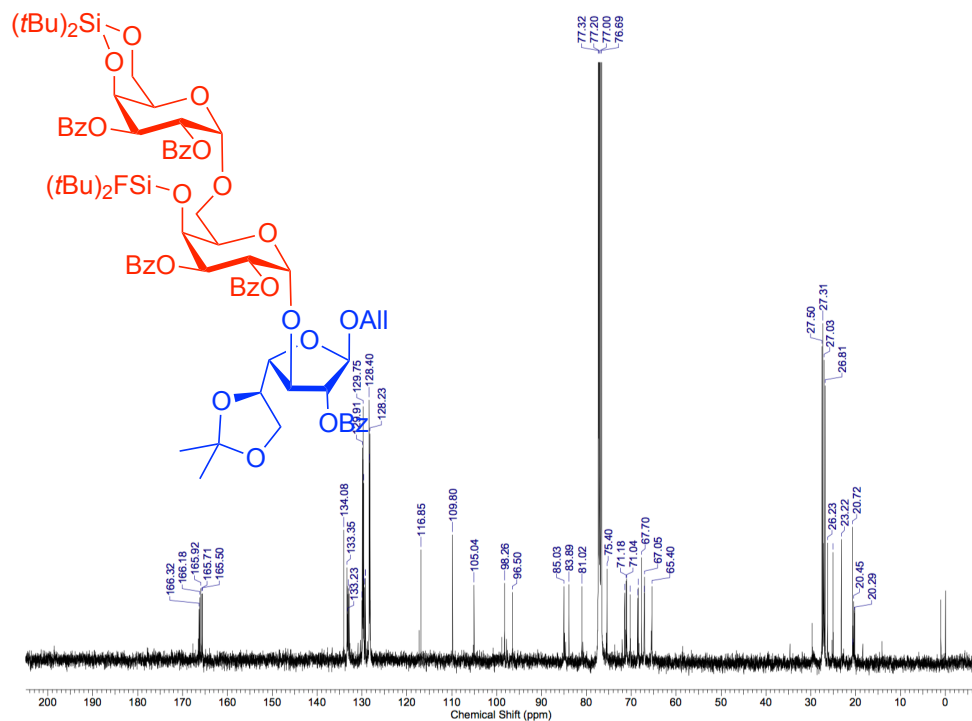
HSQC NMR, 400 MHz, CDCl₃, compound (12)

COSY NMR, 400 MHz, CDCl₃, compound (12)

142
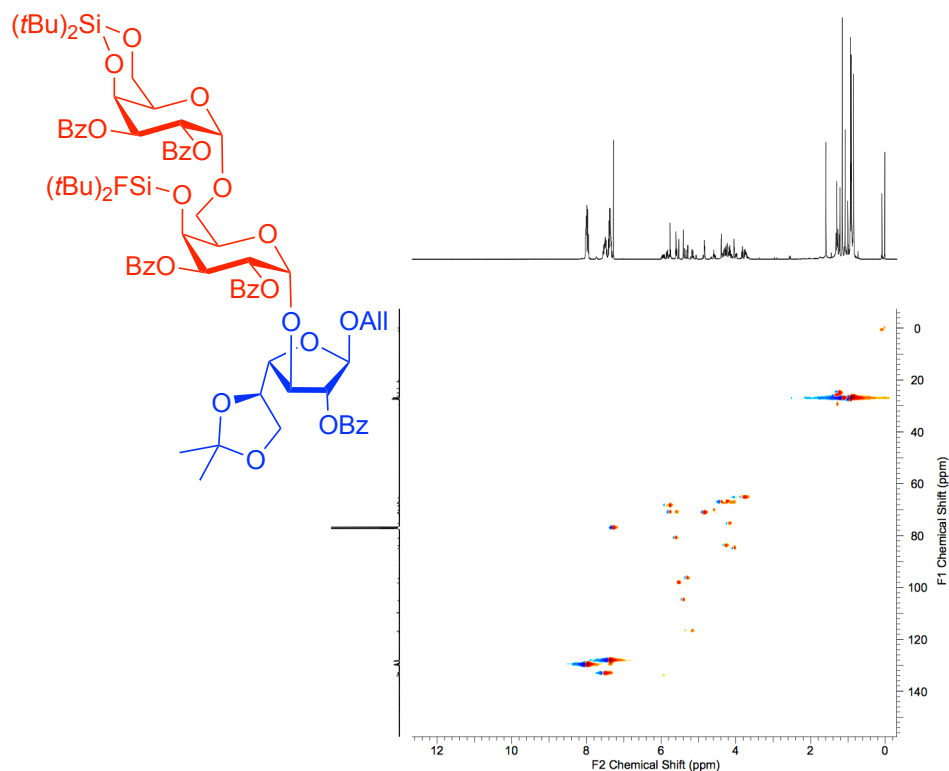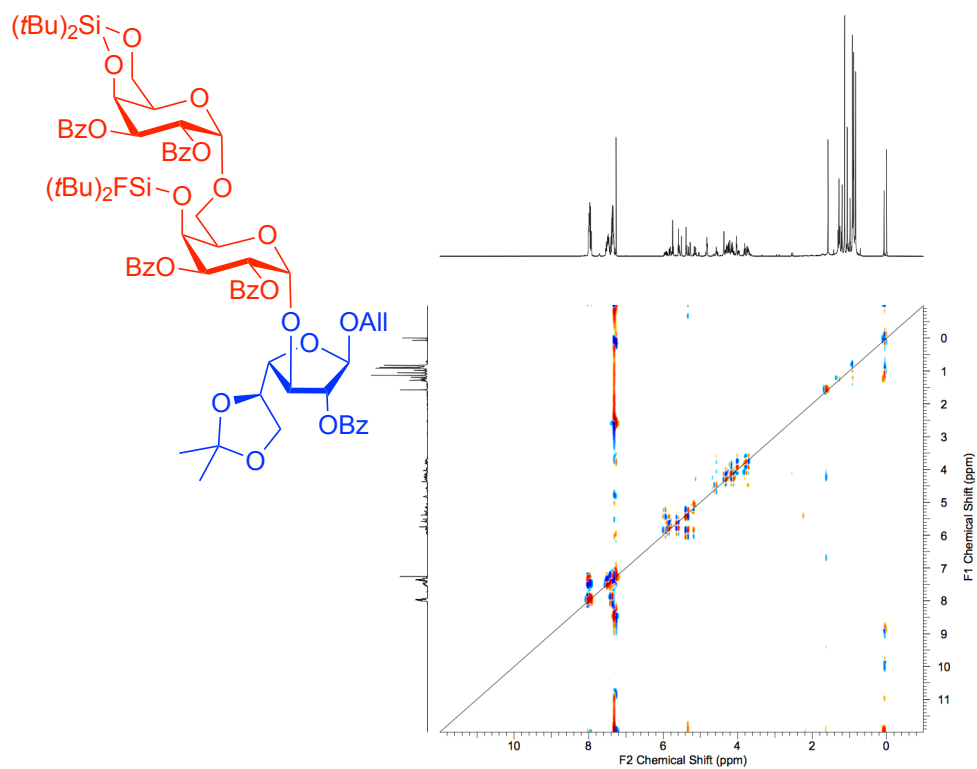
^{1}H NMR, 400 MHz, CDCl$_3$, compound (13)

^{13}C NMR, 100 MHz, CDCl$_3$, compound (13)

143
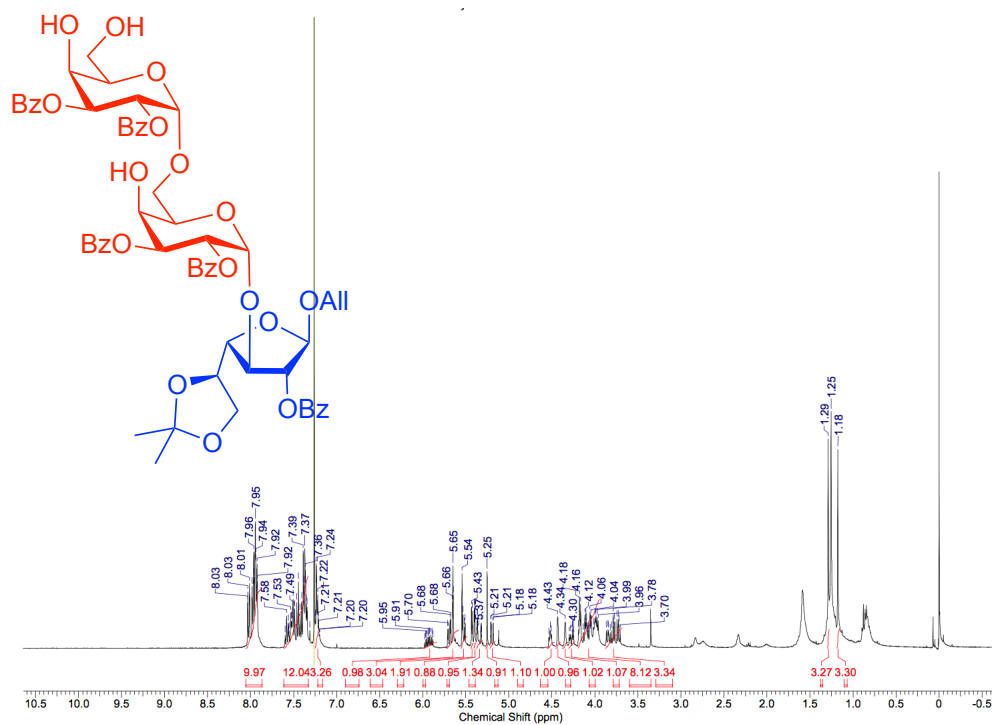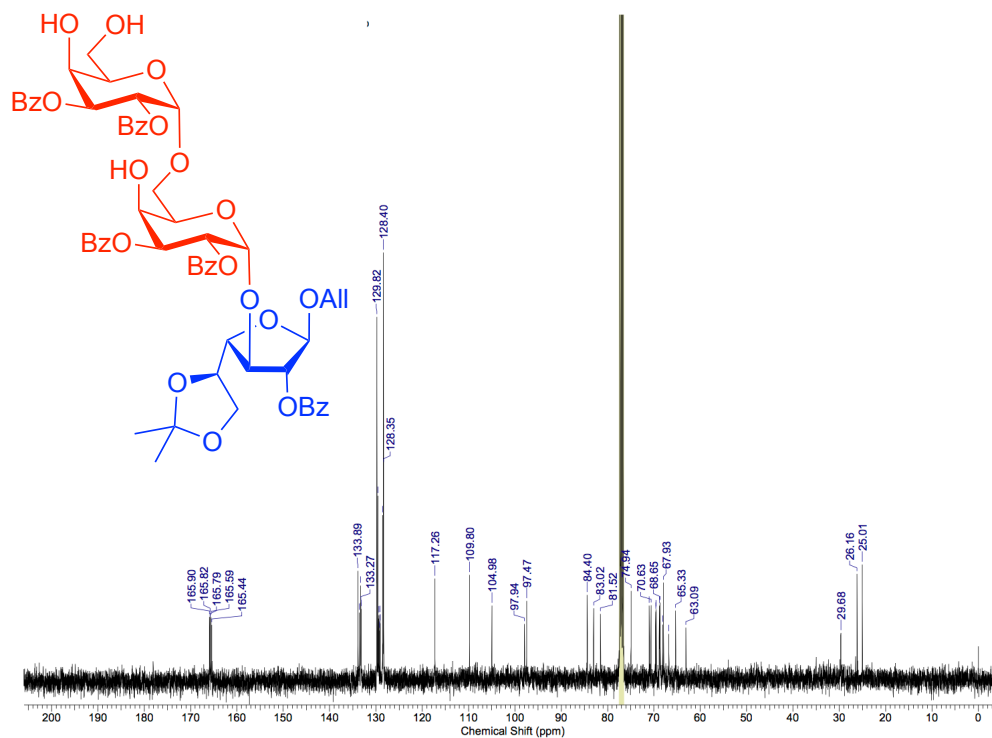
^{1}H NMR, 400 MHz, MeOD, compound (34)
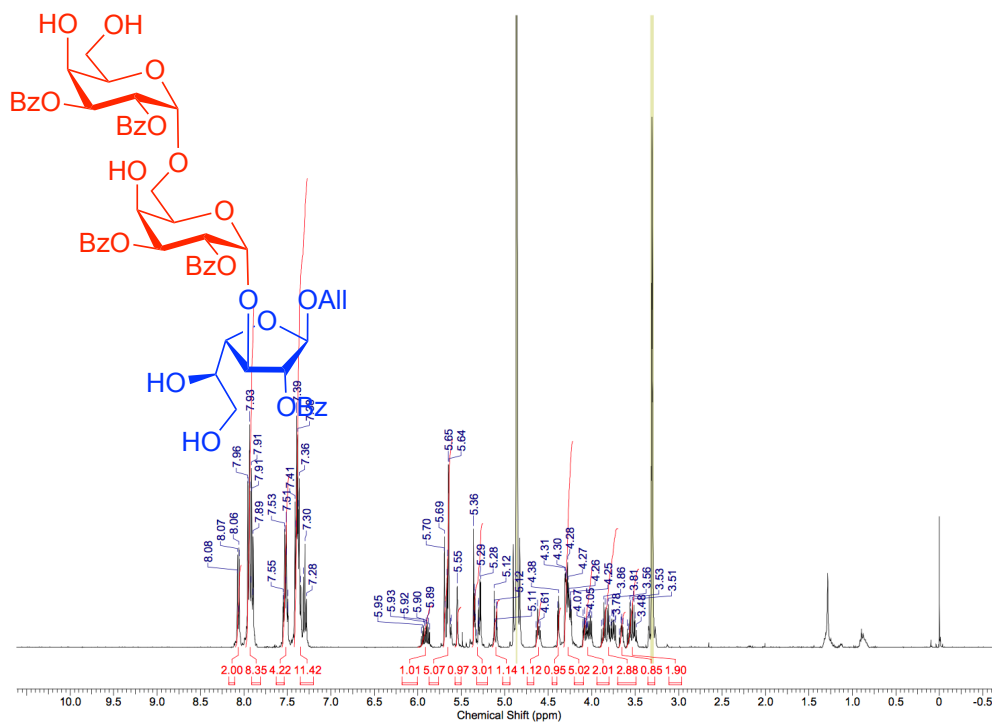
^{13}C NMR, 100 MHz, MeOD, compound (34)

144
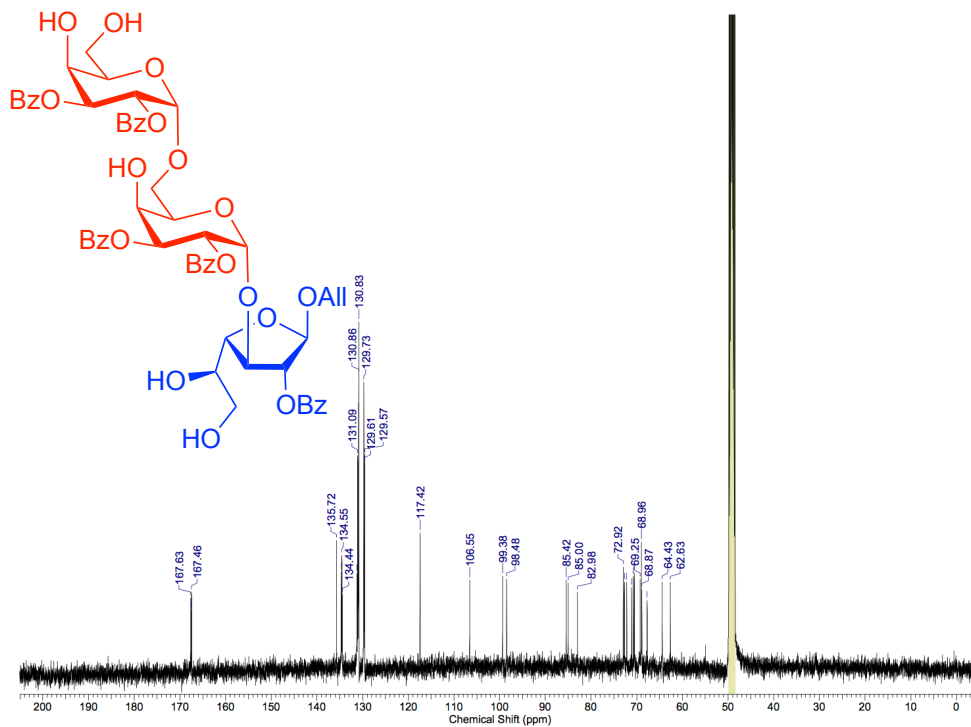
¹H NMR, 400 MHz, MeOD, compound (35)
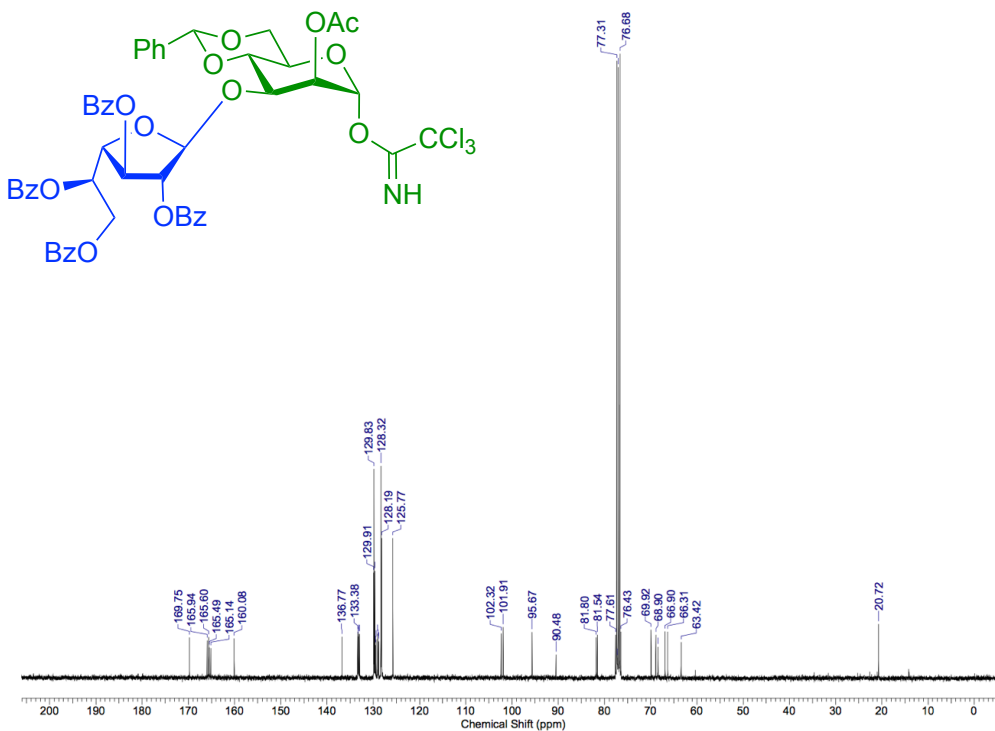

¹³C NMR, 100 MHz, MeOD, compound (35)
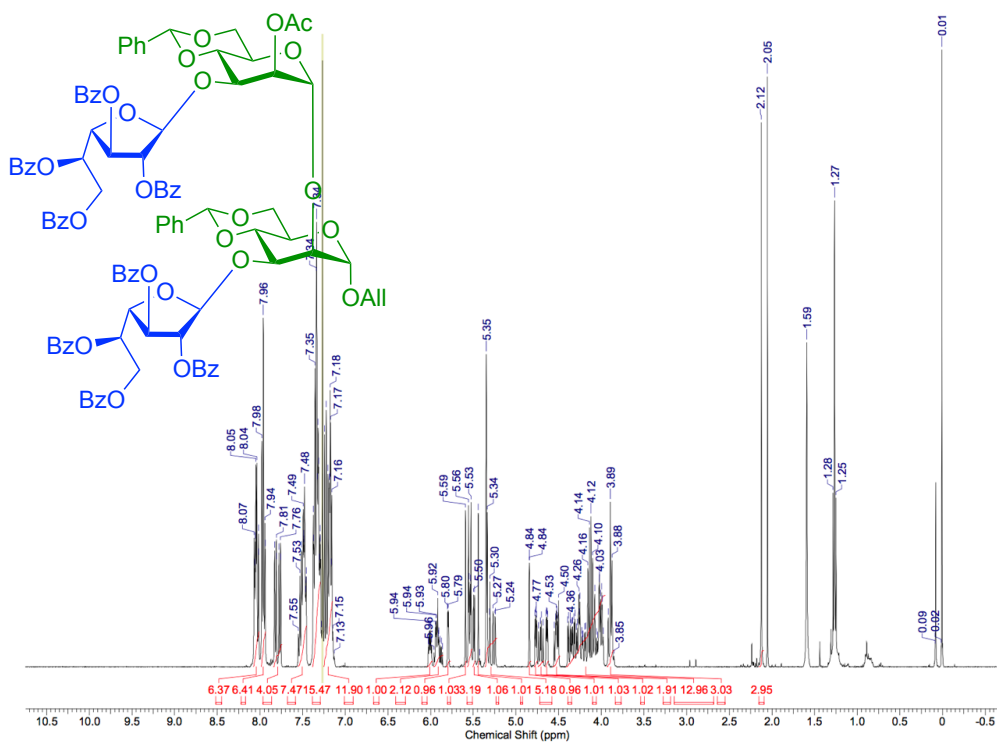

145
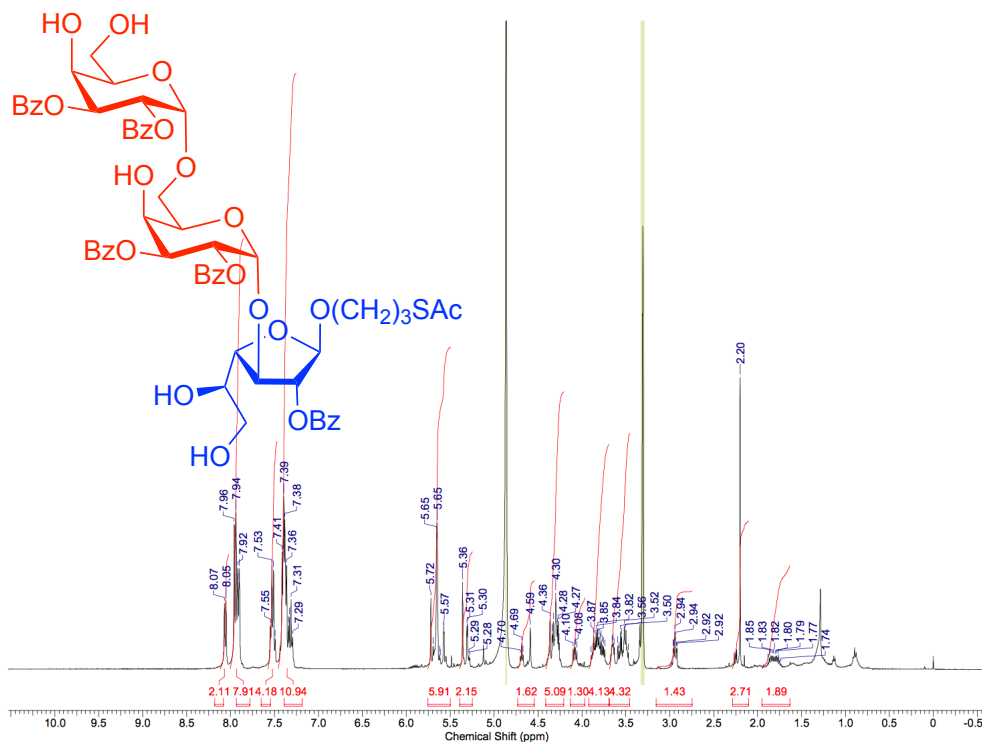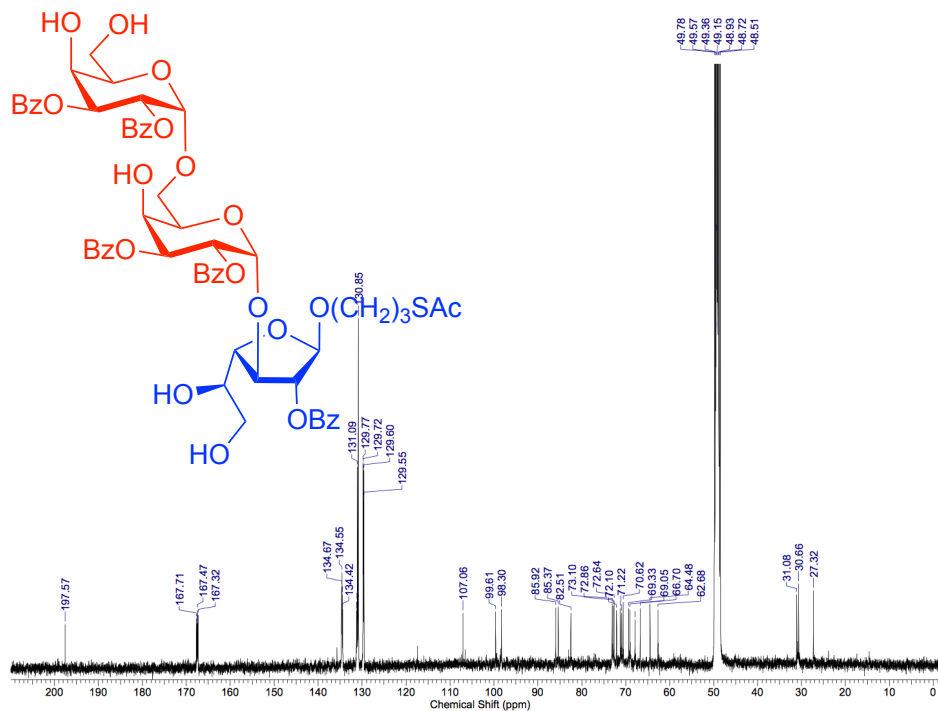
¹H NMR, 400 MHz, CDCl₃, compound (46)
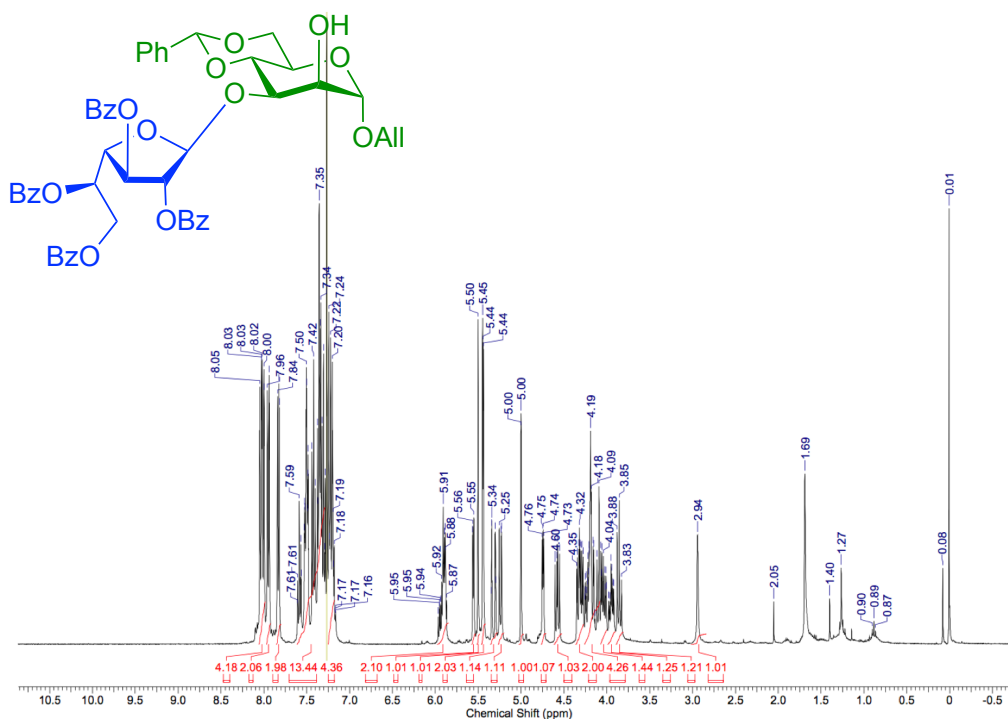
¹³C NMR, 100 MHz, CDCl₃, compound (46)

146
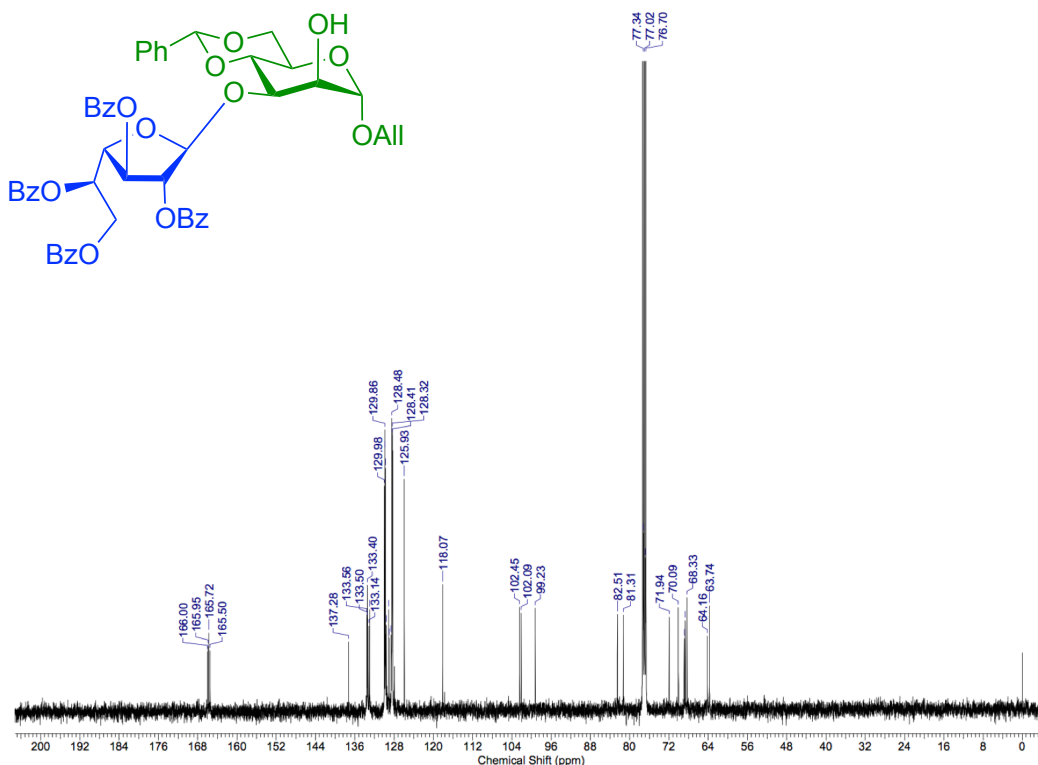
HSQC NMR, 400 MHz, CDCl₃, compound (46)

COSY NMR, 400 MHz, CDCl₃, compound (46)

147
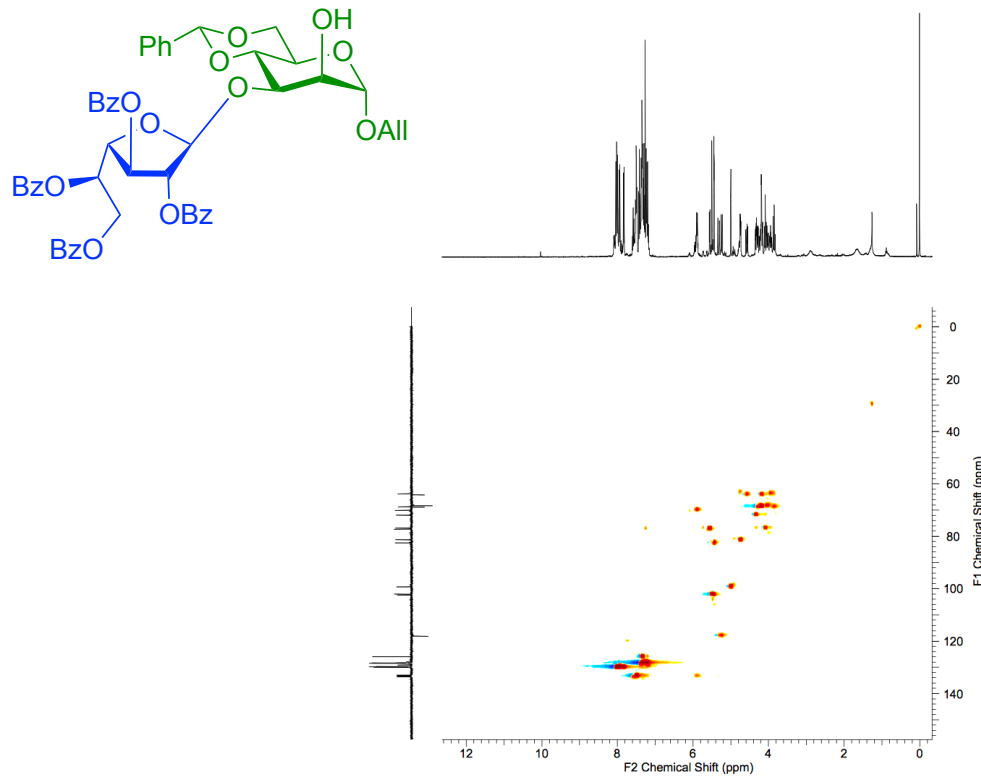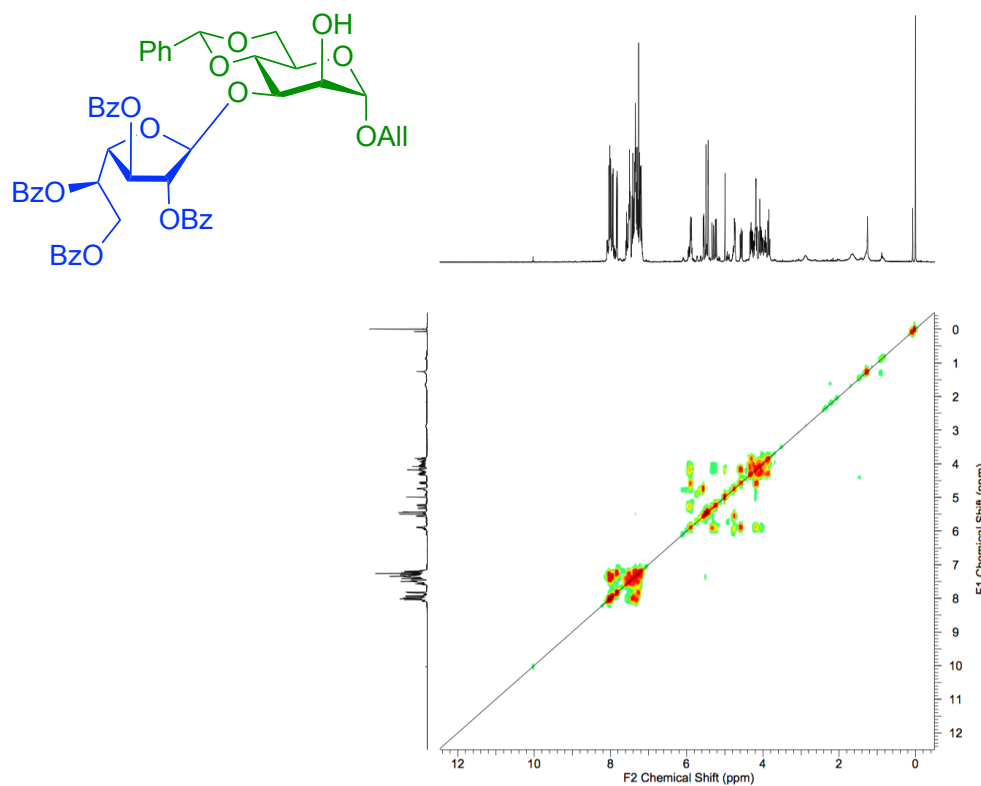
¹H NMR, 400 MHz, CDCl₃, compound (47)

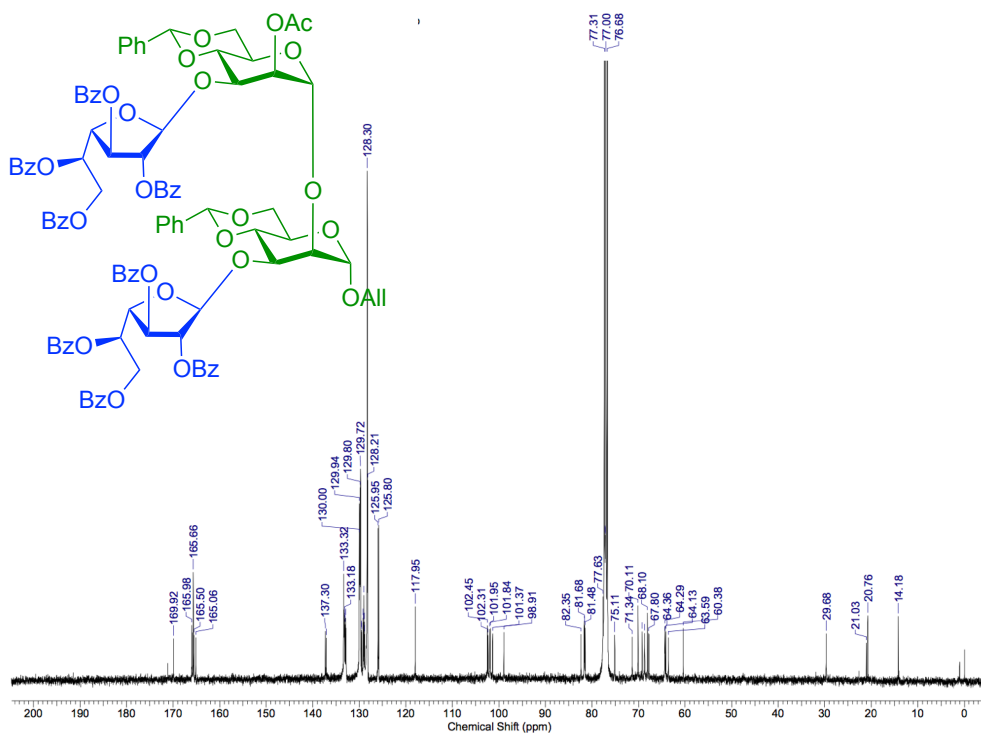**¹³C NMR, 100 MHz, CDCl₃, compound (47)**

148
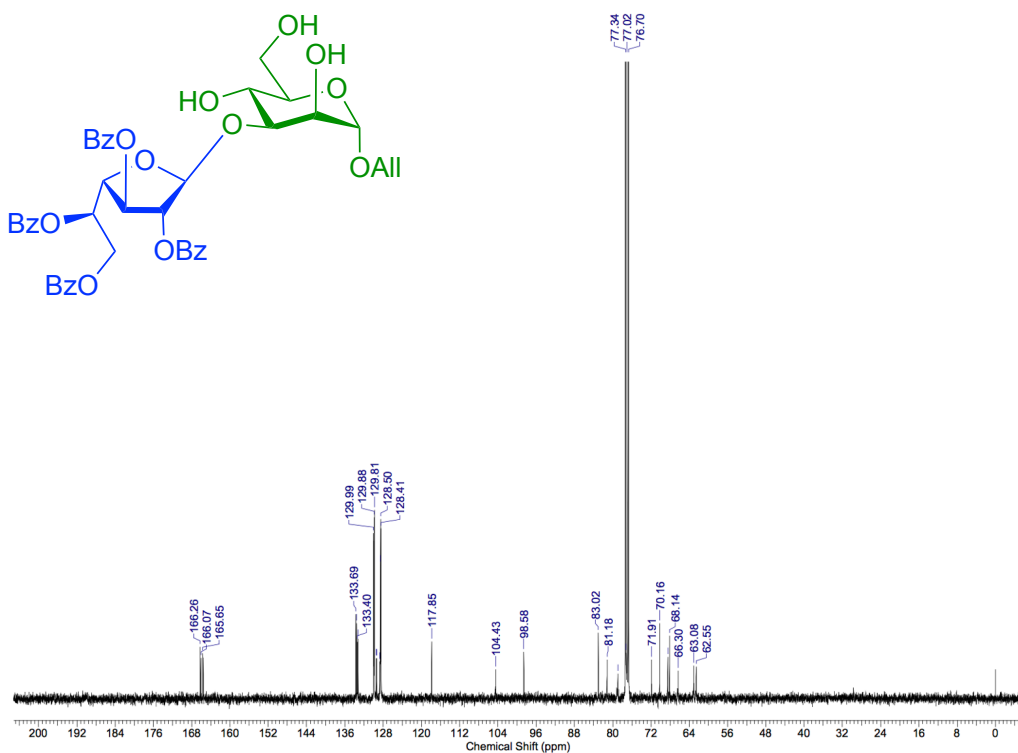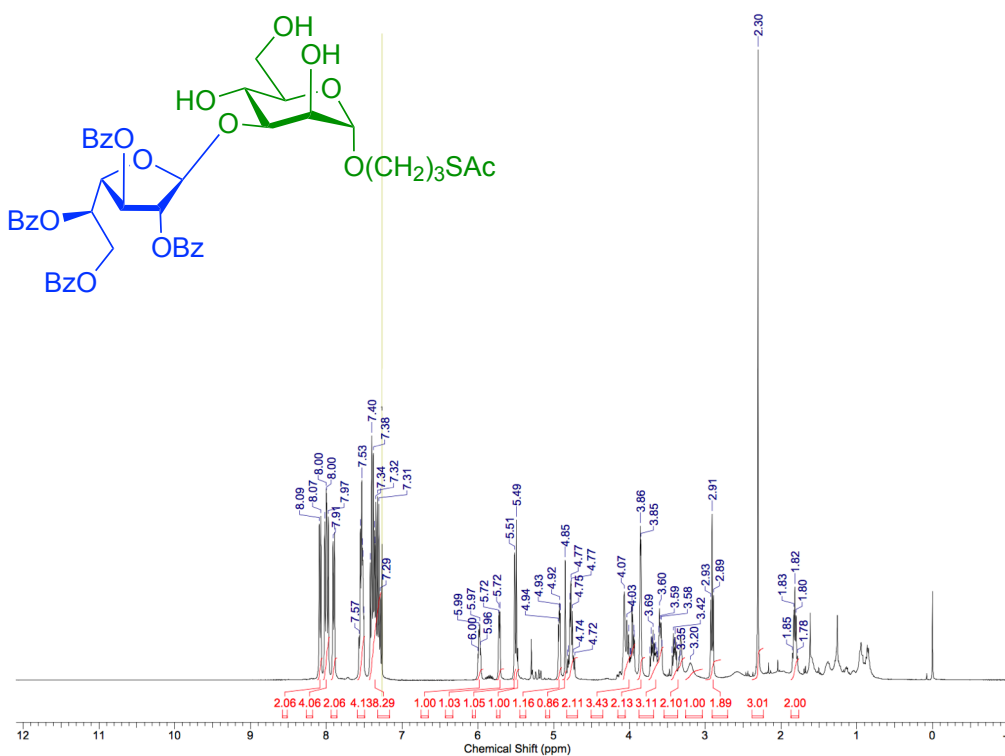
¹H NMR, 400 MHz, CDCl₃, compound (48)

¹H NMR, 400 MHz, CDCl₃, compound (48)

¹³C NMR, 100 MHz, CDCl₃, compound (48)

¹³C NMR, 100 MHz, CDCl₃, compound (48)

149
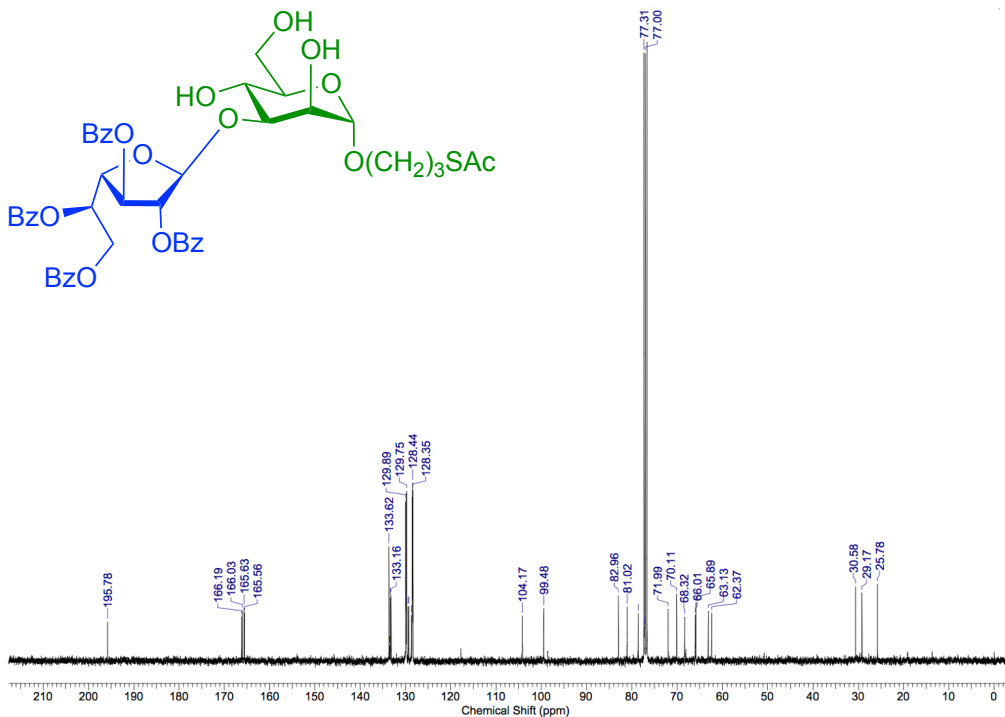
1H NMR, 400 MHz, CDCl₃, compound (5)

13C NMR, 100 MHz, CDCl₃, compound (5)

150
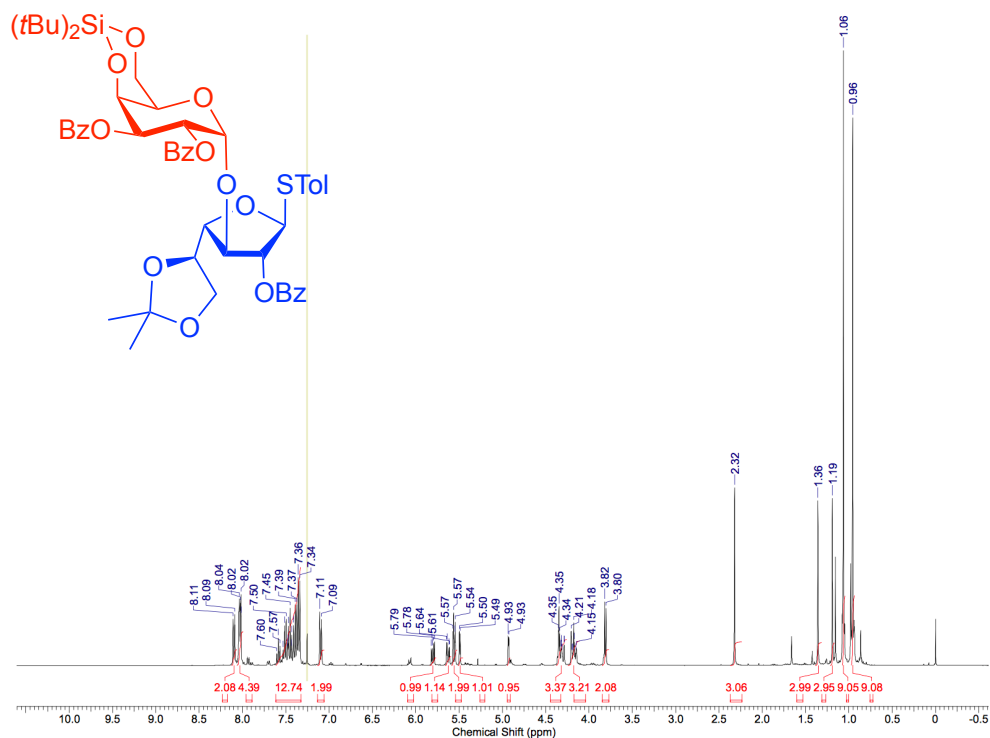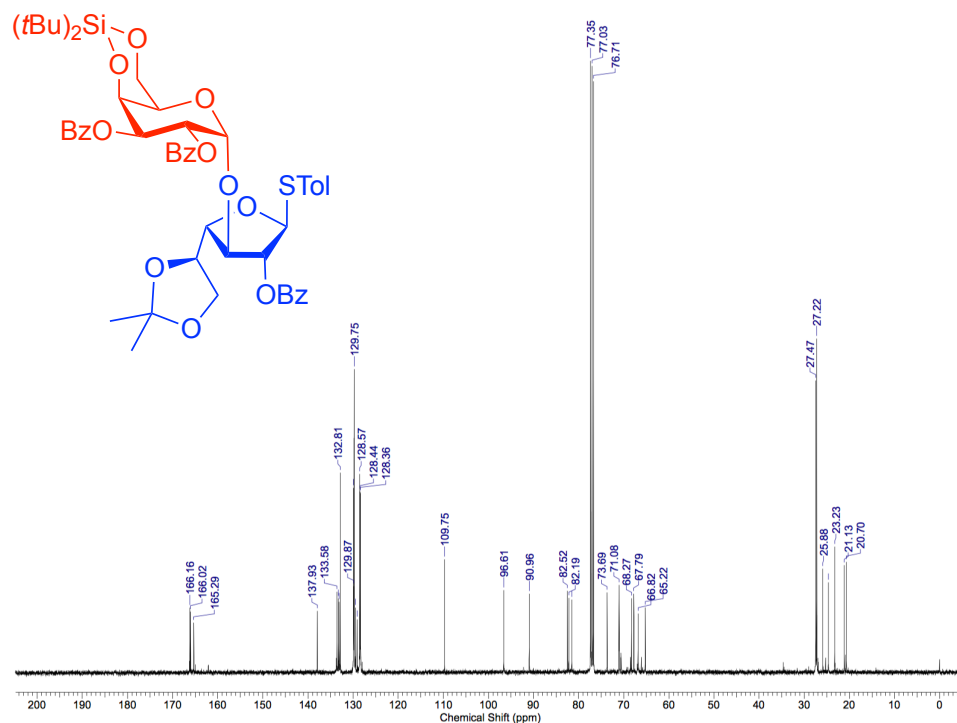
^{1}H NMR, 400 MHz, CDCl$_3$, compound (9)

^{13}C NMR, 100 MHz, CDCl$_3$, compound (9)

151
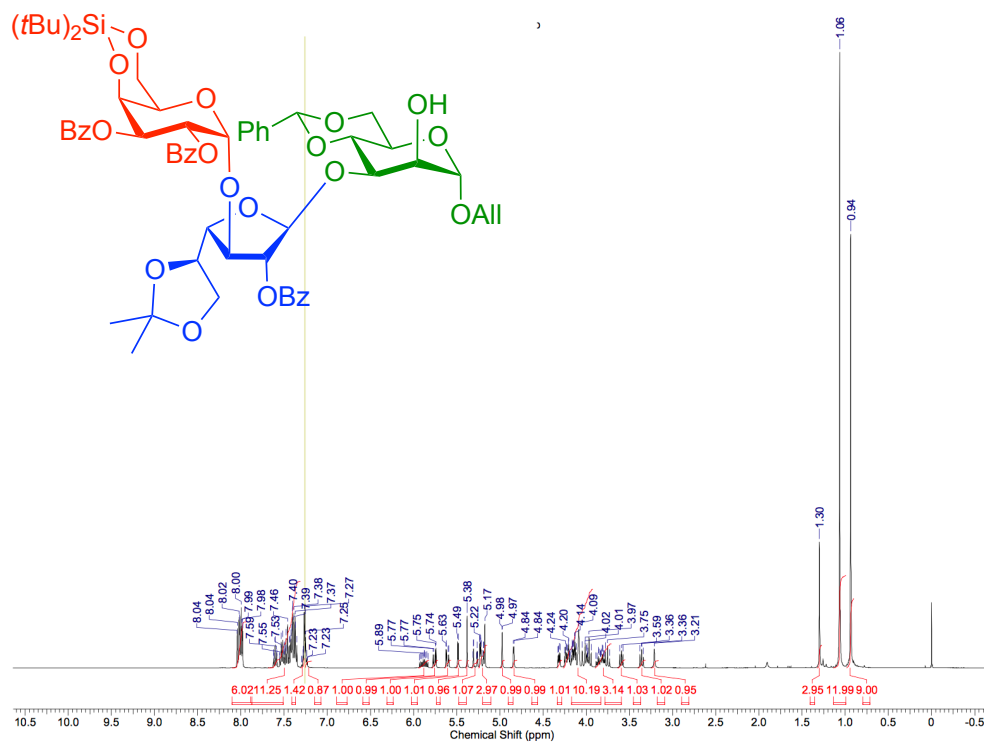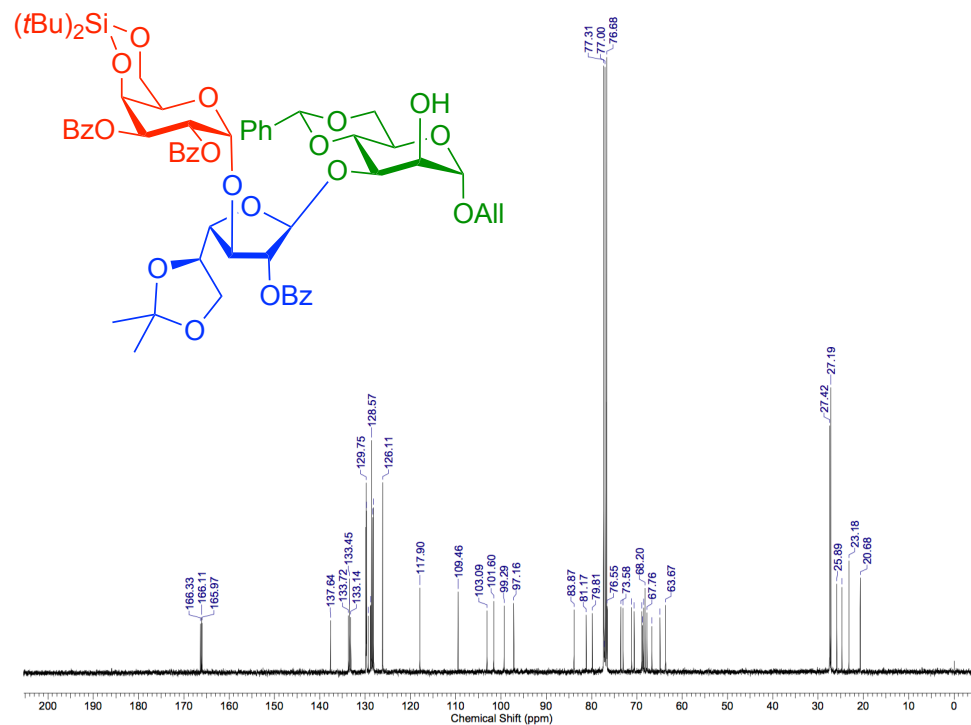
HSQC NMR, 400 MHz, CDCl₃, compound (9)

COSY NMR, 400 MHz, CDCl₃, compound (9)

152
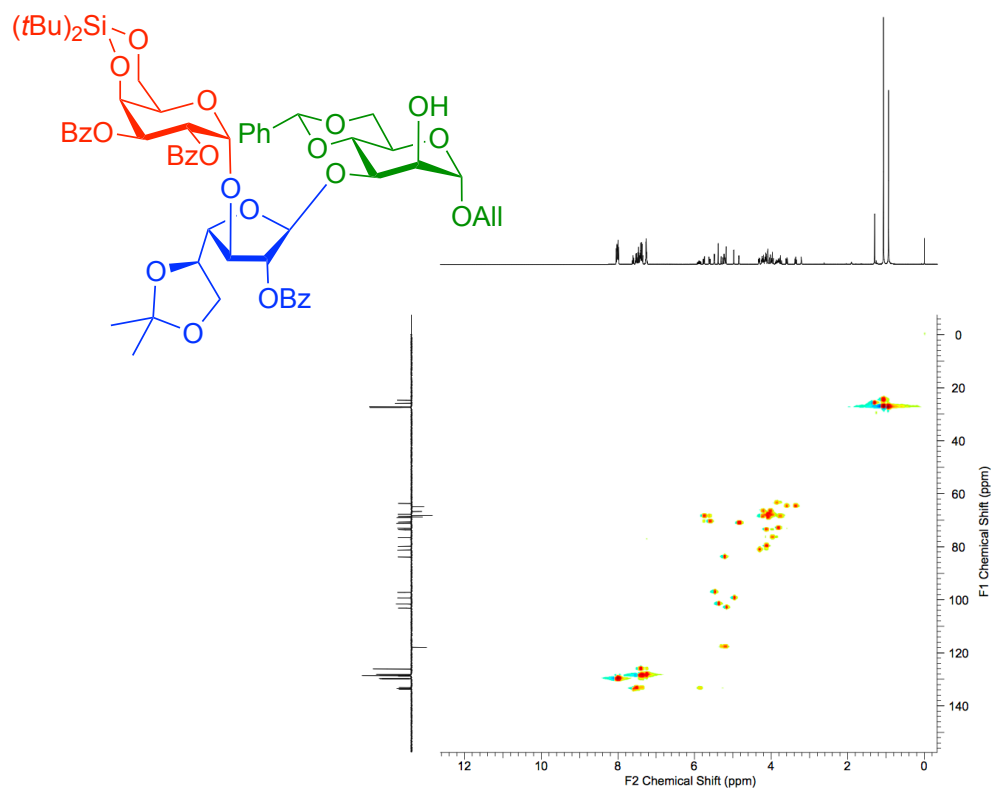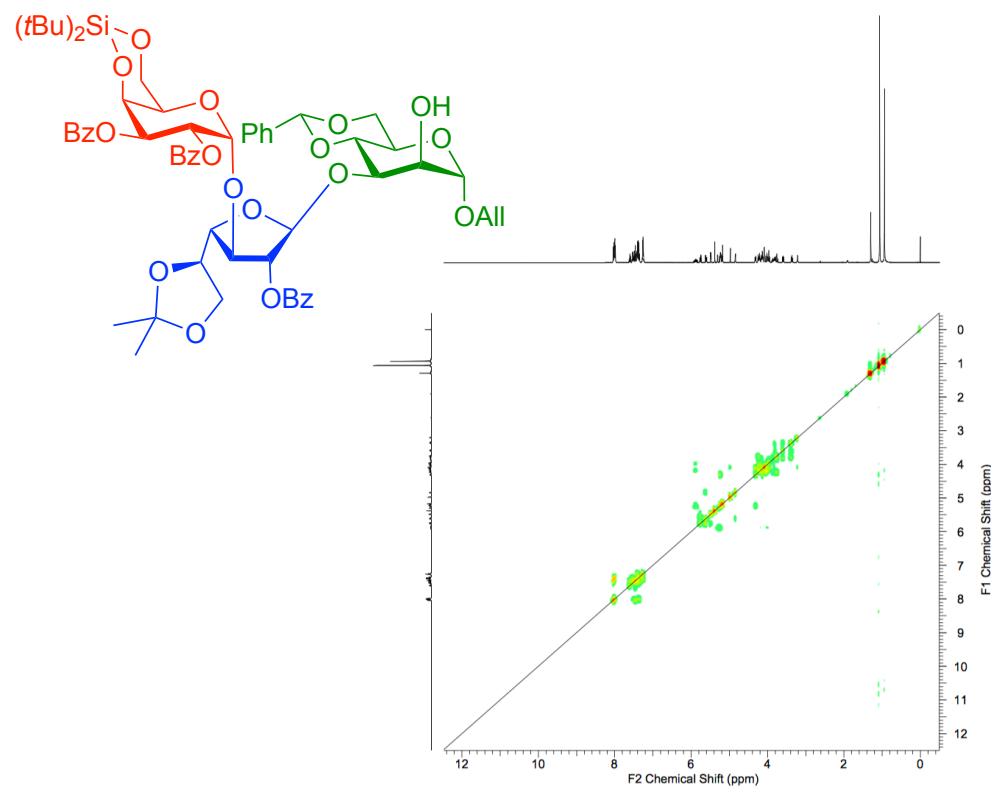
^{1}H NMR, 400 MHz, MeOD, compound (36)

^{13}C NMR, 100 MHz, MeOD, compound (36)

153
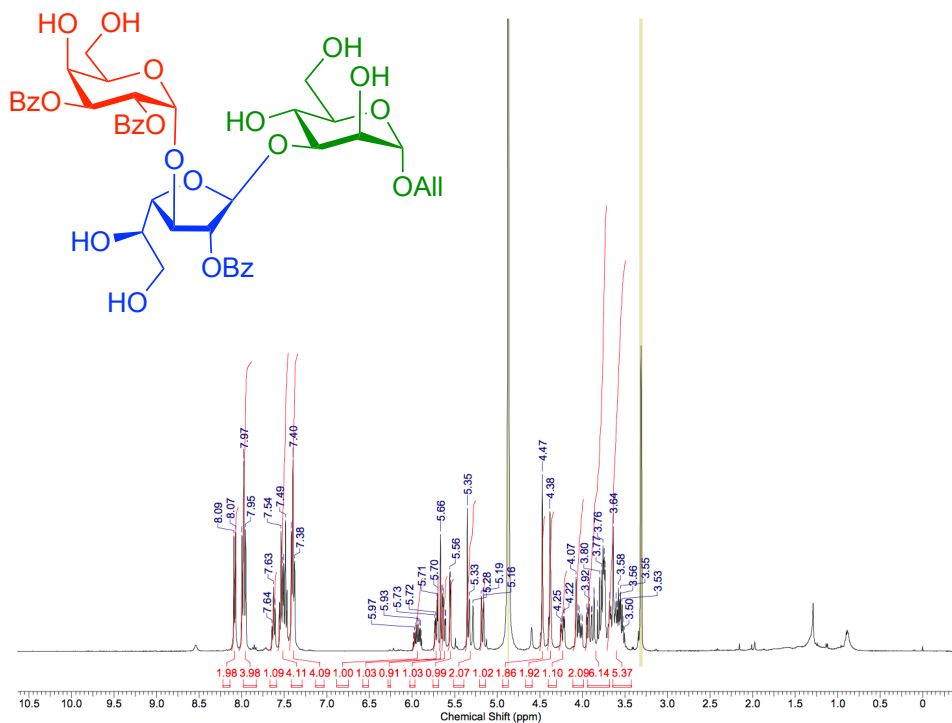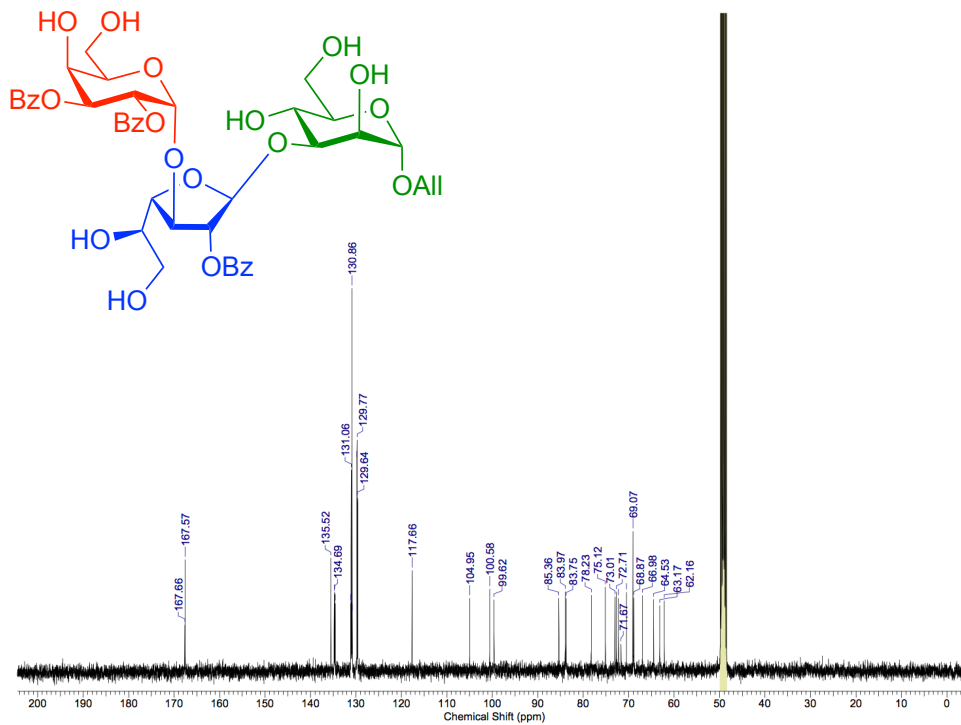
1H NMR, 400 MHz, MeOD, compound (37)

13C NMR, 100 MHz, MeOD, compound (37)

154
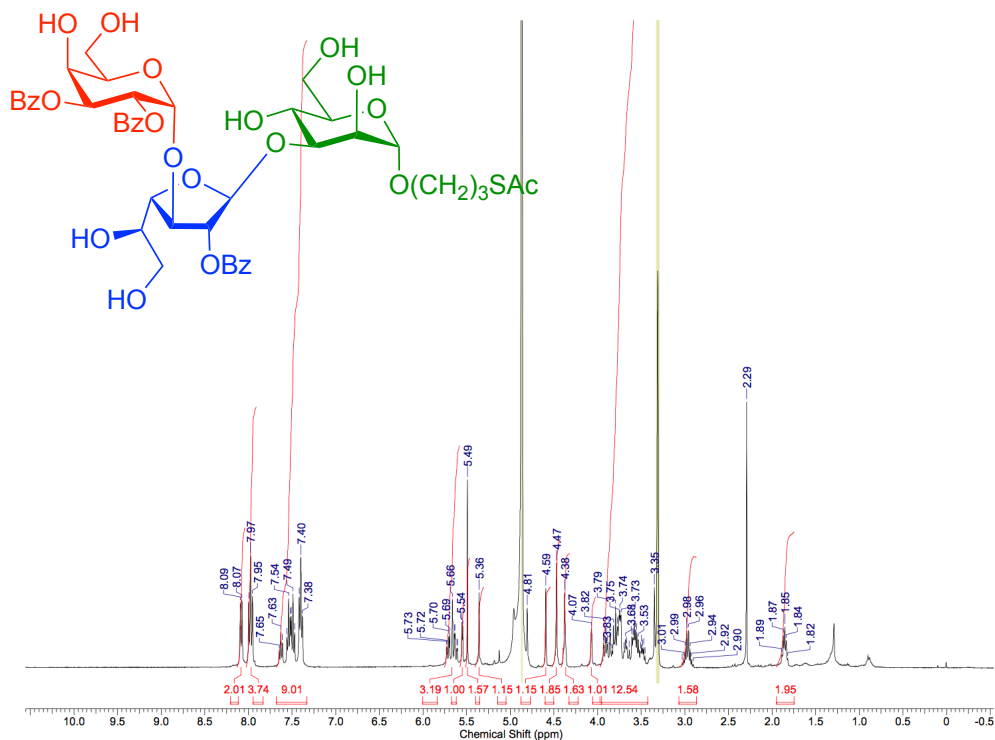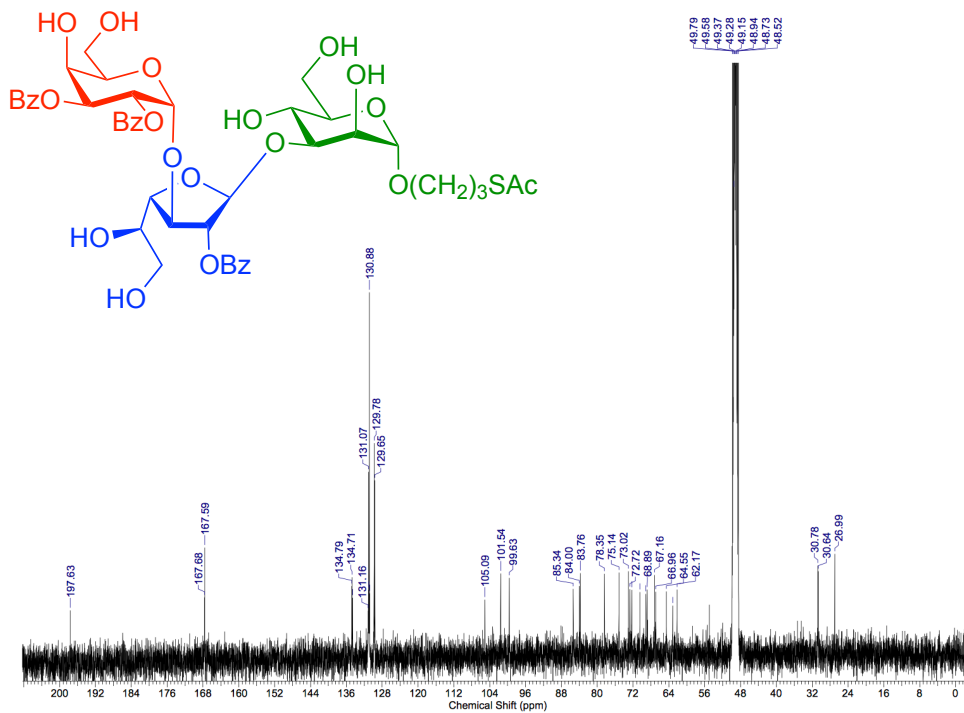
^{1}H NMR, 400 MHz, D$_2$O, compound (16)
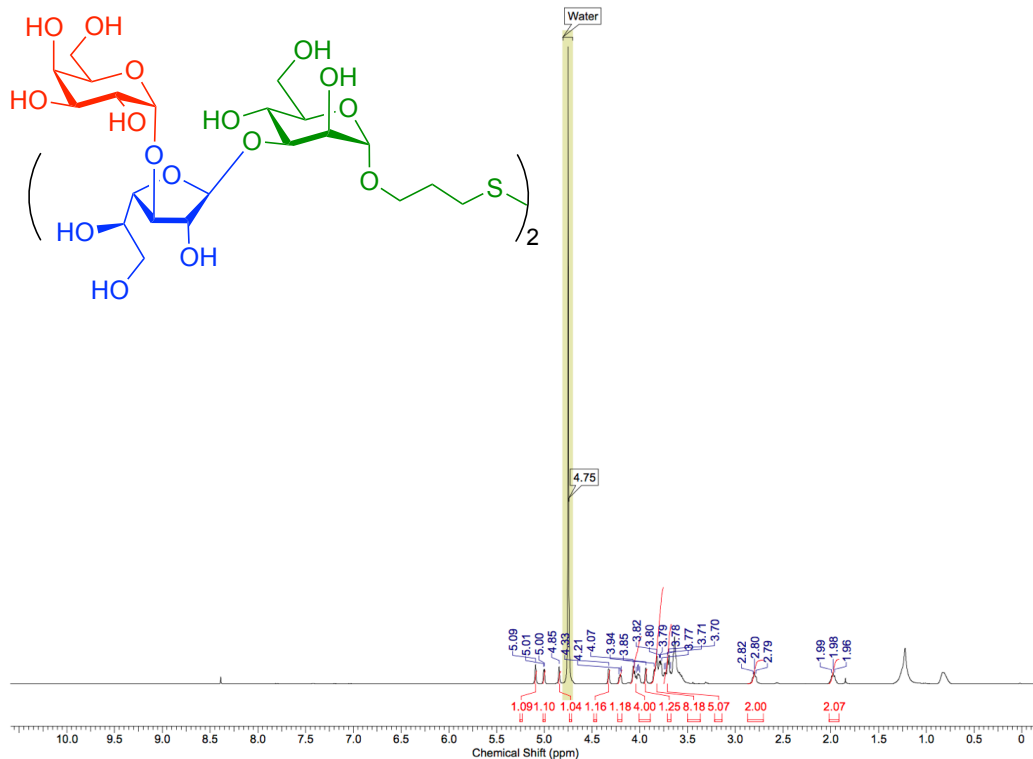
^{13}C NMR, 100 MHz, D$_2$O, compound (16)
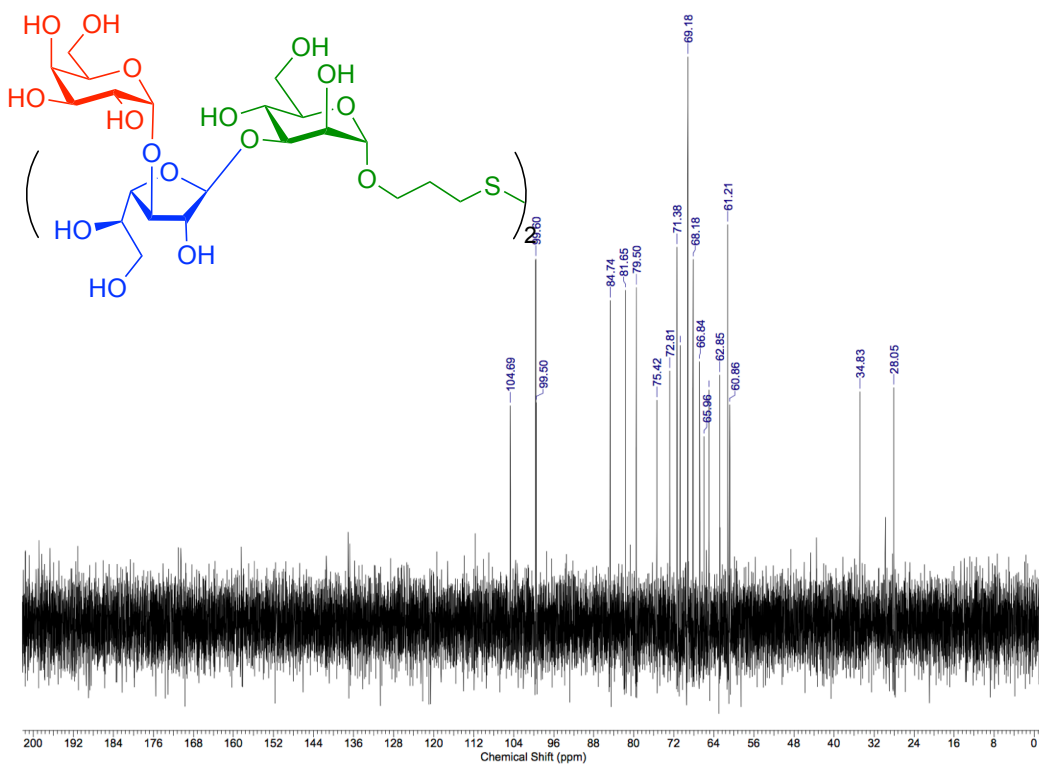
^{1}H NMR, 400 MHz, CDCl$_3$, compound (55)

^{13}C NMR, 100 MHz, CDCl$_3$, compound (55)

156
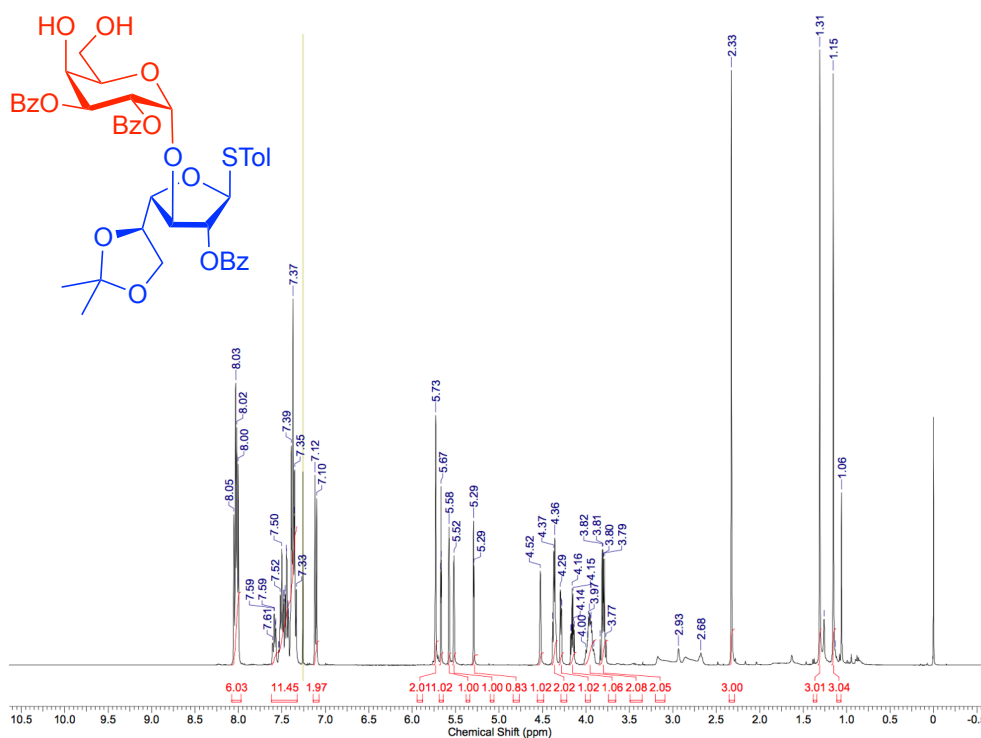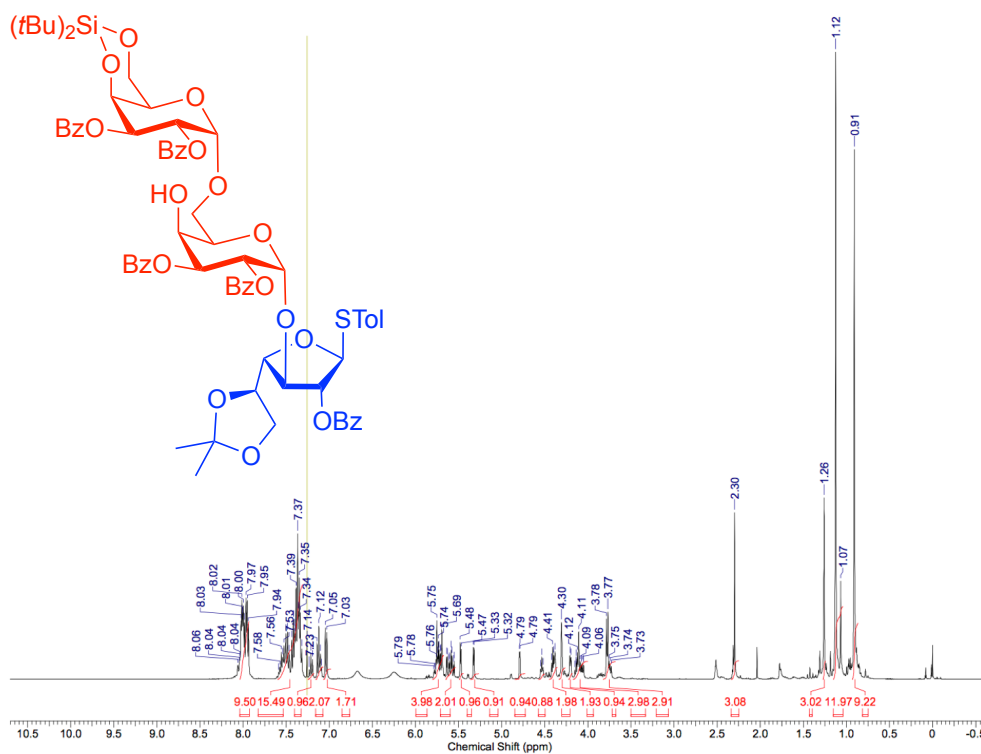
¹H NMR, 400 MHz, CDCl₃, compound (56)

^{1}H NMR, 400 MHz, CDCl$_3$, compound (56)

^{13}C NMR, 100 MHz, CDCl$_3$, compound (56)

157
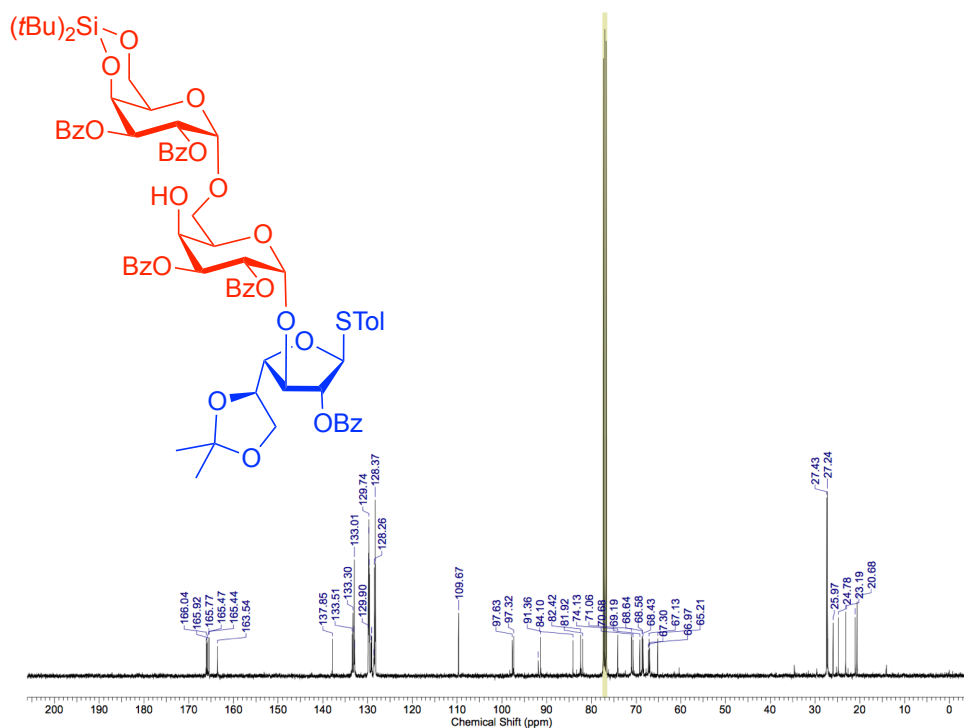
^{1}H NMR, 400 MHz, CDCl$_3$, compound (57)

^{13}C NMR, 100 MHz, CDCl$_3$, compound (57)

158
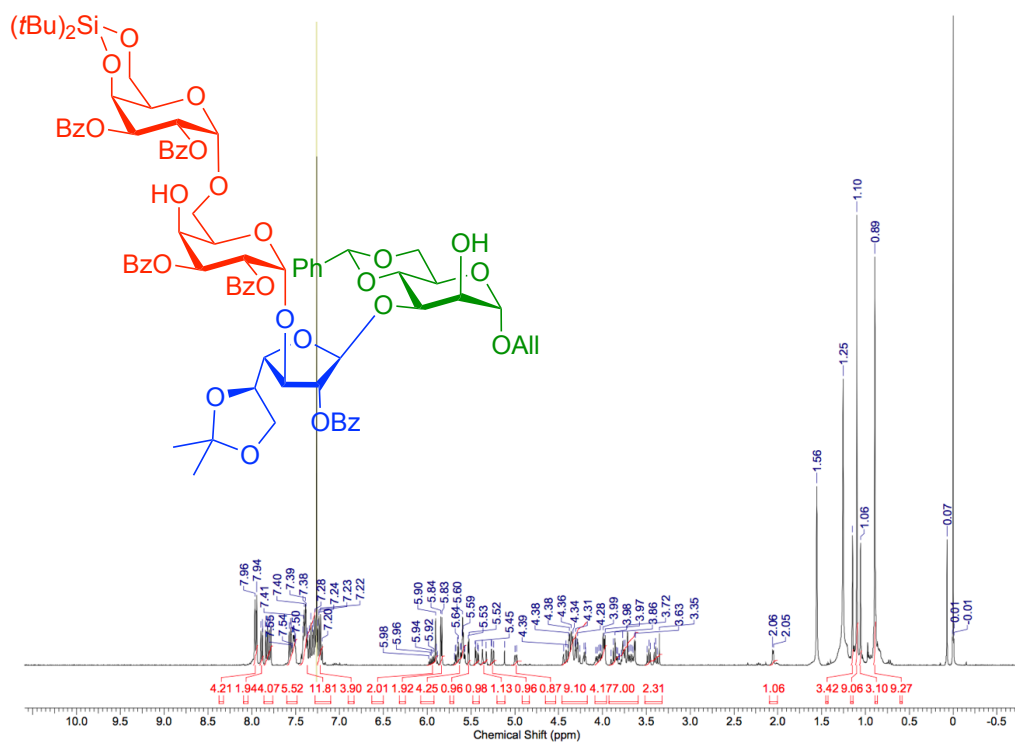
¹H NMR, 400 MHz, CDCl₃, compound (58)

¹³C NMR, 100 MHz, CDCl₃, compound (58)

159
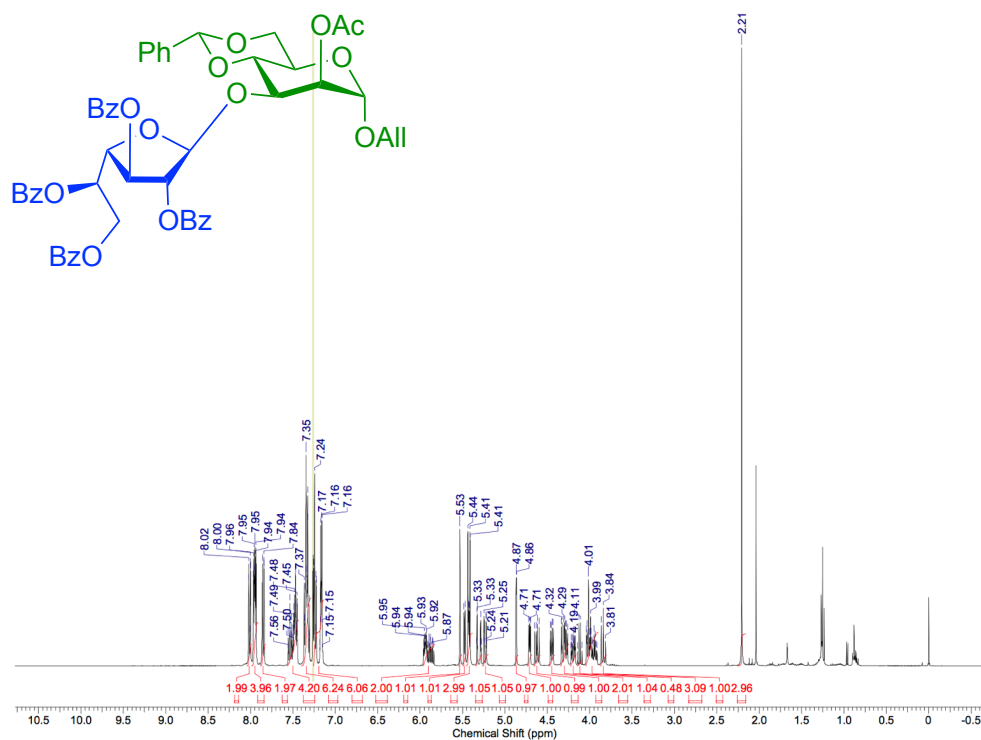
^{1}H NMR, 400 MHz, CDCl$_3$, compound (59)

^{13}C NMR, 100 MHz, CDCl$_3$, compound (59)

www.manaraa.com
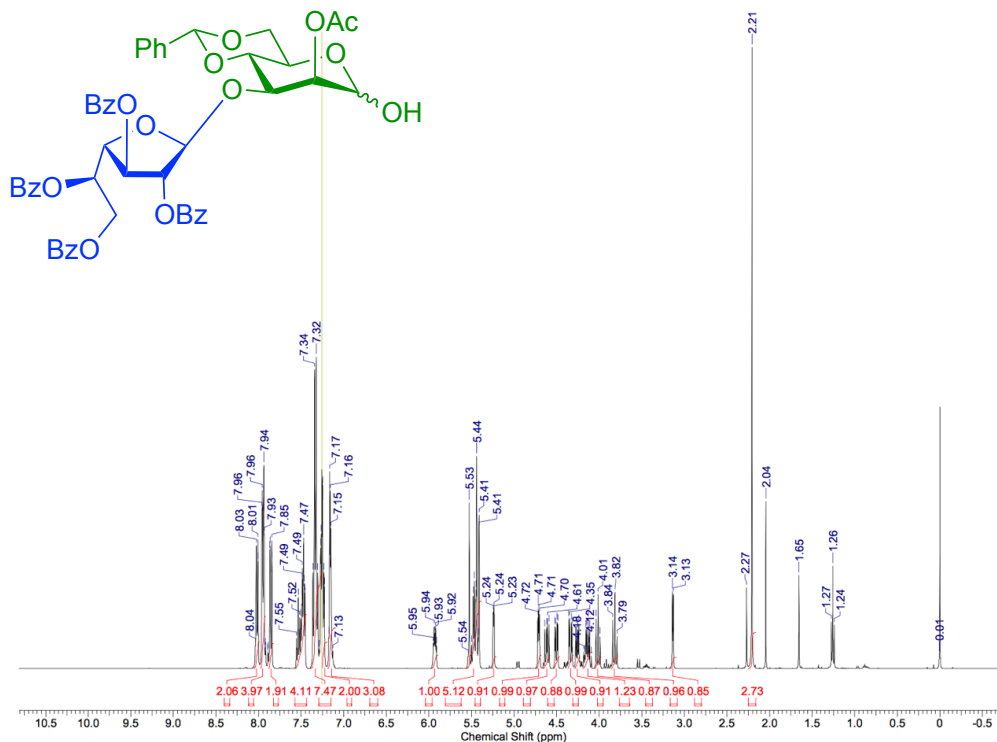
¹H NMR, 400 MHz, CDCl₃, compound (60)

¹³C NMR, 100 MHz, CDCl₃, compound (60)

161

162

ESI-TOF HR mass spectrum of compound (1)

m/z [M+Na]$^+$ calc.: 387.1420
m/z [M+Na]$^+$ exp.: 387.1346

ESI-TOF HR mass spectrum of compound (8)
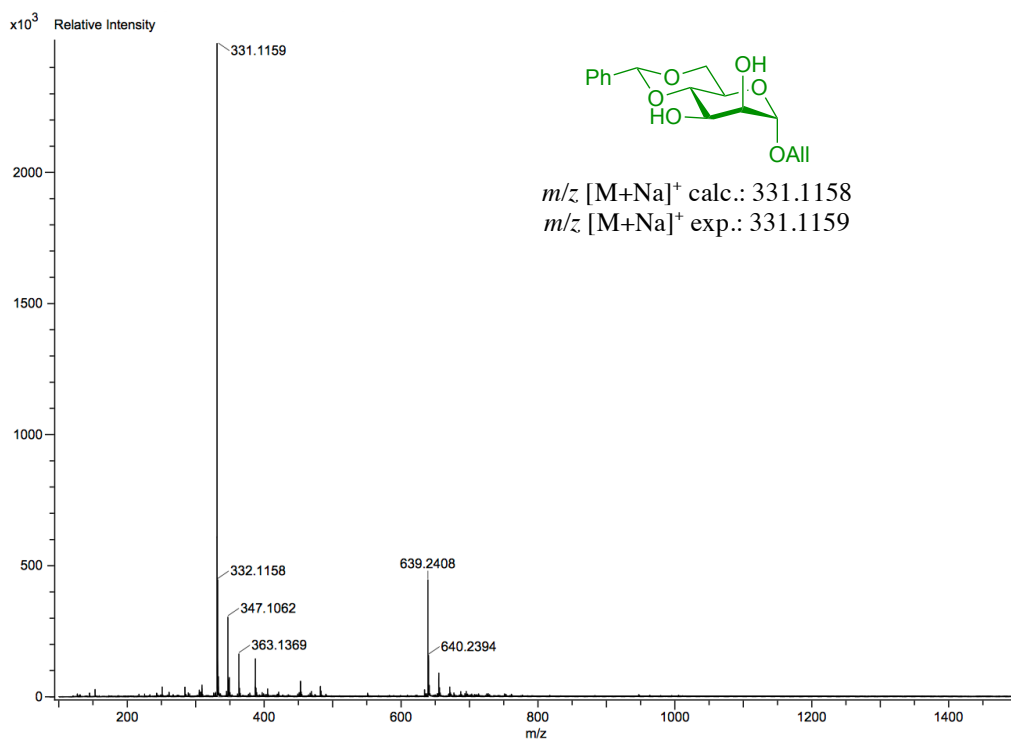
m/z [M+Na]$^+$ calc.: 331.1158
m/z [M+Na]$^+$ exp.: 331.1159

163

ESI-TOF HR mass spectrum of compound (28)
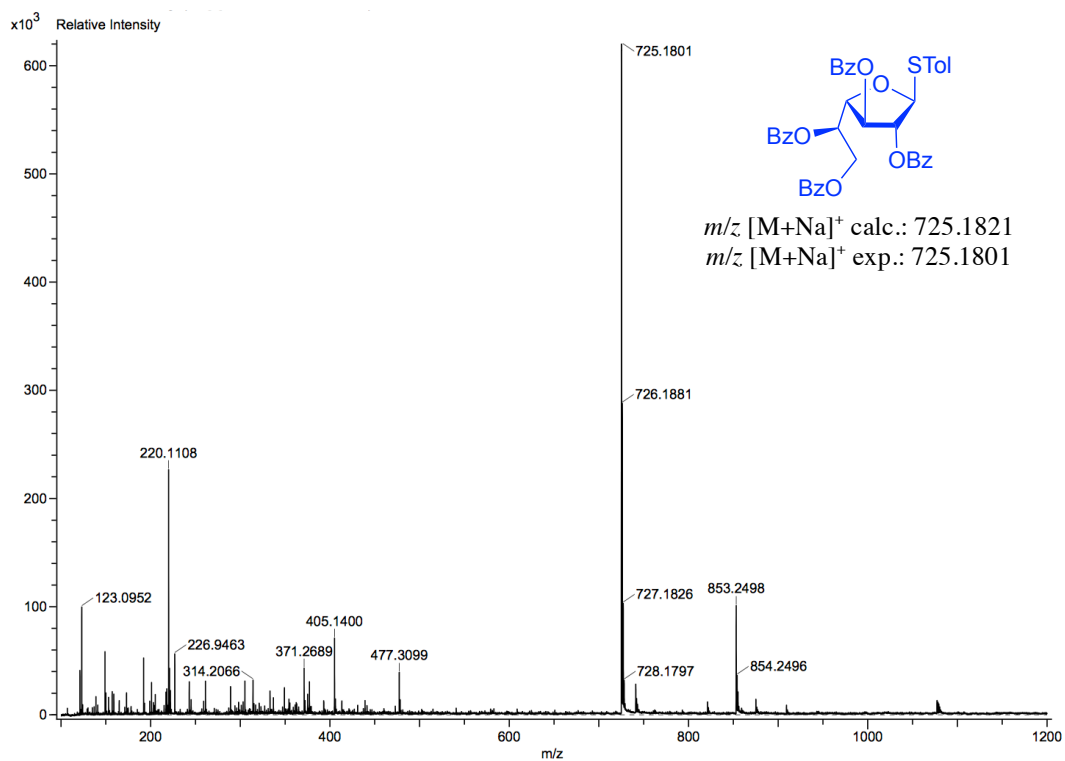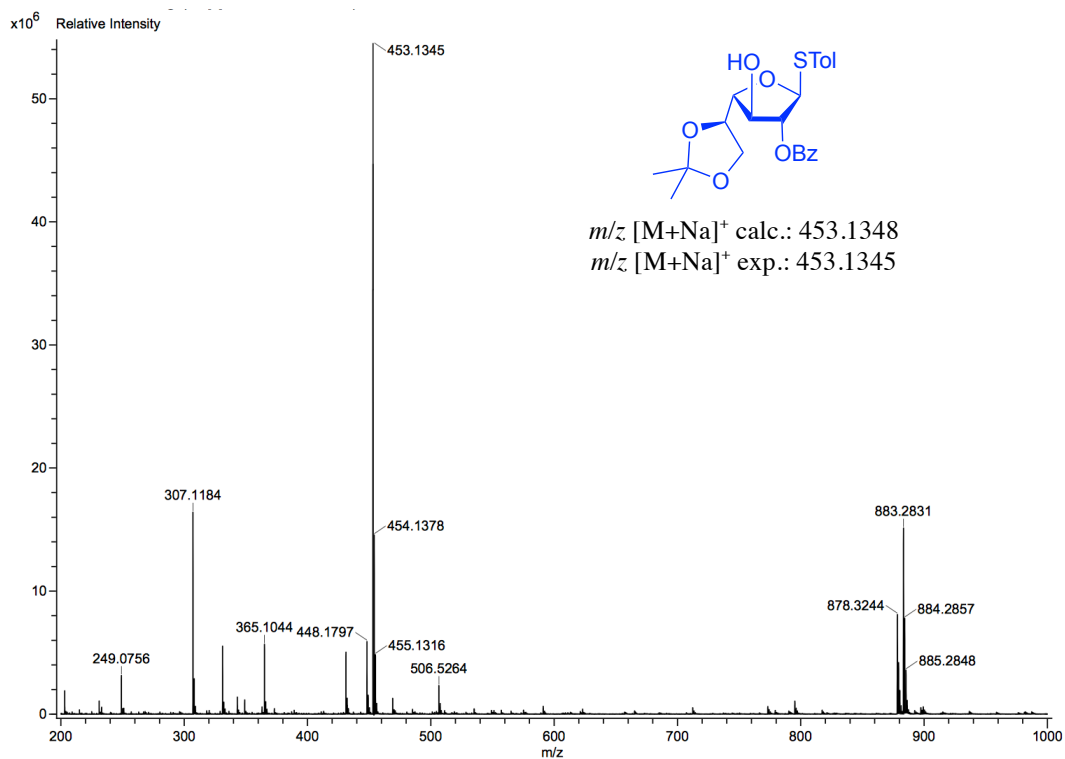
m/z [M+Na]⁺ calc.: 725.1821
m/z [M+Na]⁺ exp.: 725.1801

ESI-TOF HR mass spectrum of compound (2)

m/z [M+Na]⁺ calc.: 453.1348
m/z [M+Na]⁺ exp.: 453.1345

164

ESI-TOF HR mass spectrum of compound (3)

m/z [M+Na]+ calc.: 694.1173
m/z [M+Na]+ exp.: 694.1167

ESI-TOF HR mass spectrum of compound (4)

m/z [M+Na]+ calc.: 897.3474
m/z [M+Na]+ exp.: 897.3474

165

www.manaraa.com

ESI-TOF HR mass spectrum of compound (33)

m/z [M+Na]$^+$ calc.: 757.2472
m/z [M+Na]$^+$ exp.: 757.2470

ESI-TOF HR mass spectrum of compound (6)

m/z [M+Na]$^+$ calc.: 717.2159
m/z [M+Na]$^+$ exp.: 717.2158

166

ESI-TOF HR mass spectrum of compound (7)

m/z [M+Na]$^+$ calc.: 793.2142
m/z [M+Na]$^+$ exp.: 793.2147
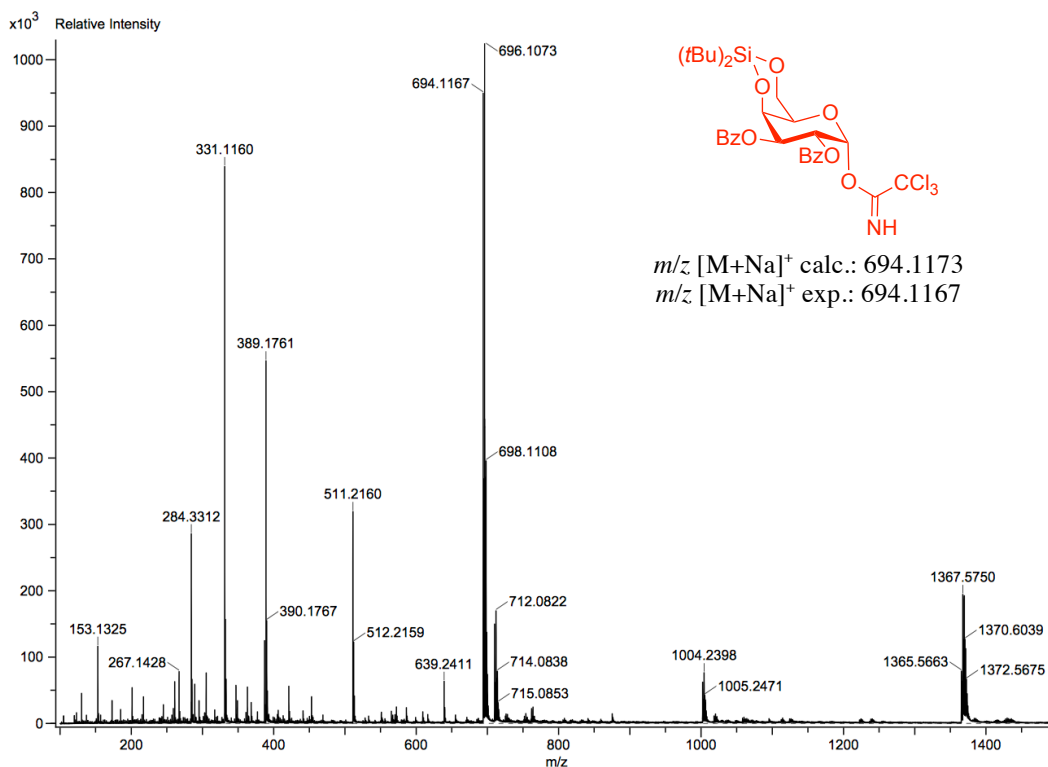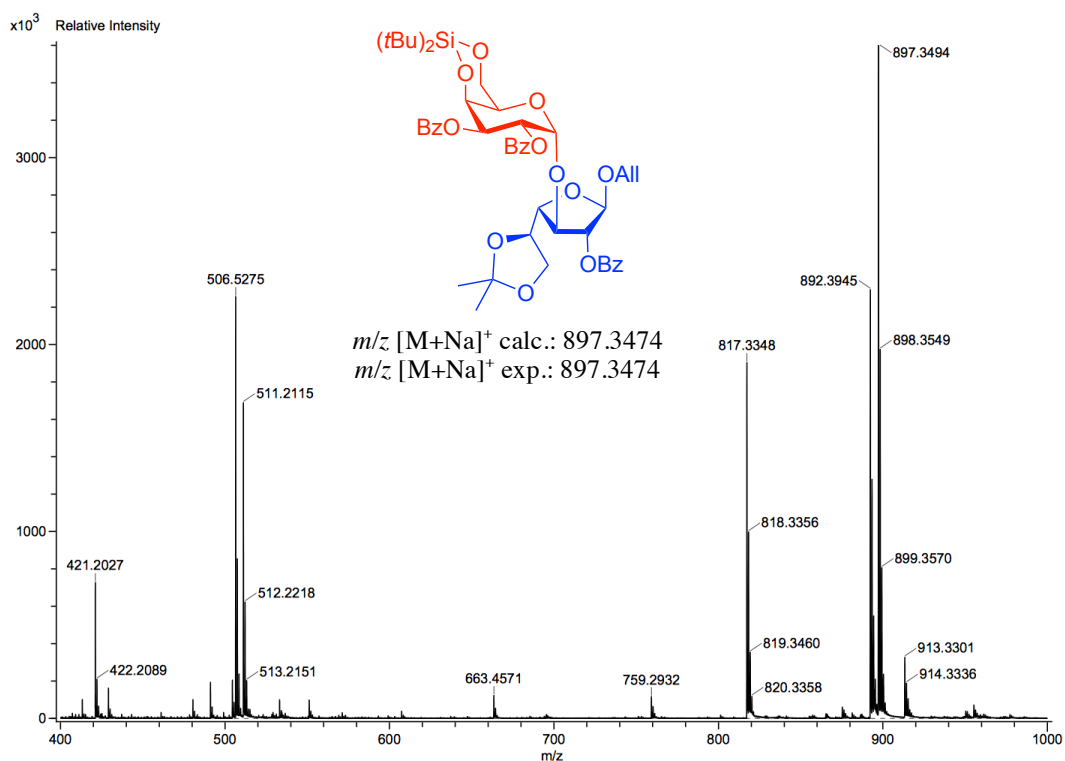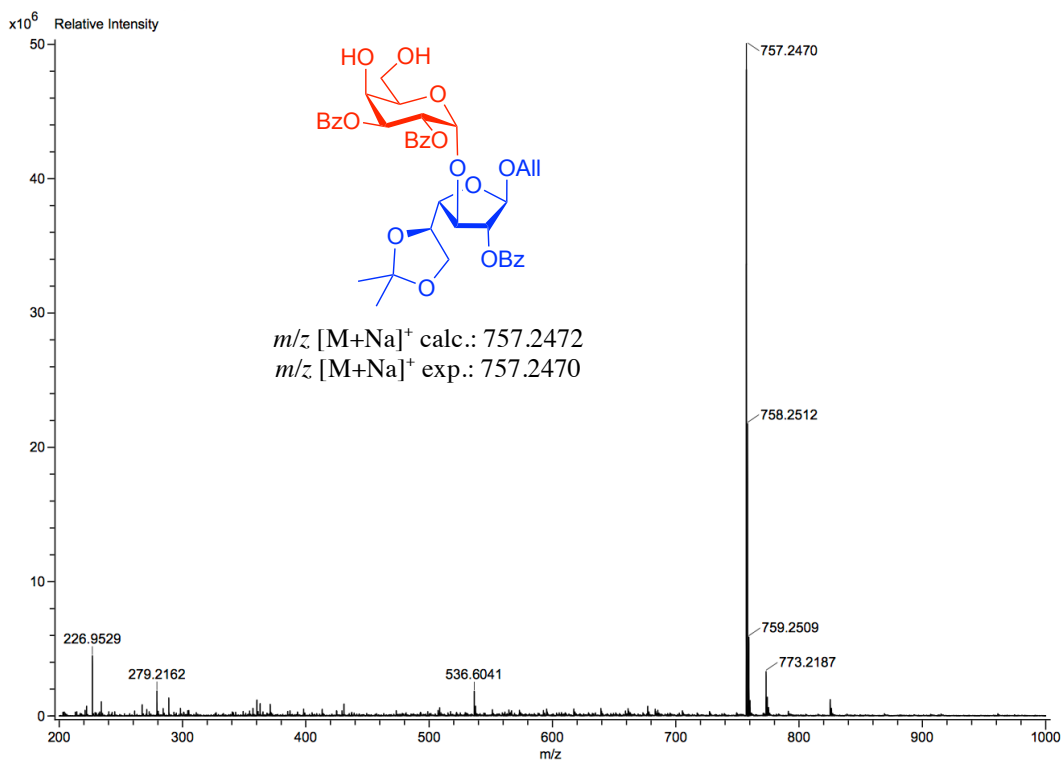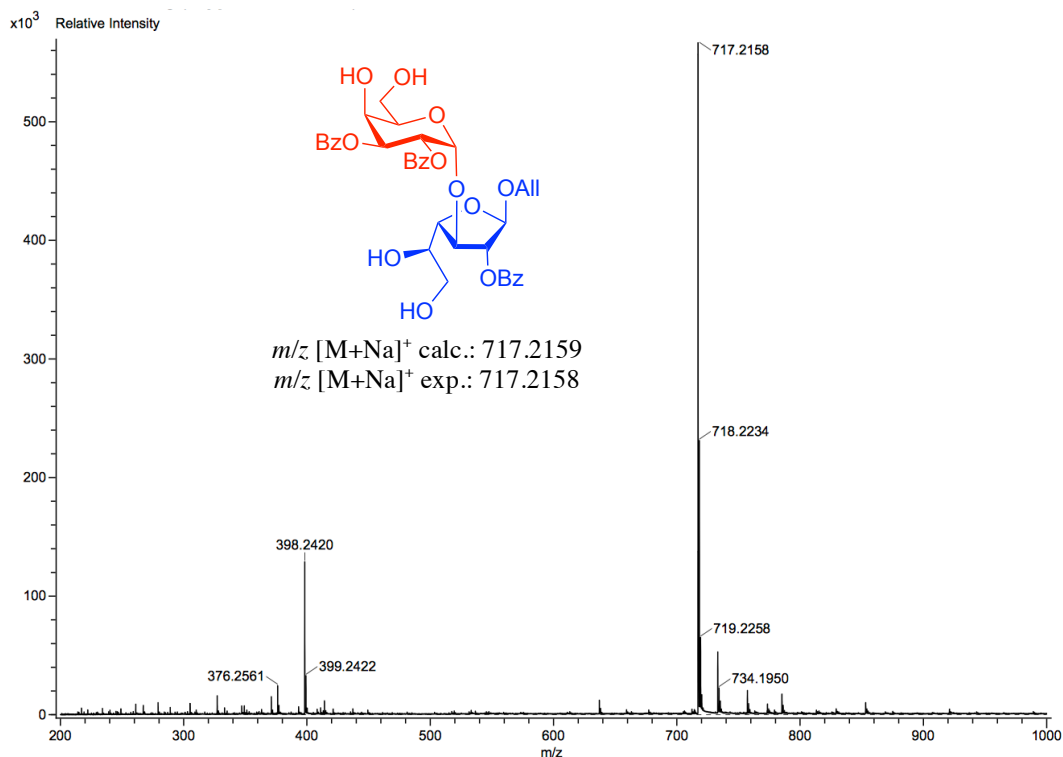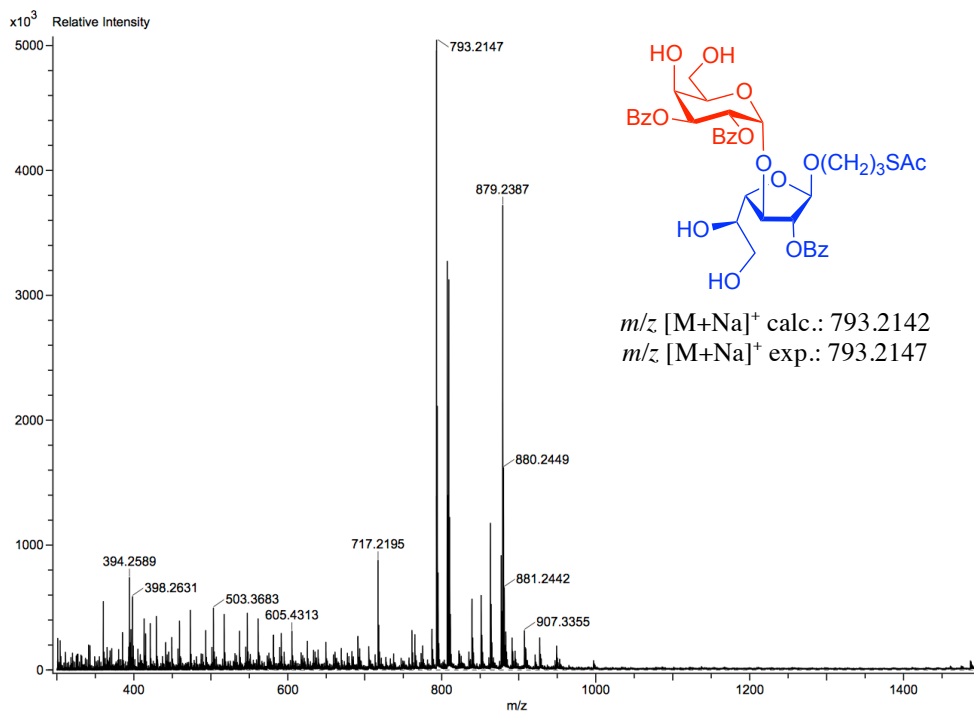
ESI-TOF HR mass spectrum of compound (G27 and 14)
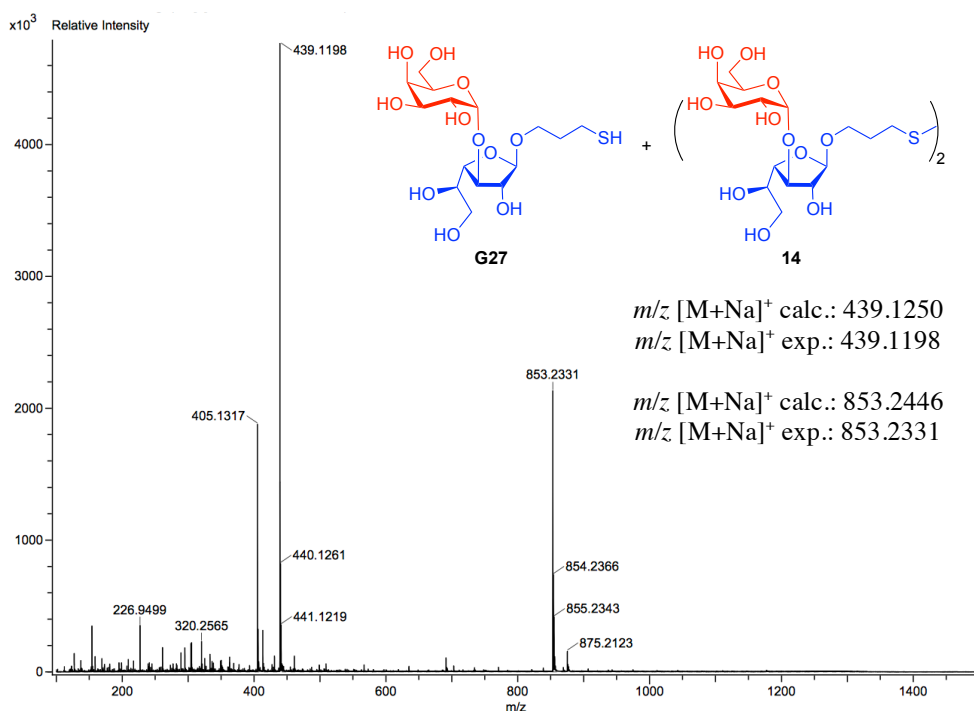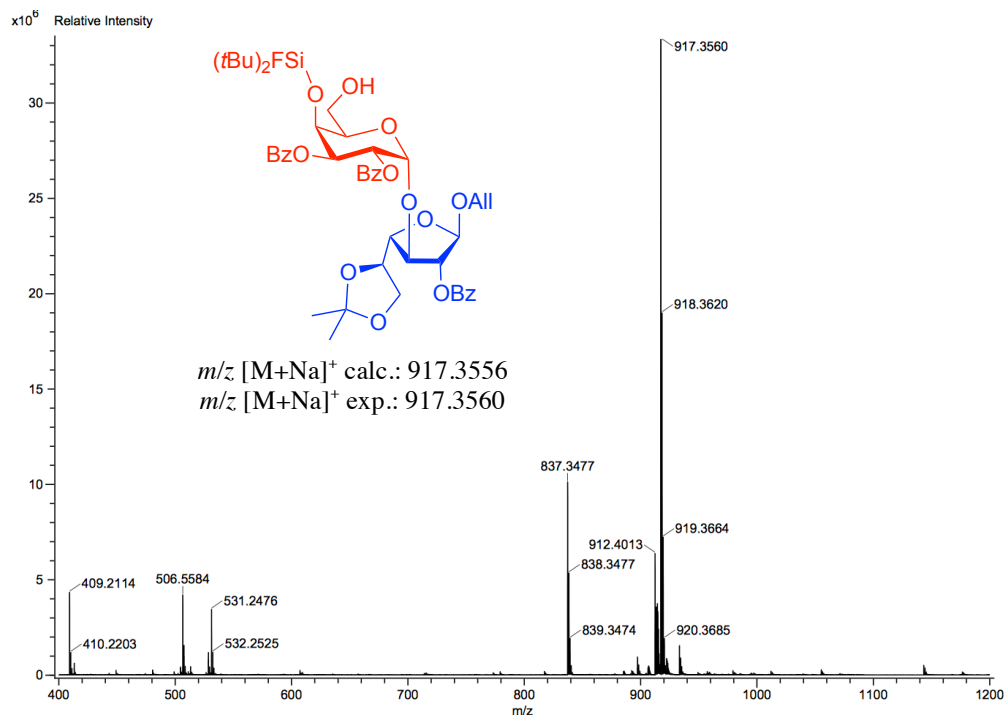
m/z [M+Na]$^+$ calc.: 439.1250
m/z [M+Na]$^+$ exp.: 439.1198

m/z [M+Na]$^+$ calc.: 853.2446
m/z [M+Na]$^+$ exp.: 853.2331

167

ESI-TOF HR mass spectrum of compound (11)

m/z [M+Na]⁺ calc.: 917.3556
m/z [M+Na]⁺ exp.: 917.3560

ESI-TOF HR mass spectrum of compound (20)

m/z [M+Na]⁺ calc.: 1021.3818
m/z [M+Na]⁺ exp.: 1021.3804

168

ESI-TOF HR mass spectrum of compound (12)

m/z [M+Na]$^+$ calc.: 1427.5630
m/z [M+Na]$^+$ exp.: 1427.5625

ESI-TOF HR mass spectrum of compound (13)

m/z [M+Na]$^+$ calc.: 1127.3525
m/z [M+Na]$^+$ exp.: 1127.3524

169

ESI-TOF HR mass spectrum of compound (34)

m/z [M+Na]⁺ calc.: 1087.3212
m/z [M+Na]⁺ exp.: 1087.3202

ESI-TOF HR mass spectrum of compound (35)

m/z [M+Na]⁺ calc.: 1163.3195
m/z [M+Na]⁺ exp.: 1163.3194

170

ESI-TOF HR mass spectrum of compound (17)

m/z [M+Na]⁺ calc.: 1177.3502
m/z [M+Na]⁺ exp.: 1177.3664

ESI-TOF HR mass spectrum of compound (46)

m/z [M+Na]⁺ calc.: 909.2734
m/z [M+Na]⁺ exp.: 909.2706

171

ESI-TOF HR mass spectrum of compound (47)

m/z [M+Na]⁺ calc.: 821.2421
m/z [M+Na]⁺ exp.: 821.2452

ESI-TOF HR mass spectrum of compound (48)

m/z [M+Na]⁺ calc.: 897.2404
m/z [M+Na]⁺ exp.: 897.2718

172
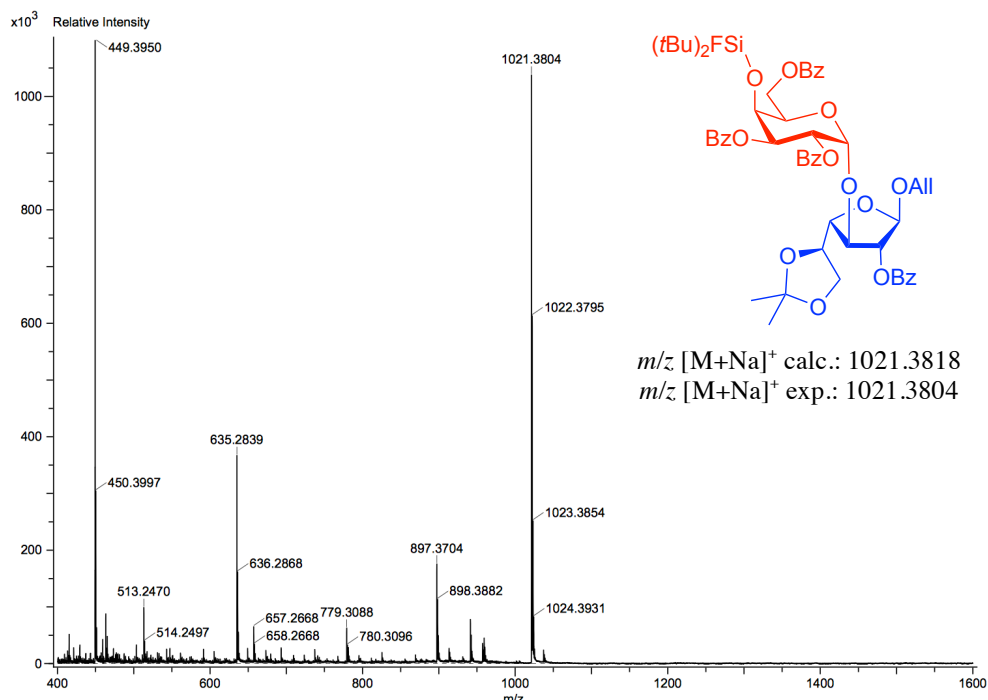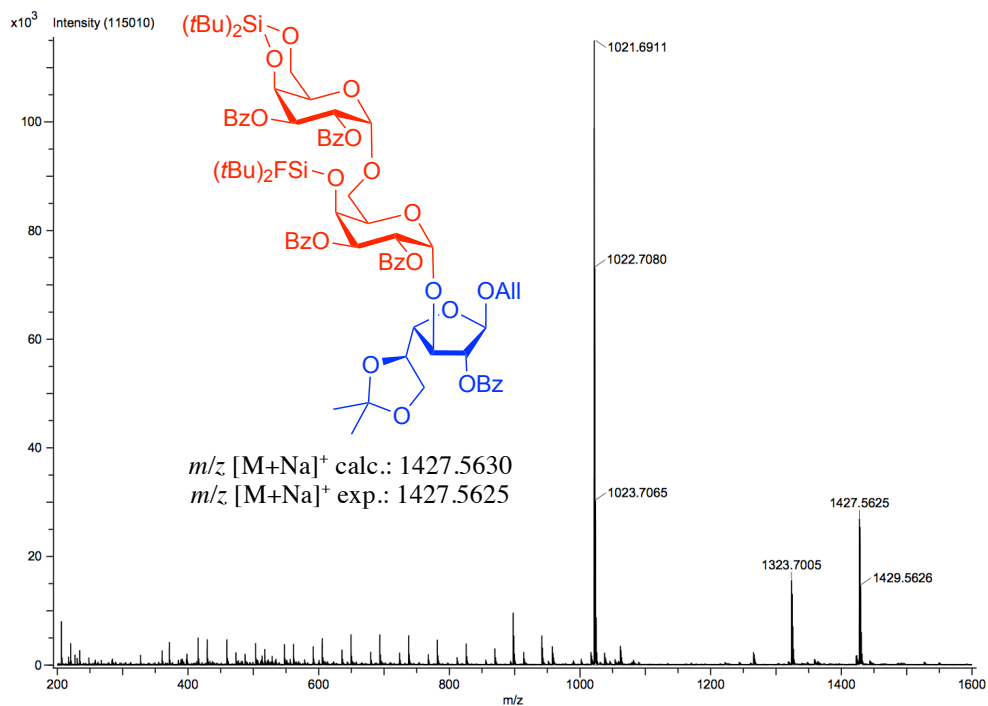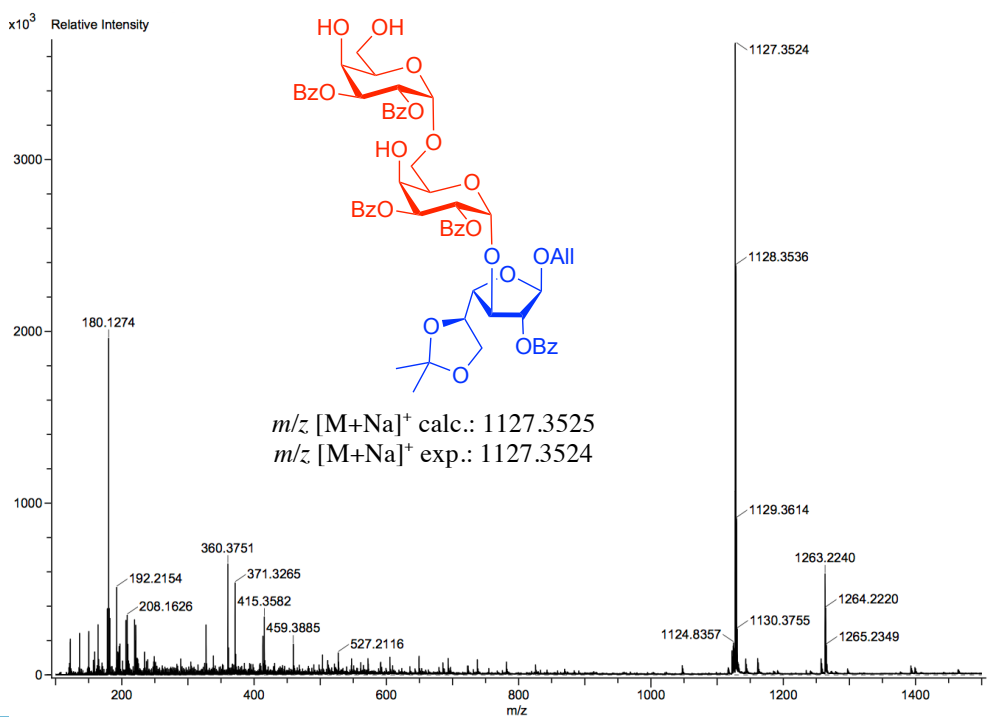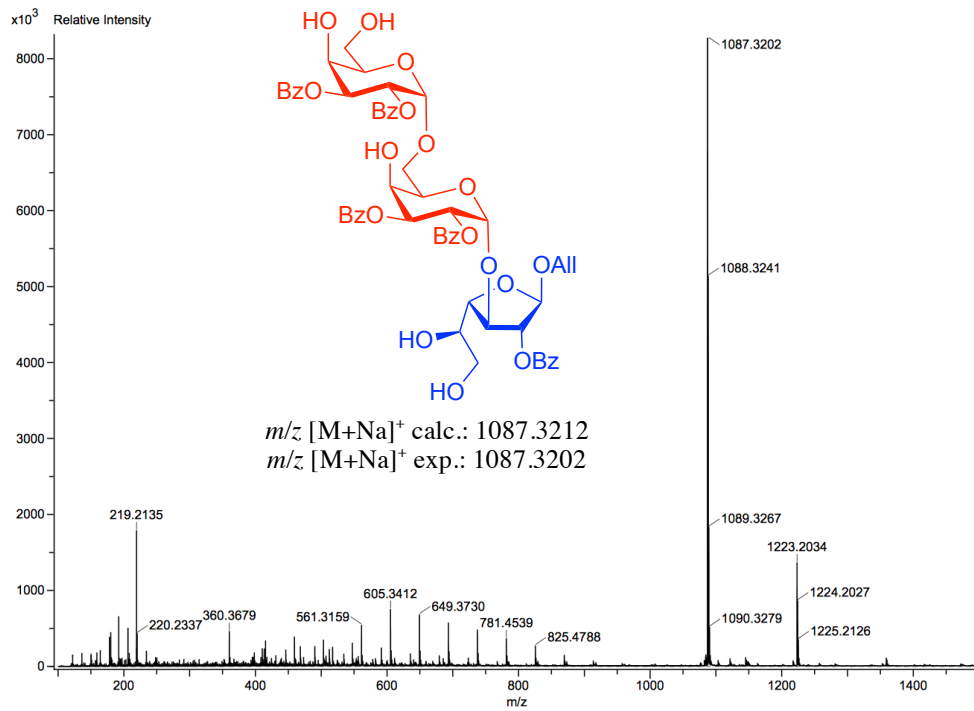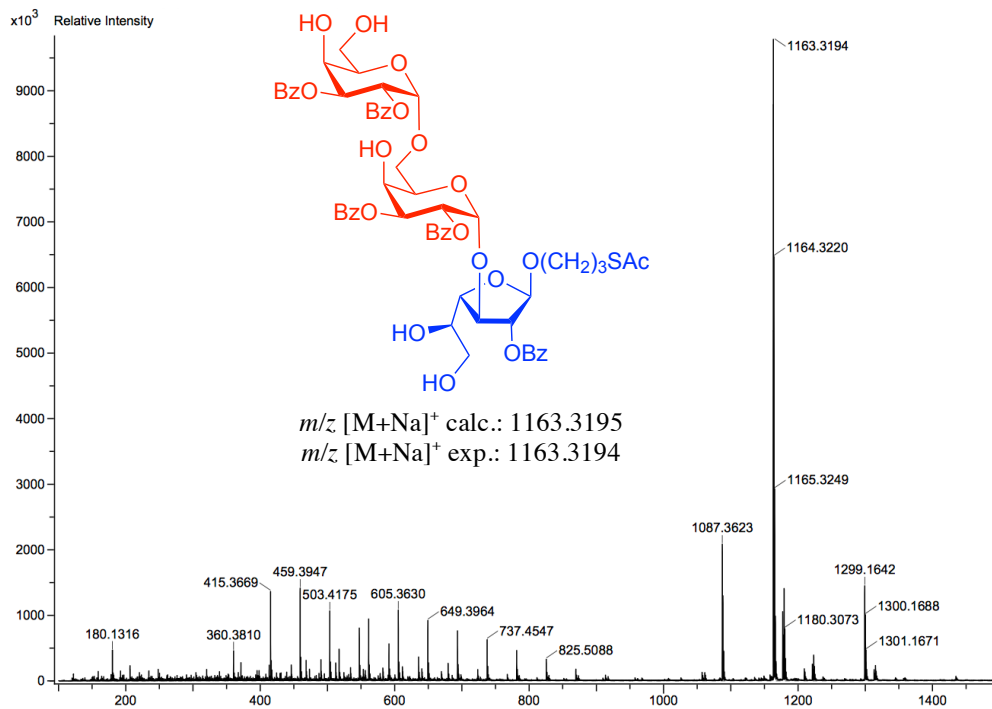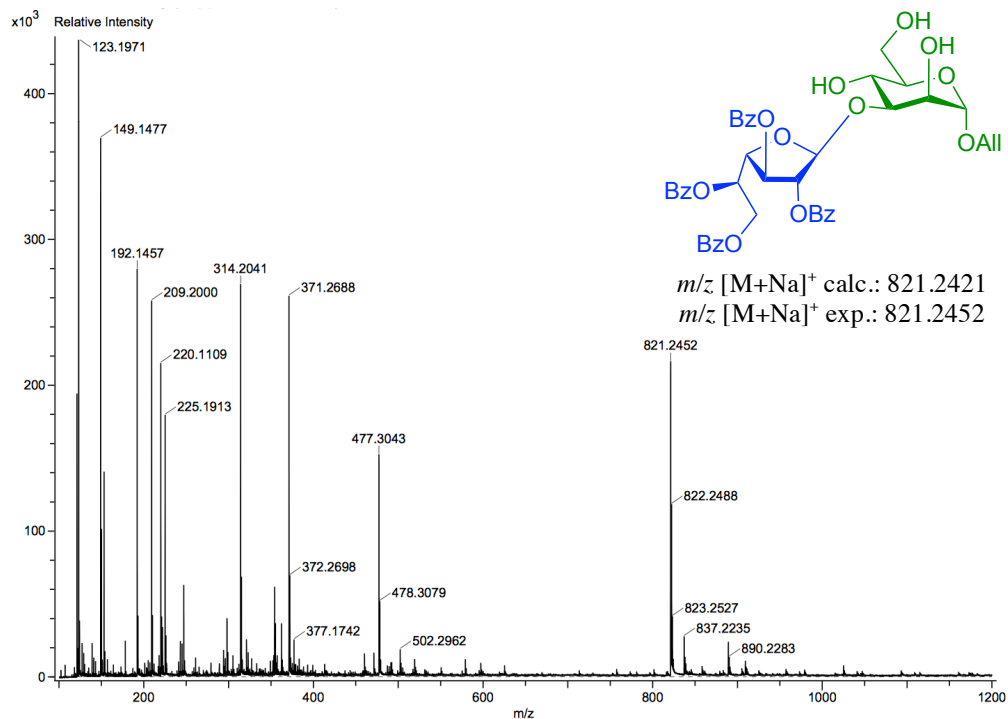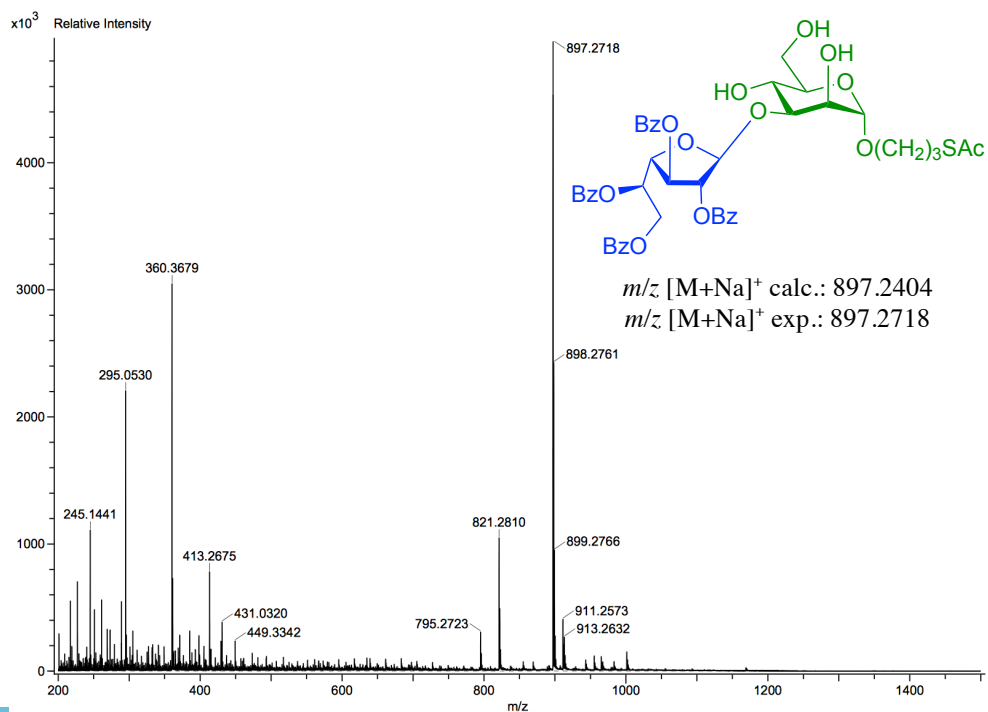
ESI-TOF HR mass spectrum of compound (G29 and 49)
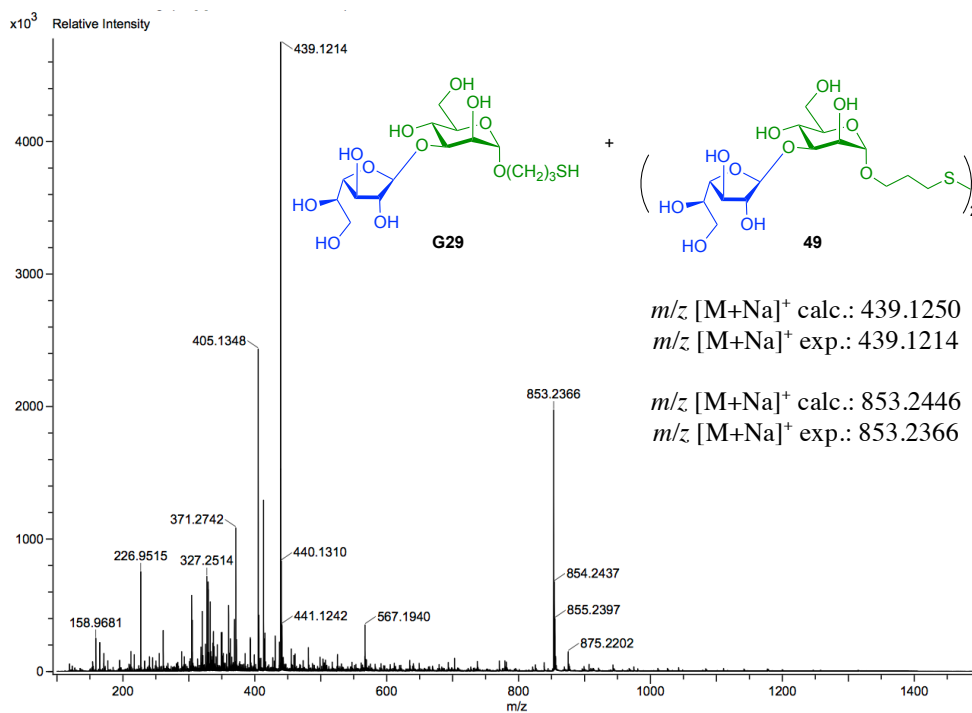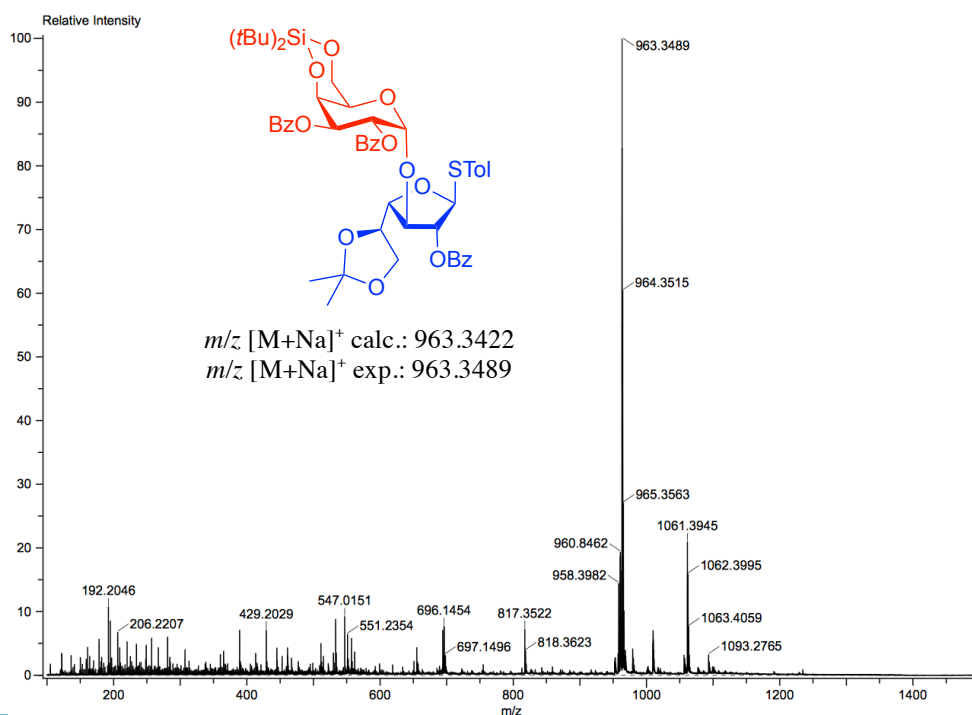
m/z [M+Na]$^+$ calc.: 439.1250
m/z [M+Na]$^+$ exp.: 439.1214

m/z [M+Na]$^+$ calc.: 853.2446
m/z [M+Na]$^+$ exp.: 853.2366

ESI-TOF HR mass spectrum of compound (5)

m/z [M+Na]$^+$ calc.: 963.3422
m/z [M+Na]$^+$ exp.: 963.3489

173

ESI-TOF HR mass spectrum of compound (9)

m/z [M+Na]⁺ calc.: 1147.4335
m/z [M+Na]⁺ exp.: 1147.4332

ESI-TOF HR mass spectrum of compound (36)

m/z [M+Na]⁺ calc.: 879.2687
m/z [M+Na]⁺ exp.: 879.2897

174

ESI-TOF HR mass spectrum of compound (37)

m/z [M+Na]⁺ calc.: 955.2670
m/z [M+Na]⁺ exp.: 955.2994

ESI-TOF HR mass spectrum of compound (16)

m/z [M+Na]⁺ calc.: 1177.3502
m/z [M+Na]⁺ exp.: 1177.3508

175

ESI-TOF HR mass spectrum of compound (56)

m/z [M+Na]$^+$ calc.: 1333.4474
m/z [M+Na]$^+$ exp.: 1333.4535

ESI-TOF HR mass spectrum of compound (57)

m/z [M+Na]$^+$ calc.: 1517.5387
m/z [M+Na]$^+$ exp.: 1517.5383

176

ESI-TOF HR mass spectrum of compound (58)

m/z [M+Na]⁺ calc.: 951.2840
m/z [M+Na]⁺ exp.: 951.2842

ESI-TOF HR mass spectrum of compound (59)

m/z [M+Na]⁺ calc.: 911.2527
m/z [M+Na]⁺ exp.: 911.2520

177

ESI-TOF HR mass spectrum of compound (60)

m/z [M+Na]$^+$ calc.: 1054.1623
m/z [M+Na]$^+$ exp.: 1054.1650

ESI-TOF HR mass spectrum of compound (61)

m/z [M+Na]$^+$ calc.: 1779.5258
m/z [M+Na]$^+$ exp.: 1779.5445

178
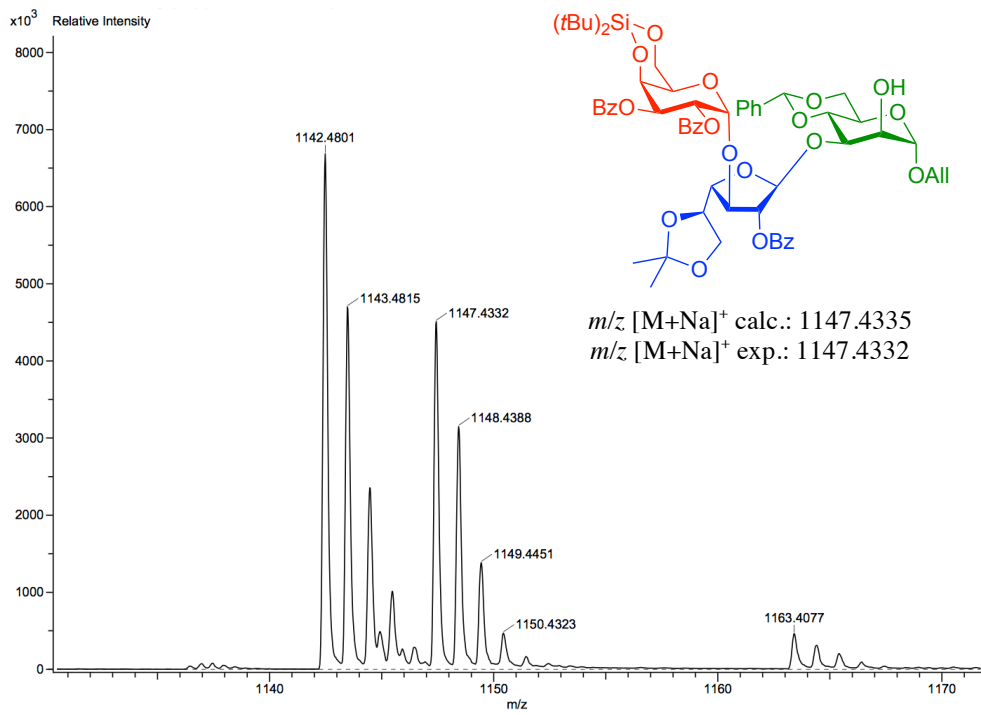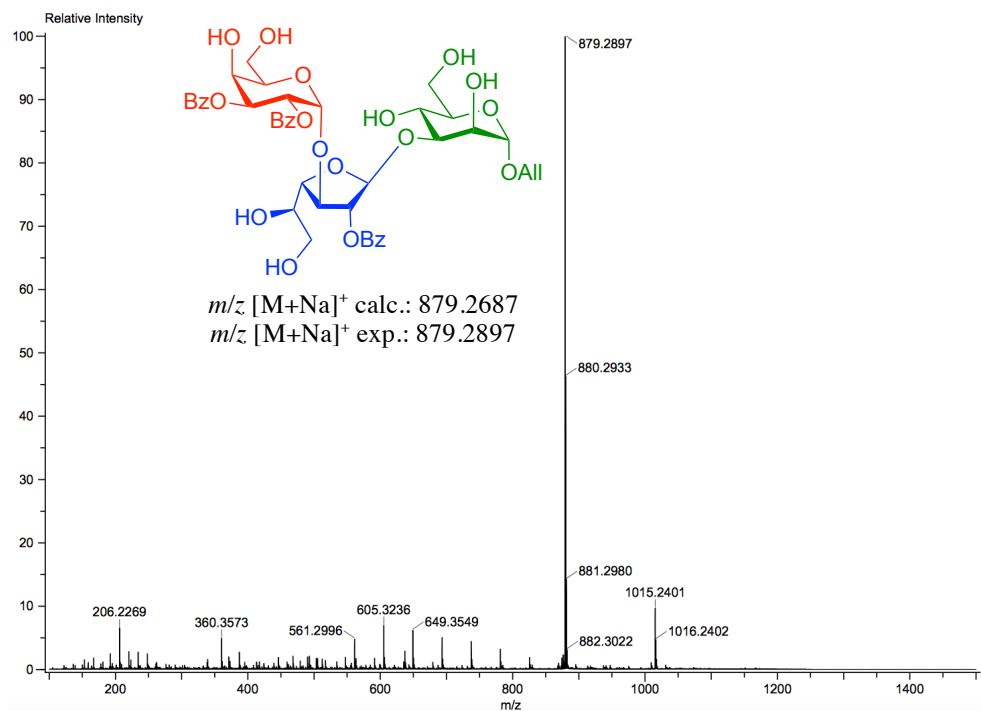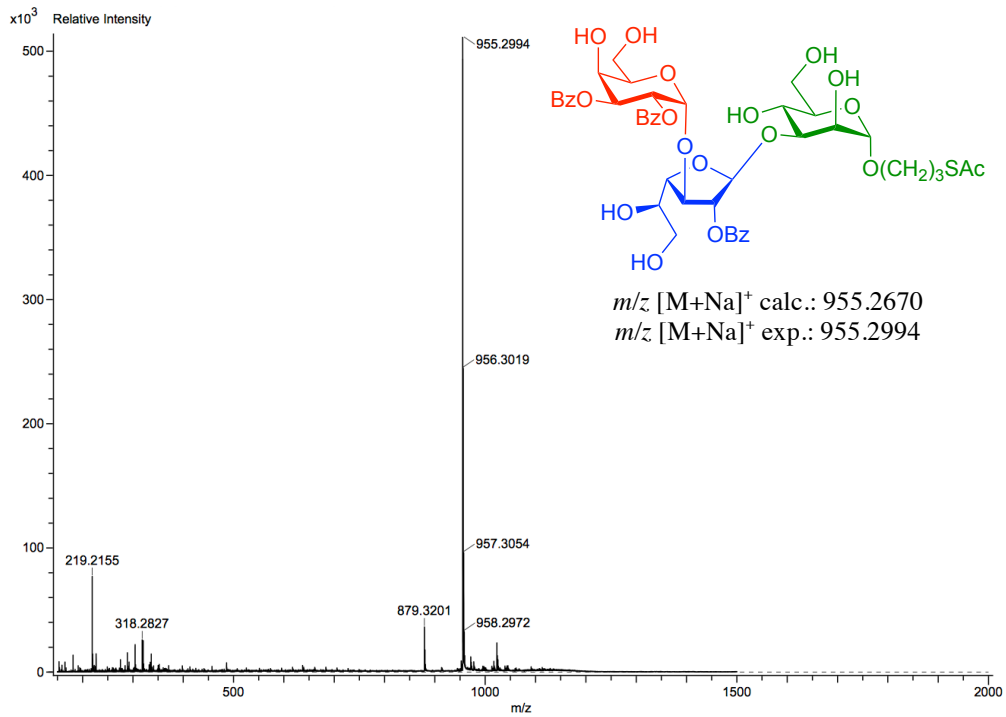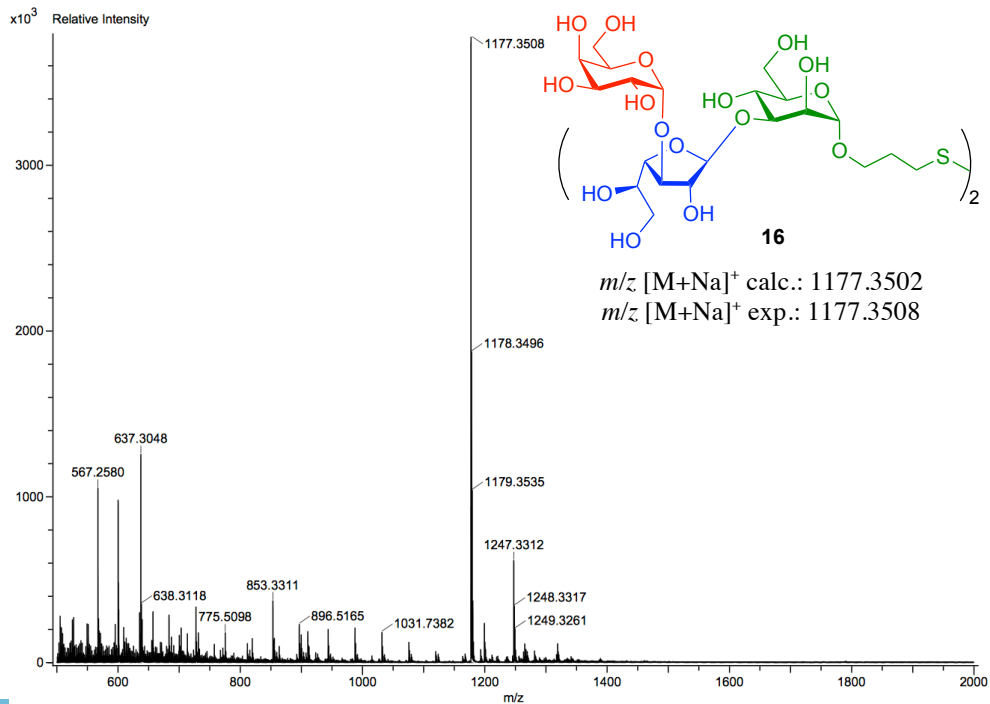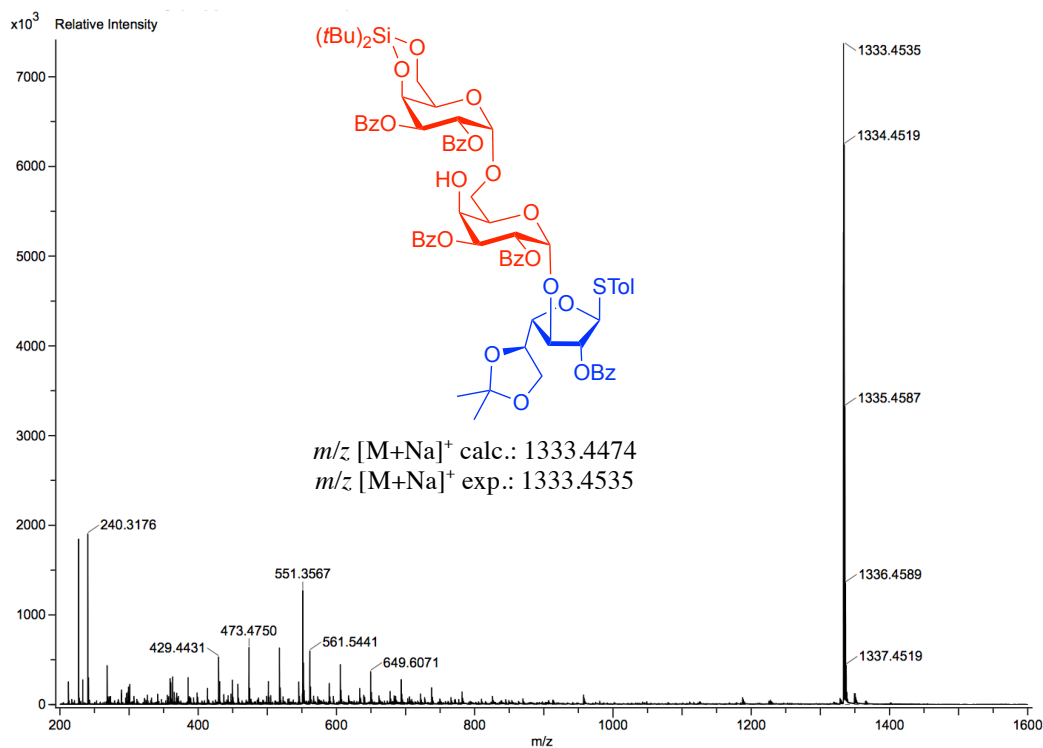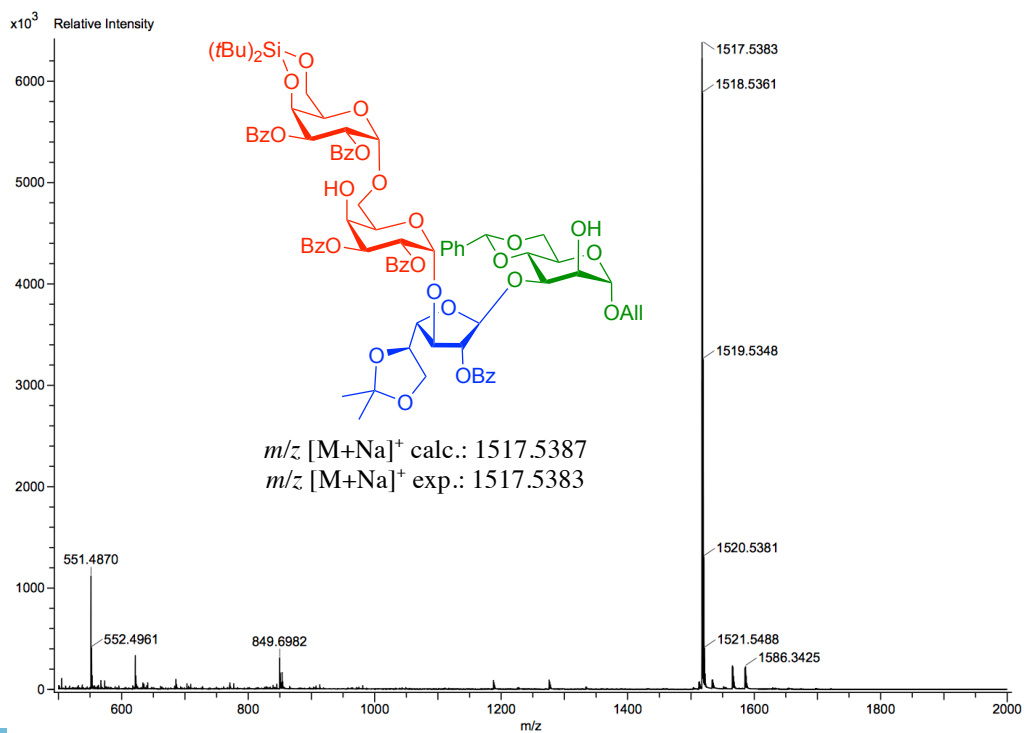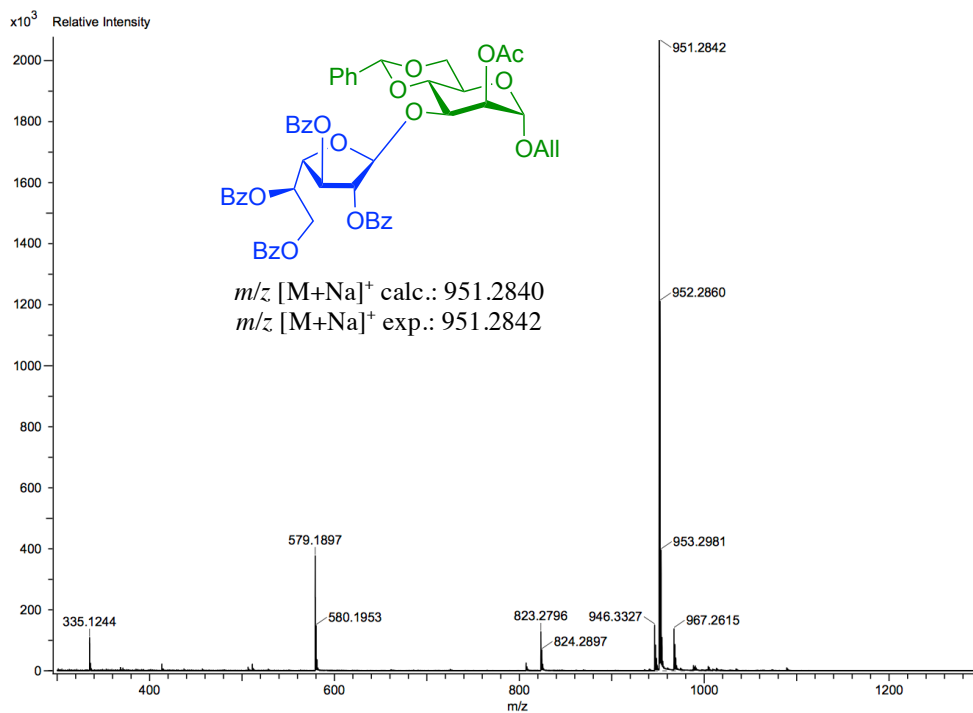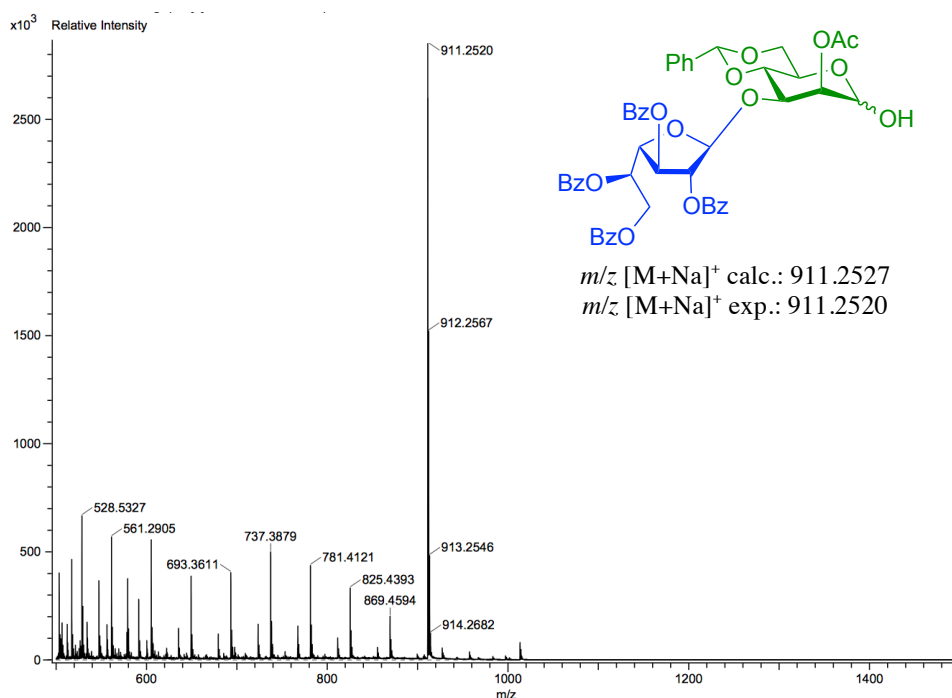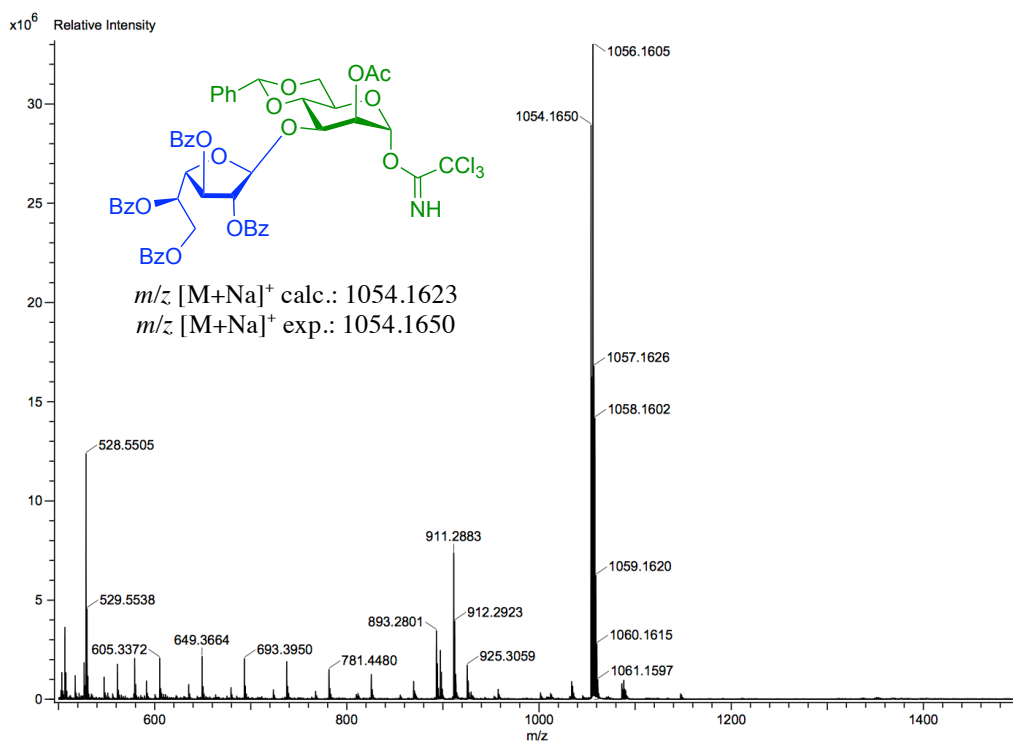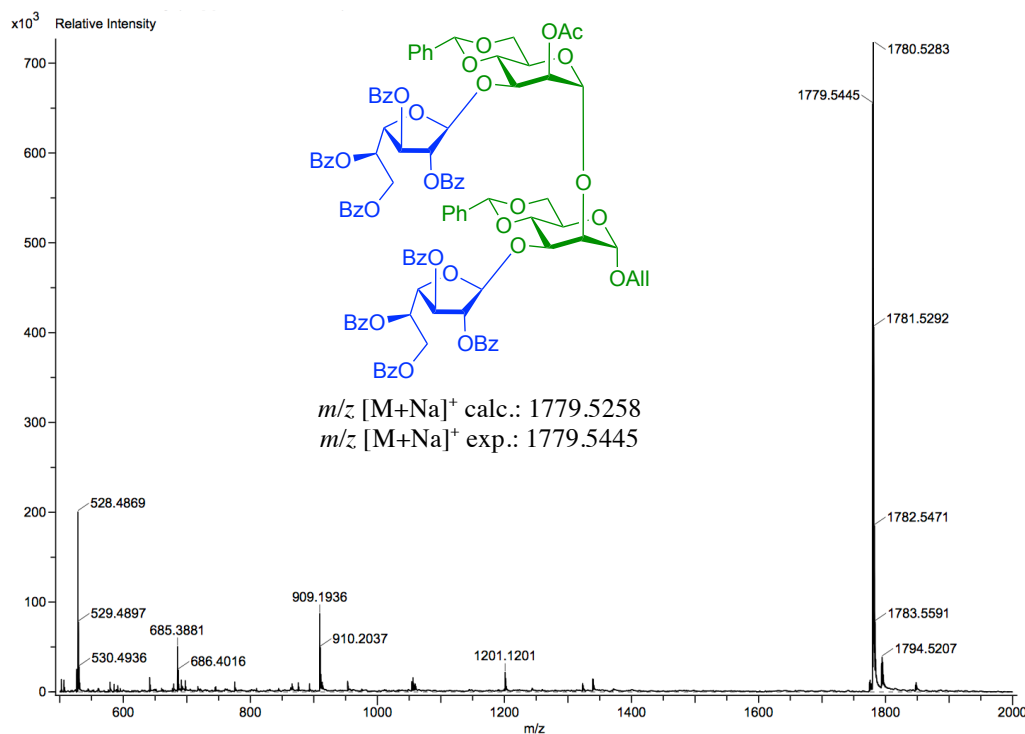
Vita

Alba Lucia Montoya Arias was born in Cali, Colombia. She graduated with the best student award from De la Presentación high school in 2006, standing out in the science area. In the same year, she met all the requirements to be accepted as a Chemistry major in the Universidad del Valle, one of the best public universities in the country. She was awarded with a tuition scholarship each academic year. In her senior year in 2010, after completing all required course work she discovered her passion for organic chemistry and joined Dr. Braulio Insuasty's research lab studying the chemistry of 4,7-dichloroquinolines. In 2011, she defended her undergraduate thesis, earned her BS degree in chemistry, and continued her education in the Chemistry MS program conducting research in the same group, where she published 5 papers in peer-reviewed journals. During her final year in 2013, she attended a departmental seminar from the University of Texas at El Paso (UTEP), which sparked her interest in obtaining her PhD degree in the US. After defending her MS thesis in 2014, she took an English course in Tallahassee, FL to improve her skills. She returned to Colombia, worked in a High School for about six months when she was accepted in 2015 in the Chemistry Doctoral Program at UTEP.

Since the beginning of the doctoral work, Alba was supported as a teaching assistant, and as a research assistant from Dr. Almeida's Kleberg Foundation grant and from Dr. Michael's R21 grant (NIH). She also received a tuition scholarship for the academic year 2018-2019 from the Pan American Round Table, a group of women who help other women in academic activities and graduate studies to support and empower women in the society. Finally, for the last two years, Alba was the recipient of the prestigious Dr. Keelung Hong Chemistry Graduate Research Fellowship.

Alba presented her research at international ACS conferences and she also did a Summer Internship at Vertex Pharmaceuticals, where she received specialized training on modern synthetic organic chemistry and medicinal chemistry.

Alba's dissertation entitled "Discovery of Biomarkers for Cutaneous Leishmaniasis and Chagas disease by reversed immunoglycomics" was supervised by Dr. Katja Michael and Dr. Igor C. Almeida. Following graduation, Alba will become a postdoctoral researcher at the University of Utah.

Contact Information: montoyaarias340@gmail.com